# NI 43-101 TECHNICAL REPORT
# Man of War Project
# Rare Earths

## Minas Gerais, Brazil

**Effective Date: December 18, 2024**
**Report Date: January 31, 2025**

**Report Prepared for**

Verde Agritech Ltd
16 Collyer Quay
#17-00
Income at Raffles
Singapore (049318)

**Report Prepared by:**

BNA Mining Solutions
Rua Desembargador Leão Starling, 200
31.310-370 Belo Horizonte, MG, Brazil

**Signed by QPs:**

Beck Nader, FAIG
Volodymyr Myadzel, MAIG

# LIST OF CONTENTS

**1. Summary ..... 15**

1.1 Introduction ..... 15

1.2 Property Description and Location ..... 15

1.3 Permit Status and Ownership ..... 16

1.4 Geology and Mineralization ..... 17

1.5 Exploration and Drilling ..... 18

1.6 Mineral Resource Estimate ..... 19

1.7 Resource Estimate Summary ..... 21

1.8 Reasonable Prospects for Eventual Economic Extraction ..... 21

1.9 Conclusions and Recommendations ..... 22

1.10 Recommendations for Future Investments in the Man of War Project ..... 23

**2 Introduction ..... 25**

2.1 Terms of Reference and Purpose of the Report ..... 25

2.2 Qualifications of Consultants ..... 26

2.3 Details of Inspection ..... 27

2.4 Sources of Information ..... 27

2.5 Effective Date ..... 27

2.6 Units of Measure ..... 27

**3 Reliance on Other Experts ..... 28**

**4 Property Description and Location ..... 29**

4.1 Project Location ..... 29

4.2 Permit Status ..... 29

4.3 Surface Rights ..... 32

4.4 Taxes and Royalties ..... 32

4.5 Environmental Liabilities and Permitting ..... 33

4.6 Other Significant Factors and Risks ..... 33

**5 Accessibility, Climate, Local Resources, Infrastructure and Physiography ..... 34**

5.1 Accessibility ..... 34
5.2 Climate ..... 35
5.3 Local Resources and Infrastructure ..... 36
5.4 Physiography ..... 37
**6 History ..... 38**
6.1 Initial Exploration and Early Discoveries ..... 38
6.2 Phosphate Resources Approved by ANM ..... 39
**7 Geological Setting and Mineralization ..... 41**
7.1 Regional Geology ..... 41
7.2 Local Geology ..... 43
7.3 Mineralization ..... 44
**8 Deposit Types ..... 46**
**9 Exploration ..... 47**
9.1 History of Phosphate Exploration ..... 47
9.2 Rare Earth Exploration ..... 47
9.3 Project targets ..... 48
**10 Drilling ..... 52**
10.1 Campaigns ..... 52
10.2 Surveying ..... 54
10.3 Logging ..... 54
10.4 Recovery Calculations ..... 56
10.5 Diamond Drilling (DDH) Sampling ..... 56
10.6 Lithologic units ..... 57
10.7 Bulk Density ..... 58
**11 Sample Preparation, Analysis and Security ..... 60**
11.1 Sample Preparation ..... 60
11.1.1 Field sample preparation ..... 60
11.1.2 Lab sample preparation ..... 61
11.2 Analysis ..... 62
11.3 QA/QC ..... 63

**12 Data Verification ..... 66**
12.1 Site Visit ..... 66
12.2 Database ..... 70
12.2.1 Database Verification Performed using the Micromine System ..... 79
12.3 QA/QC Analyses ..... 81
12.4 QA/QC – Nau de Guerra Target ..... 81
12.4.1 Sampling Precision ..... 81
12.4.2 Standards ..... 85
12.4.3 Blank Samples ..... 87
12.5 QA/QC – Balsamo and Alto da Serra Target ..... 88
12.5.1 Sampling Precision ..... 88
12.5.2 Standards ..... 91
12.5.3 Blank Samples ..... 93
**13 Mineral Processing and Metallurgical Testing ..... 94**
13.1 Objective of Leaching Tests ..... 94
13.2 Preliminary Test Conditions and Analysis ..... 94
13.3 Leaching Results and Recovery Rates ..... 95
13.4 Impurity Analysis ..... 95
**14 Mineral Resource Estimate ..... 96**
14.1 Introduction ..... 96
14.2 Statistical Analysis ..... 96
14.3 Interpretation ..... 98
14.3.1 Interpretation of the Mineralization ..... 98
14.3.2 Geological Interpretation ..... 105
14.4 Triangulation ..... 108
14.5 Data Selection ..... 113
14.6 Geostatistical Analysis ..... 116
14.7 Modelling ..... 132
14.8 Grade Interpolation and Mineral Resource Classification ..... 133
14.8.1 Grade Interpolation ..... 133

14.8.2 CAPPING ..... 137
14.9 Density Values for the Block Model ..... 140
14.10 Verification of The Block Model ..... 140
14.11 Mineral Resource Classification ..... 148
14.12 Results of the Resource Evaluation ..... 148
14.13 Reasonable Prospects for Eventual Economic Extraction ..... 152
14.14 Comments on Mineral Resources ..... 156
**15 Mineral Reserve Estimate ..... 157**
**16 Mining Methods ..... 158**
**17 Recovery Methods ..... 159**
**18 Project Infrastructure ..... 160**
**19 Market Studies and Contracts ..... 161**
**20 Environmental Studies, Permitting and Social or Community Impact ..... 162**
**21 Capital and Operating Costs ..... 163**
**22 Adjacent Properties ..... 164**
**23 Other Relevant Data and Information ..... 166**
**24 Interpretation and Conclusions ..... 167**
**25 Recommendations ..... 168**
25.1 Work Program ..... 168
25.2 Potential of Additional Elements for the Project ..... 168
25.2.1 Estimated Average Grade ..... 169
25.2.2 Highlights assays ..... 169
25.2.3 Future Studies and Exploration Directions ..... 176
25.3 Budget ..... 176
**26 References ..... 178**
**27 Date and Signature Page ..... 179**
**28 Certificates of Qualified Persons ..... 180**

# LIST OF APPENDICES

APPENDIX I – Standards Certificates ..... 184

APPENDIX II – Chemical Analysis Certificates..... 186

APPENDIX III – Qa/Qc ..... 191

APPENDIX IV - Geostatistics ..... 214

APPENDIX V – Resources Results ..... 241

APPENDIX VI – Preliminary Metallurgical Tests ..... 246

# LIST OF FIGURES

Figure 1.1 - Location Map of the Man of War Project ..... 16

Figure 1.2 - Regional geological map (Tuller et al., 2002) ..... 17

Figure 4.1 - Location Map of the Man of War Project ..... 29

Figure 4.2 - Man of War Project Targets and tenements ..... 30

Figure 5.1 - Accessibility map ..... 35

Figure 5.2 - Rainfall data from the A536 monitoring station (INMET, 2021) ..... 36

Figure 7.1 - Regional geological map (Tuller et al., 2002) ..... 41

Figure 7.2 - Stratigraphic column of the Bambuí Group in the Serra da Saudade region and surrounding areas (Lima, 2005) ..... 43

Figure 7.3 - A) Sandstone B) Conglomeratic sandstone C) Conglomerate ..... 44

Figure 9.1 - Targets drilled in the historic campaign and new prospects to be drilled ..... 49

Figure 9.2 - Surface sampling in new prospects to be drilled ..... 50

Figure 10.1 - Dimond Drilling (DDH) rig ..... 54

Figure 10.2 - A) Boxes with ½ of the cores preserved after the first exploration. B) Box of cores remarked before the new exploration phase. ..... 55

Figure 10.3 - Boxes with sample logs stored in the warehouse ..... 56

Figure 10.4 - Core storage boxes laid out in the yard to be re-logged ..... 56

Figure 10.5 - A) Contact between soil and saprolite of sandstone B) Saprolite of sandstone C) Transition zone in sandstone D) Fresh sandstone ..... 58

Figure 11.1 - Process flowchart for leaching test on Ionic Clay ..... 61

Figure 11.2 - Spatial Distribution of Samples, Blanks, Duplicates, and Standards in the Analytical QA/QC Process ..... 64

Figure 12.1 – Drilling Material – Technical site visit ..... 67

Figure 12.2 - Shed visit ..... 68

Figure 12.3 - Drill Hole Collar - Technical site visit ..... 69

Figure 12.4 - Holes and ANM limits for the Nau de Guerra Target. ..... 76

Figure 12.5 - Holes and ANM limits for the Alto da Serra Target ..... 76

Figure 12.6 - Holes and ANM limits for the Balsamo Target. ..... 77

Figure 12.7 - Linear Regression Diagram for La ppm, field duplicate, class: Diamond Drilling, internal control results for the Nau de Guerra Target. ..... 83

Figure 12.8 - Quantis plotting for La ppm, field duplicate, class: Diamond Drilling, internal control results for the Nau de Guerra Target. ..... 83

Figure 12.9 - Linear Regression Diagram for Nd ppm, field duplicate, class: Diamond Drilling, internal control results for the Nau de Guerra Target. ..... 84

Figure 12.10 - Quantis plotting for La ppm, field duplicate, class: Diamond Drilling, internal control results for the Nau de Guerra Target. ..... 84

Figure 12.11 - Standard OREAS 460, element Nd. ..... 85

Figure 12.12 - Standard OREAS 461, element Nd. ..... 86

Figure 12.13 - Standard SG-142, element Nd. ..... 86

Figure 12.14 - Linear Regression Diagram for La ppm, field duplicate, class: Diamond Drilling, internal control results for the Balsamo and Alto da Serra targets. ..... 89

Figure 12.15 - Quantis plotting for La ppm, field duplicate, class: Diamond Drilling, internal control results for the Balsamo and Alto da Serra targets. ..... 89

Figure 12.16 - Linear Regression Diagram for Nd ppm, field duplicate, class: Diamond Drilling, internal control results for the Balsamo and Alto da Serra targets. ..... 90

Figure 12.17 - Quantis plotting for La ppm, field duplicate, class: Diamond Drilling, internal control results for the Balsamo and Alto da Serra targets. ..... 90

Figure 12.18 - Standard OREAS 460, element Nd. ..... 91

Figure 12.19 - Standard OREAS 461, element Nd. ..... 92

Figure 12.20 - Standard SG-142, element Nd. ..... 92

Figure 14.1 - Histogram of TREE ppm grade distribution for all samples, Nau de Guerra target. ..... 97

Figure 14.2 - Histogram of TREE ppm grade distribution for all samples, Balsamo target. ..... 97

Figure 14.3 - Histogram of TREE ppm grade distribution for all samples, Alto da Serra target. ..... 98

Figure 14.4 - Composite sample intervals for the boreholes (red bar shows the composite sample)- Nau de Guerra target. ..... 99

Figure 14.5 - Composite sample intervals for the boreholes (red bar shows the composite sample). ..... 100

Figure 14.6 - Top (green) and Base (blue) points of the mineralized zone. ..... 100

Figure 14.7 - Digital terrain model of the Base surface of the mineralization – Nau de Guerra target ..... 101

Figure 14.8 - Digital terrain model of the Base surface of the mineralization– Nau de Guerra target ..... 102

Figure 14.9 - Digital terrain model of the Base surface of the mineralization – Balsamo and Alto da Serra targets ..... 102

Figure 14.10 - Digital terrain model of the Base surface of the mineralization - Balsamo and Alto da Serra targets ..... 103

Figure 14.11 - Geological mapping data on the Capacete Formation, Nau de Gerra target. ..... 103

Figure 14.12 - Geological mapping data on the Capacete Formation, Alto da Serra target. ..... 104

Figure 14.13 - Geological mapping data on the Capacete Formation, Balsamo target. ..... 104

Figure 14.14 - Lithological description intervals along the drill holes (Vertical Exaggeration *3), Balsamo and Alto da Serra targets ..... 106

Figure 14.15 - Lithological description intervals along the drill holes (Vertical Exaggeration *3), Nau de Guerra target ..... 106

Figure 14.16 - Points in the lithological zone ..... 107

Figure 14.17 - Digital terrain model of the base surface of the lithological types, Nau de Guerra target ..... 108

Figure 14.18 - Digital terrain model of the base surface of lithological types, Balsamo and Alto da Serra targets ..... 108

Figure 14.19 - Digital Roof Surface Model of the mineralization zone, Nau de Guerra target ..... 109

Figure 14.20 - Digital Roof Surface Model of the mineralization zone, Balsamo and Alto da Serra targets ..... 109

Figure 14.21 - Boolean operations to build the mineralization body solid, Nau de Guerra target .... 110

Figure 14.22 - Boolean operations to build the mineralization body solid, Alto da Serra target ..... 110

Figure 14.23 - Boolean operations to build the mineralization body solid, Balsamo target ..... 111

Figure 14.24 - Lithological Solids, Nau de Guerra target ..... 111

Figure 14.25 - Mineralization body solids, Balsamo target ..... 112

Figure 14.26 - Mineralization body solids, Alto da Serra target ..... 112

Figure 14.27 - Histogram of sample size distribution, Nau de Guerra target ..... 113

Figure 14.28 - Histogram of sample size distribution, Balsamo and Alto da Serra target ..... 114

Figure 14.29 - First axis to TLREE (ppm), Balsamo target ..... 117

Figure 14.30 - Second axis to TLREE (ppm), Balsamo target ..... 117

Figure 14.31 - Third axis to TLREE (ppm), Balsamo target ..... 118

Figure 14.32 - Linear diagram of dependence between composite sample data and TLREE (ppm) grade estimates, Balsamo target ..... 119

Figure 14.33 - First axis to THREE (ppm), Balsamo target ..... 119

Figure 14.34 - Second axis to THREE (ppm), Balsamo target ..... 120

Figure 14.35 - Third axis to THREE (ppm), Balsamo target ..... 120

Figure 14.36 - Linear diagram of dependence between composite samples data and THREE (ppm) grade estimates, Balsamo target ..... 121

Figure 14.37 - First axis to TLREE (ppm), Nau de Guerra target ..... 122

Figure 14.38 - Second axis to TLREE (ppm), Nau de Guerra target ..... 122

Figure 14.39 - Third axis to TLREE (ppm), Nau de Guerra target ..... 123

Figure 14.40 - Linear diagram of dependence between composite sample data and TLREE (ppm) grade estimates, Nau de Guerra target ..... 124

Figure 14.41 - First axis to THREE (ppm), Nau de Guerra target ..... 124

Figure 14.42 - Second axis to THREE (ppm), Nau de Guerra target ..... 125

Figure 14.43 - Third axis to THREE (ppm), Nau de Guerra target ..... 125

Figure 14.44 - Linear diagram of dependence between composite sample data and THREE (ppm) grade estimates, Nau de Guerra target ..... 126

Figure 14.45 - First axis to TLREE (ppm), Alto da Serra target ..... 127

Figure 14.46 - Second axis to TLREE (ppm), Alto da Serra target ..... 127

Figure 14.47 - Third axis to TLREE (ppm), Alto da Serra target ..... 128

Figure 14.48 - Linear diagram of dependence between composite sample data and TLREE (ppm) grade estimates, Alto da Serra target ..... 129

Figure 14.49 - First axis to THREE (ppm), Alto da Serra target ..... 129

Figure 14.50 - Second axis to THREE (ppm), Alto da Serra target ..... 130

Figure 14.51 - Third axis to THREE (ppm), Alto da Serra target ..... 130

Figure 14.52 - Linear diagram of dependence between composite sample data and THREE (ppm) grade estimates, Alto da Serra target ..... 131

Figure 14.53 - Histogram and graph of TREE + $Y_2O_3$ distribution probability in composite samples (left) and a block model interpolated using the Ordinary Kriging method (right) for regolith rock, Nau de Guerra target ..... 141

Figure 14.54 - Histogram and graph of TREE + $Y_2O_3$ distribution probability in composite samples (left) and block model interpolated using the Ordinary Kriging method (right), Alto da Serra target ..... 142

Figure 14.55 - Histogram and graph of TREE + $Y_2O_3$ distribution probability in composite samples (left) and block model interpolated using the Ordinary Kriging method (right), Balsamo target ..... 142

Figure 14.56 - Visualization TREO +$Y_2O_3$ with Block Model, Nau de Guerra target ..... 143

Figure 14.57 - Visualization TREO + $Y_2O_3$ with Block Model, Nau de Guerra target ..... 144

Figure 14.58 - Visualization TREO + $Y_2O_3$ with Block Model, Nau de Guerra target ..... 144

Figure 14.59 - Visualization TREO + $Y_2O_3$ with Block Model, Nau de Guerra target ..... 145

Figure 14.60 - Visualization TREO +$Y_2O_3$ with Block Model, Alto da Serra target ..... 145

Figure 14.61 – Visualization TREO + $Y_2O_3$ with Block Model, Alto da Serra target ..... 146

Figure 14.62 - Visualization TREO + $Y_2O_3$ with Block Model, Balsamo target ..... 146

Figure 14.63 - Visualization TREO + $Y_2O_3$ with Block Model, Balsamo target ..... 147

Figure 14.64 - ANM mining rights limits, Nau de Guerra target ..... 149

Figure 14.65 - ANM mining rights limits, Balsamo and Alto da Serra targets ..... 149

Figure 14.66 - ANM mining rights limits, Balsamo and Alto da Serra targets ..... 150

Figure 14.67 - Reasonable Prospects for Eventual Economic Extraction ..... 155

Figure 22.1 - Adjacent Properties to the Man of War Project ..... 165

# LIST OF TABLES

Table 1.1 - Resource Estimate Summary ..... 21

Table 1.2- Reasonable Prospects for Eventual Economic Extraction Summary ..... 21

Table 1.3 - Estimated Investment Breakdown ..... 24

Table 5.1 - Distance from São Gotardo to Major Urban Centers by Road ..... 34

Table 6.1 - Resources approved by the ANM for the Nau de Guerra target ..... 39

Table 6.2 - Resources approved by the ANM for the Alto da Serra target ..... 39

Table 6.3 - Resources approved by the ANM for the Balsamo target ..... 40

Table 9.1 - Results of surface channel samples ..... 50

Table 10.1 - Results of Drill Holes from Campaign #2 ..... 52

Table 11.1 - ICP95A Method - Determination by Fusion with Lithium Metaborate for Oxides - ICP OES Detection Ranges ..... 62

Table 11.2 - IMS95A Method - Determination by Fusion with Lithium Metaborate for Elements - ICP MS Detection Ranges ..... 63

Table 12.1 - Presentation of initial data ..... 71

Table 12.2 - Elements analyzed for all samples in the database ..... 77

Table 12.3 - Descriptive statistics for the blank sample chemical analysis results ..... 87

Table 12.4 - Descriptive statistics for the blank sample chemical analysis results ..... 93

Table 13.1 - Leaching with 0.5M Ammonium Sulfate for 30 Minutes, Analysis by ICPOES / ICPMS for Oxides/Elements - Detection Ranges ..... 94

Table 13.2 - Leached Results for Ionic Clay from Hole AP-ND-05 @5m (Interval 9m - 14m) ..... 95

Table 13.3 - Impurities Identified in Leachate Using the ICM694 Method ..... 95

Table 14.1 - Lithological codes ..... 105

Table 14.2 - Descriptive statistics for composite samples ..... 114

Table 14.3 - Cross-Validation verification results for TLREE (ppm), Balsamo target ..... 118

Table 14.4 - Cross-Validation verification results for THREE (ppm), Balsamo target ..... 120

Table 14.5 - Cross-Validation verification results for TLREE (ppm), Nau de Guerra target ..... 123

Table 14.6 - Cross-Validation verification results for THREE (ppm), Nau de Guerra target ..... 125

Table 14.7 - Cross-Validation verification results for TLREE (ppm), Alto da Serra target ..... 128

Table 14.8 - Cross-Validation verification results for THREE (ppm), Alto da Serra target ..... 131

Table 14.9 - Block model parameters, Nau de Guerra target ..... 132

Table 14.10 - Block model parameters, Balsamo and Alto da Serra targets..... 133

Table 14.11 - Direction of the search ellipsoid axes for all interpolated elements, all targets ..... 133

Table 14.12 - Direction of the search ellipsoid axes and search ellipse parameters for each interpolated element, Nau de Guerra, Balsamo and Alto da Serra targets..... 135

Table 14.13 - Search radius and interpolation parameters for all elements and interpolation methods ..... 136

Table 14.14 - Capping grade values for the Nau de Guerra, Balsamo and Alto da Serra targets ..... 137

Table 14.15 - Comparison of the average grades of components interpreted with and without capping ..... 139

Table 14.16 - Average density used for the mineralization zone..... 140

Table 14.17 - Data comparison between different estimation methods for TREO + $Y_2O_3$ ..... 147

Table 14.18 - Geological resources in situ with a Cut-off of 1000 ppm TREO on a dry basis ..... 151

Table 14.19 - Resource Estimate Summary..... 151

Table 14.20 - Optimization Parameters ..... 152

Table 14.21 - Price and Recovery..... 153

Table 14.22 - Reasonable Prospects for Eventual Economic Extraction..... 154

Table 14.23 - Reasonable Prospects for Eventual Economic Extraction Summary..... 154

Table 25.1 – Estimated Average Grades ..... 169

Table 25.2 – Highlighted Drill Hole Intersections and Niobium Oxide ($Nb_2O_5$) Concentrations for the Man of War Project..... 170

Table 25.3 – Highlighted Drill Hole Intersections and Vanadium Oxide ($V_2O_5$) Concentrations for the Man of War Project..... 171

Table 25.4 – Highlighted Drill Hole Intersections and Rubidium Oxide ($Rb_2O$) Concentrations for the Man of War Project..... 172

Table 25.5 – Highlighted Drill Hole Intersections and Hafnium Oxide ($HfO_2$) Concentrations for the Man of War Project ..... 173

Table 25.6 – Highlighted Drill Hole Intersections and Gallium Oxide ($Ga_2O_3$) Concentrations for the Man of War Project ..... 174

Table 25.7 – Highlighted Drill Hole Intersections and Cobalt Oxide (CoO) Concentrations for the Man of War Project ..... 174

Table 25.8 – Highlighted Drill Hole Intersections and Scandium Oxide ($Sc_2O_3$) Concentrations for the Man of War Project ..... 175

Table 25.9 - Estimated Investment Breakdown ..... 177

# 1. Summary

## 1.1 Introduction

Verde Agritech Ltd ("VERDE" or the "Company") commissioned BNA Mining Solutions (BNA) to prepare a Technical Report compliant with Canadian National Instrument 43-101 (NI 43-101) of the Man of War Project (or the Project) located in Brazil. The Man of War Project encompasses three primary targets spread across four mining tenements:

- **Nau de Guerra Target**:
  - Tenement No. 832543/2016 – Area: 475.19 hectares
- **Alto da Serra Target:**
  - Tenement No. 832544/2016 – Area: 452.34 hectares
- **Balsamo Target:**
  - Tenement No. 830794/2010 – Area: 1,857.56 hectares
  - Tenement No. 830796/2010 – Area: 1,923.58 hectares

The contract allows VERDE to file this report as a Technical Report with the Canadian Securities regulatory authorities pursuant to NI 43-101, Standards of Disclosure for Mineral Projects. Except for the purposes legislated under provincial securities law, any other use of this report by any third party is done so at that party's sole risk. The responsibility for any disclosure remains with VERDE. The user of this document should ensure that this is the most recent Technical Report on the property, as it is not to be considered valid if a new Technical Report has been issued.

This report provides mineral resource estimates and a classification of resources in accordance with the Canadian Institute of Mining, Metallurgy and Petroleum Standards on Mineral Resources and Reserves: Definitions and Guidelines, May 19, 2014 (https://mrmr.cim.org/media/1128/cim-definition-standards_2014.pdf).

## 1.2 Property Description and Location

The Man of War Project is located in the Midwest region of Minas Gerais, specifically within the municipalities of São Gotardo and Matutina, located in the Alto Paranaíba mesoregion. The project

area is approximately 329 km from Belo Horizonte, the capital of Minas Gerais. Geographically, it is centered around the coordinates -19°5’ latitude and -46° longitude, (Figure 1.1).




**Figure 1.1 - Location Map of the Man of War Project**

## 1.3 Permit Status and Ownership

The Man of War Project area comprises a total of 4 granted exploration permits covering an aggregate area of 4,708 ha.

The Company has agreements with landowners for mineral exploration and environmental studies, but has not yet reached agreements for mineral exploitation, as these are still being negotiated.

## 1.4 Geology and Mineralization

The study area is located in the southwestern portion of the São Francisco Craton. The regional geological framework is illustrated in Figure 1.2. The oldest stratigraphic unit in this region is the Neoproterozoic Araxá Group, comprising calciferous schists and diamictites of the Ibiá Formation. Overlying the Araxá Group is the undivided Canastra Group, which consists of phyllites, quartzites, and sericite schists.

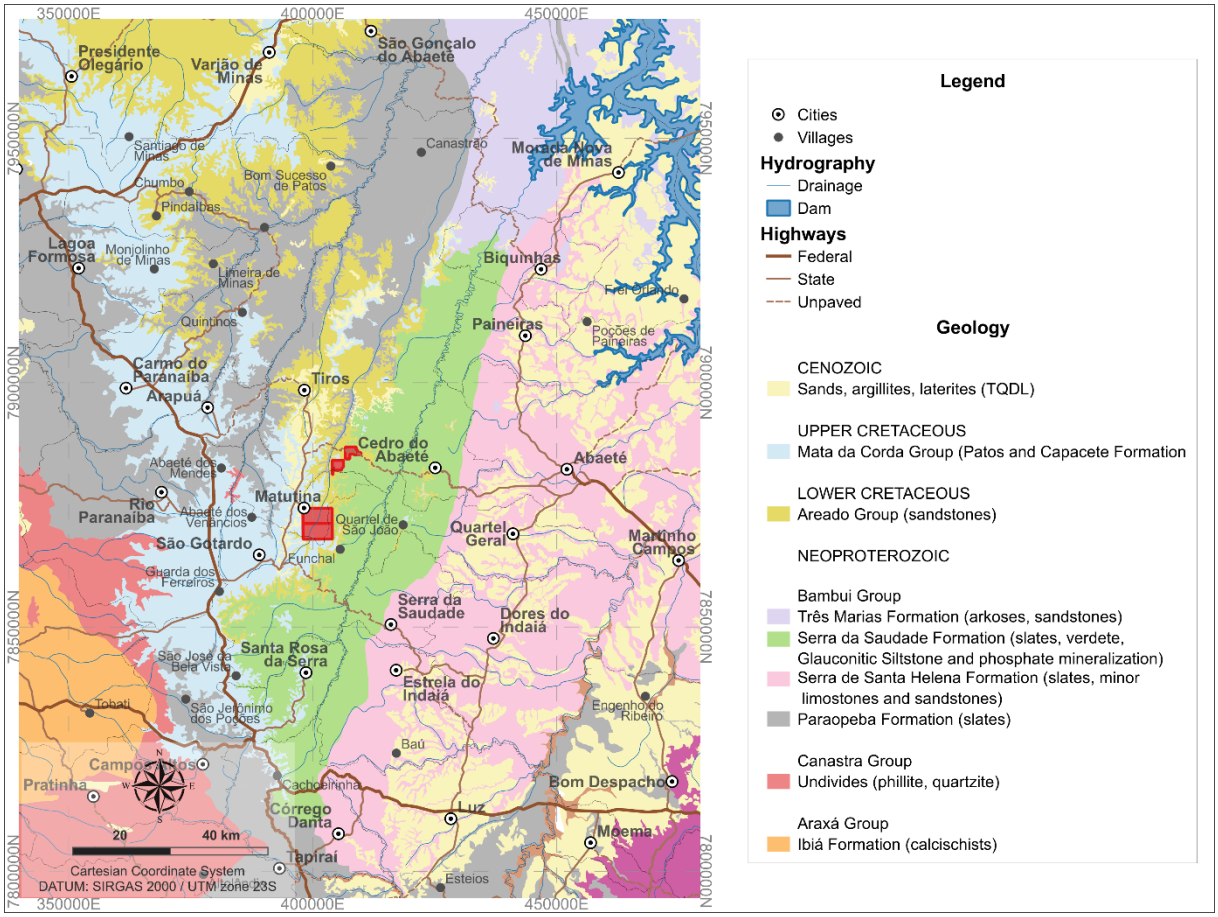



**Figure 1.2 - Regional geological map (Tuller et al., 2002)**

The Canastra Group is topped by the Bambuí Group, which is subdivided into the Paraopeba, Serra de Santa Helena, Serra da Saudade, and Três Marias formations. The Paraopeba and Serra de Santa Helena formations mainly consist of black slates with minor meta-arenites and metacarbonates. The Serra da Saudade Formation features reddish metapelites, metasiltites, and glauconite-rich metasiltites, known as "verdete". The Três Marias Formation consists of arkosic arenites.

Sedimentological, stratigraphic, and structural analyses suggest that the Bambuí Group was deposited in a foreland basin, formed as a result of compressive forces within the Brasília Belt.

Mesozoic rocks of the Areado Group overlie the Bambuí Group unconformably and are characterized by pink to reddish and whitish-yellow sandstones. The Mata da Corda Group is present above, comprising the Patos and Capacete formations. The Patos Formation includes alkaline volcanic rocks, while the Capacete Formation consists of conglomerates, sandstones, and siltstones formed from the weathering of the Patos rocks. The sequence ends with Cenozoic sediments, represented by laterized eluvial-colluvial cover (TQDL).

Rare earth elements (REEs) occur within the rocks of the Capacete Formation, which has a thickness ranging from 20 m to 100 m in the Project area. These sedimentary layers were deposited sub-horizontally over the substrate of the Areado Group.

The rocks of the Capacete Formation originated from the weathering and transport of lithologies from the Patos Formation, which is predominantly of kamafugitic composition. Both formations were deposited laterally. The REEs in the Capacete Formation are primarily sourced from the Patos Formation. During weathering, minerals such as perovskite and gorceixite underwent alteration and released rare earth ions and colloidal sediments that became incorporated into the Capacete sediments.

## 1.5 Exploration and Drilling

The exploration campaign employed diamond drilling to ensure the reliability and precision of the resource estimation process. Sampling was conducted at consistent intervals of 1 meter, with drill cores carefully stored in labeled plastic bags containing unique identification tags. These bags were sealed, double-bagged, and systematically recorded in a digital database to maintain traceability.

The drilling campaign, carried out between April and September of 2011, was executed by Rede Engenharia e Sondagens S/A (a subsidiary of SGS) and Isoágua Perfurações Especiais Ltda, using MACH 1200 and DIAKOR II rigs. Together, these campaigns saw 3,539.3 drilled meters across the Nau de Guerra (742.95 meters), Alto da Serra (1,313.85 meters), and Balsamo (1,582.5 meters) targets. The core recovery was calculated for each interval, and reliable recovery rates that formed the foundation

of the geological interpretation and resource modeling were achieved. The diamond drill cores enabled bulk density measurements to be taken and were carefully preserved for future reference.

During both the historical exploration in 2011 and the ongoing 2024 campaigns, geologists logged core details, including weathering profiles, regolith characteristics, lithology, and petrographic features. Key geotechnical parameters such as Rock Quality Designation (RQD) and degrees of weathering were also recorded. These observations were systematically entered into a centralized digital database, thus ensuring consistency and facilitating seamless integration with subsequent analyses.

## 1.6 Mineral Resource Estimate

The mineral resource estimation for the project was carried out using a systematic and robust methodology that incorporated historical data and results from the 2011–2012 drilling campaigns conducted by the Verde team. Site visits by Volodymyr Myadzel, representing BNA Mining Solutions, were conducted in July and August of 2024 to assess site conditions, verify geological documentation, and provide an general geological overview of the area.

A block model was developed, using Ordinary Kriging (OK) for grade interpolation, in Micromine software. This approach was chosen due to the log-normal distribution of the sample data. To validate and cross-check the results, Inverse Distance Weighting (IDW3) was employed as a secondary estimation method. The estimation process involved a sequential search ellipse methodology across four passes, with adjustments made to the size of the ellipsoid and the number of composite samples and drill holes required for interpolation. The block discretization process included sub-blocking, in which the initial 50x50x10-meter blocks were divided into subunits (5x5x2 meters) near mineralized wireframes. Variography guided the determination of search ellipse parameters and orientations, with the radii and azimuth orientations being customized for each REE.

Validation of the block model included statistical comparisons between interpolated grades and composite datasets. Histograms and probability plots demonstrated consistency and reliability, confirming the robustness of the model.

A cut-off grade of 1,000 ppm TREO was applied, informed by comparable projects and the Qualified Person’s experience. Dry bulk density values were calculated from 452 diamond drill core

samples, analyzed using Archimedes' principle with equipment certified by INMETRO. All estimates are reported on a dry tonnage basis.

All mineral resources have been classified as Inferred, reflecting the current state of geological continuity, drill hole spacing, variography, and density data. This classification aligns with industry standards and the Qualified Person's assessment of data reliability.

## 1.7 Resource Estimate Summary

The following table summarizes the in-situ mineral resource estimates at a cut-off grade of 1,000 ppm TREO for each target and the combined total:

**Table 1.1 - Resource Estimate Summary***

| Target | Tons | TREO[1] | MREO[2] | $Pr_6O_{11}$ | $Nd_2O_3$ | $Tb_4O_7$ | $Dy_2O_3$ |
| --- | --- | --- | --- | --- | --- | --- | --- |
| | | *ppm* | *ppm* | *ppm* | *ppm* | *ppm* | *ppm* |
| Nau de Guerra | 120,093,635 | 3,628 | 846 | 183 | 634 | 5 | 24 |
| Alto da Serra | 230,213,682 | 3,684 | 875 | 188 | 656 | 6 | 26 |
| Balsamo | 1,145,624,209 | 3,358 | 769 | 168 | 575 | 5 | 21 |
| **TOTAL** | **1,495,931,526** | **3,430** | **791** | **172** | **592** | **5** | **22** |

**Values are rounded*

The resource estimates were prepared in compliance with the NI 43-101 standards, under the supervision of Dr. Volodymyr Myadzel, PhD, MAIG, who is acting as the Qualified Person (QP) for this report. The mineral resources at the Man of War Project have been classified as Inferred due to the limitations of the hole spacing.

## 1.8 Reasonable Prospects for Eventual Economic Extraction

A preliminary economic analysis of the targets was performed to define the economically mineable resource. The results at a cut-off grade of 1,000 ppm TREO for each target and the combined total are presented in Table 1.2.

**Table 1.2- Reasonable Prospects for Eventual Economic Extraction Summary**

| Tonnes | In Situ Grades (PPM)* | | | | | |
| --- | --- | --- | --- | --- | --- | --- |
| RPEE RESOURCE | TREO | MREO | Pr6O11 | Nd2O3 | Tb4O7 | Dy2O3 |
| **1,349,820,872** | **3,437** | **793** | **173** | **594** | **5** | **22** |

**Values are rounded*

[1] Total Rare Earth Oxides (TREO) refers to the sum of the oxides of rare earth elements, which include: Lanthanum Oxide ($La_2O_3$), Cerium Oxide ($CeO_2$), Praseodymium Oxide ($Pr_6O_{11}$), Neodymium Oxide ($Nd_2O_3$), Samarium Oxide ($Sm_2O_3$), Europium Oxide ($Eu_2O_3$), Gadolinium Oxide ($Gd_2O_3$), Terbium Oxide ($Tb_4O_7$), Dysprosium Oxide ($Dy_2O_3$), Holmium Oxide ($Ho_2O_3$), Erbium Oxide ($Er_2O_3$), Thulium Oxide ($Tm_2O_3$), Ytterbium Oxide ($Yb_2O_3$), Lutetium Oxide ($Lu_2O_3$), and Yttrium Oxide ($Y_2O_3$).

[2] Magnetic Rare Earth Oxides (MREO) refers to the sum of the oxides of rare earth elements with magnetic properties, which include: Praseodymium Oxide ($Pr_6O_{11}$), Neodymium Oxide ($Nd_2O_3$), Terbium Oxide ($Tb_4O_7$), and Dysprosium Oxide ($Dy_2O_3$).

## 1.9 Conclusions and Recommendations

BNA conducted the evaluation of the mineral resources of the Man of War Project - Rare Earth, belonging to Verde, in compliance with the NI 43-101. The effective work took place from July, 2024 to December, 2024.

The main activities undertaken by BNA were:

- Verification of the status of the mining rights belonging to the project;
- A site visit, discussions with the technical staff from Verde, gaining an understanding of the geology and mineralization of the deposit, and verification of the geological work performed by Verde and contractors on site, as well as verification of the materiality of the results achieved;
- Validation of the drilling database and the topographical information;
- Verification of the QA/QC program established by Verde for geological work and of its conduction, especially during the drilling work;
- Verification of the Verde Agritech – Declaração SGSGeosol.pdf document demonstrating the recovery of rare earth elements for the ionic clay mineralization of the Man of War project;
- Selection of the drilling data used in the definition of mineral resources;
- Interpretation of the geological model;
- Conduction of statistical and geostatistical studies;
- Estimation of mineral resources, as well as their quantification and classification;
- Disclosure of the mineral resources from the Man of War Project in accordance with the Canadian Institute of Mining, Metallurgy and Petroleum Standards on Mineral Resources and Reserves: Definitions and Guidelines, May 19, 2014 (https://mrmr.cim.org/media/1128/cim-definition-standards_2014.pdf).

The materiality of the work undertaken by Verde, as well as the materiality of the deposit and the studies conducted, are sufficient to support the declaration of mineral resources of the Man of War Project. This project includes the Nau de Guerra, Balsamo and Alto da Serra targets.

Furthermore, the work conducted revealed notable concentrations of Nb, Sc, Hf, Ga, Rb, V and Co, highlighting the need for studies on these elements, a further description is provided in **item 25.2**.

**Recommendations:**

- Perform cross-validation between the geological description and the chemical analysis results;
- Perform interlaboratory verification of the analysis results;
- Designate a professional or team to be responsible for the database feed and handling;
- Densify and regularize the exploratory drill grid;
- Standardize lithological codes in the geological descriptions;
- Conduct a detailed topographic survey of the site;
- Perform detailed geological mapping of the Capacete Formation;
- Perform additional metallurgical test work for rare earth elements as a critical component in advancing the project;
- Perform metallurgical test work for additional elements (Nb, Sc, Hf, Ga, Rb, V and Co), to verify their potential for economic exploitation.

## 1.10 Recommendations for Future Investments in the Man of War Project

The Man of War rare earths project has demonstrated significant potential for further development through strategic investments in exploration and resource evaluation. The current data suggests that the deposit contains a substantial rare earth element resource with promising economic prospects.

It is recommended to advance the project towards the Preliminary Economic Assessment (PEA) stage by implementing a comprehensive work program. This program should focus on infill drilling, exploration of new targets, resource estimation updates, and economic viability studies.

To enhance the confidence level in the existing resource, an infill drilling campaign is recommended. This will aid in converting Inferred Mineral Resources into Indicated or Measured categories, thereby improving the reliability of future feasibility studies. In addition, drilling new targets, specifically the Fragata and Caravela targets, will provide valuable insights into the lateral and depth extensions of the mineralization, ensuring a more comprehensive understanding of the deposit's potential.

An updated NI 43-101 resource estimate is necessary to incorporate new geological data and ensure that the project aligns with industry standards. This updated estimate will serve as a foundation for further economic evaluations and decision-making processes. Additionally, it is crucial to initiate a

PEA to assess the project's economic feasibility, including mining methods, processing options, environmental considerations, and market analysis. The PEA will provide essential inputs to guide future investments and strategic planning.

Metallurgical test work is also a critical component in advancing the project. Future studies with specialized companies will focus on advanced leaching processes, impurity treatment methodologies, and recovery optimization. These efforts are expected to significantly enhance recovery rates and contribute to the overall economic potential of the project. Additionally, other elements identified in the deposit will require preliminary metallurgical studies to better understand their processing requirements and economic viability.

Overall, the recommended investment plan aims to position the Man of War project for future development and value realization. By conducting targeted exploration, resource assessment, and economic evaluation, the project will move closer to achieving its objectives and attracting potential investors. It is advised to secure adequate funding and resources to successfully implement the proposed work plan and advance the project to the next stage of development.

The estimated budget for this work program is shown in Table 1.3.

**Table 1.3 - Estimated Investment Breakdown**

| Description | Value (CAD) | Value (BRL) |
|---|---|---|
| Infill Drilling | $4,004,854 | R$ 16,500,000 |
| Drilling New Targets | $485,437 | R$ 2,000,000 |
| NI 43-101 Resource Update | $145,631 | R$ 600,000 |
| Preliminary Economic Assessment (PEA) | $533,981 | R$ 2,200,000 |
| Metallurgical Flowsheet Design | $121,359 | R$ 500,000 |
| Initial Environmental Studies (EIS/PCA) | $266,990 | R$ 1,100,000 |
| **Total Investment** | **$5,558,252** | **R$ 22,900,000** |

# 2 Introduction

## 2.1 Terms of Reference and Purpose of the Report

Verde Agritech Ltd ("VERDE" or the "Company") commissioned BNA Mining Solutions (BNA) to prepare a Technical Report compliant with Canadian National Instrument 43-101 (NI 43-101) for the Man of War Project (or the Project) located in Brazil. The Man of War Project encompasses three primary targets spread across four mining tenements:

- **Nau de Guerra Target**:
  - Tenement No. 832543/2016 – Area: 475.19 hectares
- **Alto da Serra Target:**
  - Tenement No. 832544/2016 – Area: 452.34 hectares
- **Balsamo Target:**
  - Tenement No. 830794/2010 – Area: 1,857.56 hectares
  - Tenement No. 830796/2010 – Area: 1,923.58 hectares

The contract allows VERDE to file this report as a Technical Report with the Canadian Securities regulatory authorities pursuant to NI 43-101, Standards of Disclosure for Mineral Projects. Except for the purposes legislated under provincial securities law, any other uses of this report by any third party is done so at that party's sole risk. The responsibility for any disclosure remains with VERDE. The user of this document should ensure that this is the most recent Technical Report for the property, as it is not to be considered valid if a new Technical Report has been issued.

This report provides mineral resource estimates and a classification of resources in accordance with the Canadian Institute of Mining, Metallurgy and Petroleum Standards on Mineral Resources and Reserves: Definitions and Guidelines, May 10, 2014 (CIM).

Verde AgriTech Ltd Group is listed on the Canadian Stock Exchange since 2007 and on the OTCQB Venture Market in the United States ("U.S.") since 2017. Verde AgriTech is dedicated to advancing sustainable agriculture through the innovation of specialty multi-nutrient potassium fertilizers. The company's mission is to increase agricultural productivity, enhance soil health, and significantly contribute to environmental sustainability. Utilizing a unique position in Brazil, proprietary technologies are harnessed to develop solutions that not only meet the immediate needs of farmers but also address global challenges such as food security and climate change. A strong commitment to

carbon capture and the production of eco-friendly fertilizers underscores a vision for a future where agriculture contributes positively to the health of the planet.

For more information on the efforts toward sustainable agriculture and climate change mitigation in Brazil, visit the website at https://verde.ag/en/home/.

## 2.2 Qualifications of Consultants

The Consultants preparing this technical report are specialists in the fields of geology, exploration and mineral resource estimation and classification. The information in this announcement that relates to exploration results is based on the information reviewed and the use of recommended data collection methodologies. This work was overseen by QP Beck Nader and QP Volodymyr Myadzel.

Dr. Beck Nader, who is a DSc. in Mineral Engineering and a Fellow of the Australian Institute of Geoscientists (MAIG), brings over 43 years of experience in mineral resource and reserve estimation of deposits, including economical evaluation of mineral projects, risk assessment and multidisciplinary coordination and integration. Dr. Beck Nader is Qualified Person (QP) under Canada's NI 43-101 standards. He will serve as the Qualified Person acting as the Peer Reviewer of this current report.

Dr. Myadzel, who is a PhD in Geology and a Member of the Australian Institute of Geoscientists (MAIG), brings over 25 years of experience in mineral exploration, resource modeling, and the estimation of mineral deposits. His expertise spans the origin of mineralization and ore precipitation mechanisms across various geological environments. Dr. Myadzel has extensive experience in fieldwork, exploration, and the mineralogy, and petrography of metamorphic rocks and mineral deposits. He is also skilled in the preparation of core samples for analysis, sedimentology of alluvial and talus sediments, and the investigation of primary and secondary lithogeochemical dispersion patterns. His laboratory capabilities include transmitted-light microscopy and ore microscopy for petrography and ore mineralogy. Dr. Myadzel is a recognized Qualified Person (QP) under Canada's NI 43-101 standards. He will serve as the Qualified Person for Mineral Resource estimation.

Other consultants who contributed to this report:

- Kelly Pereira, Systems Engineer at BNA.
- Jean Lacerda, Mining Engineer at BNA.

None of the Consultants or any associates employed in the preparation of this report have any beneficial interest in VERDE. The Consultants are not insiders, associates, or affiliates of VERDE. The results of this Technical Report are not dependent upon any prior agreements concerning the conclusions to be reached, nor are there any undisclosed understandings concerning any future business dealings between VERDE and the Consultants. The Consultants are being paid a fee for their work in accordance with normal professional consulting practice.

## 2.3 Details of Inspection

A site visit was carried out by Volodymyr Myadzel on behalf of BNA Mining Solutions on July 1-2 and August 13, 2024. The visit was attended by Verde officials: Thiago Siqueira (Geology & Projects/Project Manager) and Guido Pessoa (Environmental Manager).

## 2.4 Sources of Information

The information used to support this Technical Report was derived from previous technical reports on the property and the reports and documents listed in the References section of this Technical Report. BNA has used, primarily, information provided by Verde Agritech or its consultants to prepare this study.

## 2.5 Effective Date

The effective date of this report is December 18, 2024.

There were no material changes to the information on the Project between the effective date and the signature date of the Technical Report.

## 2.6 Units of Measure

The Metric System for weights and units has been used throughout this report, unless noted otherwise. All currency is in U.S. dollars (US$) unless otherwise stated, and all geographical coordinates are in UTM, SIRGAS 2000, zone 23S.

# 3 Reliance on Other Experts

The Consultants' opinion contained herein is based on information provided by Verde Agritech throughout the course of the investigations conducted. The sources of information include data and reports supplied by Verde Agritech personnel, and documents. The Consultants have relied upon the work of other consultants in the Project areas to prepare this Technical Report.

VERDE has warranted, to the authors, that the information provided for the preparation of this report correctly represents all material information relevant to the Man of War Project. VERDE has taken reasonable measures to ensure that permits covering its properties are in good standing.

The Consultants used their experience to determine whether the information from previous reports was suitable for inclusion in this Technical Report and adjusted information that required amendment. The QP Volodymyr Myadzel has examined the data for the Project provided by VERDE and has relied upon that basic data to support the statements and opinions presented in this Technical Report. In the opinion of the QP, the data is of sufficient detail, is credible and verifiable in the field, and is an accurate representation of the Project.

This report includes technical information that requires subsequent calculations to derive sub-totals, totals, and weighted averages. Such calculations inherently involve a degree of rounding and consequently can introduce a margin of error. Where these rounding errors occur, they are not considered to be material.

The authors have relied upon the work of others to describe the geology and exploration.

# 4 Property Description and Location

## 4.1 Project Location

The Man of War Project is located in the Midwest region of Minas Gerais, specifically within the municipalities of São Gotardo and Matutina, located in the Alto Paranaíba mesoregion. The project area is approximately 329 km from Belo Horizonte, the capital of Minas Gerais. Geographically, it is centered around the coordinates -19°5’ latitude and -46° longitude, (Figure 4.1).




**Figure 4.1 - Location Map of the Man of War Project**

## 4.2 Permit Status

The Man of War Project encompasses three primary targets spread across four mining tenements:

- **Nau de Guerra Target**:
  - Tenement No. 832543/2016 – Area: 475.19 hectares
- **Alto da Serra Target:**

- Tenement No. 832544/2016 – Area: 452.34 hectares

- **Balsamo Target:**
  - Tenement No. 830794/2010 – Area: 1,857.56 hectares
  - Tenement No. 830796/2010 – Area: 1,923.58 hectares

In total, these tenements cover a combined area of 4,708.67 hectares. All tenements within the Man of War Project are currently in the "Application for Mining Concession" stage, meaning that the request for a mining license has already been submitted. The Figure 4.2 shows the layout of the project tenements.

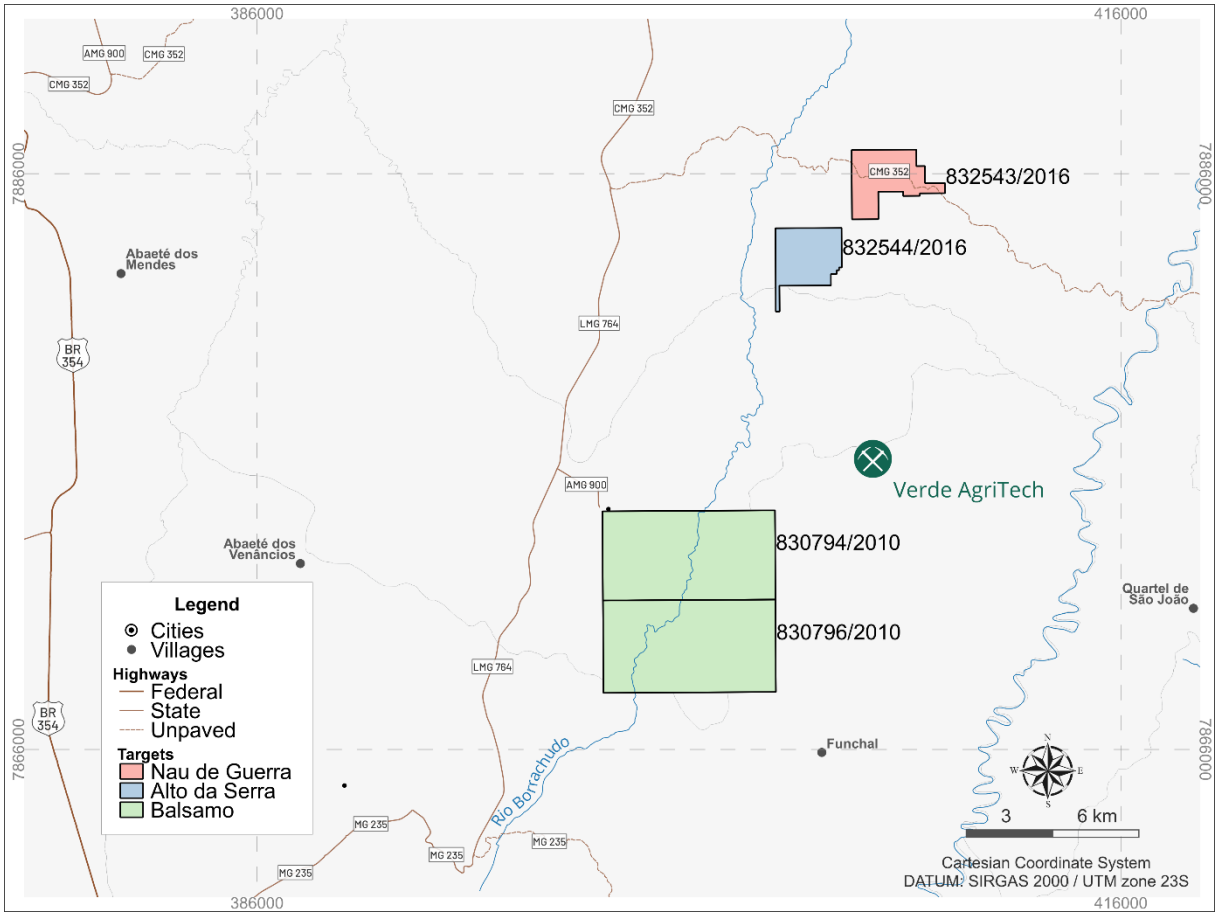



**Figure 4.2 - Man of War Project Targets and tenements**

The National Mining Agency (Agência Nacional de Mineração – ANM), established by Federal Law No. 13,575/2017 as the successor to the National Department of Mineral Production (DNPM), is responsible for overseeing mineral exploration, promoting resource development, and ensuring regulatory compliance across Brazil. This includes geological research, mineral technology oversight,

and mining activity inspection in alignment with the Mining Code, Mineral Water Code, and related regulations.

The key stages in the mining concession application process are as follows:

1. Application for Exploration Permit (*Alvará de Pesquisa*)
2. Filing of the Final Exploration Report
3. Application for the Mining Concession
4. Granting of the Mining Concession

The Exploration Permit allows the holder—whether an individual or legal entity—to conduct mineral research within the designated area and typically grants exploration rights for two to four years, with possible extensions.

Upon completion of exploration activities, the titleholder must submit a Final Exploration Report (*Relatório Final de Pesquisa*) detailing the geological, quantitative, and technological assessment of the mineral deposit and demonstrating its technical and economic viability. The ANM then conducts a site visit to evaluate the report.

If the report is approved, the titleholder has one year to complete a Feasibility Study (*Plano de Aproveitamento Econômico – PAE*) and file the Mining Concession Application with the Ministry of Mines and Energy (*Ministério de Minas e Energia – MME*). This federal body is tasked with managing geological, mineral, and energy resource policies, as well as overseeing the hydroelectric, mining, and metallurgical sectors.

During the ANM's review of the Mining Concession Application (*Requerimento de Lavra*), the applicant retains exclusive rights to the tenement area. Development and construction of the mine can only commence once the MME has issued a Mining Concession (*Portaria de Concessão de Lavra*), in compliance with applicable environmental licensing requirements under Brazilian law. The Mining Concession grants the owner the right to exploit the deposit until it is exhausted, without a predetermined expiration date.

In Brazil, a mining site is granted full leave to operate once the owner has both a Mining Concession/Permit and an Environmental License for the area.

## 4.3 Surface Rights

According to Brazilian law, surface rights are separate from mining rights. Therefore, a landowner has no title to the minerals contained in the soil or in the sub-soil, which are deemed the property of the federal government. The federal government can grant private companies or individuals the right to explore for and mine sub-surface minerals.

Private companies or individuals that are holders of an Exploration Permit are supposed to enter into agreements with landowners to gain access to areas and conduct exploration activities. If such agreements are not reached, the Brazilian Mining Code establishes a judicial procedure by means of which mining companies or individuals may secure access to these areas by paying landowners compensation for any damages to their property and/or loss of income due to the exploration activities undertaken.

Private companies or individuals holding a Mining Permit are entitled to access the area necessary for the mine infrastructure. Such surface rights are obtained through agreements with landowners, which provide compensation that covers the price of the land and any additional losses caused by the occupation of said land. In the event such an agreement is not reached, surface rights may be granted by the local Court once payments have been made by the mining company or individual in the amount determined by a court for such compensation.

The Company has agreements with landowners for mineral exploration and environmental studies but has not yet reached agreements for mineral exploitation. These are still being negotiated.

## 4.4 Taxes and Royalties

In Brazil, the ANM monitors exploration, mining and mineral processing. This regulatory agency also administers mineral exploration permits and mining concessions. Mineral exploration permits are issued by the ANM, and mining concessions are issued by the Ministry of Mines and Energy.

A mining concession carries an obligation to pay royalties to the federal government, known as Financial Compensation for the Exploitation of Mineral Resources (“CFEM”), the rate for which is set at 2% of the gross sale price of the mineral product, less taxes levied on its sale.

In addition to compensation for damages, landowners are entitled by law to a royalty equal to 50% of the CFEM. However, there may be an agreement between a mining company and a landowner that establishes a level of compensation that is satisfactory to both (MENDO, 2009).

## 4.5 Environmental Liabilities and Permitting

The authors are unaware of any environmental liabilities to which the Man of War Project is subject.

Environmental regulations and general environmental rules and obligations in Brazil are relatively similar to those applicable in Canada and Australia. Brazilian environmental policy is the responsibility of the Ministry of the Environment and is executed at three levels: federal, state, and municipal.

As the tenement was being developed with regard to other mineral substances, activities related to the application for environmental licenses were ongoing. Currently the Company is engaging its consultants to prepare Environmental Impact Assessment (Estudo de Impacto Ambiental – EIA) and undertaking a three-phase licensing process. This means that the Company expects to obtain the Preliminary License (*Licença Prévia - LP*), Installation License (*Licença de Instalação - LI*) and Operating License (*Licença de Operação - LO*) separately.

## 4.6 Other Significant Factors and Risks

There are no other significant factors or risks known at this time that may affect access, title, or the right or ability to perform work on the Project.

# 5 Accessibility, Climate, Local Resources, Infrastructure and Physiography

## 5.1 Accessibility

The project areas are approximately 20 km from the city of São Gotardo, accessible by unpaved local roads that connect the farms in the region. Reaching São Gotardo from Belo Horizonte involves a 20 km trip to reach the BR-262 highway, which leads to the Triângulo Mineiro region, followed by 230 km along this highway to the intersection with the BR-354 highway heading towards Patos de Minas, followed by another 140 km to São Gotardo.

São Gotardo is 101 km from Patos de Minas and 250 km from Uberaba. Via the Ferrovia Centro Atlântica railway, which has a station in Campos Altos, the area is 413 km from Belo Horizonte, 765 km from Rio de Janeiro, 836 km from São Paulo, 760 km from Brasília, and 1,119 km from the port of Vitória.

Key municipalities for this project include Matutina and São Gotardo. Detailed information about these municipalities, including physiographic aspects, infrastructure, services, and road and rail distances to major consumer centers, is presented below.

**Table 5.1 - Distance from São Gotardo to Major Urban Centers by Road**

| Urban Centers | São Gotardo (km) |
| --- | --- |
| Belo Horizonte | 312 |
| Brasília | 546 |
| Rio de Janeiro | 723 |
| São Paulo | 646 |
| Vitória | 825 |




**Figure 5.1 - Accessibility map**

## 5.2 Climate

The typical climate is high-altitude tropical, with two different seasons: rainy and dry. The dry season, with a total rainfall volume of 200 mm, runs from April to September. The annual rainy season, with a total rainfall volume of 1,115 mm, runs from October to March, when 85% of the precipitation in the area falls. The average annual relative humidity is 50%. Winds are predominantly from the NNE in the dry season and from the SSE in the rainy season. The total annual rainfall volume is 1,315 mm. This figure was obtained from the A536 monitoring station, located in Dores do Indaiá, during a time frame beginning in May, 2007, when the station started operating, and ending in June, 2021 (Figure 5.2). The station is located approximately 45 km in a straight line from the project location and is the closest one operated by the National Institute of Meteorology (INMET).

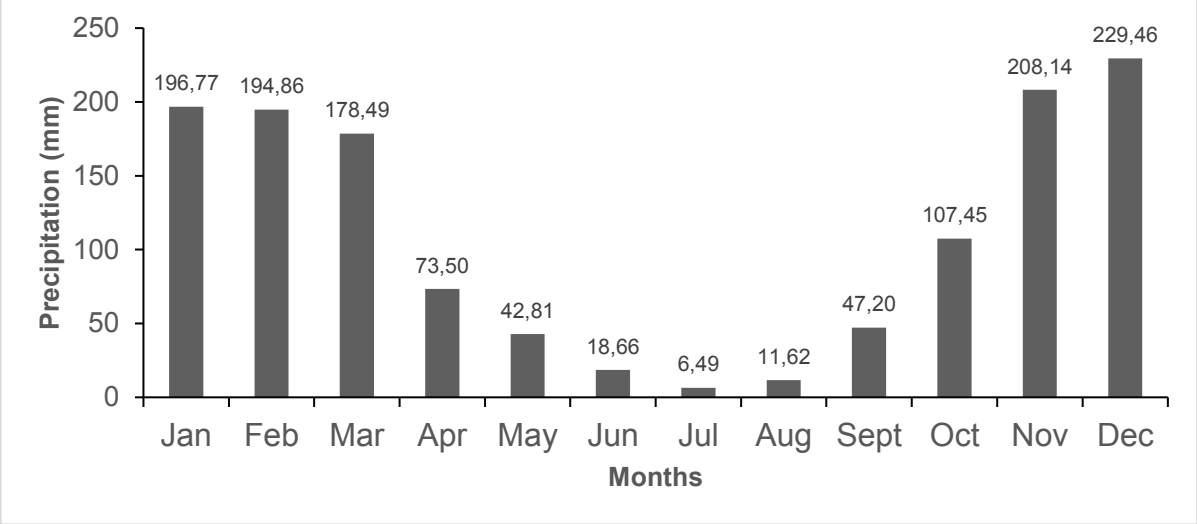



**Figure 5.2 - Rainfall data from the A536 monitoring station (INMET, 2021)**

According to INMET data, the average annual temperature is between 19.5°C and 24.2°C and the annual potential evapotranspiration (PET) is around 1,187 m (calculated for the Patos de Minas region). The annual evapotranspiration (ETR) is on the order of 13 mm, which, according to the Turc formula, is based on the figures for annual mean and total temperature.

Exploration and mining operations can be conducted year-round.

## 5.3 Local Resources and Infrastructure

The project is located in the municipalities of Matutina and São Gotardo, which offer essential infrastructure and resources for potential mining operations.

São Gotardo has a population of approximately 36,084 and serves as a regional hub. The municipality features electricity service, telephone services, and a strong agricultural and livestock economy. It is accessible via the BR-262, BR-354, and MG-235 highways, ensuring good connectivity for logistical needs.

Matutina, with a smaller population of 3,733, is known for its agriculture and its natural source of mineral water, commercially marketed as Matutina Mineral Water since 2007. Located at an altitude of approximately 1,000 meters, the municipality benefits from a favorable climate for farming.

The project area is also well-positioned relative to key infrastructure. Patos de Minas, 129 km away, is the primary urban center in the Alto Paranaíba region and offers economic, cultural, and educational resources. The Ibiá railway station, 83 km from the site, connects to the Centro Atlântica railroad.

For more extensive services, Belo Horizonte, the capital of Minas Gerais, is located 320 km from the site. The city is a mining industry hub, with a population of over 2.5 million and a wealth of skilled labor, government agencies, and private businesses supporting mining operations. It also has a large commercial airport with domestic and international connections.

These municipalities and infrastructure resources provide vital support for the logistical and operational needs of the project.

## 5.4 Physiography

The region is part of the Indaiá river basin, with the Indaiá river forming a left-bank tributary of the São Francisco River downstream. The main rivers are the Indaiá and Borrachudo, along with a major tributary, the Pirapitinga das Perobas stream. The area is intersected by the Indaiazinho stream, Fragata stream, Bastos stream, Pirapitinga stream, Barreiro stream, Do Meio stream, and Sítio stream, among others. These streams generally exhibit a dendritic pattern, characterized by irregular branching of watercourses in all directions, with tributaries forming at varied angles to the main course, predominantly over the pelitic substrate.

# 6 History

This section provides a comprehensive overview of the project history, from its inception to the present, highlighting the key milestones, ownership transitions, and strategic decisions that have driven its development. Originally focused on phosphate rock, the direction of the project has evolved significantly following the discovery of REEs in the area. This shift reflects a strategic pivot from phosphate extraction toward rare earth exploitation.

As a brief contextual background, the Man of War project is divided into three targets: Nau de Guerra (tenement No. 832.543/2016), Alto da Serra (No. 832.544/2016), and Balsamo (tenements No. 830794/2010 and 830796/2010). Historically, the Nau de Guerra and Alto da Serra targets have shared a closely aligned development path, while the Balsamo target has followed a somewhat distinct trajectory.

## 6.1 Initial Exploration and Early Discoveries

The origins of this project date back to the late 2000s under the management of FVS Mineração Ltda and Verde Fertilizantes Ltda, subsidiaries of Verde AgriTech. FVS Mineração was granted exploration permits (Alvarás) Nos. 14084 and 11928 for tenements 833.324/2008 and 833.326/2008, respectively. Verde Fertilizantes was granted exploration permits Nos. 8461 and 8462 for tenements 830.794/2010 and 830.796/2010, respectively.

These permits covered substantial areas across the municipalities of São Gotardo and Matutina in the state of Minas Gerais, Brazil. Initial exploration activities primarily focused on assessing the potential for phosphate and potash rock deposits.

Following extensive geological surveys and resource evaluations, the Final Exploration Reports for phosphate and potash deposits in the tenements were completed between the second half of 2012 and the first half of 2013. In 2016, the ANM approved the Final Exploration Reports for tenements 833.324/2008 and 833.326/2008, followed shortly by approval for tenements 830.794/2010 and 830.796/2010.

Tenements 833.324/2008 and 833.326/2008 were originally part of the Cerrado Verde Project, which was focused on potash for fertilizer production. Therefore, Verde decided to separate the potash and phosphate deposits within these areas. On November 18, 2016, a request was submitted to the ANM to partially transfer the phosphate rock deposits from FVS Mineração to Verde

Fertilizantes. This process resulted in the creation of new tenements, 832.543/2016 and 832.544/2016, covering areas of 475.19 hectares and 452.34 hectares, respectively.

On July 14, 2017, a mining application was filed for tenements 832.543/2016 and 832.544/2016, A single Feasibility Study (*Plano de Aproveitamento Econômico Integrado* - PAE) was filed for both tenements. On July 9, 2019, ANM – Agência Nacional de Mineração issued a dispatch approving the partial transfer. This transfer was officially recorded in the Book of Annotations as No. 224, on page 157, marking a significant milestone in the development of the project.

With the transfer completed, the mining application was evaluated and approved on September 13, 2019, on the condition that Verde Fertilizantes obtain, at a minimum, an environmental license for installation or and equivalent license/permit.

## 6.2 Phosphate Resources Approved by ANM

This subsection aims to present the phosphate and potash resources approved by the Brazilian National Mining Agency (ANM). These resources were estimated based on the legislation currently in force in Brazil, following the scope of the RFP protocol, and have been approved by the ANM, as detailed in a previous section of this report.

The tables below present the approved phosphate rock resource classification for each target, including their corresponding grades for key elements such as $P_2O_5$, $K_2O$, CaO, and others.

**Table 6.1 - Resources approved by the ANM for the Nau de Guerra target**

| Classification | Resource (t) | $P_2O_5$ (%) | $K_2O$ (%) | CaO (%) | $Al_2O_3$ (%) | $Fe_2O_3$ (%) | $SiO_2$ (%) | MgO (%) | $TiO_2$ (%) | MnO (%) |
|---|---|---|---|---|---|---|---|---|---|---|
| **Measured** | 12,775,905 | 3.03 | 4.88 | 4.04 | 6.77 | 21.61 | 39.41 | 4.21 | 11.25 | 0.29 |
| **Indicated** | 2,955,378 | 3.05 | 4.2 | 3.87 | 6.86 | 22.89 | 37.03 | 3.91 | 12.65 | 0.33 |
| **Total** | **15,731,284** | **3.03** | **4.79** | **4.01** | **6.79** | **21** | **38.96** | **4.16** | **11.51** | **0.29** |

**Table 6.2 - Resources approved by the ANM for the Alto da Serra target**

| Classification | Resource (t) | $P_2O_5$ (%) | $K_2O$ (%) | CaO (%) | $Al_2O_3$ (%) | $Fe_2O_3$ (%) | $SiO_2$ (%) | MgO (%) | $TiO_2$ (%) | MnO (%) |
|---|---|---|---|---|---|---|---|---|---|---|
| **Measured** | 13,172,445 | 3.12 | 5.17 | 4.66 | 6.92 | 19.8 | 42.05 | 4.18 | 10.13 | 0.29 |
| **Indicated** | 8,698,460 | 3.1 | 5.14 | 4.78 | 6.96 | 19.7 | 42.23 | 4.2 | 10.09 | 0.33 |
| **Inferred** | 2,092,568 | 3.29 | 5.05 | 5.16 | 6.84 | 19.59 | 42.25 | 4.14 | 10.01 | 0.38 |
| **Total** | **23,963,473** | **3.13** | **5.15** | **4.75** | **6.92** | **19.75** | **42.13** | **4.19** | **10.11** | **0.31** |

**Table 6.3 - Resources approved by the ANM for the Balsamo target**

| Tenement | Classification | Resource (t) | $P_2O_5$ (%) |
|---|---|---|---|
| **830.794/2010** | Measured | 6,917,108 | 3.29 |
| | Indicated | 6,780,971 | 3.33 |
| | **Subtotal** | **13,698,079** | **3.31** |
| **830.796/2010** | Measured | 6,931,413 | 2.85 |
| | Indicated | 9,656,585 | 2.75 |
| | **Subtotal** | **16,587,998** | **2.79** |
| **Total** | | **30,286,077** | **3.03** |

The Nau de Guerra target has a total resource of 15.7 million tonnes, with a $P_2O_5$ grade of 3.03%. The resource also contains 4.79% $K_2O$ and 4.01% CaO. The Alto da Serra target contains 24 million tonnes of resource, with a $P_2O_5$ grade of 3.13%. It also has 5.15% $K_2O$ and significant levels of $SiO_2$ (42.13%) and CaO (4.75%). The Balsamo target has a total resource of 30.3 million tonnes, with a $P_2O_5$ grade of 3.03%.

BNA did not conduct the mineral resource estimate for the Man of War deposit filed with and approved by the ANM. Additionally, these mineral resources were not prepared in accordance with the CIM (CIM 2014) guidelines, which are part of the NI 43-101 standards.

# 7 Geological Setting and Mineralization

## 7.1 Regional Geology

The study area is located in the southwestern portion of the São Francisco Craton. The regional geological framework is shown in Figure 7.1. The oldest stratigraphic unit in this region is the Neoproterozoic Araxá Group, which is comprised of calciferous schists and diamictites of the Ibiá Formation. Overlying the Araxá Group is the undivided Canastra Group, which consists of phyllites, quartzites, and sericite schists.

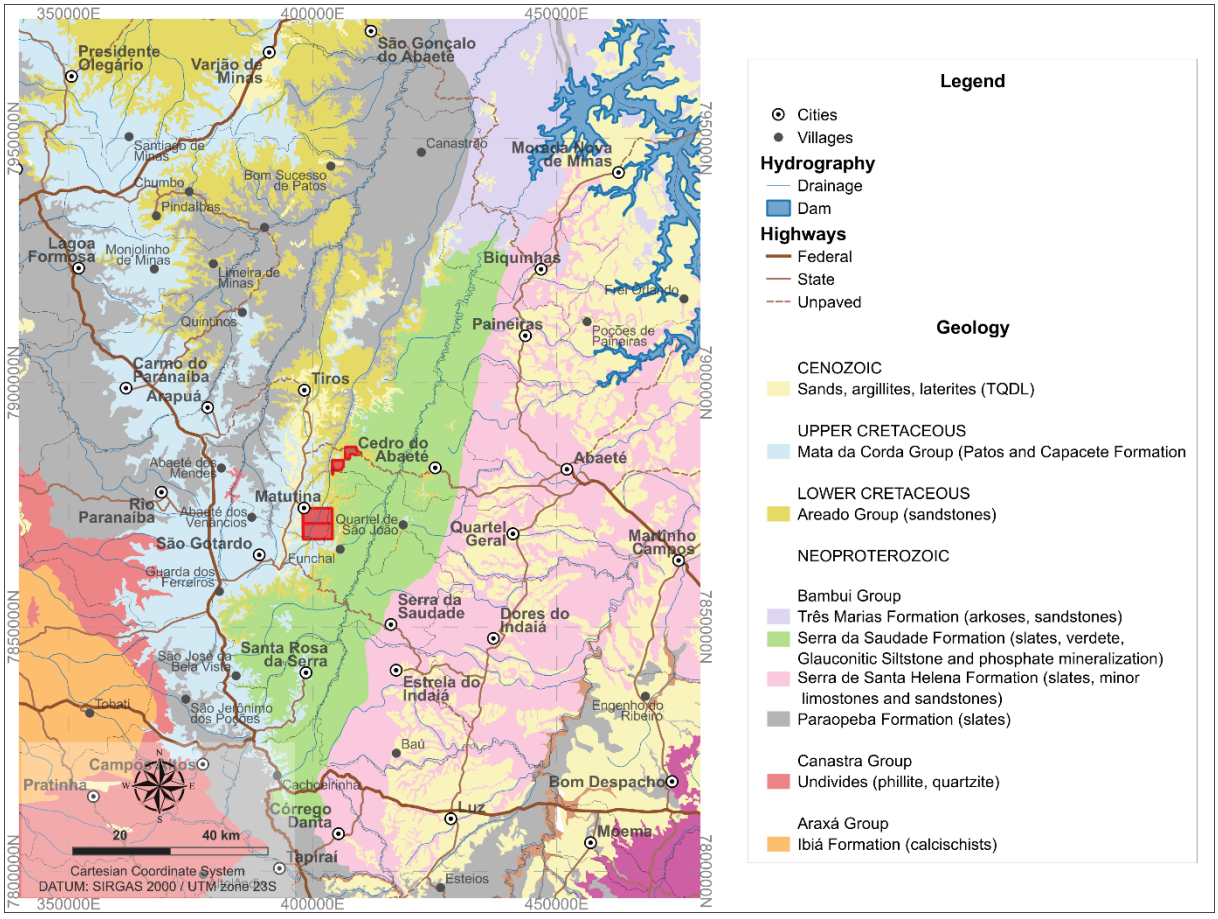



**Figure 7.1 - Regional geological map (Tuller et al., 2002)**

The Canastra Group is overlain by the Bambuí Group, the stratigraphic column of which, located in the Serra da Saudade region and surrounding areas, is shown in Figure 7.2. The Bambuí Group is subdivided, from base to top, into the Paraopeba, Serra de Santa Helena, Serra da Saudade, and Três Marias formations. The Paraopeba and Serra de Santa Helena formations are dominated by homogeneous black slates with minor intercalations of meta-arenites and metacarbonates. The Serra da Saudade Formation comprises massive reddish metapelites and metasiltites, interbedded with

glauconite-rich greenish metasiltites. At the top of the sequence lies the Três Marias Formation, primarily composed of arkosic arenites.

Stratigraphic, sedimentological, and structural analyses of the Bambuí Group in this region suggest that deposition occurred in a foreland basin, formed in response to compressive regimes within the Brasília Belt.

Mesozoic rocks of the Areado Group unconformably overlie the Bambuí Group. The Areado Group is characterized by pink to reddish and whitish-yellow sandstones, which are occasionally silicified. Above this, the Mata da Corda Group is divided into the Patos and Capacete formations, which occur laterally. The Patos Formation features alkaline volcanic rocks of kamafugitic composition, alkaline plutonics, and epiclastic sediments, while the Capacete Formation consists of conglomerates, sandstones, and siltstones derived from the weathering and transport of Patos Formation rocks.

The stratigraphic sequence concludes with Cenozoic sediments (TQDL), represented by an undifferentiated laterized eluvial-colluvial cover.

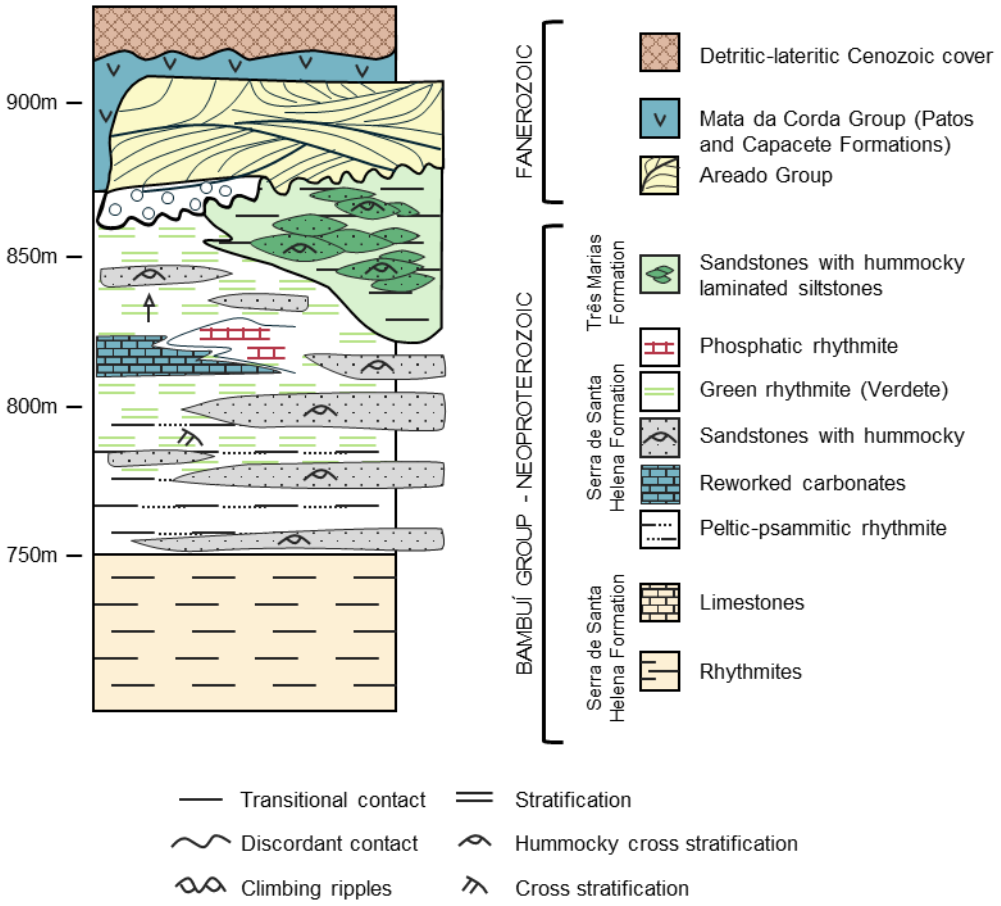



**Figure 7.2 - Stratigraphic column of the Bambuí Group in the Serra da Saudade region and surrounding areas (Lima, 2005)**

## 7.2 Local Geology

The Capacete Formation, from the Upper Cretaceous epoch, represents a sedimentary sequence deposited sub-horizontally over the sandstones of the Areado Formation.

The primary lithology is a sandstone with a clayey matrix composed of smectite (nontronite and montmorillonite), wavellite, crandallite, and apatite. This sandstone, shown in Figure 7.3A, is intercalated with thin conglomeratic layers containing millimetric fragments (Figure 7.3B). Magnetite is a common mineral within the sandstone.

This sequence also features alternating centimetric to metric layers of conglomerates and sandstones. The conglomerates (Figure 7.3 C) contain rounded to sub-rounded fragments of varying sizes, composed of quartz, magnetite, siltstone, chert, kamafugite, and sandstone, with occasional

apatite fragments. These fragments are embedded in a clayey matrix similar in composition to that of the sandstone.

Thin siltstone layers, on the centimeter scale, are also observed within the sequence.

Rock classifications were conducted using thin-section petrography and X-ray diffraction analyses, which provided detailed mineralogical insights.

The Capacete Formation is well-defined in aero gamma spectrometric surveys, particularly due to the presence of thorium (Th) anomalies. These anomalies remain prominent even beneath the detrital-lateritic cover (TQDL). The aerogeophysical data were acquired through surveys conducted by CODEMIG, a government agency of the state of Minas Gerais.

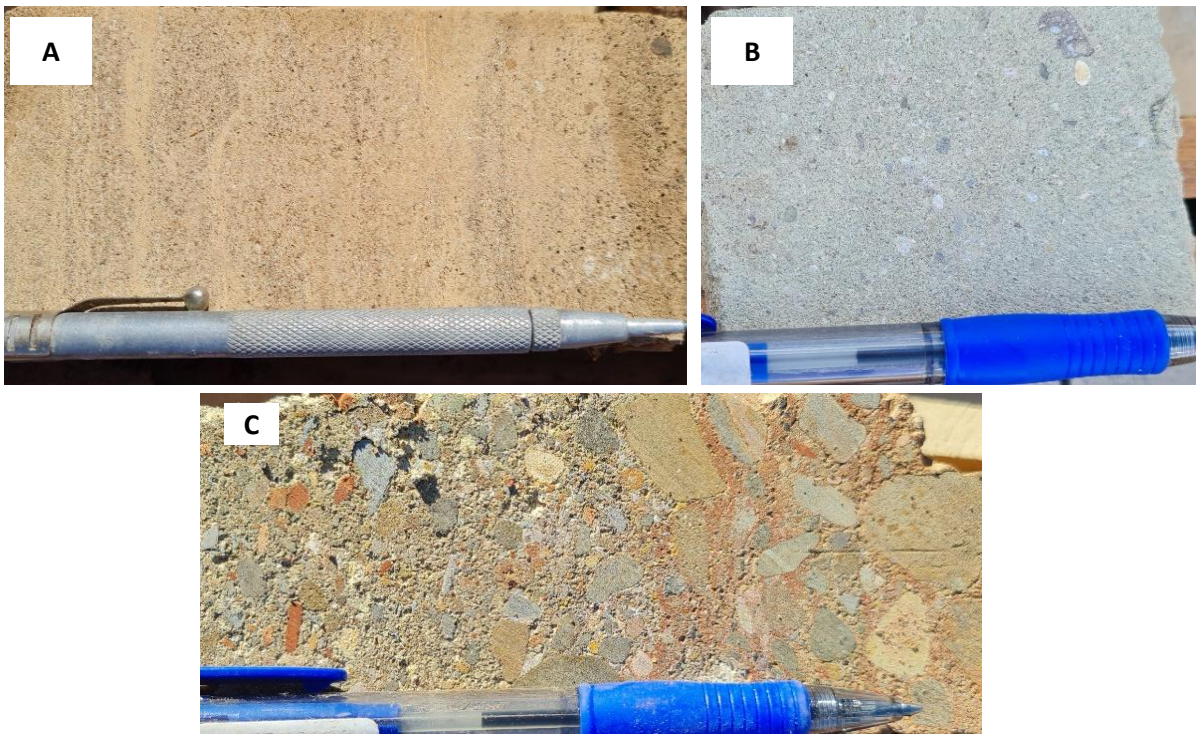



**Figure 7.3 - A) Sandstone B) Conglomeratic sandstone C) Conglomerate**

## 7.3 Mineralization

Rare earth elements (REEs) occur within the rocks of the Capacete Formation, which has a thickness ranging from 20 m to 100 m in the Project area. These sedimentary layers were deposited sub-horizontally over the substrate of the Areado Group.

The rocks of the Capacete Formation originated from the weathering and transport of lithologies from the Patos Formation, which is predominantly of kamafugitic composition. Both formations were deposited laterally. The REEs in the Capacete Formation are primarily sourced from the Patos Formation. During weathering, minerals such as perovskite and gorceixite underwent alteration and released rare earth ions and colloidal sediments that became incorporated into the Capacete sediments.

# 8 Deposit Types

The mineralization in the project area is classified as a sediment-hosted deposit, primarily composed of ion-adsorption clays rich in REEs, hosted within the matrix of arenites and conglomerates.

# 9 Exploration

This section outlines the exploration activities conducted in the project areas, highlighting the transition from phosphate exploration to a focus on REEs.

## 9.1 History of Phosphate Exploration

Occurrences of potassic and phosphate rocks in the Serra da Saudade region were first noted in the 1960s by the Comissão do Vale do São Francisco under Professor Djalma Guimarães. Later, the ANM conducted geological and economic assessments, including drilling, trenching, and mapping. In 1970, the Fosfato de Cedro do Abaeté Project conducted by the CPRM identified phosphate occurrences in the Bambuí, Areado, and Mata da Corda groups, with significant concentrations found at the base of the Mata da Corda Group.

Since 2008, FVS and Verde have been investigating phosphate deposits in sedimentary rocks with volcanic clasts in the Mata da Corda Group. Agronomic studies have confirmed the potential for these rocks for the manufacture of high-quality fertilizers, thus providing essential nutrients such as phosphate, calcium, magnesium and potassium, and micronutrients such as silicon and manganese, all of which contribute to improved agricultural productivity and sustainability.

## 9.2 Rare Earth Exploration

The focus of the project shifted from phosphate to rare earth elements (REEs) during a new phase of exploration aimed at better characterizing the deposit. This change was motivated by the need for a deeper geological understanding of the area.

Exploration efforts began with a thorough review of existing literature and geophysical data, including high-resolution airborne surveys conducted between 2000 and 2013. These surveys identified thorium anomalies in the Capacete Formation, which is also associated with phosphate mineralization. Gamma-spectrometric and magnetometric analyses were used to map thorium and potassium distributions. This revealed significant correlations that guided further investigations.

To verify REE mineralization, 3,640 meters of drill core were reanalyzed, starting with selected drill holes from key target areas. Initially, 200 samples from six drill holes were sent to the SGS Laboratory for testing. Once the presence of REEs had been confirmed, the remaining core samples were promptly analyzed to refine the understanding of the mineralization.

The reanalysis performed using ICP-OES/MS—an advanced and precise technique—identified notable concentrations of Total Rare Earth Oxides (TREO), with a significant enrichment of Magnetic Rare Earth Oxides (MREO). Among these, neodymium (Nd) and praseodymium (Pr) oxides stood out due to their high value and critical applications in the production of high-performance permanent magnets for electric vehicles, wind turbines, and advanced technologies.

These findings underscore the economic potential of the deposit, with high TREO and NdPr concentrations indicating strong viability for extraction.

## 9.3 Project targets

The Man of War Project comprises three primary targets:

- **Nau de Guerra** Target: Approximately 2.90 km²
- **Alto da Serra** Target: Approximately 3.40 km²
- **Balsamo** Target: Approximately 11.40 km²

Together, these targets cover a combined area of approximately 17.70 km².

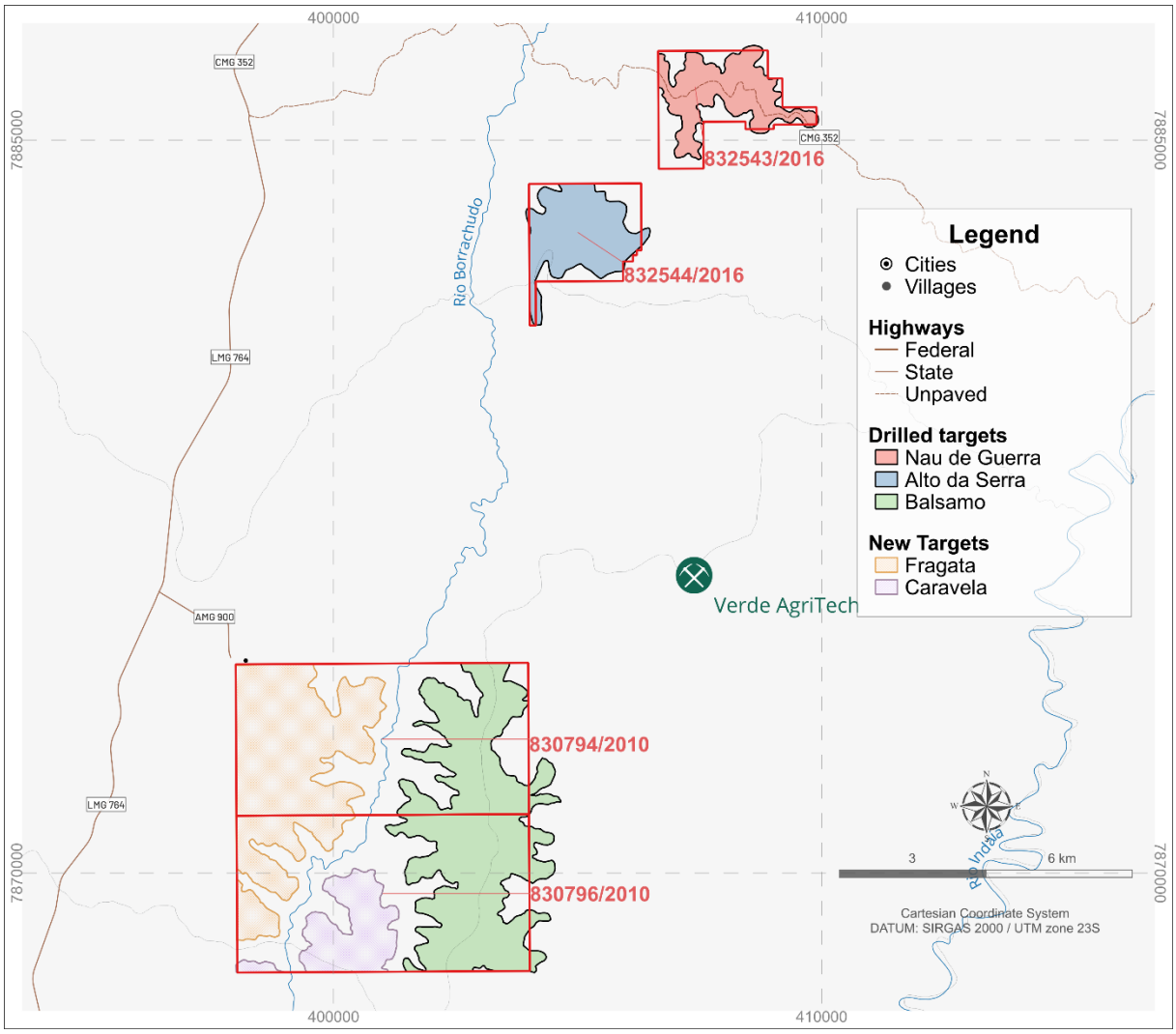



**Figure 9.1 - Targets drilled in the historic campaign and new prospects to be drilled**

Recent exploration efforts have identified two new targets, Fragata and Caravela, located west of the Balsamo target within the same tenement area. Covering approximately 10.08 km² and 3.03 km², respectively, these additions have expanded the project area from 17.7 km².

Surface sampling, conducted through channel samples and analyzed at the SGS laboratory, confirmed the presence of rare earth element mineralization in both targets. Notable results include TREO values of up to 15,613 ppm and MREO values of up to 3,562 ppm at Fragata, while Caravela recorded up to 7,563 ppm TREO and 2,611 ppm MREO. Key REE concentrations, including $Nd_2O_3$, $Pr_6O_{11}$, $Tb_4O_7$, and $Dy_2O_3$, further highlight the potential of these newly identified zones. A map showing the sample collection locations and results is presented in Figure 9.2.

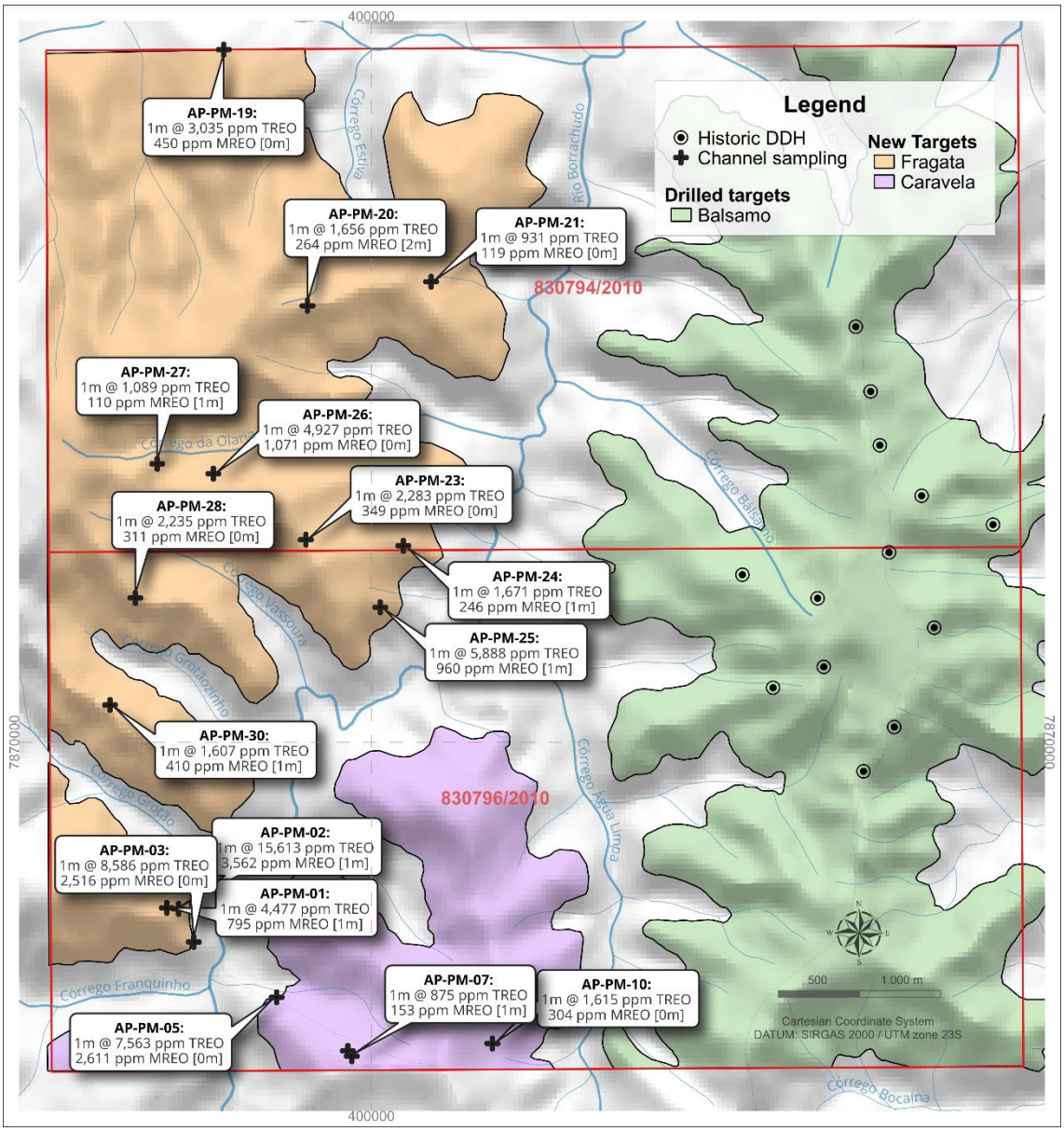



**Figure 9.2 - Surface sampling in new prospects to be drilled**

The Table 9.1 shows the results of the channel samples collected on the surface at the Fragata and Caravela targets.

**Table 9.1 - Results of surface channel samples**

| Hole ID | Total Length (m) | From (m) | To (m) | TREO (ppm) | MREO (ppm) | Nd2O3 (ppm) | Pr6O11 (ppm) | Tb4O7 (ppm) | Dy2O3 (ppm) |
|---|---|---|---|---|---|---|---|---|---|
| AP-PM-01 | 4 | 0 | 4 | 4,092 | 724 | 525 | 171 | 5 | 23 |
| | Including | 1 | 2 | 4,477 | 795 | 577 | 188 | 5 | 25 |
| AP-PM-02 | 4 | 0 | 4 | 11,951 | 2,277 | 1,707 | 498 | 13 | 59 |
| | Including | 1 | 2 | 15,613 | 3,562 | 2,729 | 723 | 20 | 90 |
| AP-PM-03 | 7 | 0 | 7 | 6,546 | 1,797 | 1,353 | 373 | 12 | 58 |

| Hole ID | Total Length (m) | From (m) | To (m) | TREO (ppm) | MREO (ppm) | Nd2O3 (ppm) | Pr6O11 (ppm) | Tb4O7 (ppm) | Dy2O3 (ppm) |
|---|---|---|---|---|---|---|---|---|---|
| | Including | 0 | 1 | 8,586 | 2,516 | 1,904 | 518 | 16 | 79 |
| AP-PM-05 | 4 | 0 | 4 | 7,153 | 1,757 | 1,313 | 387 | 10 | 47 |
| | Including | 0 | 1 | 7,563 | 2,611 | 2,014 | 511 | 15 | 71 |
| AP-PM-06 | 1 | 0 | 1 | 1,436 | 249 | 181 | 57 | 2 | 9 |
| | Including | 0 | 1 | 1,436 | 249 | 181 | 57 | 2 | 9 |
| AP-PM-07 | 2 | 0 | 2 | 855 | 133 | 97 | 30 | 1 | 5 |
| | Including | 1 | 2 | 875 | 153 | 113 | 34 | 1 | 6 |
| AP-PM-10 | 1 | 0 | 1 | 1,615 | 304 | 224 | 67 | 2 | 11 |
| | Including | 0 | 1 | 1,615 | 304 | 224 | 67 | 2 | 11 |
| AP-PM-19 | 3 | 0 | 3 | 2,906 | 427 | 308 | 106 | 2 | 11 |
| | Including | 0 | 1 | 3,035 | 450 | 325 | 112 | 2 | 11 |
| AP-PM-20 | 3 | 0 | 3 | 1,476 | 158 | 115 | 37 | 1 | 5 |
| | Including | 2 | 3 | 1,656 | 264 | 194 | 61 | 1 | 8 |
| AP-PM-21 | 1 | 0 | 1 | 931 | 119 | 84 | 30 | 1 | 4 |
| | Including | 0 | 1 | 931 | 119 | 84 | 30 | 1 | 4 |
| AP-PM-23 | 1 | 0 | 1 | 2,283 | 349 | 254 | 81 | 2 | 11 |
| | Including | 0 | 1 | 2,283 | 349 | 254 | 81 | 2 | 11 |
| AP-PM-24 | 2 | 0 | 2 | 1,335 | 208 | 149 | 50 | 1 | 7 |
| | Including | 1 | 2 | 1,671 | 246 | 176 | 59 | 2 | 9 |
| AP-PM-25 | 2 | 0 | 2 | 5,389 | 819 | 597 | 194 | 5 | 24 |
| | Including | 1 | 2 | 5,888 | 960 | 703 | 224 | 6 | 28 |
| AP-PM-26 | 1 | 0 | 1 | 4,927 | 1,071 | 805 | 228 | 7 | 31 |
| | Including | 0 | 1 | 4,927 | 1,071 | 805 | 228 | 7 | 31 |
| AP-PM-27 | 3 | 0 | 3 | 1,015 | 96 | 67 | 24 | 1 | 3 |
| | Including | 1 | 2 | 1,089 | 110 | 78 | 27 | 1 | 4 |
| AP-PM-28 | 1 | 0 | 1 | 2,235 | 311 | 224 | 75 | 2 | 11 |
| | Including | 0 | 1 | 2,235 | 311 | 224 | 75 | 2 | 11 |
| AP-PM-30 | 2 | 0 | 2 | 1,425 | 348 | 260 | 76 | 2 | 10 |
| | Including | 1 | 2 | 1,607 | 410 | 308 | 89 | 2 | 11 |

# 10 Drilling

The primary drilling method employed for the Man of War Project was Diamond Drilling (DDH), chosen for its ability to produce the high-quality core samples essential for detailed geological analysis.

## 10.1 Campaigns

The drilling campaign took place between April and September, 2011, and covered a total of 3,539.3 meters. The average drill depth was 96.54 meters, ranging from a minimum of 21.45 meters to a maximum depth of 139 meters. Two companies performed the drilling work: Rede Engenharia e Sondagens S/A ("REDE") and Isoágua Perfurações Especiais Ltda ("ISOAGUA").

REDE served as the primary contractor, drilling 42 holes for a total of 3,470.55 meters using a MACH 1200 drill rig with an HQ-diameter core. ISOAGUA was responsible for an additional 3 holes, totaling 168.75 meters, utilizing a DIAKOR II rig, also with an HQ-diameter core.

The campaign targeted three areas: 742.95 meters were drilled at the Nau de Guerra target, 1,313.85 meters at the Alto da Serra target, and 1,582.5 meters at the Balsamo target.

The diamond drill cores obtained provided high-quality samples for further bulk density measurements. Details of the drill holes are summarized in Table 10.1 below:

**Table 10.1 - Results of Drill Holes from Campaign #2**

| Prospect | Hole | X | Y | Z | Depth (m) | Company | Drill |
|---|---|---|---|---|---|---|---|
| ALTO DA SERRA | AP-AD-01 | 404561.279 | 7883712.996 | 1039.30 | 55.00 | REDE | MACH 1200 |
| | AP-AD-02 | 405029.799 | 7883797.756 | 1071.45 | 90.00 | REDE | MACH 1200 |
| | AP-AD-03 | 404883.619 | 7883339.817 | 1091.41 | 106.95 | REDE | MACH 1200 |
| | AP-AD-04 | 405149.869 | 7883333.807 | 1095.68 | 112.95 | REDE | MACH 1200 |
| | AP-AD-05 | 405623.618 | 7883346.547 | 1068.07 | 82.45 | REDE | MACH 1200 |
| | AP-AD-06 | 404434.659 | 7882931.868 | 1083.66 | 94.65 | REDE | MACH 1200 |
| | AP-AD-07 | 404814.879 | 7882950.058 | 1099.89 | 116.15 | REDE | MACH 1200 |
| | AP-AD-08 | 405210.978 | 7882954.638 | 1078.29 | 96.30 | REDE | MACH 1200 |
| | AP-AD-09 | 405625.628 | 7882964.788 | 1083.84 | 100.85 | REDE | MACH 1200 |
| | AP-AD-11 | 404555.349 | 7882489.338 | 1025.37 | 33.65 | REDE | MACH 1200 |
| | AP-AD-12 | 405298.088 | 7882545.688 | 1059.12 | 73.30 | REDE | MACH 1200 |
| | AP-AD-13 | 404097.399 | 7882385.508 | 1018.69 | 29.05 | REDE | MACH 1200 |
| | AP-AD-14 | 403931.460 | 7882723.217 | 1040.60 | 53.65 | REDE | MACH 1200 |
| | AP-AD-16 | 404210.069 | 7882816.317 | 1044.13 | 55.00 | REDE | MACH 1200 |
| | AP-AD-17 | 404651.899 | 7883488.677 | 1055.06 | 70.35 | REDE | MACH 1200 |
| | AP-AD-18 | 404843.989 | 7883541.857 | 1059.94 | 76.35 | REDE | MACH 1200 |

| Prospect | Hole | X | Y | Z | Depth (m) | Company | Drill |
|---|---|---|---|---|---|---|---|
| | AP-AD-19 | 405468.108 | 7883230.067 | 1055.67 | 67.20 | REDE | MACH 1200 |
| BALSAMO | AP-BD-01 | 402936.803 | 7872513.361 | 1131.78 | 131.25 | REDE | MACH 1200 |
| | AP-BD-02 | 403028.453 | 7872113.761 | 1130.96 | 134.30 | REDE | MACH 1200 |
| | AP-BD-03 | 403085.153 | 7871781.482 | 1132.69 | 135.80 | REDE | MACH 1200 |
| | AP-BD-04 | 403342.993 | 7871469.542 | 1134.68 | 138.50 | REDE | MACH 1200 |
| | AP-BD-05 | 402237.964 | 7870981.782 | 1093.83 | 97.70 | REDE | MACH 1200 |
| | AP-BD-06 | 402701.624 | 7870836.343 | 1140.00 | 136.95 | REDE | MACH 1200 |
| | AP-BD-07 | 403141.723 | 7871119.613 | 1131.37 | 135.85 | REDE | MACH 1200 |
| | AP-BD-08 | 403783.012 | 7871291.312 | 1077.21 | 78.45 | REDE | MACH 1200 |
| | AP-BD-09 | 402427.064 | 7870284.283 | 1089.60 | 85.45 | REDE | MACH 1200 |
| | AP-BD-10 | 402739.574 | 7870412.953 | 1126.13 | 128.05 | REDE | MACH 1200 |
| | AP-BD-11 | 403420.343 | 7870654.963 | 1137.73 | 139.00 | REDE | MACH 1200 |
| | AP-BD-12 | 403173.883 | 7870041.404 | 1131.65 | 134.35 | REDE | MACH 1200 |
| | AP-BD-13 | 402984.593 | 7869768.034 | 1107.59 | 106.85 | REDE | MACH 1200 |
| NAU DE GUERRA | AP-ND-02 | 407936.41 | 7886126.373 | 1026.66 | 47.35 | ISOAGUA | DIAKOR II |
| | AP-ND-03 | 408520.06 | 7886165.824 | 1059.74 | 79.4 | REDE | MACH 1200 |
| | AP-ND-04 | 406990.25 | 7885854.774 | 1025.54 | 51.95 | REDE | MACH 1200 |
| | AP-ND-05 | 407244.02 | 7885937.784 | 1055.04 | 71.65 | REDE | MACH 1200 |
| | AP-ND-06 | 408076.45 | 7885921.344 | 1029.4 | 47.4 | REDE | MACH 1200 |
| | AP-ND-07 | 407311.93 | 7885466.314 | 1014.8 | 33.25 | REDE | MACH 1200 |
| | AP-ND-08 | 408264.7 | 7885723.054 | 1020.64 | 42.8 | REDE | MACH 1200 |
| | AP-ND-09 | 408830.08 | 7885727.044 | 1060.48 | 78.7 | ISOAGUA | DIAKOR II |
| | AP-ND-11 | 407186.09 | 7884999.565 | 1021.45 | 42.7 | ISOAGUA | DIAKOR II |
| | AP-ND-12 | 406741.18 | 7886245.433 | 1005.42 | 24.5 | REDE | MACH 1200 |
| | AP-ND-13 | 407321.16 | 7885270.944 | 1000.33 | 21.45 | REDE | MACH 1200 |
| | AP-ND-14 | 407749.91 | 7886317.553 | 1049.36 | 67.2 | REDE | MACH 1200 |
| | AP-ND-15 | 408292.57 | 7886267.163 | 1039.29 | 59.65 | REDE | MACH 1200 |
| | AP-ND-16 | 408687.12 | 7885899.414 | 1032.19 | 51.95 | REDE | MACH 1200 |
| | AP-ND-17 | 409253.08 | 7885504.304 | 1000.76 | 23 | REDE | MACH 1200 |



**Figure 10.1 - Dimond Drilling (DDH) rig**

## 10.2 Surveying

The boreholes were drilled in a vertical orientation, eliminating the need for downhole deviation surveys due to their shallow depth. The drilling direction was perpendicular to the mineralization, and thus accurately represented its true width. BNA conducted a review of the historical drilling during a July, 2024 site visit, which included an inspection by the Project QP.

Surveying of the drillhole collars was performed using a Trimble® Pathfinder Pro XR DGPS and the data underwent post-correction validation by IBGE, referencing the Santiago & Cintra station in Belo Horizonte (vertex 93,621; coordinates: East 608,308.23 m, North 7,799,827.00 m, altitude 879.06 m HAE – with a recording rate of 0.5s, C/A code + L1). The precision of these measurements is within the acceptable range for the type of mineralization encountered, with an accuracy level of approximately 1 cm after 45 minutes of satellite tracking, which conforms to industry standards for this mineralization category.

This drilling information was then integrated into a 3D geological model.

## 10.3 Logging

During the initial phosphate exploration in 2011, the diamond drill cores were placed in core boxes for storage (Figure 10.2-A). The weathering, regolith, and lithology, including petrographic features, were logged by the geologists. Basic geotechnical observations, such as rock quality

designation (RQD), degree of weathering, and impact resistance, were recorded. All information was entered into a digital database (Microsoft Excel). After logging and sample preparation for analysis, during which ½ of each core was consumed, though for some intervals, ¾ were required, the core boxes were stored in the warehouse (Figure 10.3).

In this phase of rare earth exploration, before reanalysis of the drill cores, new procedures were followed. The boxes with the remaining portions of the cores were laid out in the yard (Figure 10.4) and the logging procedures were redone. First, all the boxes and their respective intervals were properly identified and photographed one by one (Figure 10.2-B). The geologists then repeated the logging of weathering, regolith, and lithology, including petrographic features, and recorded basic geotechnical observations (RQD, degree of weathering, and impact resistance). This information was also entered into the digital database (Microsoft Excel).




**Figure 10.2 - A) Boxes with ½ of the cores preserved after the first exploration. B) Box of cores remarked before the new exploration phase.**



**Figure 10.3 - Boxes with sample logs stored in the warehouse**



**Figure 10.4 - Core storage boxes laid out in the yard to be re-logged**

## 10.4 Recovery Calculations

The recovery determinations are calculated using the sum of the length of core pieces compared against the total length of the core run.

## 10.5 Diamond Drilling (DDH) Sampling

As discussed in previous sections, the exploration project was undertaken in two distinct phases, focusing on different minerals. This has resulted in a somewhat unique sampling process.

During the phosphate exploration phase, after logging, the selected diamond drill core was cut lengthwise using a diamond core saw. Half of the core was sent for analysis, while the other half was retained in the core box for future reference. For some intervals, three-quarters of the core was utilized for analysis.

In the subsequent rare earth exploration phase, a different sampling approach was necessary due to the limited amount of core remaining. Following the advice of the Qualified Person for the Project, the remaining half of the core was further split longitudinally. This procedure was implemented to ensure the representativeness of the interval, with only a quarter of the sample being sent for analysis while the other quarter was preserved for materiality purposes. However, for intervals where only a quarter of the core remained from the initial exploration, the entire sample had to be consumed for analysis.

For the diamond drilling core sampling procedure, the samples, typically 1 meter in length, were carefully packed into plastic bags. Each sample was labeled with an identification number written on the bag using a marker, accompanied by an identification tag. The bags were then double-bagged, sealed with clamps, and labeled accordingly. All sampling data was meticulously recorded in an Excel database, allowing for subsequent correlation with the analytical results once they were returned from the laboratory.

## 10.6 Lithologic units

The lithological units identified in the study area encompass a variety of rock types, each with distinct characteristics and compositions. These units include soil, saprolite, a transition zone, and fresh rock. Each lithology is associated with specific geological features and weathering processes.

The soil layer is typically thin, ranging from a few centimeters to a meter in thickness. It is predominantly red due to its argillaceous nature and the presence of iron oxides (Figure 10.5-A).

Saprolite appears reddish, a coloration attributed to the weathering of magnetite. Other colors include light beige, yellow, white, gray, green, and brown. This unit is formed from the weathering of siltstone, sandstone, conglomeratic sandstone, and conglomerate and retains the structure of the original rock to varying degrees. Occasionally, thin zones of iron-rich laterite can be observed within the saprolite (Figure 10.5-B).

The transition zone, or saprock, represents an intermediate stage of weathering. This zone comprises materials derived from siltstone, sandstone, conglomeratic sandstone, and conglomerate, and exhibits colors such as light beige, reddish, white, and gray. The degree of weathering in this zone is less advanced compared to the saprolite (Figure 10.5-C).

Fresh rock units include unweathered siltstones, sandstones, conglomeratic sandstones, and conglomerates. These rocks have not undergone significant weathering and therefore retain their original physical and chemical properties (Figure 10.5-D).
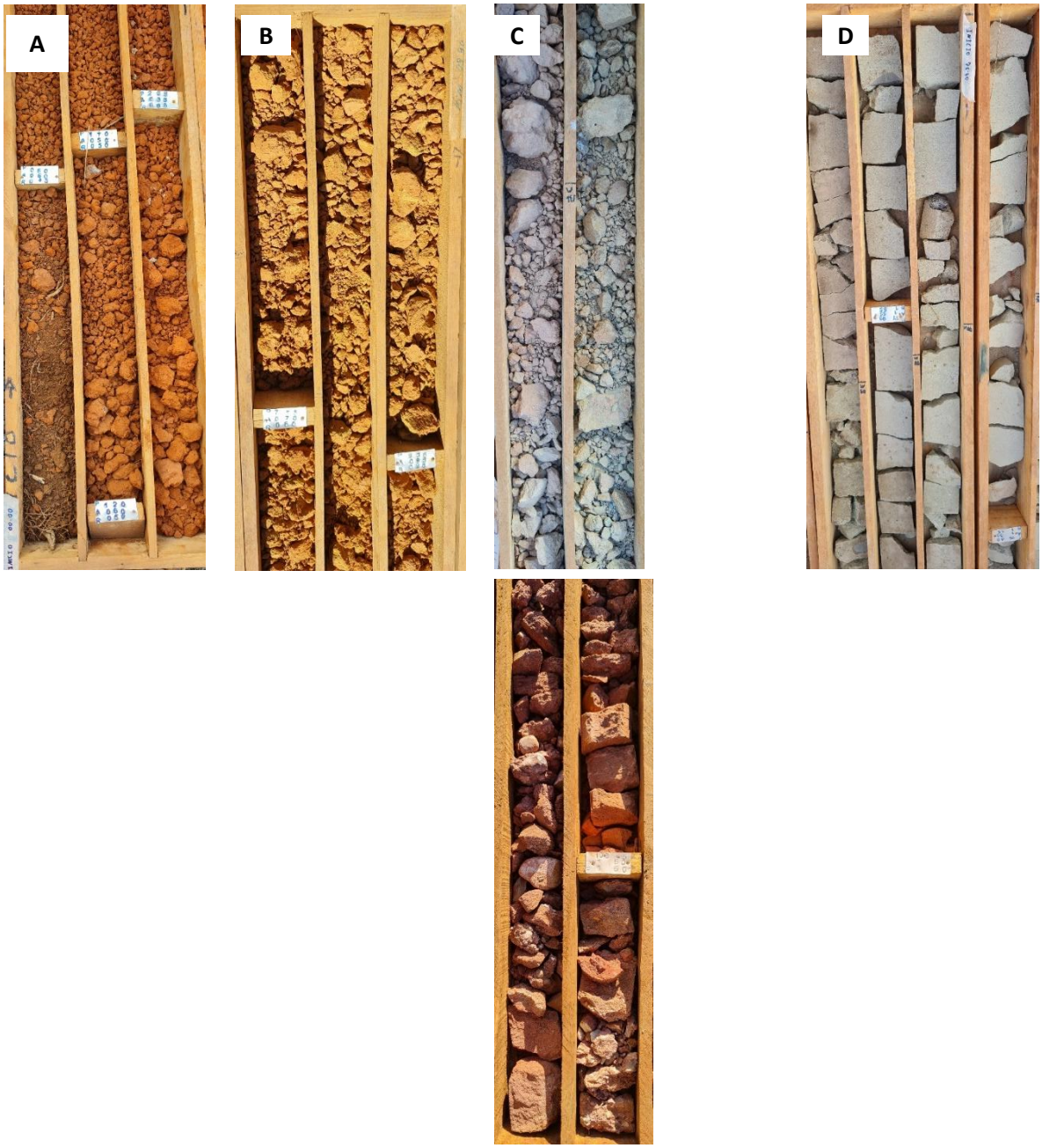



**Figure 10.5 - A) Contact between soil and saprolite of sandstone B) Saprolite of sandstone C) Transition zone in sandstone D) Fresh sandstone**

## 10.7 Bulk Density

For resource estimation, dry bulk density values were calculated for select samples of the diamond drill core. Whole core pieces were selected for density measurements at intervals of 2 meters along each hole. The samples were placed on properly labeled aluminum plates and taken to an electric oven for 24 hours at 90°C to eliminate moisture. After drying, they were wrapped in PVC film and weighed in the open air on an OHAUS Adventurer® precision digital scale. Then, they were completely

immersed in a basin of water, suspended by a thread of negligible mass, to obtain the submerged weight.

Bulk density measurements were conducted on samples ranging from 10 to 20 centimeters throughout the mineralized interval. The density calculation was based on Archimedes' Principle, which states that any solid body immersed in a fluid loses weight equivalent to the volume of fluid displaced. Water, with a known density, was used as the displacement fluid for these measurements.

The initial weight measurements were taken in the open air using an OHAUS Adventurer® digital scale, approved by INMETRO (the National Institute of Meteorology, Normalization and Industrial Quality), which measures weights to a precision of at least 0.02 grams. The scale stored the data in its memory, allowing for retrieval in the event any issues arose. Following the open air weighing, the samples were fully submerged in water to record their submerged weight. Subsequently, the samples were returned to their respective positions in the core boxes. A total of 452 dry density measurements were conducted.

# 11 Sample Preparation, Analysis and Security

The primary laboratory involved in the analysis of samples for the Man of War Project is SGS Geosol Laboratórios Ltda., with the analyses being conducted at their main facility in Vespasiano, Minas Gerais (MG). For interlaboratory quality control, additional analyses were performed by the ALS Laboratory Group, also located in Vespasiano, MG. As detailed in previous sections, the current project initially preserved only half of the DDH (diamond drill hole) cores, as the other half was consumed during the exploration campaign for phosphate rock (for some holes only one quarter of the core was preserved).

SGS Geosol Laboratórios Ltda., a joint venture between SGS do Brasil and Geosol Geologia e Sondagens, is internationally recognized for its high-quality analytical chemistry services. The company is ISO 9001, ISO 14001 certified and ISO/IEC 17025:2017 accredited, ensuring quality, safety, respect for the environment, and social responsibility. ALS is a leading global provider of analytical and testing services, with a workforce of over 20,000 people working in more than 420 locations in 70+ countries, ensuring extensive and reliable services.

The following subsections will provide a detailed overview of sample preparation, analytical methods, and quality assurance/quality control (QA/QC) procedures.

## 11.1 Sample Preparation

### 11.1.1 Field sample preparation

Before the sampling work commenced, all core boxes were laid out in the yard and photographed individually. The geological descriptions were redone by the geologist responsible to ensure accuracy and completeness. Given that only half of the diamond drill core was available, a longitudinal cut was made to collect a quarter of the original sample, thus ensuring the representativity of the sample. The remaining quarter was preserved in the boxes.

Sampling was conducted at 1-meter intervals, with the intervals clearly marked on the boxes. All density samples from the initial exploration campaign were also preserved in the boxes. The samples were packed in plastic bags, with one label attached inside the bag and another outside to ensure proper identification and control by the company.

Experienced geologists supervised the entire sample preparation process to maintain quality and consistency.

### 11.1.2 Lab sample preparation

After initial sample preparation at the company's facilities, batches of 50 samples were shipped to SGS for further processing and analysis. Upon receipt, the samples were re-coded and prepared according to a standardized procedure, as outlined in Figure 11.1.

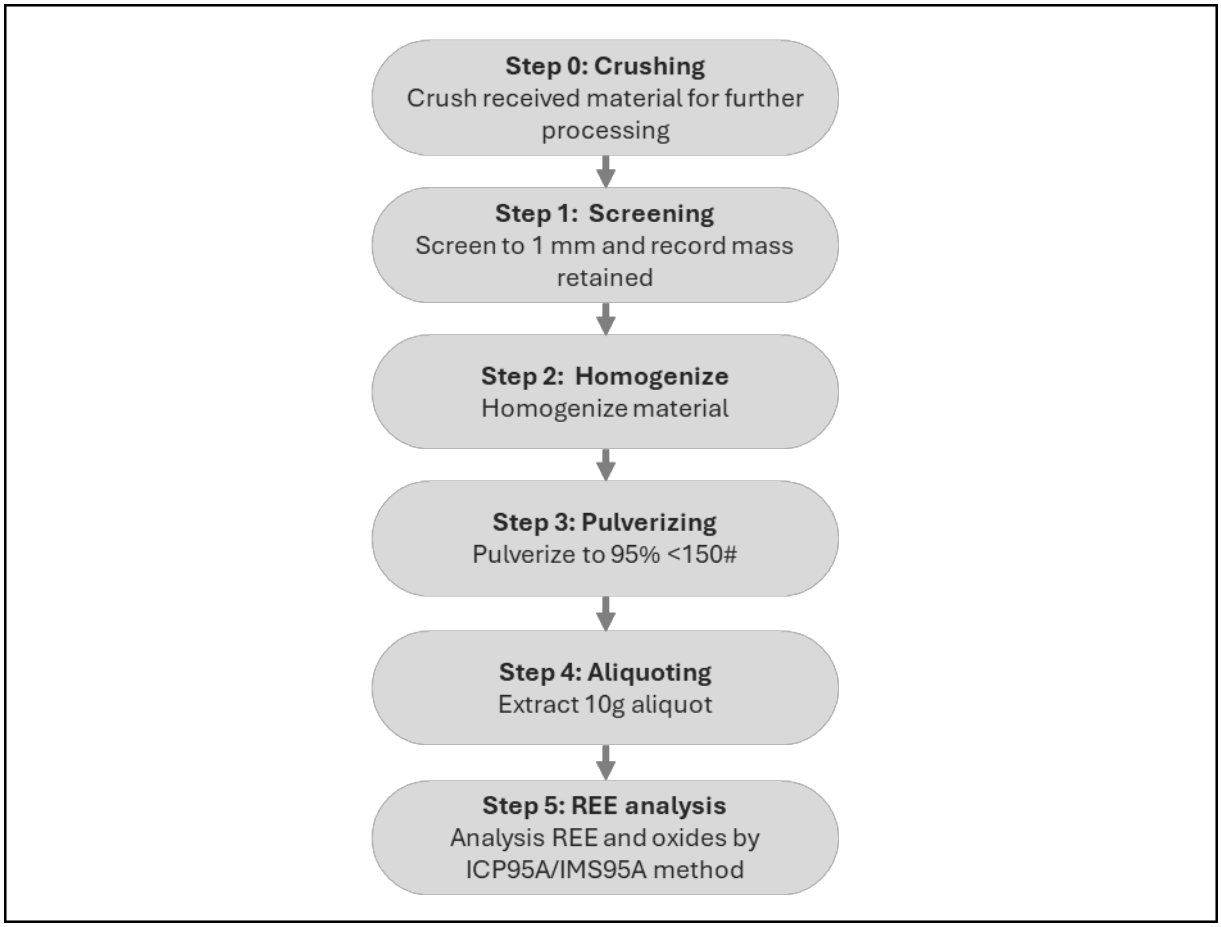



**Figure 11.1 - Process flowchart for leaching test on Ionic Clay**

The process began with crushing the material to facilitate further handling (Step 0). The crushed material was then sieved to achieve a particle size of 1 mm, with the mass retained being meticulously recorded (Step 1). After sieving, the material was homogenized to ensure consistency across the batch. A Jones riffle splitter was employed to divide the homogenized material into two equal portions, ensuring each portion was representative of the original sample (Step 2).

One half was pulverized to 95% passing through a 150# mesh sieve (105 microns) (Step 3), and a 10g aliquot was collected (Step 4) for the ICP95A/IMS95A analysis, which provides comprehensive data on rare earth elements and other oxides (Step 5).

SGS adhered to strict quality control criteria for particle size and mass loss during the sample preparation process. Crushing was performed to ensure that 75% of the sample was reduced to a particle size of less than 3 mm, with a maximum mass loss of 5%. The sample was pulverized to ensure that 95% of the sample passed through a 105-micron sieve, with the same 5% maximum allowable mass loss.

In addition to these internal controls, such as the preparation of duplicate crushed samples and the use of preparation blanks to monitor contamination, SGS implemented a robust analytical quality control (QA/QC) system. This included the use of reference materials (RM) or certified reference materials (CRM), analytical blanks (BLK), and replicates (REP) within each batch. The number of QA/QC samples was determined based on the size of the rack and the analytical method used.

Moreover, in addition to SGS's internal QA/QC protocols, the project managers and staff implemented their own stringent quality control procedures, which are detailed in Section 11.3. This additional layer of QA/QC ensures the accuracy, precision, and reliability of the analytical results and maintains the highest standards throughout the sample preparation and analysis phases.

## 11.2 Analysis

For the global analysis, the ICP95A/IMS95A method was employed, utilizing lithium metaborate fusion for the determination of 48 elements. Inductively Coupled Plasma Optical Emission Spectrometry (ICP-OES) was used for oxide determination (see Table 11.1).

**Table 11.1 - ICP95A Method - Determination by Fusion with Lithium Metaborate for Oxides - ICP OES Detection Ranges**

| Oxides/elements | Detection interval | Oxides/elements | Detection interval |
|---|---|---|---|
| **$Al_2O_3$** | 0.01 – 75 (%) | **CaO** | 0.01 – 60 (%) |
| **$Fe_2O_3$** | 0.01 – 30 (%) | **MgO** | 0.01 – 30 (%) |
| **$Na_2O$** | 0.01 – 25 (%) | **$SiO_2$** | 0.01 – 90 (%) |
| **$TiO_2$** | 0.01 – 25 (%) | **Zn** | 5 – 10000 (ppm) |
| **Ba** | 10 – 100000 (ppm) | **$Cr_2O_3$** | 0.01 – 10 (%) |
| **$K_2O$** | 0.01 – 25 (%) | **MnO** | 0.01 – 10 (%) |
| **$P_2O_5$** | 0.01 – 25 (%) | **Sr** | 10 – 100000 (ppm) |
| **V** | 5 – 10000 (ppm) | **Zr** | 10 – 100000 (ppm) |

Inductively Coupled Plasma Mass Spectrometry (ICP-MS) was employed for rare earth element analysis (see Table 11.2).

**Table 11.2 - IMS95A Method - Determination by Fusion with Lithium Metaborate for Elements - ICP MS Detection Ranges**

| Elements | Detection interval | Elements | Detection interval |
|---|---|---|---|
| **Ce** | 0.1 - 10000 (ppm) | **Yb** | 0.1 - 1000 (ppm) |
| **Dy** | 0.05 - 1000 (ppm) | **Cs** | 0.05 - 1000 (ppm) |
| **Gd** | 0.05 - 1000 (ppm) | **Eu** | 0.05 - 1000 (ppm) |
| **Lu** | 0.05 - 1000 (ppm) | **Ho** | 0.05 - 1000 (ppm) |
| **Ni** | 5 - 10000 (ppm) | **Nb** | 0.05 - 1000 (ppm) |
| **Sn** | 0.3 - 1000 (ppm) | **Rb** | 0.2 - 10000 (ppm) |
| **Tl** | 0.5 - 1000 (ppm) | **Tb** | 0.05 - 1000 (ppm) |
| **Y** | 0.05 - 10000 (ppm) | **U** | 0.05 - 10000 (ppm) |
| **Co** | 0.5 - 10000 (ppm) | **Cu** | 5 - 10000 (ppm) |
| **Er** | 0.05 - 1000 (ppm) | **Ga** | 0.1 - 10000 (ppm) |
| **Hf** | 0.05 - 1000 (ppm) | **La** | 0.1 - 10000 (ppm) |
| **Mo** | 2 - 10000 (ppm) | **Nd** | 0.1 - 10000 (ppm) |
| **Pr** | 0.05 - 1000 (ppm) | **Sm** | 0.1 - 1000 (ppm) |
| **Ta** | 0.05 - 10000 (ppm) | **Th** | 0.1 - 10000 (ppm) |
| **Tm** | 0.05 - 1000 (ppm) | **W** | 0.1 - 10000 (ppm) |

## 11.3 QA/QC

Quality Assurance/Quality Control (QA/QC) is a systematic approach to ensuring the reliability and accuracy of analytical results through rigorous testing and validation procedures. It involves implementing protocols to monitor and maintain the quality of data throughout the entire analytical process.

In addition to SGS's internal quality assurance and control system, Verde applied its own QA/QC process to each batch sent to the laboratory. During the QA/QC process for this project, samples were processed in batches of 50, with each batch containing 44 samples of the material to be analyzed, 2 blanks, 2 standards, and 2 duplicates.

Blanks, consisting of quartz samples devoid of the analyte of interest, were placed at positions 1 and 50 in each batch to detect and correct for potential contamination during sample handling and analysis. This precaution ensures that the analytical process begins and ends without introducing unintended substances. Additionally, for quality control purposes, results were required to be below the detectable limit, as detailed in Section 12.2.

Standards, known solutions or materials with a known concentration of the analyte, were inserted at positions 20 and 40 within each batch. These standards serve to verify the quality, accuracy, and biases of the laboratory's analyses throughout the batch. Criteria based on the Shewart control chart were adopted for quality control and the results are presented in Section 12.2. Certified Reference Materials (CRMs) used for standardization included OREAS 461, OREAS 460, and SGS 142, sourced from ORE Research & Exploration P/L in Australia and SGS Geosol Laboratories in Brazil.

Duplicates (field duplicates), identical samples analyzed separately, were included at positions 10 and 30 in each batch to assess the reproducibility and consistency of the analytical results. Analyzing duplicates helps identify any experimental errors or inconsistencies in the analytical procedure. For quality control purposes, an ideal difference limit of 5% was established between duplicate results. Differences of up to 15% were acceptable, provided there was sufficient justification. Results showing differences exceeding 15% required a plausible explanation. Detailed results are outlined in Section 12.2.

Inter-laboratory comparisons (pulp duplicates) were performed to further verify the bias and accuracy of results from SGS Laboratory. In this procedure, 3% of the samples were selected, at 30 routine material sample intervals, and pulps of this material were sent to ALS Laboratory for reanalysis. This inter-laboratory comparison ensures the reliability and accuracy of the analytical data by comparing results obtained from different laboratories using the same samples.

Below is a diagram that shows the positions of samples, blanks, field duplicates, standards and Inter-laboratory comparisons:

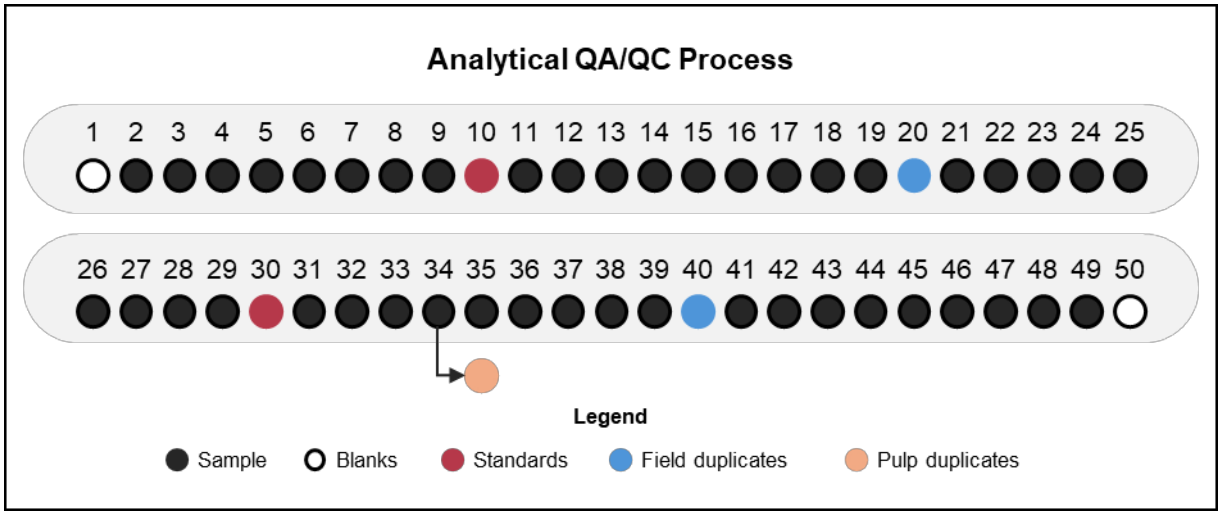



**Figure 11.2 - Spatial Distribution of Samples, Blanks, Duplicates, and Standards in the Analytical QA/QC Process**

It is also important to mention that a portion of the samples from holes (totaling 200 samples) did not undergo the QA/QC process, as they were used during the preliminary studies to confirm the presence of rare earths in the deposit.

# 12 Data Verification

## 12.1 Site Visit

A site visit was carried out by Volodymyr Myadzel on behalf of BNA Mining Solutions on July 1 & 2 and August 13, 2024. The visit was attended by Verde officials Thiago Siqueira (Geology & Projects/Project Manager) and Guido Pessoa (Environment Manager).

The purpose of the visit was to learn about the project and verify the work done in the field, in terms of geological exploration, in accordance with the basic principles governing the application and operation of the NI 43-101 standards: transparency, materiality and competence, and also in accordance with the best practices of the mineral industry.

The technical visit covered the core storage shed, the project area and the mineralized zone in the field.

The images below show photos taken during the site visit (Figure 12.1 and Figure 12.2).




**Figure 12.1 – Drilling Material – Technical site visit**




**Figure 12.2 - Shed visit**

Most drillholes were clearly marked with concrete plugs (Figure 12.3). A metal tag, hammered into the concrete plugs, displayed the hole number, depth and azimuth. All drill holes were identified following the drilling campaign by a surveyor using a GPS RTK device.




**Figure 12.3 - Drill Hole Collar - Technical site visit**

During the visit, it was observed that the Verde technical team had been performing the work in accordance with the best practices of the mining industry. The author is of the opinion that the company has adequately followed proper sample preparation, security and analytical procedures, and that industry best practices have been applied regarding the collection of information and maintenance of the database.

## 12.2 Database

BNA received two large batches of data from Verde. The first contained data from the Nau de Guerra target and the second contained data from the Balsamo and Alto da Serra targets.

To save time, BNA began working with data from the Nau de Guerra target. The data from Balsamo and Alto da Serra were received after the resource estimate for the Nau de Guerra target had been completed. Due to the similarity between the targets, the data from Balsamo and Alto da Serra were worked on together whenever possible.

The main database used in this work is in the form tables in various formats, including the tables listed here:

- Drill holes tables:
  - DATASET_Nau_de_Guerra_v2_2024-09-13.xlsx - Target Nau de Guerra Database:
  - COLLAR - collar Nau de Guerra;
  - ASSAY - assay Nau de Guerra;
  - ASSAY_Historic - assay Nau de Guerra, chemical results of the first phase of mineral exploration;
  - RECOVERY - recovery data Nau de Guerra;
  - DENSITY - density data Nau de Guerra;
  - GEOTECHINAL - geotechnical data Nau de Guerra;
  - GEOLOGY - lithology description Nau de Guerra;
  - Legend - legend used in the database Nau de Guerra.
  - DNPM_SIRGAS2000.STR - license limits of Nau de Guerra Target.
  - DATASET_Alto da Serra & Balsamo_v1_2024-11-01.xlsx - Targets Alto da Serra and Balsamo Database:
  - COLLAR - collar Alto da Serra and Balsamo;
  - ASSAY - assay Alto da Serra and Balsamo;
  - ASSAY_Historic - assay Alto da Serra and Balsamo, chemical results of the first phase of mineral exploration;
  - RECOVERY - recovery data Alto da Serra and Balsamo;
  - DENSITY - density data Alto da Serra and Balsamo;
  - GEOTECHINAL - geotechnical data Alto da Serra and Balsamo;

- GEOLOGY - lithology description Alto da Serra and Balsamo;
- Legend - legend used in the database Alto da Serra and Balsamo.
- *ANM_ BALSAMO & ALTO DA SERRA.STR - license limits of Alto da Serra and Balsamo Target.*

- DTM.tridb - topography of Nau de Guerra Target.
- Geologia_nau_de_guerra_SIRGAS2000.STR - geological mapping data of Nau de Guerra Target.
- DTM.tridb - topography of Alto da Serra and Balsamo Target.
- Geology_ALTO_DA_SERRA.STR - geological mapping data of Alto da Serra Target.
- Geology_BALSAMO.STR - geological mapping data of Balsamo Target.
- DNPM_SIRGAS2000.STR - license limits of Nau de Guerra Target.
- DTM.tridb - topography of Nau de Guerra Target.
- Geologia_nau_de_guerra_SIRGAS2000.STR - geological mapping data of Nau de Guerra Target.

Information on the initial data from the database is presented in Table 12.1.

**Table 12.1 - Presentation of initial data**

| Description | Quantity |
|---|---|
| Nau de Guerra Target | |
| Diamond Drilling | 15 |
| Diamond Drilling metreage | 742.95 |
| Drill hole sampling notes | 626 |
| Lithological descriptions | 142 |
| Density Analyses | 175 |
| Blank | 32 |
| Standard | 32 |
| Duplicate | 32 |
| $Al_2O_3$ | 743 |
| Ba | 675 |
| CaO | 743 |
| $Cr_2O_3$ | 675 |
| $Fe_2O_3$ | 743 |
| $K_2O$ | 743 |
| MgO | 743 |
| MnO | 743 |
| $Na_2O$ | 743 |
| Nb1 | 244 |
| $P_2O_5$ | 743 |

| Description | Quantity |
|---|---|
| $SiO_2$ | 743 |
| Sr | 675 |
| $TiO_2$ | 743 |
| Zn | 675 |
| Zr | 675 |
| V | 675 |
| LOI | 743 |
| Ce | 745 |
| Co | 745 |
| Cs | 745 |
| Cu | 745 |
| Dy | 745 |
| Er | 745 |
| Eu | 745 |
| Ga | 211 |
| Gd | 745 |
| Hf | 745 |
| Ho | 745 |
| La | 745 |
| Lu | 745 |
| Mo | 745 |
| Nb2 | 701 |
| Nd | 745 |
| Ni | 745 |
| Pr | 745 |
| Rb | 745 |
| Sm | 745 |
| Sn | 745 |
| Ta | 745 |
| Tb | 745 |
| Th | 745 |
| Tl | 745 |
| Tm | 745 |
| U | 745 |
| W | 745 |
| Y | 745 |
| Yb | 745 |
| Sc | 671 |
| Nb3 | 745 |
| Balsamo Target | |
| Diamond Drilling | 13 |
| Diamond Drilling metreage | 1582.5 |
| Drill hole sampling notes | 1577 |
| Lithological descriptions | 487 |

| Description | Quantity |
|---|---|
| Density Analyses | 167 |
| Blank | 70 |
| Standard | 70 |
| Duplicate | 70 |
| $Al_2O_3$ | 1551 |
| Ba | 1517 |
| CaO | 1551 |
| $Cr_2O_3$ | 1517 |
| $Fe_2O_3$ | 1551 |
| $K_2O$ | 1551 |
| MgO | 1551 |
| MnO | 1551 |
| $Na_2O$ | 1572 |
| $Nb_3$ | 1577 |
| $Nb_1$ | 12 |
| $Nb_2$ | 1577 |
| $P_2O_5$ | 1551 |
| $SiO_2$ | 1551 |
| Sr | 1517 |
| $TiO_2$ | 1551 |
| Zn | 1517 |
| Zr | 1517 |
| V | 1517 |
| LOI | 1572 |
| Ce | 1577 |
| Co | 1577 |
| Cs | 1577 |
| Cu | 1577 |
| Dy | 1577 |
| Er | 1577 |
| Eu | 1577 |
| Ga | 813 |
| Gd | 1577 |
| Hf | 1577 |
| Ho | 1577 |
| La | 1577 |
| Lu | 1577 |
| Mo | 1577 |
| Nd | 1577 |
| Ni | 1577 |
| Pr | 1577 |
| Rb | 1577 |
| Sm | 1577 |
| Sn | 1577 |

| Description | Quantity |
|---|---|
| Ta | 1577 |
| Tb | 1577 |
| Th | 1577 |
| Tl | 1577 |
| Tm | 1577 |
| U | 1577 |
| W | 1577 |
| Y | 1577 |
| Yb | 1577 |
| Alto da Serra Target | |
| Diamond Drilling | 17 |
| Diamond Drilling metreage | 1313.85 |
| Drill hole sampling notes | 1250 |
| Lithological descriptions | 375 |
| Density Analyses | 303 |
| Blank | 55 |
| Standard | 54 |
| Duplicate | 54 |
| $Al_2O_3$ | 1242 |
| Ba | 1180 |
| CaO | 1242 |
| $Cr_2O_3$ | 1180 |
| $Fe_2O_3$ | 1242 |
| $K_2O$ | 1242 |
| MgO | 1242 |
| MnO | 1242 |
| $Na_2O$ | 1242 |
| $Nb_3$ | 1250 |
| $Nb_1$ | 43 |
| $Nb_2$ | 1250 |
| $P_2O_5$ | 1242 |
| $SiO_2$ | 1242 |
| Sr | 1180 |
| $TiO_2$ | 1242 |
| Zn | 1180 |
| Zr | 1180 |
| V | 1180 |
| LOI | 1242 |
| Ce | 1250 |
| Co | 1250 |
| Cs | 1250 |
| Cu | 1250 |
| Dy | 1250 |
| Er | 1250 |

| Description | Quantity |
|---|---|
| Eu | 1250 |
| Ga | 655 |
| Gd | 1250 |
| Hf | 1250 |
| Ho | 1250 |
| La | 1250 |
| Lu | 1250 |
| Mo | 1250 |
| Nd | 1250 |
| Ni | 1250 |
| Pr | 1250 |
| Rb | 1250 |
| Sm | 1250 |
| Sn | 1250 |
| Ta | 1250 |
| Tb | 1250 |
| Th | 1250 |
| Tl | 1250 |
| Tm | 1250 |
| U | 1250 |
| W | 1250 |
| Y | 1250 |
| Yb | 1250 |

The drill holes are distributed in an irregular grid, with distances between holes that vary between 200 and 500 meters. The drill holes that were provided and used in the interpretation are shown in Figure 12.4 to Figure 12.6.

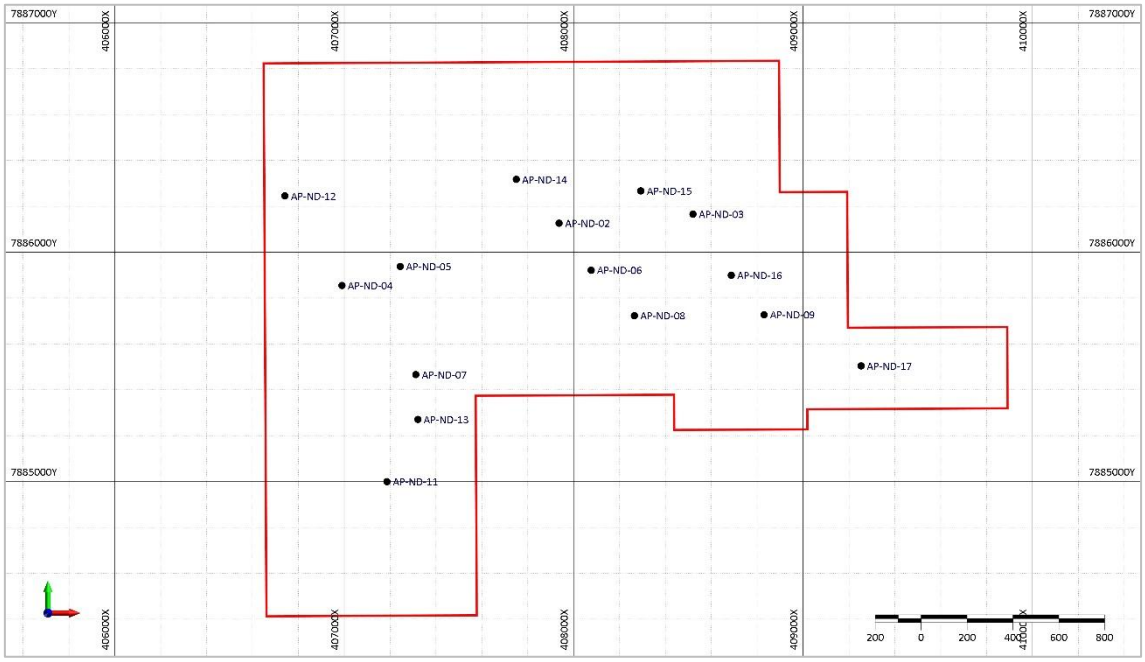



**Figure 12.4 - Holes and ANM limits for the Nau de Guerra Target.**

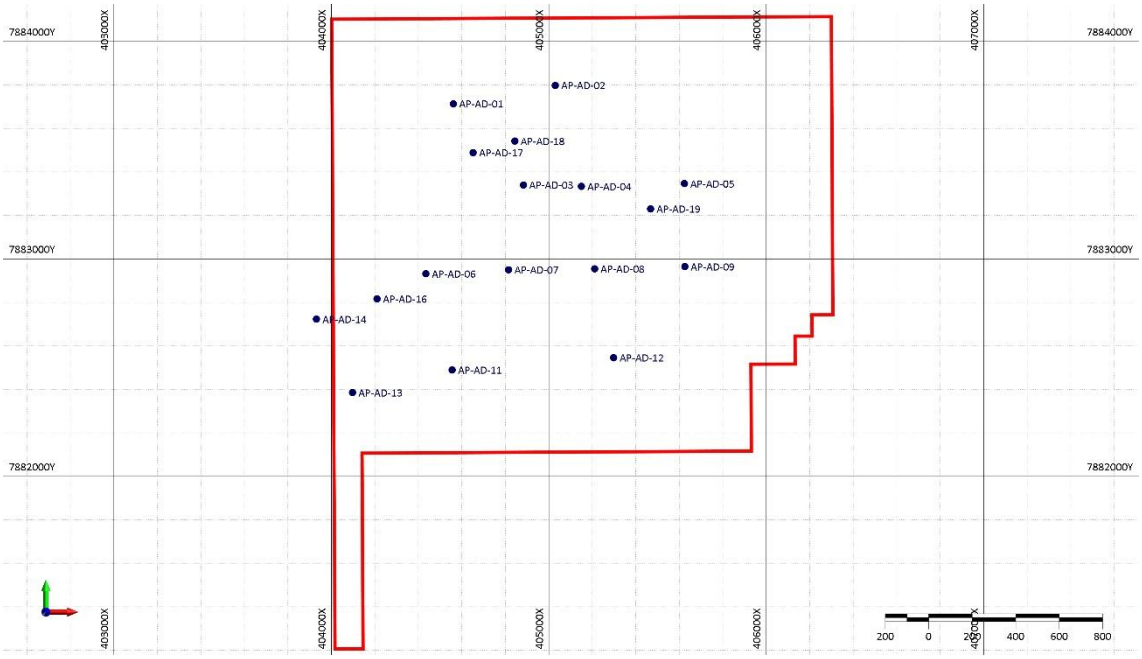



**Figure 12.5 - Holes and ANM limits for the Alto da Serra Target.**

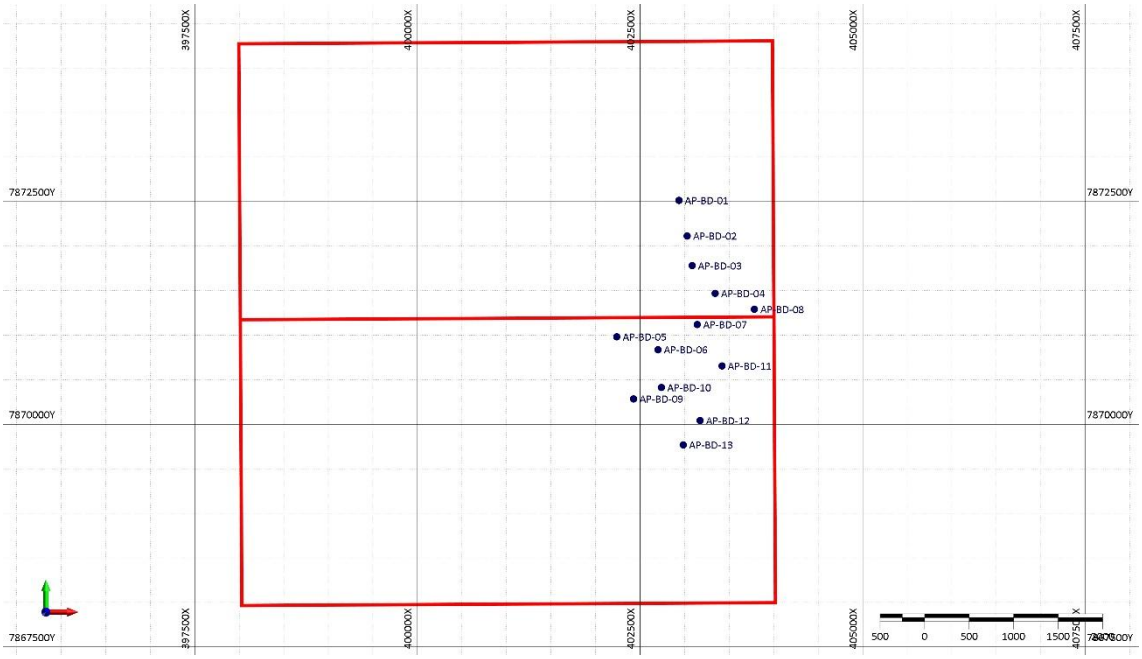



**Figure 12.6 - Holes and ANM limits for the Balsamo Target.**

The descriptive statistics are presented in Table 12.2.

**Table 12.2 - Elements analyzed for all samples in the database**

| Chemical analyses | Quantity | Minimum | Maximum | Average | Variance | Std. Deviation | Variation Coef. |
|---|---|---|---|---|---|---|---|
| Nau de Guerra Target | | | | | | | |
| $Al_2O_3$ | 743 | 2.83 | 17.8 | 6.837 | 5.06502 | 2.25056 | 0.329 |
| Ba | 675 | 5 | 15491 | 2262.92 | 3458021 | 1859.57537 | 0.822 |
| CaO | 743 | 0.01 | 21.98 | 3.191 | 22.49805 | 4.74321 | 1.486 |
| $Cr_2O_3$ | 675 | 0.005 | 0.64 | 0.132 | 0.00904 | 0.09509 | 0.719 |
| $Fe_2O_3$ | 743 | 0.97 | 50.05 | 19.019 | 83.07814 | 9.11472 | 0.479 |
| $K_2O$ | 743 | 0.07 | 7.77 | 3.647 | 3.85036 | 1.96223 | 0.538 |
| MgO | 743 | 0.03 | 11.19 | 3.63 | 4.77223 | 2.18454 | 0.602 |
| MnO | 743 | 0.01 | 1.3 | 0.258 | 0.02408 | 0.15518 | 0.601 |
| $Na_2O$ | 743 | 0.005 | 0.62 | 0.09 | 0.00499 | 0.07061 | 0.784 |
| Nb | 745 | 2.67 | 1312 | 422.631 | 51693.99 | 227.36313 | 0.538 |
| $Nb_1$ | 244 | 0 | 1312 | 122.951 | 69053.92 | 262.78112 | 2.137 |
| $Nb_2$ | 701 | 2.67 | 1010 | 416.448 | 52326.17 | 228.74913 | 0.549 |
| $P_2O_5$ | 743 | 0.02 | 7.27 | 1.34 | 1.23979 | 1.11346 | 0.831 |
| $SiO_2$ | 743 | 7.65 | 90.9 | 45.768 | 317.6638 | 17.82313 | 0.389 |
| Sr | 675 | 12 | 2889 | 861.834 | 316184.8 | 562.30316 | 0.652 |
| $TiO_2$ | 743 | 0.14 | 25.25 | 8.999 | 21.44422 | 4.63079 | 0.515 |
| Zn | 675 | 2.5 | 366 | 141.137 | 4826.804 | 69.47521 | 0.492 |
| Zr | 675 | 77 | 2360 | 725.07 | 134291.2 | 366.4576 | 0.505 |
| V | 675 | 2.5 | 1035 | 356.353 | 27462.61 | 165.71847 | 0.465 |
| LOI | 743 | -0.25 | 22.59 | 5.361 | 15.89504 | 3.98686 | 0.744 |

| Chemical analyses | Quantity | Minimum | Maximum | Average | Variance | Std. Deviation | Variation Coef. |
|---|---|---|---|---|---|---|---|
| Ce | 745 | 9.5 | 5220.3 | 1228.75 | 586465.2 | 765.81016 | 0.623 |
| Co | 745 | 0.25 | 738.1 | 74.012 | 3041.324 | 55.1482 | 0.745 |
| Cs | 745 | 0.12 | 23.1 | 3.137 | 8.10873 | 2.84758 | 0.908 |
| Cu | 745 | 2.5 | 639 | 83.155 | 2150.428 | 46.37271 | 0.558 |
| Dy | 745 | 0.91 | 132.49 | 18.855 | 159.8215 | 12.64205 | 0.67 |
| Er | 745 | 0.54 | 54.75 | 6.066 | 15.83514 | 3.97934 | 0.656 |
| Eu | 745 | 0.3 | 85.33 | 16.533 | 133.3268 | 11.54672 | 0.698 |
| Ga | 211 | 0.05 | 26.6 | 7.295 | 33.30129 | 5.77073 | 0.791 |
| Gd | 745 | 1.19 | 246.29 | 40.325 | 797.7761 | 28.24493 | 0.7 |
| Hf | 745 | 2.01 | 59.81 | 18.073 | 75.04697 | 8.66297 | 0.479 |
| Ho | 745 | 0.21 | 21.73 | 2.747 | 3.24385 | 1.80107 | 0.656 |
| La | 745 | 6.5 | 2549.3 | 608.339 | 153723 | 392.07519 | 0.645 |
| Lu | 745 | 0.09 | 4.55 | 0.494 | 0.08851 | 0.2975 | 0.603 |
| Mo | 745 | 1 | 133 | 5.848 | 129.0186 | 11.35864 | 1.942 |
| Nd | 745 | 4.2 | 2428 | 485.644 | 111542.7 | 333.98005 | 0.688 |
| Ni | 745 | 5 | 628 | 264.293 | 22761.74 | 150.86995 | 0.571 |
| Pr | 745 | 1.45 | 649.97 | 135.225 | 8431.663 | 91.82409 | 0.679 |
| Rb | 745 | 2.2 | 393.4 | 136.922 | 6443.346 | 80.27046 | 0.586 |
| Sm | 745 | 1.2 | 347.7 | 67.282 | 2181.726 | 46.70895 | 0.694 |
| Sn | 745 | 0.15 | 18.2 | 6.71 | 9.52024 | 3.08549 | 0.46 |
| Ta | 745 | 0.025 | 103.19 | 27.491 | 235.3413 | 15.34084 | 0.558 |
| Tb | 745 | 0.18 | 26.49 | 4.188 | 8.15186 | 2.85515 | 0.682 |
| Th | 745 | 1 | 236.7 | 65.599 | 1356.29 | 36.82784 | 0.561 |
| Tl | 745 | 0.25 | 2.1 | 0.286 | 0.02722 | 0.16499 | 0.577 |
| Tm | 745 | 0.1 | 5.92 | 0.686 | 0.18084 | 0.42526 | 0.62 |
| U | 745 | 0.38 | 23.94 | 6.692 | 12.75743 | 3.57175 | 0.534 |
| W | 745 | 0.05 | 508.9 | 13.916 | 1269.033 | 35.62348 | 2.56 |
| Y | 745 | 5.81 | 685.32 | 63.659 | 2084.623 | 45.65767 | 0.717 |
| Yb | 745 | 0.6 | 33.2 | 3.825 | 5.39019 | 2.32168 | 0.607 |
| Sc | 45 | 1.9 | 80.8 | 28.264 | 603.0278 | 24.55662 | 0.869 |
| Alto da Serra and Balsamo Target | | | | | | | |
| $Al_2O_3$ | 2793 | 1.22 | 38.01 | 10 | 6.98 | 71.19491 | 8.43771 |
| Ba | 2697 | 21 | 23503 | 2199.397 | 1503 | 6019334.213 | 2453.43315 |
| CaO | 2793 | 0 | 21.93 | 3.425 | 0.31 | 27.19974 | 5.21534 |
| $Cr_2O_3$ | 2697 | 0 | 0.56 | 0.1 | 0.08 | 0.00724 | 0.08506 |
| $Fe_2O_3$ | 2793 | 0.42 | 60.3 | 16.993 | 15.66 | 95.70602 | 9.78295 |
| $K_2O$ | 2793 | 0 | 9.03 | 2.652 | 2.72 | 5.62122 | 2.37091 |
| MgO | 2793 | 0 | 16.31 | 3.937 | 3.46 | 18.59246 | 4.3119 |
| MnO | 2793 | 0 | 5.96 | 0.212 | 0.2 | 0.07782 | 0.27897 |
| Na2O | 2814 | 0 | 0.95 | 0.107 | 0.08 | 0.01466 | 0.12106 |
| $Nb_3$ | 2827 | 0.24 | 1589 | 337.234 | 311.88 | 58198.61687 | 241.24389 |
| $Nb_1$ | 55 | 1001 | 1589 | 1197.455 | 1190 | 19596.69697 | 139.9882 |
| $Nb_2$ | 2827 | 0.24 | 1010 | 333.739 | 311.88 | 52448.83937 | 229.01712 |
| $P_2O_5$ | 2793 | 0 | 12.25 | 0.936 | 0.77 | 0.93516 | 0.96704 |

| Chemical analyses | Quantity | Minimum | Maximum | Average | Variance | Std. Deviation | Variation Coef. |
|---|---|---|---|---|---|---|---|
| $SiO_2$ | 2793 | 5.06 | 90.9 | 46.008 | 41.96 | 356.0158 | 18.86838 |
| Sr | 2697 | 5 | 4414 | 844.019 | 695 | 575187.7957 | 758.41136 |
| $TiO_2$ | 2793 | 0.07 | 31.3 | 7.634 | 6.92 | 26.81039 | 5.17788 |
| Zn | 2697 | 2.5 | 739 | 121.484 | 108 | 6340.00467 | 79.62415 |
| Zr | 2697 | 86 | 8040 | 747.973 | 624 | 210653.3023 | 458.96983 |
| V | 2697 | 2.5 | 2366 | 367.977 | 325 | 46740.44393 | 216.19538 |
| LOI | 2814 | 0.33 | 24.77 | 7.681 | 5.26 | 27.62956 | 5.25638 |
| Ce | 2827 | 2.5 | 6784.9 | 998.02 | 943.8 | 744065.674 | 862.59241 |
| Co | 2827 | 0 | 542 | 54.503 | 55.8 | 2576.01268 | 50.75444 |
| Cs | 2827 | 0 | 37.95 | 2.238 | 1.5 | 8.21072 | 2.86544 |
| Cu | 2827 | 2.5 | 1405 | 73.349 | 63 | 3628.59561 | 60.23783 |
| Dy | 2827 | 0.32 | 153.18 | 15.435 | 13.53 | 195.8311 | 13.99397 |
| Er | 2827 | 0.17 | 52.01 | 5.347 | 4.32 | 22.06414 | 4.69725 |
| Eu | 2827 | 0.13 | 115.67 | 12.775 | 11.58 | 164.40556 | 12.82207 |
| Ga | 1468 | 0 | 59.2 | 17.995 | 12.9 | 218.82956 | 14.79289 |
| Gd | 2827 | 0.6 | 303.82 | 31.429 | 28.31 | 950.59605 | 30.83174 |
| Hf | 2827 | 0.93 | 60.67 | 17.237 | 15.24 | 83.27695 | 9.12562 |
| Ho | 2827 | 0 | 22.11 | 2.335 | 1.97 | 4.33745 | 2.08265 |
| La | 2827 | 4.4 | 3436.1 | 484.579 | 447.1 | 183627.5407 | 428.51784 |
| Lu | 2827 | 0.05 | 5.96 | 0.49 | 0.4 | 0.16899 | 0.41108 |
| Mo | 2827 | 1 | 106 | 4.253 | 3 | 31.27465 | 5.59237 |
| Nd | 2827 | 2.9 | 3460.2 | 385.113 | 342.5 | 145776.5198 | 381.80691 |
| Ni | 2827 | 2.5 | 835 | 201.732 | 196 | 25382.28284 | 159.31818 |
| Pr | 2827 | 0.82 | 896.7 | 107.829 | 95.42 | 10856.16735 | 104.19293 |
| Rb | 2827 | 0 | 389.4 | 97.406 | 90.4 | 7956.05346 | 89.19671 |
| Sm | 2827 | 0.6 | 484.6 | 52.438 | 47.1 | 2691.18107 | 51.87659 |
| Sn | 2827 | 0 | 88.7 | 6.429 | 6 | 13.02395 | 3.60887 |
| Ta | 2827 | 0 | 123.42 | 22.031 | 19.8 | 284.8859 | 16.87856 |
| Tb | 2827 | 0.11 | 31.99 | 3.362 | 3.01 | 9.9409 | 3.15292 |
| Th | 2827 | 0.8 | 299.8 | 54.779 | 47.6 | 1336.58193 | 36.55929 |
| Tl | 2827 | 0 | 2.3 | 0.009 | 0 | 0.00863 | 0.09292 |
| Tm | 2827 | 0.08 | 6.88 | 0.633 | 0.51 | 0.29049 | 0.53897 |
| U | 2827 | 0.4 | 35.33 | 6.296 | 5.3 | 19.41571 | 4.40633 |
| W | 2827 | 0 | 1319.2 | 19.585 | 6 | 4520.16166 | 67.23215 |
| Y | 2827 | 3.31 | 797.96 | 55.28 | 44.52 | 3212.82831 | 56.68182 |
| Yb | 2827 | 0.5 | 40.1 | 3.659 | 3.1 | 8.93724 | 2.98952 |

### 12.2.1 Database Verification Performed using the Micromine System

The database was tested using specific processes to determine the existence of any of the errors listed below:

- The name of the drill hole is present in the collar file but is missing from the analytical database;
- The name of the drill hole is present in the analytical database, but is absent in the collar file;
- The name of the drill hole is repeated in the analytical database and in the collar file;
- The name of the drill hole does not appear in the collar file and in the analytical database;
- One or more coordinate notes are absent from the collar file;
- FROM or TO are not present in the analytical database;
- FROM > TO in the analytical database;
- Sampling intervals are not continuous in the analytical database (there are gaps between the logs);
- Sampling intervals overlap in the analytical database;
- The first sample does not correspond to 0 m in the analytical database;
- The azimuth is not within the range of 0-360 degrees;
- The dip is not within the range of 0-90 degrees;
- The azimuth or dip of the hole is missing;
- The total depth of the hole is shallower than the depth of the last sample.

After performing the aforementioned analysis, no errors were found in the database, as its structure was found to be consistent. It was therefore concluded that the verification was satisfactory.

BNA conducted random checks on approximately 10% of the assay certificates per target to validate the assay values entered into the database. No errors were detected.

With regard to the drilling program, the author has been able to confirm the accuracy of the locations of the drill holes by checking them using his own handheld GPS unit. Some drill holes were not located because due to the fact that they are located on agricultural land (private property) and had been removed by landowners during farming activities.

During his visits to the property during the drilling programs, the author confirmed that sampling was being conducted in accordance with the protocols, described in Chapter 11 above, and that the data collected on drill samples to date is therefore accurate.

There have been no limitations on the author in terms of his ability to verify any of the data presented in this report. The author's opinion is that all data presented in this report are adequate for the purposes of this report and are presented in a manner that is not misleading.

## 12.3 QA/QC Analyses

The laboratory SGS GEOSOL LABORATÓRIOS LTDA. was hired by Verde to serve as the main laboratory for physical preparation and chemical analysis of the resource samples for the three targets.

One drilling campaign and round of chemical analysis were carried out. The verifications and conclusions of this work are described in the following items.

For the Nau de Guerra target, 15 batches of chemical analysis were delivered to BNA. A total of 62 quality control samples were selected. Of these, 32 are Duplicates, 32 are Standards and 32 are Blanks. The following elements were analyzed: Ba, Ce, Cs, Dy, Er, Eu, Ga, Gd, Hf, Ho, La, Lu, Nb, Nd, Pr, Rb, Sm, Sn, Sr, Ta, Tb, Th, Tm, U, V, W, Y, Yb, Zr, $SiO_2$, $Al_2O_3$, $Fe_2O_3$, CaO, MgO, $Na_2O$, $K_2O$, $Cr_2O_3$, $TiO_2$, MnO, $P_2O_5$ and LOI.

For the Alto da Serra and Balsamo targets, 57 batches of chemical analysis were delivered to BNA. A total of 373 quality control samples were selected. Of these, 124 are Duplicates, 124 are Standards and 125 are Blanks. The following elements were analyzed: Ba, Ce, Cs, Dy, Er, Eu, Ga, Gd, Hf, Ho, La, Lu, Nb, Nd, Pr, Rb, Sm, Sn, Sr, Ta, Tb, Th, Tm, U, V, W, Y, Yb, Zr, $SiO_2$, $Al_2O_3$, $Fe_2O_3$, CaO, MgO, Na2O, $K_2O$, $Cr_2O_3$, $TiO_2$, MnO, $P_2O_5$ and LOI.

The analytical results were received by BNA and imported into the corresponding spreadsheet.

The topics below present the accuracy of the quality control analyses, in terms of the percentage difference between an initial analysis and its repetition. For example, an accuracy of 10% would mean that the initial analysis and the repetition differ by 10%.

## 12.4 QA/QC – Nau de Guerra Target

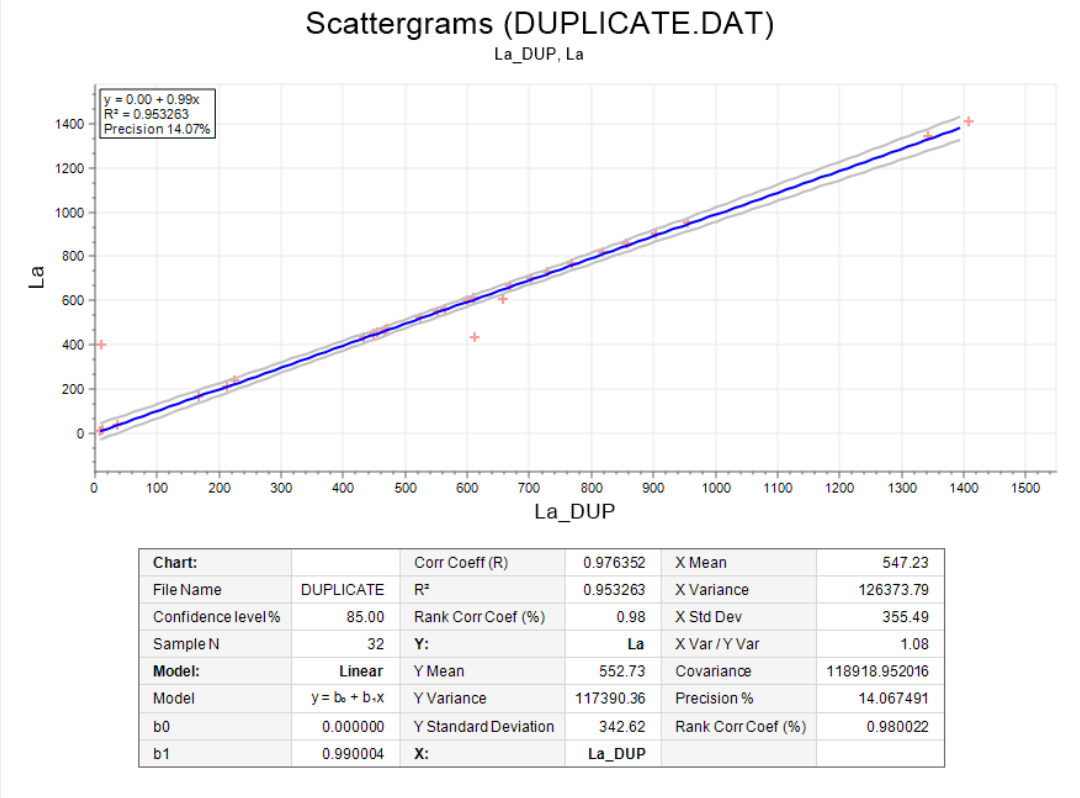
### 12.4.1 Sampling Precision

Sampling precision was assessed using the repeated analysis method, for REE (Y, Ce, La, Nd, Tb and Pr). From a total of 745 samples, 32 samples were reanalyzed. This represents 4.3% of the total number of assays.

The internal quality control data were presented as a single batch of data, with no separation of the samples by grade ranges or by sample collection dates. Two evaluative methods were used: Simple Linear Regression and Q-Q plot (quantile--quantile plot).

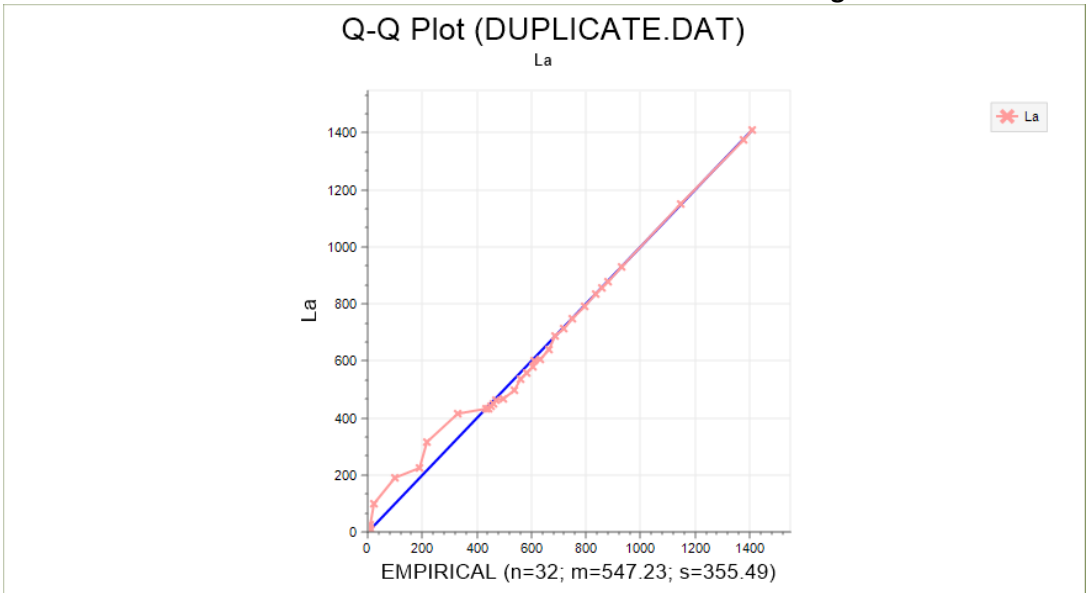
In general, the Diamond Drilling showed satisfactory quality and accuracy in the statistical analysis, with precision rates of up to 10-15%.

The correlation coefficient of the regular control sample values is above 0.99. One can therefore conclude that the tests for the most important elements of the studied ore were conducted with satisfactory and acceptable levels of precision. The results of the data processing for La and Nd are shown in Figure 12.7 to Figure 12.10. Graphs for Ce, Pr, Tb and Y can be found in APPENDIX III.



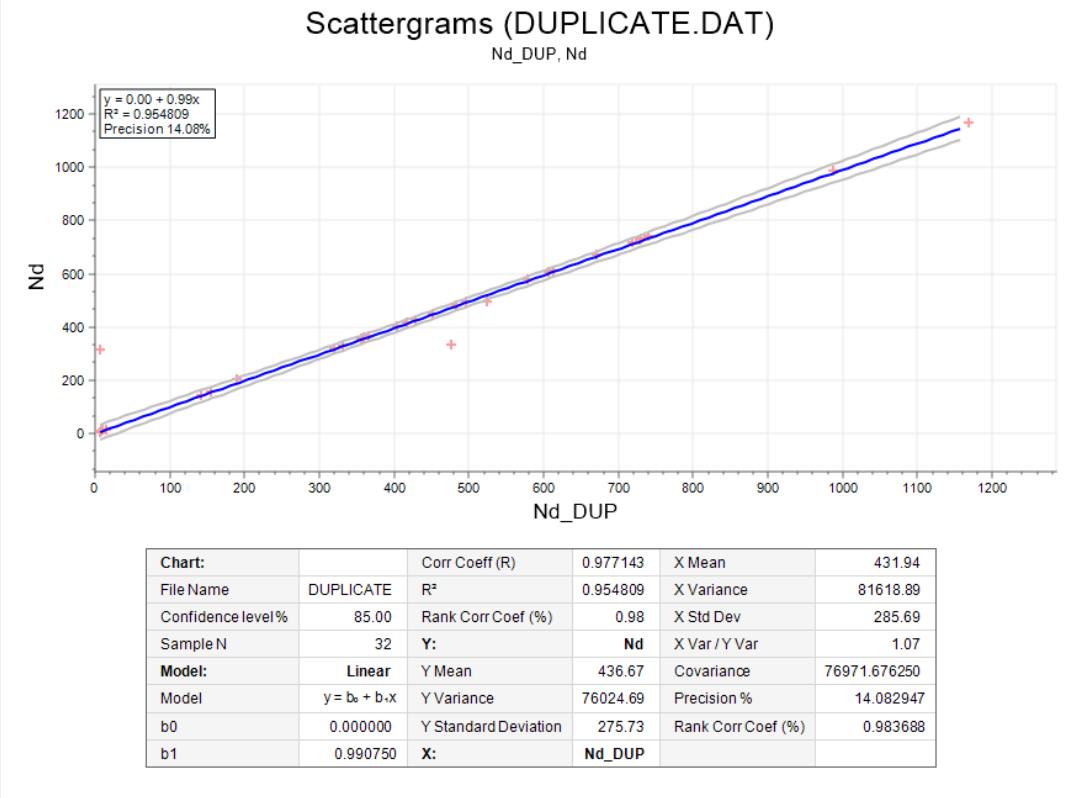

| Chart: | | Corr Coeff (R) | 0.976352 | X Mean | 547.23 |
|---|---|---|---|---|---|
| File Name | DUPLICATE | R² | 0.953263 | X Variance | 126373.79 |
| Confidence level % | 85.00 | Rank Corr Coef (%) | 0.98 | X Std Dev | 355.49 |
| Sample N | 32 | **Y:** | **La** | X Var / Y Var | 1.08 |
| **Model:** | **Linear** | Y Mean | 552.73 | Covariance | 118918.952016 |
| Model | $y = b_0 + b_1x$ | Y Variance | 117390.36 | Precision % | 14.067491 |
| b0 | 0.000000 | Y Standard Deviation | 342.62 | Rank Corr Coef (%) | 0.980022 |
| b1 | 0.990004 | **X:** | **La_DUP** | | |

**Figure 12.7 - Linear Regression Diagram for La ppm, field duplicate, class: Diamond Drilling, internal control results for the Nau de Guerra Target.**



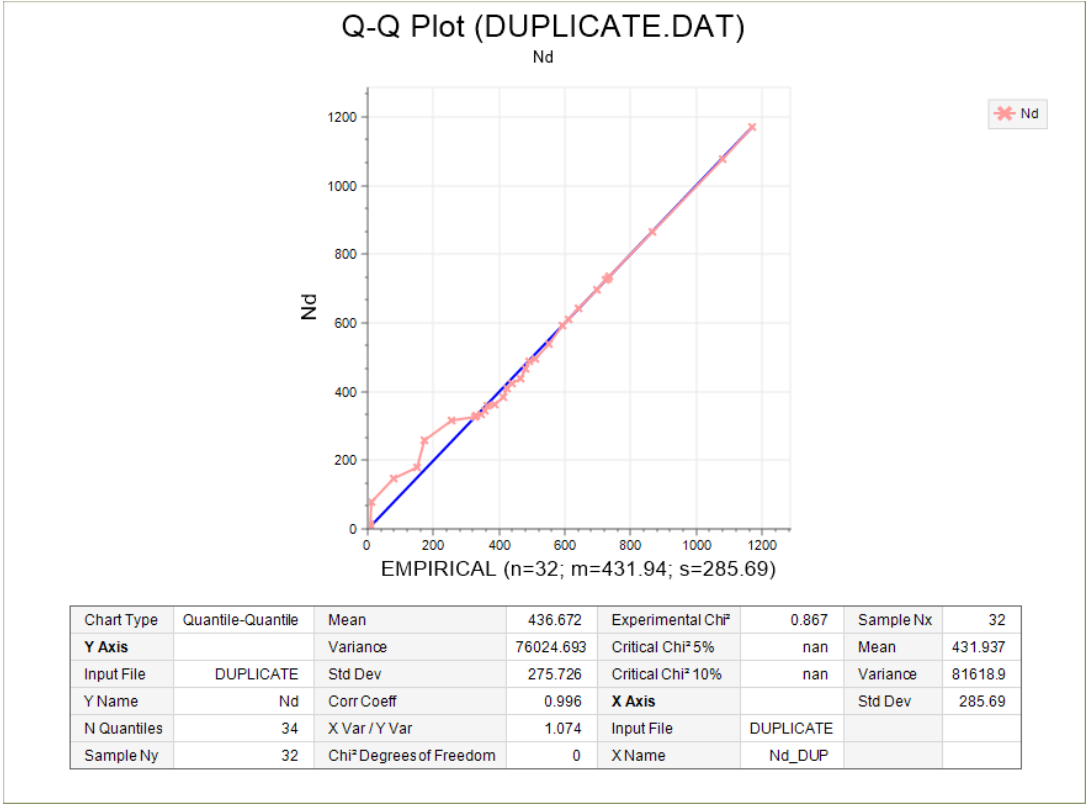

| Chart Type | Quantile-Quantile | Mean | 552.725 | Experimental Chi² | 0.833 | Sample Nx | 32 |
|---|---|---|---|---|---|---|---|
| **Y Axis** | | Variance | 117390.362 | Critical Chi² 5% | nan | Mean | 547.234 |
| Input File | DUPLICATE | Std Dev | 342.623 | Critical Chi² 10% | nan | Variance | 126374 |
| Y Name | La | Corr Coeff | 0.996 | **X Axis** | | Std Dev | 355.491 |
| N Quantiles | 34 | X Var / Y Var | 1.077 | Input File | DUPLICATE | | |
| Sample Ny | 32 | Chi² Degrees of Freedom | 0 | X Name | La_DUP | | |

**Figure 12.8 - Quantis plotting for La ppm, field duplicate, class: Diamond Drilling, internal control results for the Nau de Guerra Target.**




| Chart: | | Corr Coeff (R) | 0.977143 | X Mean | 431.94 |
|---|---|---|---|---|---|
| File Name | DUPLICATE | R² | 0.954809 | X Variance | 81618.89 |
| Confidence level % | 85.00 | Rank Corr Coef (%) | 0.98 | X Std Dev | 285.69 |
| Sample N | 32 | **Y:** | **Nd** | X Var / Y Var | 1.07 |
| **Model:** | **Linear** | Y Mean | 436.67 | Covariance | 76971.676250 |
| Model | $y = b_0 + b_1 x$ | Y Variance | 76024.69 | Precision % | 14.082947 |
| b0 | 0.000000 | Y Standard Deviation | 275.73 | Rank Corr Coef (%) | 0.983688 |
| b1 | 0.990750 | **X:** | **Nd_DUP** | | |

**Figure 12.9 - Linear Regression Diagram for Nd ppm, field duplicate, class: Diamond Drilling, internal control results for the Nau de Guerra Target.**




| Chart Type | Quantile-Quantile | Mean | 436.672 | Experimental Chi² | 0.867 | Sample Nx | 32 |
|---|---|---|---|---|---|---|---|
| **Y Axis** | | Variance | 76024.693 | Critical Chi² 5% | nan | Mean | 431.937 |
| Input File | DUPLICATE | Std Dev | 275.726 | Critical Chi² 10% | nan | Variance | 81618.9 |
| Y Name | Nd | Corr Coeff | 0.996 | **X Axis** | | Std Dev | 285.69 |
| N Quantiles | 34 | X Var / Y Var | 1.074 | Input File | DUPLICATE | | |
| Sample Ny | 32 | Chi² Degrees of Freedom | 0 | X Name | Nd_DUP | | |

**Figure 12.10 - Quantis plotting for La ppm, field duplicate, class: Diamond Drilling, internal control results for the Nau de Guerra Target.**

### 12.4.2 Standards

32 Standards were used for the quality control process. These, represented 4.3% of the total number of samples analyzed.

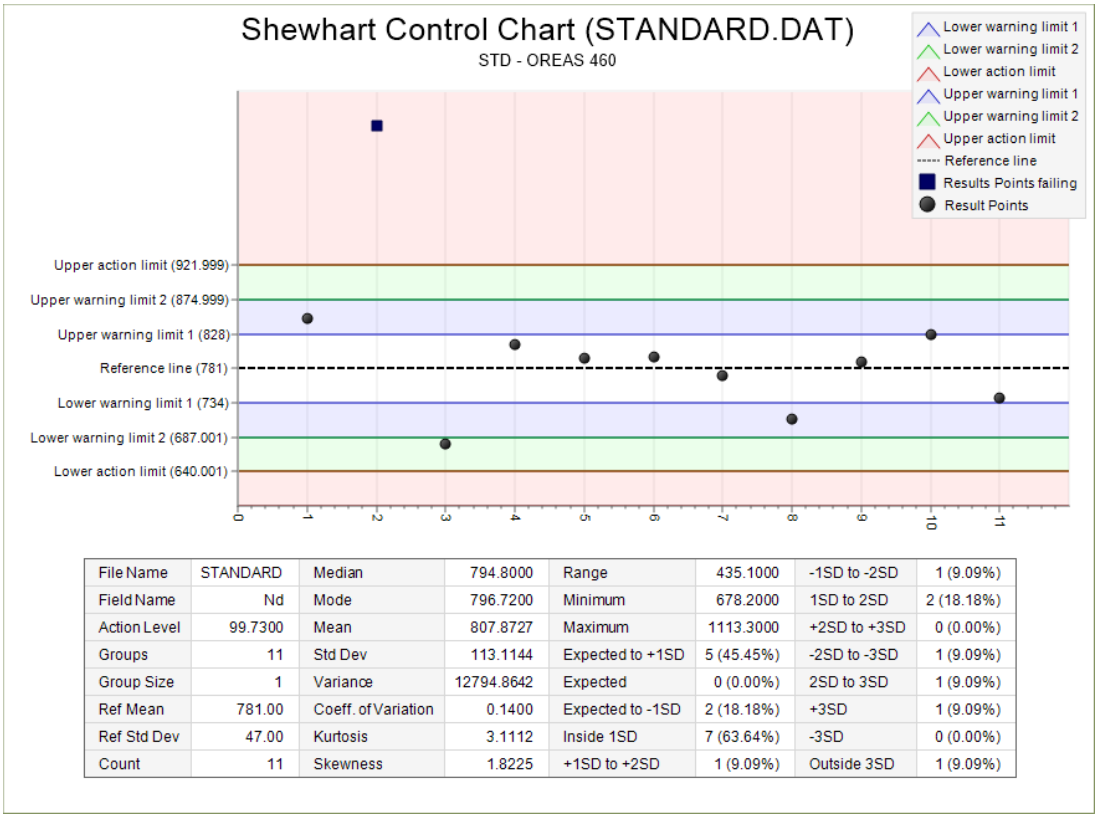
List of the standard samples used:

- OREAS 460 Certificate, (results from 11 analyses);
- OREAS 461 Certificate (results from 10 analyses);
- SG-142 Certificate (results from 11 analyses);

These certificates are presented in the APPENDIX I section of this report.

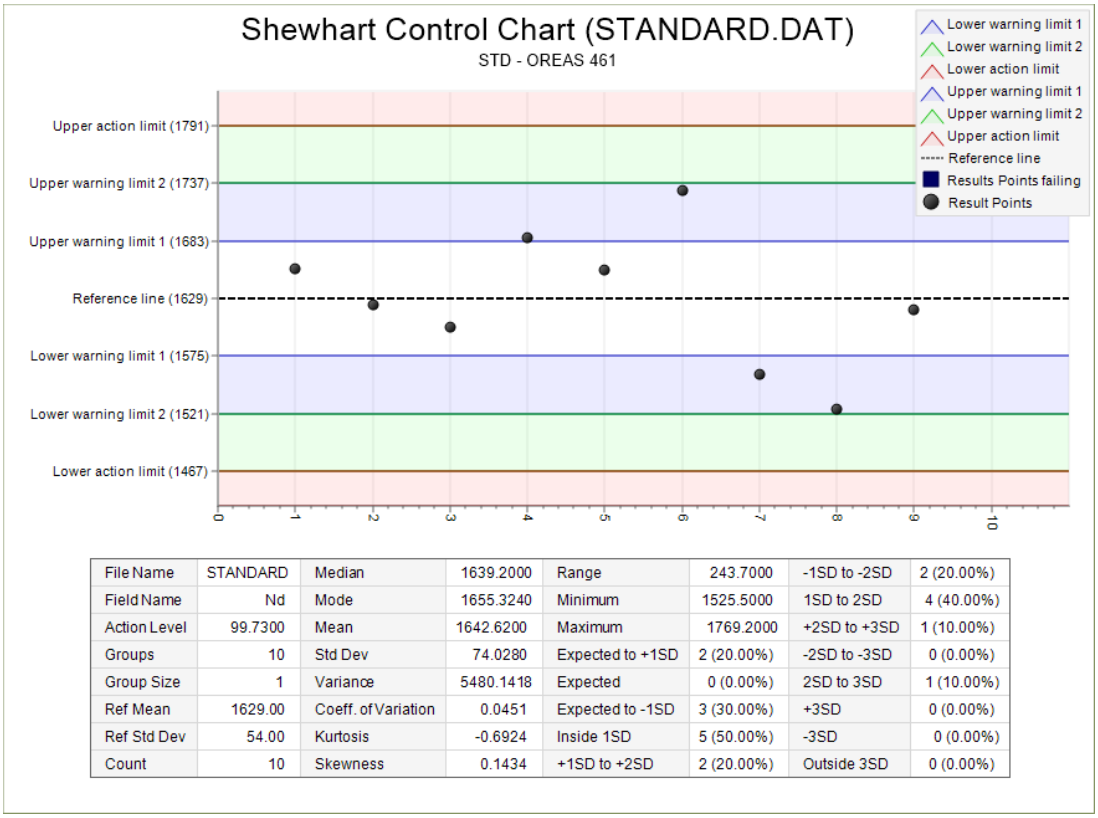
For each type of standard, the results were analyzed using a Shewhart Control Chart.

The data analyzed for Nd are shown in Figure 12.11 to Figure 12.13 Graphs for La, Ce and Y can be found in APPENDIX III.



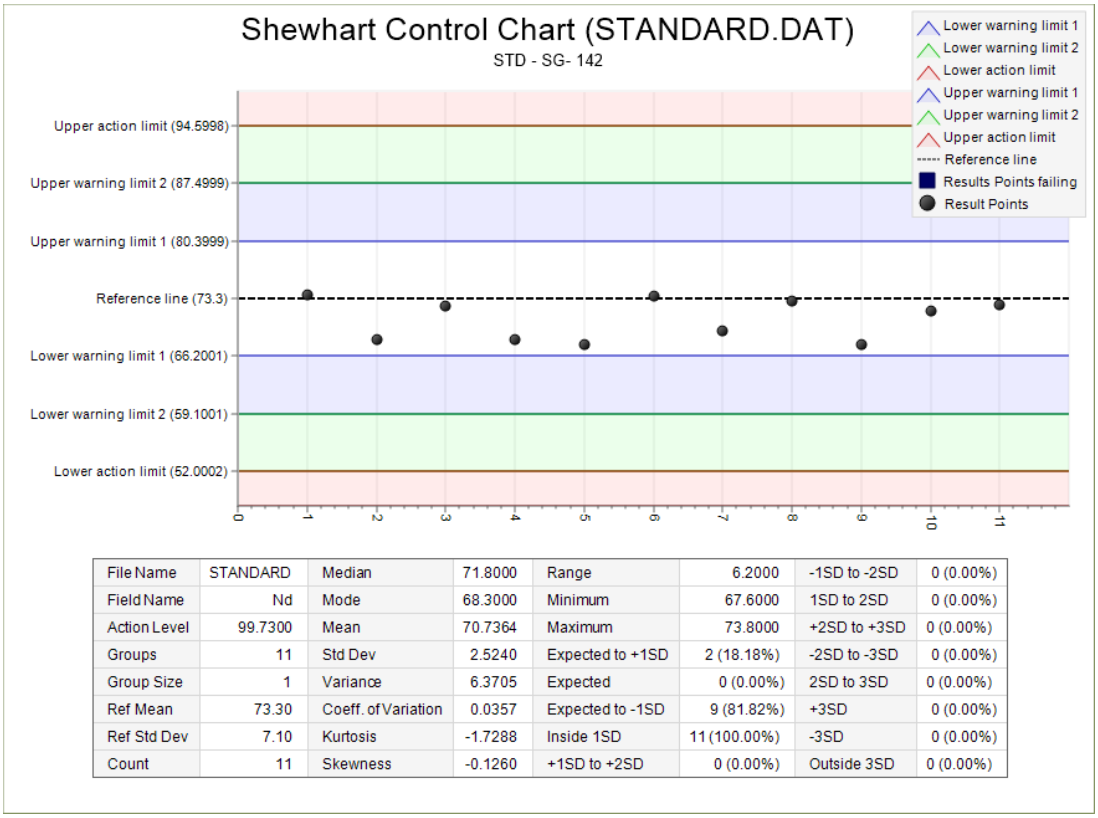

| File Name | STANDARD | Median | 794.8000 | Range | 435.1000 | -1SD to -2SD | 1 (9.09%) |
| --- | --- | --- | --- | --- | --- | --- | --- |
| Field Name | Nd | Mode | 796.7200 | Minimum | 678.2000 | 1SD to 2SD | 2 (18.18%) |
| Action Level | 99.7300 | Mean | 807.8727 | Maximum | 1113.3000 | +2SD to +3SD | 0 (0.00%) |
| Groups | 11 | Std Dev | 113.1144 | Expected to +1SD | 5 (45.45%) | -2SD to -3SD | 1 (9.09%) |
| Group Size | 1 | Variance | 12794.8642 | Expected | 0 (0.00%) | 2SD to 3SD | 1 (9.09%) |
| Ref Mean | 781.00 | Coeff. of Variation | 0.1400 | Expected to -1SD | 2 (18.18%) | +3SD | 1 (9.09%) |
| Ref Std Dev | 47.00 | Kurtosis | 3.1112 | Inside 1SD | 7 (63.64%) | -3SD | 0 (0.00%) |
| Count | 11 | Skewness | 1.8225 | +1SD to +2SD | 1 (9.09%) | Outside 3SD | 1 (9.09%) |

**Figure 12.11 - Standard OREAS 460, element Nd.**




| File Name | STANDARD | Median | 1639.2000 | Range | 243.7000 | -1SD to -2SD | 2 (20.00%) |
| --- | --- | --- | --- | --- | --- | --- | --- |
| Field Name | Nd | Mode | 1655.3240 | Minimum | 1525.5000 | 1SD to 2SD | 4 (40.00%) |
| Action Level | 99.7300 | Mean | 1642.6200 | Maximum | 1769.2000 | +2SD to +3SD | 1 (10.00%) |
| Groups | 10 | Std Dev | 74.0280 | Expected to +1SD | 2 (20.00%) | -2SD to -3SD | 0 (0.00%) |
| Group Size | 1 | Variance | 5480.1418 | Expected | 0 (0.00%) | 2SD to 3SD | 1 (10.00%) |
| Ref Mean | 1629.00 | Coeff. of Variation | 0.0451 | Expected to -1SD | 3 (30.00%) | +3SD | 0 (0.00%) |
| Ref Std Dev | 54.00 | Kurtosis | -0.6924 | Inside 1SD | 5 (50.00%) | -3SD | 0 (0.00%) |
| Count | 10 | Skewness | 0.1434 | +1SD to +2SD | 2 (20.00%) | Outside 3SD | 0 (0.00%) |

**Figure 12.12 - Standard OREAS 461, element Nd.**




| File Name | STANDARD | Median | 71.8000 | Range | 6.2000 | -1SD to -2SD | 0 (0.00%) |
| --- | --- | --- | --- | --- | --- | --- | --- |
| Field Name | Nd | Mode | 68.3000 | Minimum | 67.6000 | 1SD to 2SD | 0 (0.00%) |
| Action Level | 99.7300 | Mean | 70.7364 | Maximum | 73.8000 | +2SD to +3SD | 0 (0.00%) |
| Groups | 11 | Std Dev | 2.5240 | Expected to +1SD | 2 (18.18%) | -2SD to -3SD | 0 (0.00%) |
| Group Size | 1 | Variance | 6.3705 | Expected | 0 (0.00%) | 2SD to 3SD | 0 (0.00%) |
| Ref Mean | 73.30 | Coeff. of Variation | 0.0357 | Expected to -1SD | 9 (81.82%) | +3SD | 0 (0.00%) |
| Ref Std Dev | 7.10 | Kurtosis | -1.7288 | Inside 1SD | 11 (100.00%) | -3SD | 0 (0.00%) |
| Count | 11 | Skewness | -0.1260 | +1SD to +2SD | 0 (0.00%) | Outside 3SD | 0 (0.00%) |

**Figure 12.13 - Standard SG-142, element Nd.**

In general, the results for rare earth elements that were analyzed, provided by SGS, do not present problems when compared with the known results. Only one standard sample, YM 399 from batch GQ2407379, shows values in excess of three standard deviations. The other standard samples from this batch do not, however, exhibit this issue.

### 12.4.3 Blank Samples

32 Blank Samples were used for contamination control of the sample preparation process. These represent 4.3% of the total number of samples analyzed.

The reference material used in the blank samples is a Quartz Blank.

The results of the analyses performed for the elements are shown in Table 12.3 below. In general, the results for rare earth elements that were analyzed, provided by SGS, do not present problems in terms of contamination during sample preparation, and/or due to wear and cleanliness of the equipment.

**Table 12.3 - Descriptive statistics for the blank sample chemical analysis results**

| Chemical analyses | Quantity | Minimum | Maximum | Average | Median | Variance | Std. Deviation |
|---|---|---|---|---|---|---|---|
| Y | 32 | 0.025 | 8.67 | 1.429 | 1.155 | 2.14281 | 1.46383 |
| La | 32 | 0.05 | 22.6 | 3.264 | 2.2 | 18.14197 | 4.25934 |
| Ce | 32 | 0.05 | 15.5 | 5.278 | 4.65 | 17.03515 | 4.12737 |
| Pr | 32 | 0.025 | 4.44 | 0.88 | 0.72 | 0.66834 | 0.81752 |
| Nd | 32 | 0.05 | 13.6 | 2.989 | 2.55 | 7.05092 | 2.65536 |
| Sm | 32 | 0.05 | 2 | 0.536 | 0.4 | 0.14842 | 0.38526 |
| Eu | 32 | 0.025 | 0.32 | 0.099 | 0.085 | 0.00518 | 0.07195 |
| Gd | 32 | 0.025 | 1.76 | 0.396 | 0.295 | 0.12496 | 0.35349 |
| Tb | 32 | 0.025 | 0.29 | 0.056 | 0.025 | 0.00294 | 0.0542 |
| Dy | 32 | 0.025 | 1.25 | 0.258 | 0.21 | 0.05979 | 0.24452 |
| Ho | 32 | 0.025 | 0.29 | 0.056 | 0.025 | 0.00298 | 0.05458 |
| Er | 32 | 0.025 | 0.78 | 0.153 | 0.12 | 0.01882 | 0.13719 |
| Tm | 32 | 0.025 | 0.14 | 0.03 | 0.025 | 0.00044 | 0.02106 |
| Yb | 32 | 0.05 | 0.6 | 0.091 | 0.05 | 0.01184 | 0.10883 |
| Lu | 32 | 0.025 | 0.12 | 0.03 | 0.025 | 0.00037 | 0.01911 |

## 12.5 QA/QC – Balsamo and Alto da Serra Target

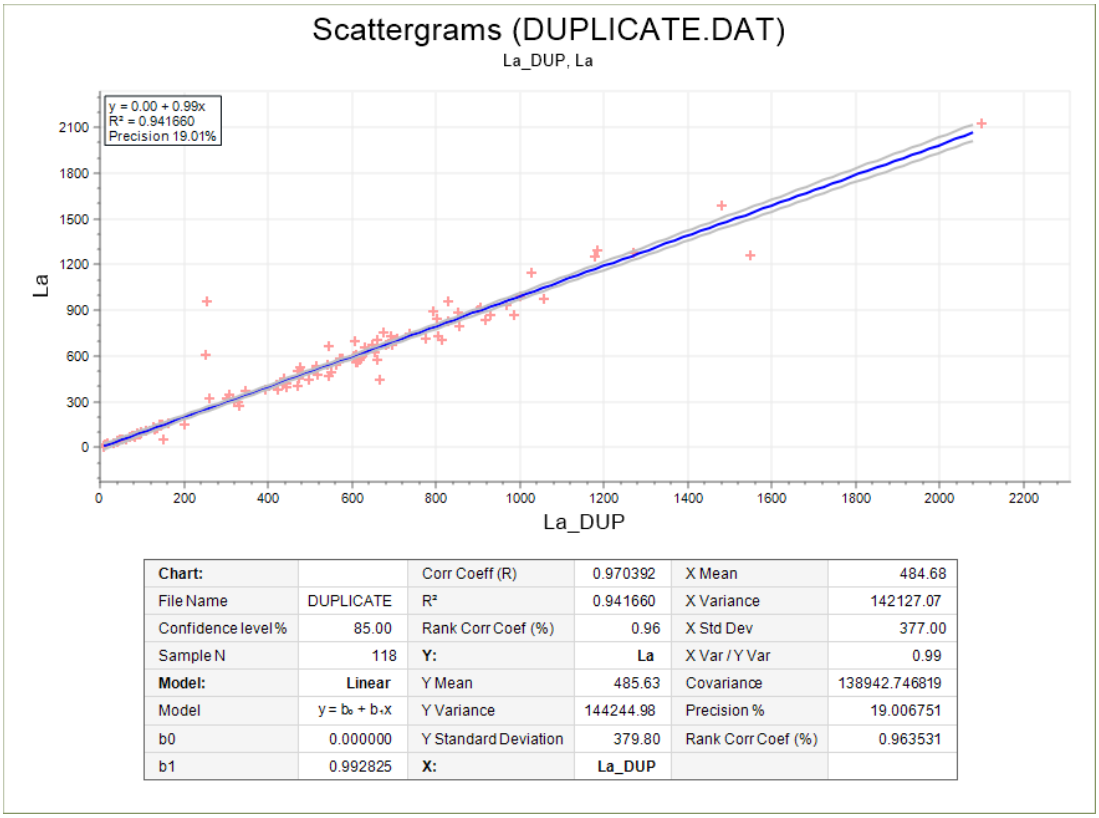
### 12.5.1 Sampling Precision

Sampling precision was assessed using the repeated analysis method, for REE (Y, Ce, La, Nd, Tb and Pr). From a total of 2827 samples, 124 samples, representing 4.4% of the total number of assays, were reanalyzed.

The internal quality control data were presented as a single batch of data, with no separation of the samples by grade ranges or by sample collection date. Two evaluative methods were used: Simple Linear Regression and Q-Q plot (quantile-quantile plot).

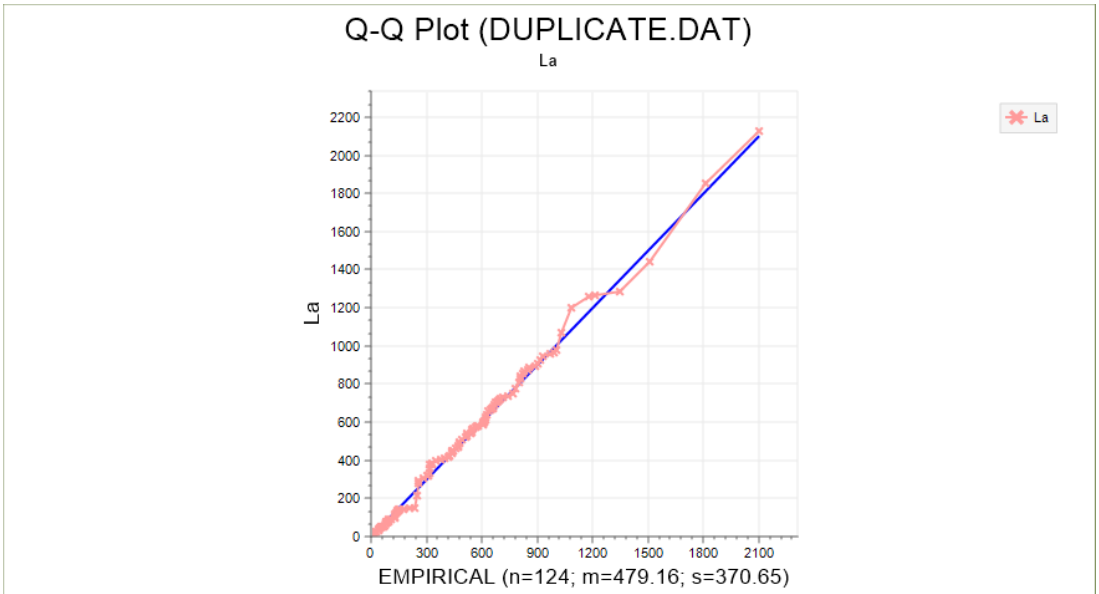
In general, Diamond Drilling showed satisfactory quality and accuracy in the statistical analysis, with a precision level of approximately 19-22%.

The correlation coefficient for the regular control samples values is above 0.96. One can therefore conclude that the tests for the most important elements of the studied ore were conducted with satisfactory and acceptable levels of precision. The results of the data processing for La are Nd are shown in Figure 12.14 to Figure 12.17. Graphs for Ce, Pr, Tb and Y can be found in APPENDIX III.



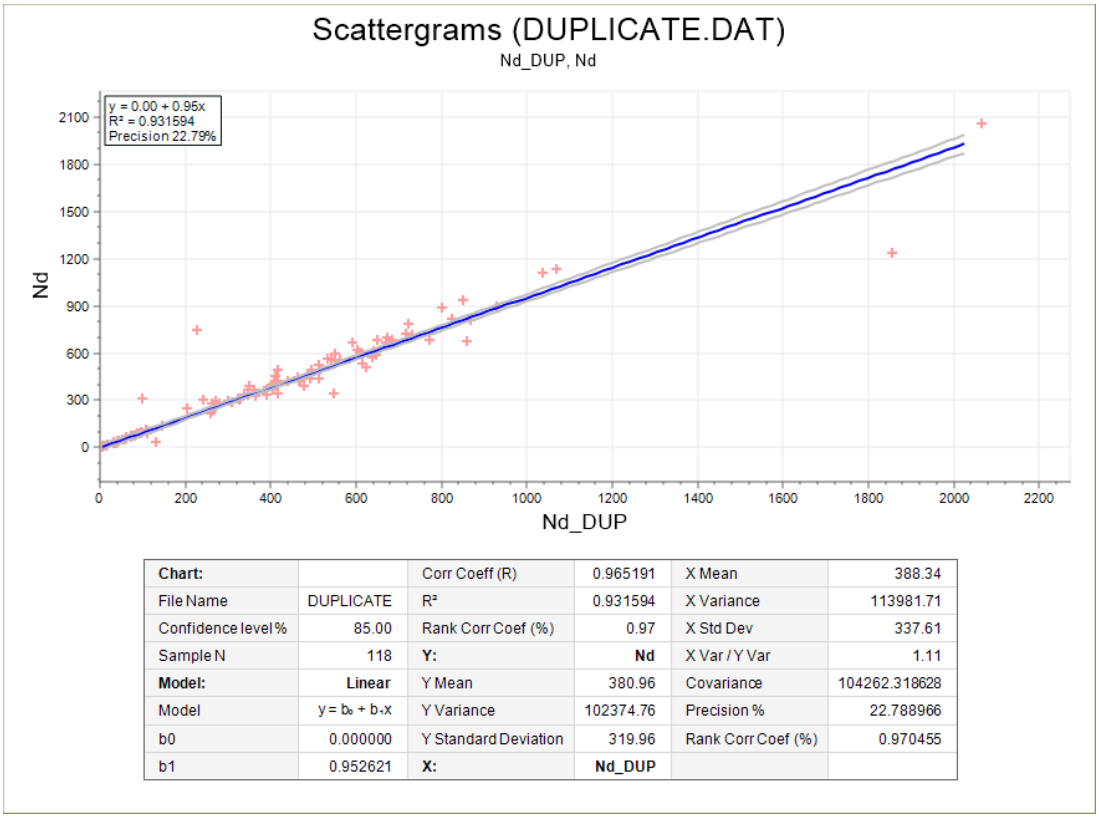

| Chart: | | Corr Coeff (R) | 0.970392 | X Mean | 484.68 |
|---|---|---|---|---|---|
| File Name | DUPLICATE | R² | 0.941660 | X Variance | 142127.07 |
| Confidence level % | 85.00 | Rank Corr Coef (%) | 0.96 | X Std Dev | 377.00 |
| Sample N | 118 | **Y:** | **La** | X Var / Y Var | 0.99 |
| **Model:** | **Linear** | Y Mean | 485.63 | Covariance | 138942.746819 |
| Model | $y = b_0 + b_1 x$ | Y Variance | 144244.98 | Precision % | 19.006751 |
| b0 | 0.000000 | Y Standard Deviation | 379.80 | Rank Corr Coef (%) | 0.963531 |
| b1 | 0.992825 | **X:** | **La_DUP** | | |

**Figure 12.14 - Linear Regression Diagram for La ppm, field duplicate, class: Diamond Drilling, internal control results for the Balsamo and Alto da Serra targets.**



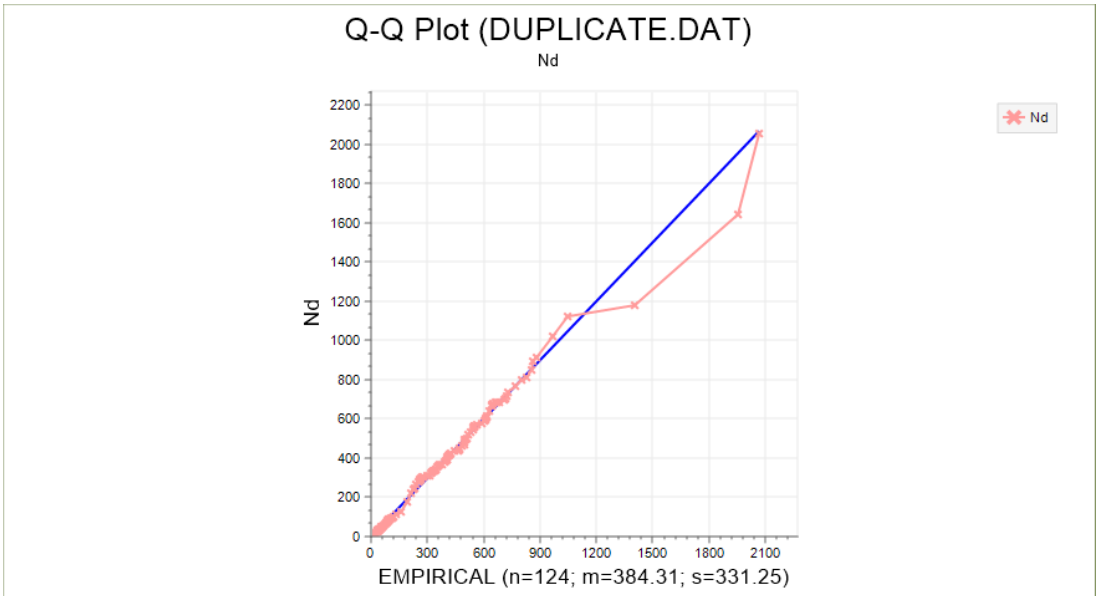

| Chart Type | Quantile-Quantile | Mean | 485.634 | Experimental Chi² | 7.810 | Sample Nx | 124 |
|---|---|---|---|---|---|---|---|
| **Y Axis** | | Variance | 144244.980 | Critical Chi² 5% | 5.991 | Mean | 479.16 |
| Input File | DUPLICATE | Std Dev | 379.796 | Critical Chi² 10% | 4.605 | Variance | 137380 |
| Y Name | La | Corr Coeff | 0.998 | **X Axis** | | Std Dev | 370.648 |
| N Quantiles | 120 | X Var / Y Var | 0.952 | Input File | DUPLICATE | | |
| Sample Ny | 118 | Chi² Degrees of Freedom | 2 | X Name | La_DUP | | |

**Figure 12.15 - Quantis plotting for La ppm, field duplicate, class: Diamond Drilling, internal control results for the Balsamo and Alto da Serra targets.**




| Chart: | | Corr Coeff (R) | 0.965191 | X Mean | 388.34 |
|---|---|---|---|---|---|
| File Name | DUPLICATE | $R^2$ | 0.931594 | X Variance | 113981.71 |
| Confidence level % | 85.00 | Rank Corr Coef (%) | 0.97 | X Std Dev | 337.61 |
| Sample N | 118 | **Y:** | **Nd** | X Var / Y Var | 1.11 |
| **Model:** | **Linear** | Y Mean | 380.96 | Covariance | 104262.318628 |
| Model | $y = b_0 + b_1 x$ | Y Variance | 102374.76 | Precision % | 22.788966 |
| b0 | 0.000000 | Y Standard Deviation | 319.96 | Rank Corr Coef (%) | 0.970455 |
| b1 | 0.952621 | **X:** | **Nd_DUP** | | |

**Figure 12.16 - Linear Regression Diagram for Nd ppm, field duplicate, class: Diamond Drilling, internal control results for the Balsamo and Alto da Serra targets.**




| Chart Type | Quantile-Quantile | Mean | 380.964 | Experimental Chi² | 8.319 | Sample Nx | 124 |
|---|---|---|---|---|---|---|---|
| **Y Axis** | | Variance | 102374.760 | Critical Chi² 5% | 5.991 | Mean | 384.314 |
| Input File | DUPLICATE | Std Dev | 319.961 | Critical Chi² 10% | 4.605 | Variance | 109729 |
| Y Name | Nd | Corr Coeff | 0.994 | **X Axis** | | Std Dev | 331.253 |
| N Quantiles | 120 | X Var / Y Var | 1.072 | Input File | DUPLICATE | | |
| Sample Ny | 118 | Chi² Degrees of Freedom | 2 | X Name | Nd_DUP | | |

**Figure 12.17 - Quantis plotting for La ppm, field duplicate, class: Diamond Drilling, internal control results for the Balsamo and Alto da Serra targets.**

### 12.5.2 Standards

124 Standards were used for quality control. These represented 4.5% of the total number of samples analyzed.

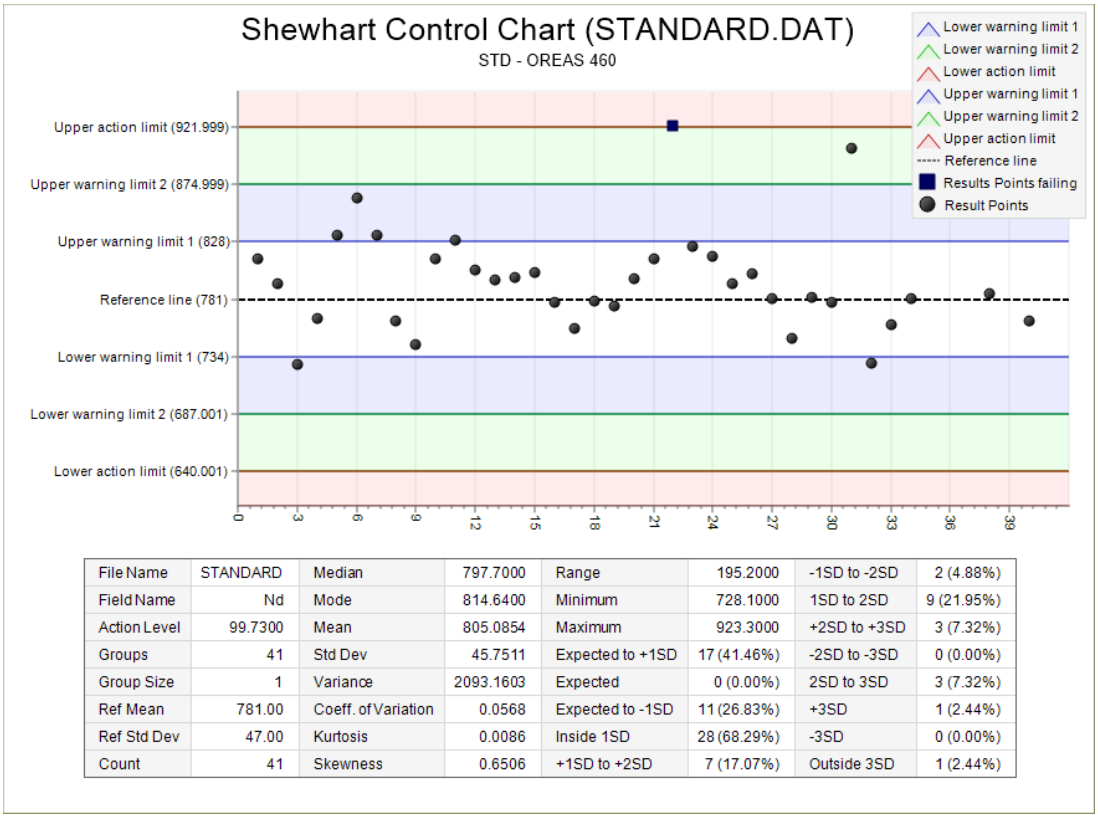
List of the standard samples used:

- OREAS 460 Certificate, (results from 41 analyses);
- OREAS 461 Certificate (results from 41 analyses);
- SG-142 Certificate (results from 42 analyses);

These certificates are presented in APPENDIX I of this report.

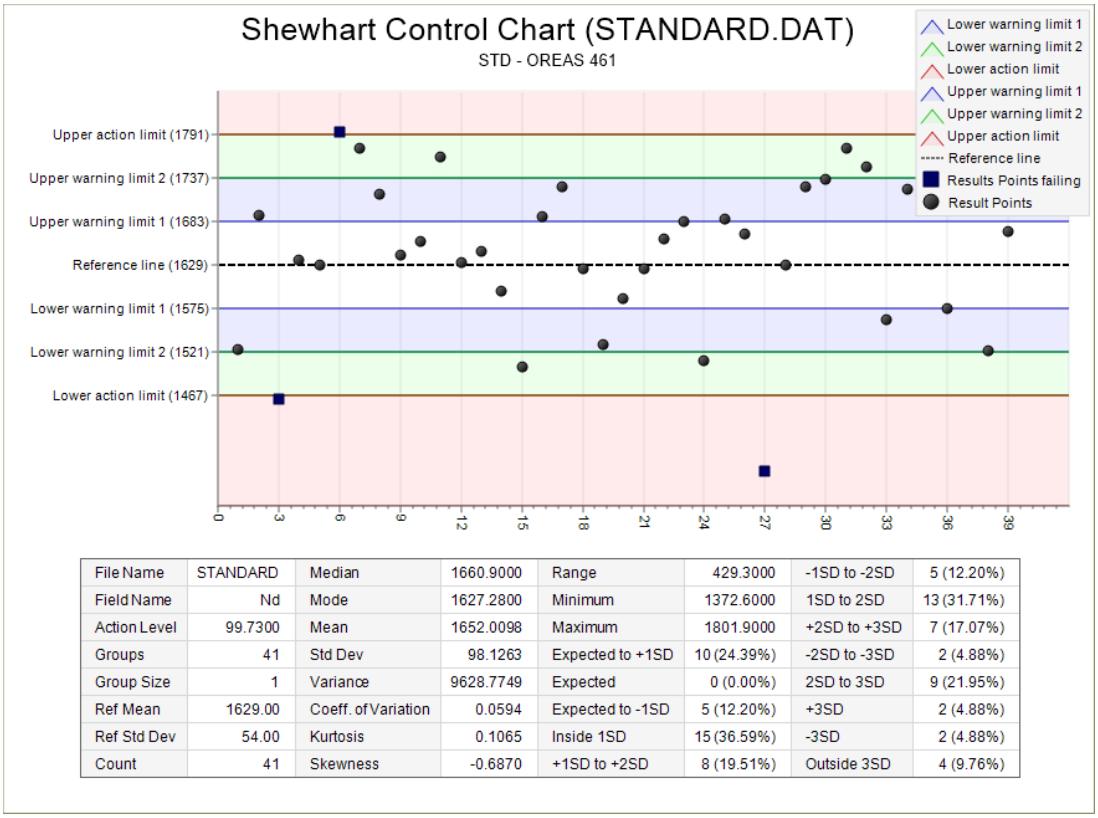
For each type of standard, the results were analyzed using a Shewhart Control Chart.

The data analyzed for Nd are shown in Figure 12.18 to Figure 12.20. Graphics for La, Ce and Y can be found in APPENDIX III.



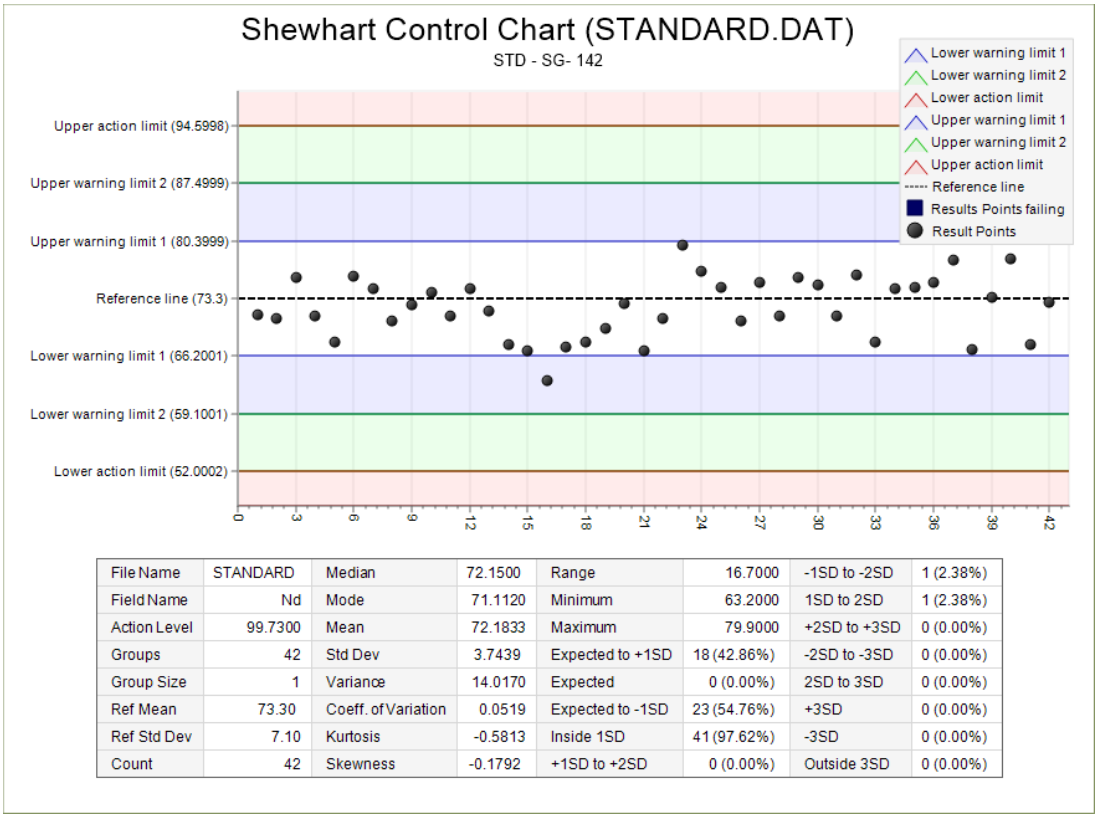

| File Name | STANDARD | Median | 797.7000 | Range | 195.2000 | -1SD to -2SD | 2 (4.88%) |
| --- | --- | --- | --- | --- | --- | --- | --- |
| Field Name | Nd | Mode | 814.6400 | Minimum | 728.1000 | 1SD to 2SD | 9 (21.95%) |
| Action Level | 99.7300 | Mean | 805.0854 | Maximum | 923.3000 | +2SD to +3SD | 3 (7.32%) |
| Groups | 41 | Std Dev | 45.7511 | Expected to +1SD | 17 (41.46%) | -2SD to -3SD | 0 (0.00%) |
| Group Size | 1 | Variance | 2093.1603 | Expected | 0 (0.00%) | 2SD to 3SD | 3 (7.32%) |
| Ref Mean | 781.00 | Coeff. of Variation | 0.0568 | Expected to -1SD | 11 (26.83%) | +3SD | 1 (2.44%) |
| Ref Std Dev | 47.00 | Kurtosis | 0.0086 | Inside 1SD | 28 (68.29%) | -3SD | 0 (0.00%) |
| Count | 41 | Skewness | 0.6506 | +1SD to +2SD | 7 (17.07%) | Outside 3SD | 1 (2.44%) |

**Figure 12.18 - Standard OREAS 460, element Nd.**




| | | | | | | | |
|---|---|---|---|---|---|---|---|
| File Name | STANDARD | Median | 1660.9000 | Range | 429.3000 | -1SD to -2SD | 5 (12.20%) |
| Field Name | Nd | Mode | 1627.2800 | Minimum | 1372.6000 | 1SD to 2SD | 13 (31.71%) |
| Action Level | 99.7300 | Mean | 1652.0098 | Maximum | 1801.9000 | +2SD to +3SD | 7 (17.07%) |
| Groups | 41 | Std Dev | 98.1263 | Expected to +1SD | 10 (24.39%) | -2SD to -3SD | 2 (4.88%) |
| Group Size | 1 | Variance | 9628.7749 | Expected | 0 (0.00%) | 2SD to 3SD | 9 (21.95%) |
| Ref Mean | 1629.00 | Coeff. of Variation | 0.0594 | Expected to -1SD | 5 (12.20%) | +3SD | 2 (4.88%) |
| Ref Std Dev | 54.00 | Kurtosis | 0.1065 | Inside 1SD | 15 (36.59%) | -3SD | 2 (4.88%) |
| Count | 41 | Skewness | -0.6870 | +1SD to +2SD | 8 (19.51%) | Outside 3SD | 4 (9.76%) |

**Figure 12.19 - Standard OREAS 461, element Nd.**




| | | | | | | | |
|---|---|---|---|---|---|---|---|
| File Name | STANDARD | Median | 72.1500 | Range | 16.7000 | -1SD to -2SD | 1 (2.38%) |
| Field Name | Nd | Mode | 71.1120 | Minimum | 63.2000 | 1SD to 2SD | 1 (2.38%) |
| Action Level | 99.7300 | Mean | 72.1833 | Maximum | 79.9000 | +2SD to +3SD | 0 (0.00%) |
| Groups | 42 | Std Dev | 3.7439 | Expected to +1SD | 18 (42.86%) | -2SD to -3SD | 0 (0.00%) |
| Group Size | 1 | Variance | 14.0170 | Expected | 0 (0.00%) | 2SD to 3SD | 0 (0.00%) |
| Ref Mean | 73.30 | Coeff. of Variation | 0.0519 | Expected to -1SD | 23 (54.76%) | +3SD | 0 (0.00%) |
| Ref Std Dev | 7.10 | Kurtosis | -0.5813 | Inside 1SD | 41 (97.62%) | -3SD | 0 (0.00%) |
| Count | 42 | Skewness | -0.1792 | +1SD to +2SD | 0 (0.00%) | Outside 3SD | 0 (0.00%) |

**Figure 12.20 - Standard SG-142, element Nd.**

In general, the results for rare earth elements that were analyzed, provided by SGS, do not present problems when compared with the known results.

### 12.5.3 Blank Samples

125 Blank Samples were used for contamination control of the sample preparation process. These represent 4.4% of the total number of samples analyzed.

The reference material used in the blank samples is a Quartz Blank.

The results of the analyses performed for the elements are shown in Table 12.4 below. In general, the results for rare earth elements that were analyzed, provided by SGS, do not present problems in terms of contamination during sample preparation, and/or due to wear and cleanliness of the equipment.

**Table 12.4 - Descriptive statistics for the blank sample chemical analysis results**

| Chemical analyses | Quantity | Minimum | Maximum | Average | Median | Variance | Std. Deviation |
|---|---|---|---|---|---|---|---|
| Y | 125 | 0.025 | 3.160 | 1.154 | 1.040 | 0.50938 | 0.71371 |
| La | 125 | 0.050 | 9.100 | 3.190 | 3.100 | 3.76074 | 1.93926 |
| Ce | 125 | 0.050 | 13.600 | 4.325 | 4.200 | 5.31696 | 2.30585 |
| Pr | 125 | 0.025 | 1.780 | 0.689 | 0.650 | 0.09017 | 0.30028 |
| Nd | 125 | 0.050 | 6.500 | 2.432 | 2.200 | 1.50006 | 1.22477 |
| Sm | 125 | 0.050 | 1.100 | 0.409 | 0.400 | 0.04078 | 0.20194 |
| Eu | 125 | 0.025 | 0.240 | 0.070 | 0.070 | 0.00163 | 0.04035 |
| Gd | 125 | 0.025 | 0.860 | 0.313 | 0.280 | 0.02799 | 0.16731 |
| Tb | 125 | 0.025 | 0.130 | 0.040 | 0.025 | 0.00061 | 0.02476 |
| Dy | 125 | 0.025 | 0.720 | 0.232 | 0.210 | 0.01833 | 0.13540 |
| Ho | 125 | 0.025 | 0.150 | 0.040 | 0.025 | 0.00076 | 0.02758 |
| Er | 125 | 0.025 | 0.440 | 0.124 | 0.110 | 0.00590 | 0.07681 |
| Tm | 125 | 0.025 | 0.060 | 0.025 | 0.025 | 0.00001 | 0.00313 |
| Yb | 125 | 0.050 | 0.300 | 0.070 | 0.050 | 0.00267 | 0.05163 |
| Lu | 125 | 0.025 | 0.050 | 0.025 | 0.025 | 0.00001 | 0.00224 |

# 13 Mineral Processing and Metallurgical Testing

## 13.1 Objective of Leaching Tests

The primary objective of the leaching tests was to conduct a preliminary evaluation of the feasibility of extracting rare earth elements (REEs) from the ionic clay mineralization. These initial tests were focused on assessing the potential for REE release using a low-cost, weak acid wash at room temperature.

## 13.2 Preliminary Test Conditions and Analysis

Leaching tests were conducted by SGS under standardized conditions: a leaching time of 30 minutes using a 40g aliquot of material in a 0.5M ammonium sulfate solution at pH 4, with a solids-to-liquid ratio of 25%. Leachate recovery was quantified using the ICM694 method, analyzed via ICP-OES and ICP-MS. The specific methods for quantifying these leachate recoveries are detailed below:

For quantification of the leachate recovery, an analysis was performed using the ICM694 method, employing Inductively Coupled Plasma Optical Emission Spectrometry (ICP-OES) / Inductively Coupled Plasma Mass Spectrometry (ICP-MS) (Table 13.1).

**Table 13.1 - Leaching with 0.5M Ammonium Sulfate for 30 Minutes, Analysis by ICPOES / ICPMS for Oxides/Elements - Detection Ranges**

| Elements | Detection interval | Elements | Detection interval | Elements | Detection interval |
|---|---|---|---|---|---|
| **Al** | 2 - 8000 (mg/kg) | **In** | 0.08 - 200 (mg/kg) | **Sc** | 0.24 - 800 (mg/kg) |
| **Ca** | 10 - 8000 (mg/kg) | **Lu** | 0.04 - 200 (mg/kg) | **Ta** | 0.2 - 200 (mg/kg) |
| **Cr** | 1 - 800 (mg/kg) | **Na** | 20 - 8000 (mg/kg) | **Tl** | 0.08 - 200 (mg/kg) |
| **Er** | 0.02 - 200 (mg/kg) | **P** | 4 - 8000 (mg/kg) | **W** | 1 - 800 (mg/kg) |
| **Ho** | 0.016 - 200 (mg/kg) | **Re** | 0.4 - 200 (mg/kg) | **Zr** | 0.2 - 800 (mg/kg) |
| **Li** | 0.4 - 800 (mg/kg) | **Sr** | 0.16 - 800 (mg/kg) | **Bi** | 0.8 - 800 (mg/kg) |
| **Mo** | 0.2 - 200 (mg/kg) | **Ti** | 5 - 8000 (mg/kg) | **Co** | 0.2 - 800 (mg/kg) |
| **Ni** | 0.2 - 800 (mg/kg) | **V** | 2 - 800 (mg/kg) | **Dy** | 0.028 - 200 (mg/kg) |
| **Rb** | 0.8 - 200 (mg/kg) | **Zn** | 0.5 - 800 (mg/kg) | **Gd** | 0.028 - 200 (mg/kg) |
| **Sn** | 1.2 - 200 (mg/kg) | **Be** | 0.4 - 800 (mg/kg) | **La** | 1 - 800 (mg/kg) |
| **Th** | 0.2 - 200 (mg/kg) | **Ce** | 0.2 - 800 (mg/kg) | **Mn** | 0.4 - 8000 (mg/kg) |
| **U** | 0.04 - 200 (mg/kg) | **Cu** | 0.04 - 800 (mg/kg) | **Nd** | 2.4 - 800 (mg/kg) |
| **Yb** | 0.4 - 200 (mg/kg) | **Fe** | 2 - 8000 (mg/kg) | **Pr** | 0.06 - 800 (mg/kg) |
| **Ba** | 20 - 800 (mg/kg) | **K** | 20 - 8000 (mg/kg) | **Sm** | 0.04 - 200 (mg/kg) |
| **Cd** | 0.12 - 800 (mg/kg) | **Mg** | 2 - 8000 (mg/kg) | **Tb** | 0.08 - 200 (mg/kg) |
| **Cs** | 0.2 - 200 (mg/kg) | **Nb** | 0.2 - 200 (mg/kg) | **Tm** | 0.012 - 200 (mg/kg) |
| **Eu** | 0.02 - 200 (mg/kg) | **Pb** | 0.32 - 800 (mg/kg) | **Y** | 0.2 - 800 (mg/kg) |

## 13.3 Leaching Results and Recovery Rates

Table 13.2 presents leaching results and highlights key figures for Heavy, Light, and Magnetic Rare Earth Oxides, as well as for Neodymium and Praseodymium content. The data also includes recovery rates, indicating the preliminary efficiency of the process employing a conventional ionic adsorption clay metallurgical route:

**Table 13.2 - Leached Results for Ionic Clay from Hole AP-ND-05 @5m (Interval 9m - 14m)**

| Description | HREO | LREO | MREO | NdPr | TREO |
| --- | --- | --- | --- | --- | --- |
| Head Grade (ppm) | 371 | 4,004 | 1,187 | 1,149 | 4,375 |
| Leached Grade (ppm) | 133 | 894 | 399 | 386 | 1,027 |
| Recovery (%) | 36% | 22% | 34% | 34% | 23% |

Heavy Rare Earth Oxides (HREO): $Sm_2O_3 + Eu_2O_3 + Gd_2O_3 + Tb_4O_7 + Dy_2O_3 + Ho_2O_3 + Er_2O_3 + Tm_2O_3 + Yb_2O_3 + Lu_2O_3$

Light Rare Earth Oxides (LREO): $La_2O_3 + Ce_2O_3 + Pr_2O_3 + Nd_2O_3$

Magnetic Rare Earth Oxides (MREO): $Sm_2O_3 + Tb4O7 + Dy_2O_3 + Pr_6O_{11} + Nd_2O_3$

Neodymium and Praseodymium Oxides (NdPr): $Nd_2O_3 + Pr_6O_{11}$

Total Rare Earth Oxides (TREO): $Y_2O_3 + Eu_2O_3 + Gd_2O_3 + Tb_2O_3 + Dy_2O_3 + Ho_2O_3 + Er_2O_3 + Tm_2O_3 + Yb_2O_3 + Lu_2O_3 + La_2O_3 + Ce_2O3 + Pr_2O_3 + Nd_2O_3 + Sm_2O_3$

## 13.4 Impurity Analysis

Additionally, Table 13.3 presents the results of an analysis of impurities in the leachate, these results demonstrate that the content of these elements remains minimal, further supporting the feasibility of the process:

**Table 13.3 - Impurities Identified in Leachate Using the ICM694 Method**

| Impurity | Ca | Al | Ni | Fe | U | Th |
| --- | --- | --- | --- | --- | --- | --- |
| **Content (ppm)** | 117 | 75 | 5 | 5 | <0.04 | 0.6 |

The initial results show encouraging recoveries and low levels of impurities, underscoring the potential of the project.

# 14 Mineral Resource Estimate

## 14.1 Introduction

This topic describes the methodology and devices used in the resource evaluation for the Rare Earth deposits in the Nau de Guerra, Balsamo and Alto da Serra targets. These targets make up the Man of War project, which is located in the city of Tiros, Minas Gerais, Brazil.

BNA initially received data from the Nau de Guerra target, which was modeled and processed first. BNA then received data from the Balsamo and Alto da Serra targets. Data from both targets were processed together whenever possible.

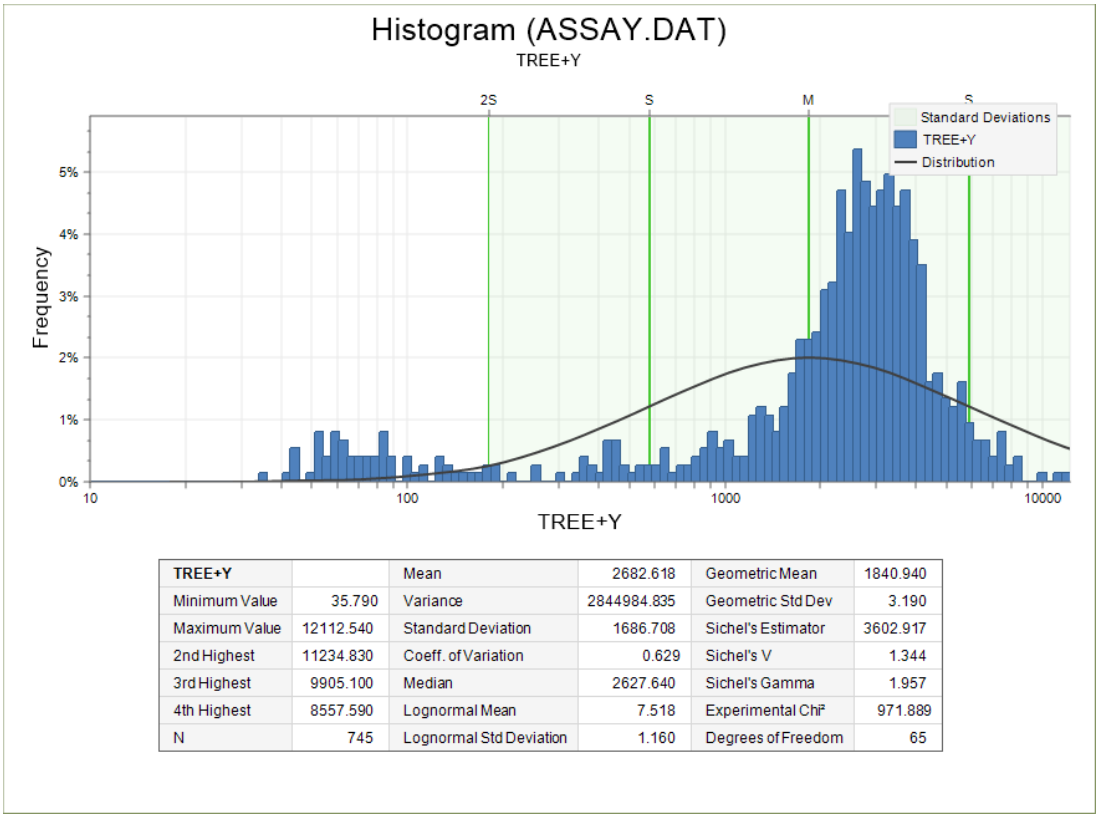
Dr. Myadzel is responsible for the resource estimation methodology. Dr. Myadzel is independent of the issuer of this report. The effective date of this estimate is the date on which the latest data on the resource estimate was received, or that is, November 28, 2024.

## 14.2 Statistical Analysis

This report used a classical statistical analysis methodology to perform the following tasks:

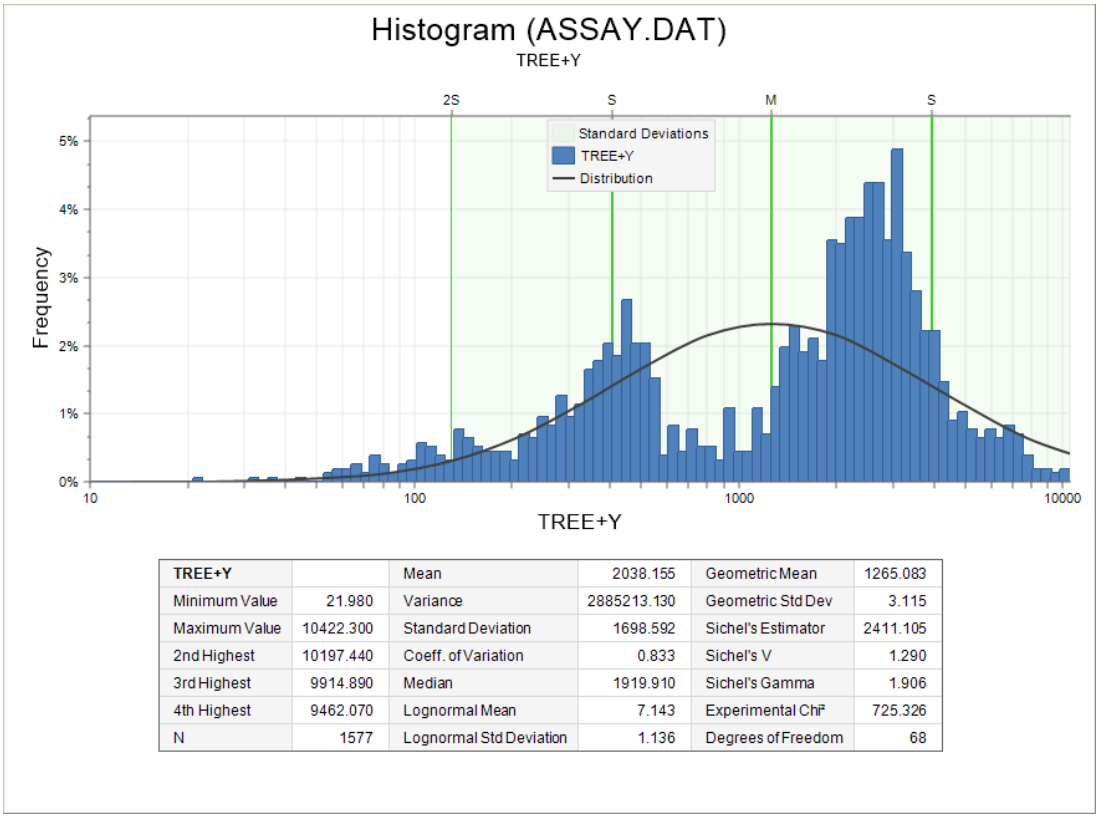
- Assess the need to separate populations, when there is more than one population;
- Evaluate the effect of population mixing;
- Determine the grade distribution.

Statistical analyses was performed for all TREE ppm samples grouped throughout the data matrix, as shown in Figure 14.1, Figure 14.2 and Figure 14.3.



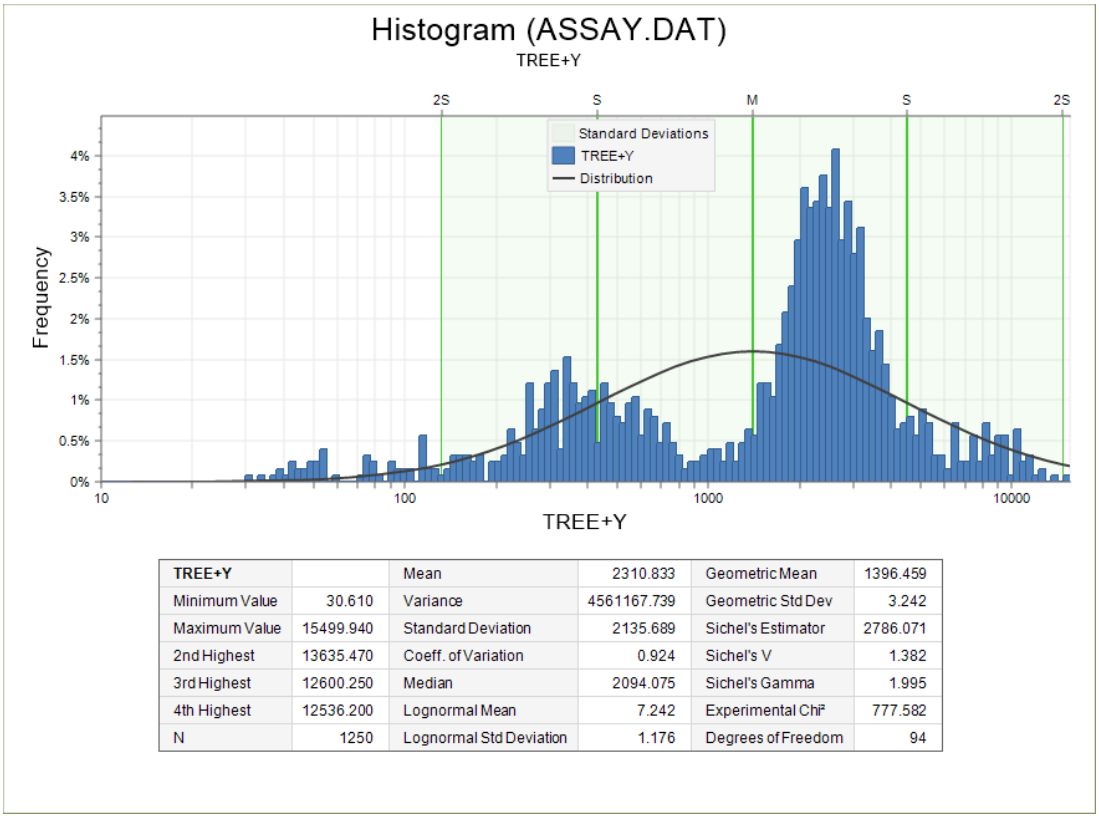

| TREE+Y | | Mean | 2682.618 | Geometric Mean | 1840.940 |
| --- | --- | --- | --- | --- | --- |
| Minimum Value | 35.790 | Variance | 2844984.835 | Geometric Std Dev | 3.190 |
| Maximum Value | 12112.540 | Standard Deviation | 1686.708 | Sichel's Estimator | 3602.917 |
| 2nd Highest | 11234.830 | Coeff. of Variation | 0.629 | Sichel's V | 1.344 |
| 3rd Highest | 9905.100 | Median | 2627.640 | Sichel's Gamma | 1.957 |
| 4th Highest | 8557.590 | Lognormal Mean | 7.518 | Experimental Chi² | 971.889 |
| N | 745 | Lognormal Std Deviation | 1.160 | Degrees of Freedom | 65 |

**Figure 14.1 - Histogram of TREE ppm grade distribution for all samples, Nau de Guerra target.**




| TREE+Y | | Mean | 2038.155 | Geometric Mean | 1265.083 |
| --- | --- | --- | --- | --- | --- |
| Minimum Value | 21.980 | Variance | 2885213.130 | Geometric Std Dev | 3.115 |
| Maximum Value | 10422.300 | Standard Deviation | 1698.592 | Sichel's Estimator | 2411.105 |
| 2nd Highest | 10197.440 | Coeff. of Variation | 0.833 | Sichel's V | 1.290 |
| 3rd Highest | 9914.890 | Median | 1919.910 | Sichel's Gamma | 1.906 |
| 4th Highest | 9462.070 | Lognormal Mean | 7.143 | Experimental Chi² | 725.326 |
| N | 1577 | Lognormal Std Deviation | 1.136 | Degrees of Freedom | 68 |

**Figure 14.2 - Histogram of TREE ppm grade distribution for all samples, Balsamo target.**




| TREE+Y | | Mean | 2310.833 | Geometric Mean | 1396.459 |
| --- | --- | --- | --- | --- | --- |
| Minimum Value | 30.610 | Variance | 4561167.739 | Geometric Std Dev | 3.242 |
| Maximum Value | 15499.940 | Standard Deviation | 2135.689 | Sichel's Estimator | 2786.071 |
| 2nd Highest | 13635.470 | Coeff. of Variation | 0.924 | Sichel's V | 1.382 |
| 3rd Highest | 12600.250 | Median | 2094.075 | Sichel's Gamma | 1.995 |
| 4th Highest | 12536.200 | Lognormal Mean | 7.242 | Experimental Chi² | 777.582 |
| N | 1250 | Lognormal Std Deviation | 1.176 | Degrees of Freedom | 94 |

**Figure 14.3 - Histogram of TREE ppm grade distribution for all samples, Alto da Serra target.**

Following an analysis of the statistical data, we conclude that the variables associated with rare earth mineralization exhibit a log-normal behavior.

.

## 14.3 Interpretation

The geological interpretation consisted of two parts: the interpretation of the mineralization zone and the interpretation of the lithological model for the accurate assignment of rock density.

### 14.3.1 Interpretation of the Mineralization

For the Nau de Guerra target, an interpretation of the mineralization was performed for content levels above 600 ppm of TREE. Levels below 600 ppm with a length equal to or greater than 5 meters were individualized.

Using the ASSAY.DAT worksheet (chemical analysis results), a file named COMP_GRADE.DAT was created, containing all samples with a TREE grade of 600 ppm or higher. Only samples with results equal to or exceeding 600 ppm TREE were included, as illustrated in Figure 14.4.

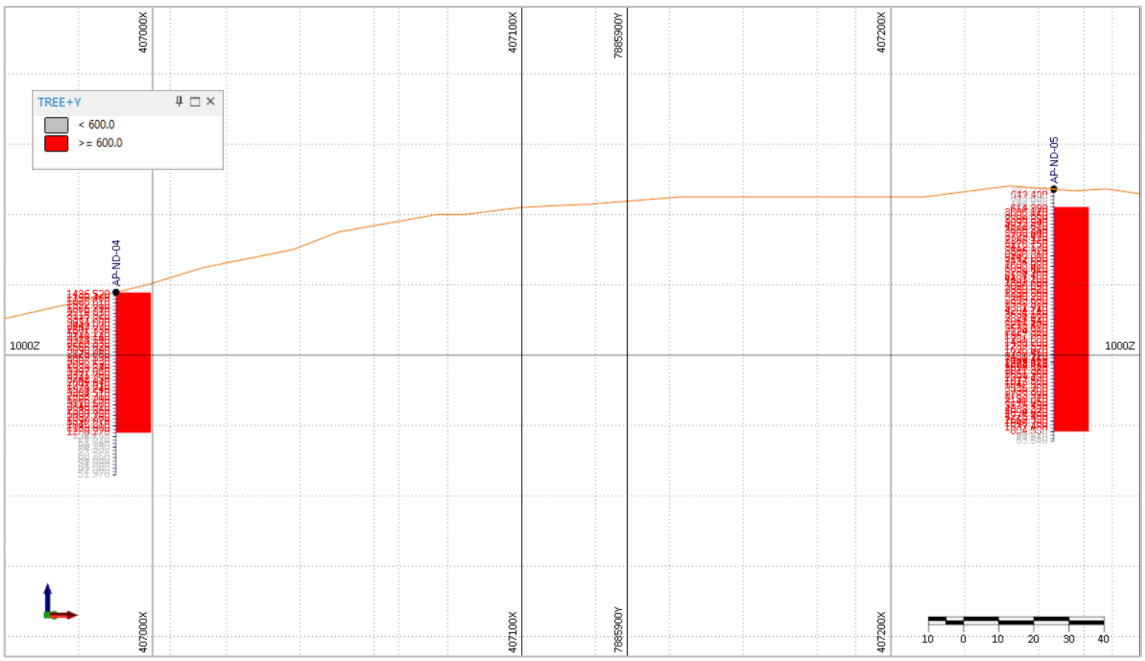



**Figure 14.4 - Composite sample intervals for the boreholes (red bar shows the composite sample)- Nau de Guerra target.**

For the Balsamo and Alto da Serra target, an interpretation of the mineralization was performed for content levels above 500 ppm of TREE. Levels below 500 ppm with a length equal to or greater than 5 meters were individualized. Using the ASSAY.DAT worksheet (chemical analysis results), a file named COMP_GRADE.DAT was created, containing all samples with a TREE grade of 500 ppm or higher. Only samples with results equal to or exceeding 500 ppm TREE were included, as illustrated in Figure 14.5.

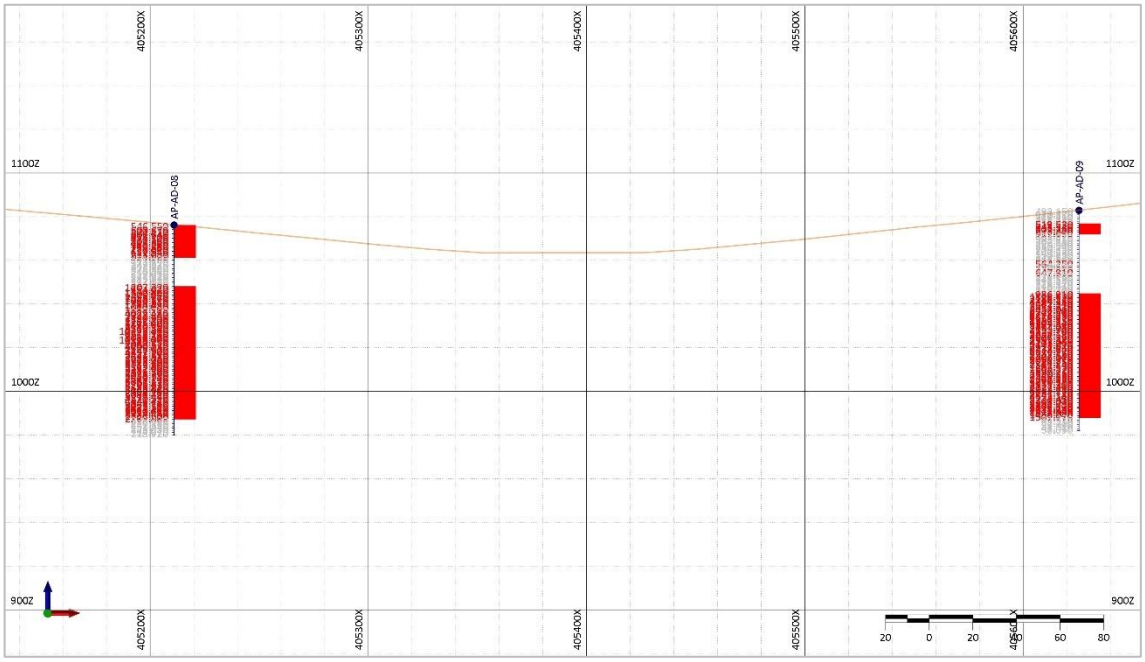



**Figure 14.5 - Composite sample intervals for the boreholes (red bar shows the composite sample).**

The **COMP_GRADE.DAT** file was used to generate a new file, **SEAM_ORE.DAT**, which contains the coordinates of each sample composed of 500 ppm of TREE for the Balsamo and Alto da Serra targets and 600 ppm of TREE for the Nau de Guerra target, and a new code, with TOPO representing the top of the mineralized zone and BASE representing the base of the zone, as shown in Figure 14.6.

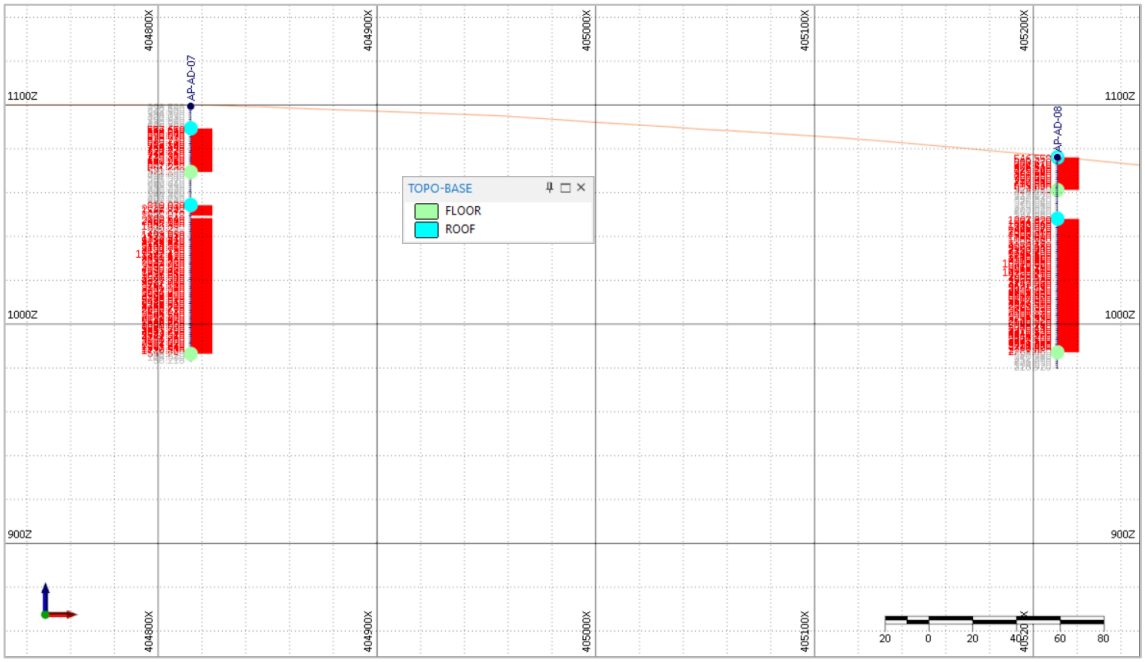



**Figure 14.6 - Top (green) and Base (blue) points of the mineralized zone.**

In collaboration with the Verde team, the following geological interpretation criteria and parameters were defined for the Balsamo and Alto da Serra targets:

- For interpretation, the TREE grade criterion was used, including the use of composite samples with a content of at least 500 ppm of TREE for the Balsamo and Alto da Serra targets and 600 ppm of TREE for the Nau de Guerra target
- The minimum thickness of the body is 5 meters
- Internal dilution is 2 meters, up to 1 meter of internal waste was included for the continuation of the orebody.

Using data from the **SEAM_ORE.DAT** file, which was corrected manually, top and base surfaces of the mineralization zone were created. The grid creation method was used together with the IDW2 interpolation method. The cell size is 5 × 5 meters. Grids were converted into digital surfaces DTM (Digital Terrain Model), as shown in Figure 14.7 to Figure 14.10.

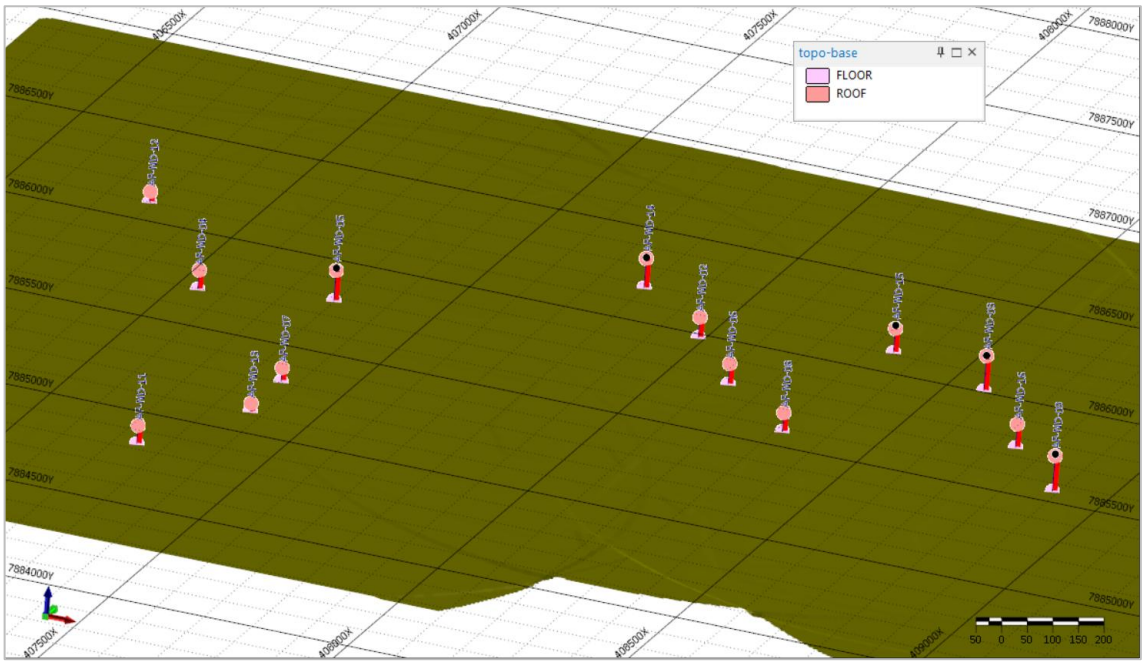



**Figure 14.7 - Digital terrain model of the Base surface of the mineralization – Nau de Guerra target**

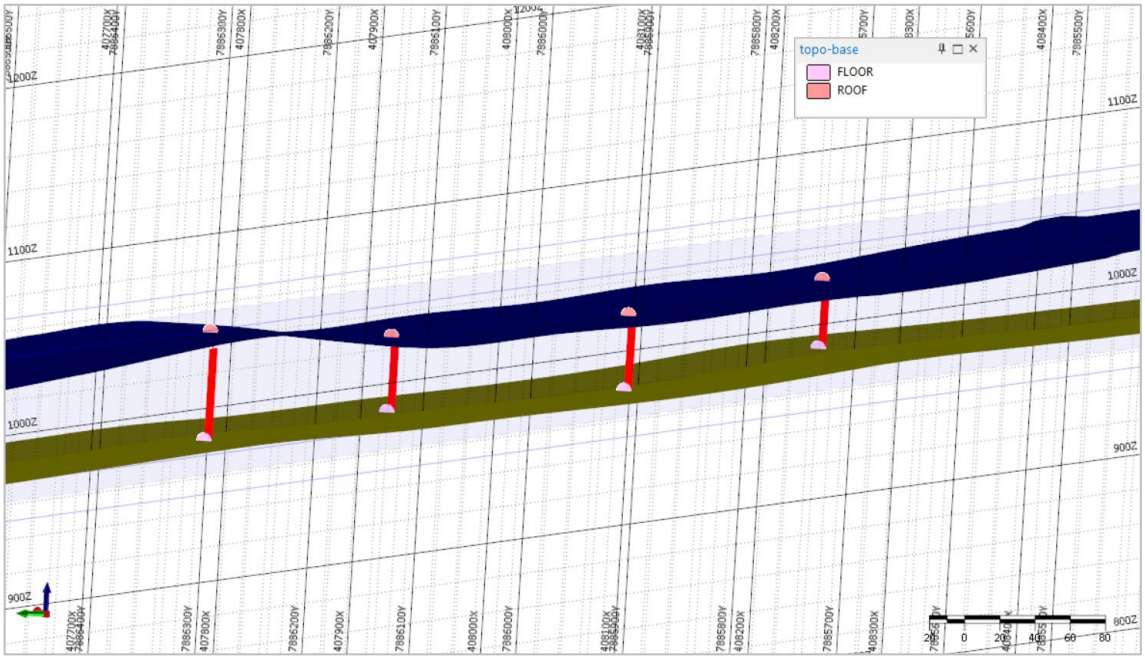



**Figure 14.8 - Digital terrain model of the Base surface of the mineralization– Nau de Guerra target**

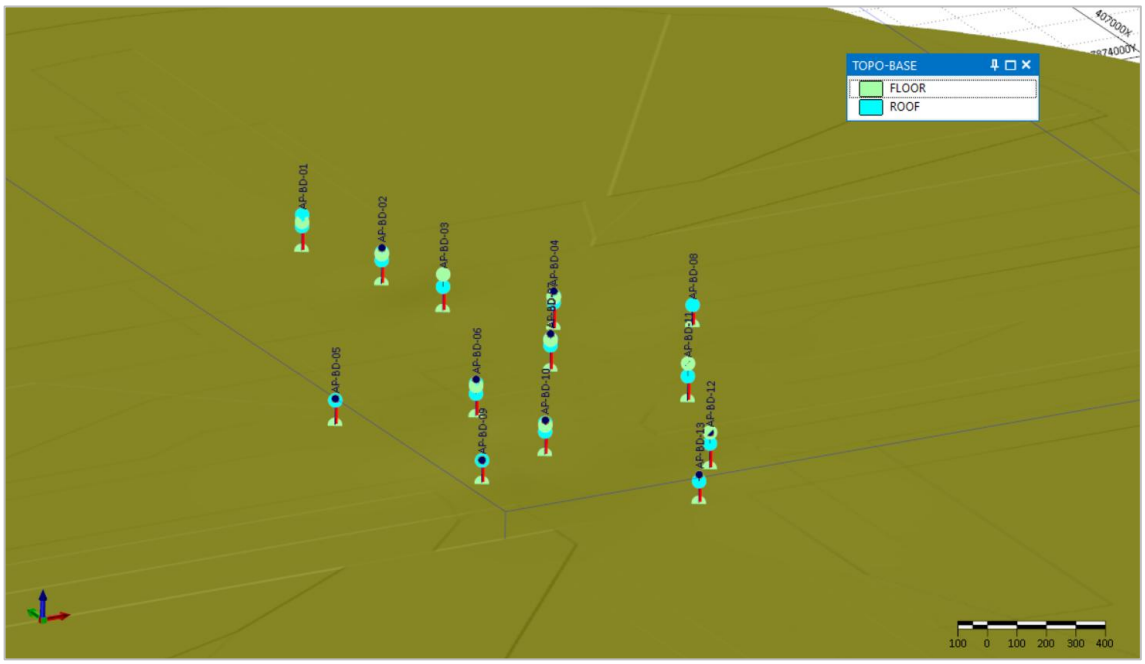



**Figure 14.9 - Digital terrain model of the Base surface of the mineralization – Balsamo and Alto da Serra targets**

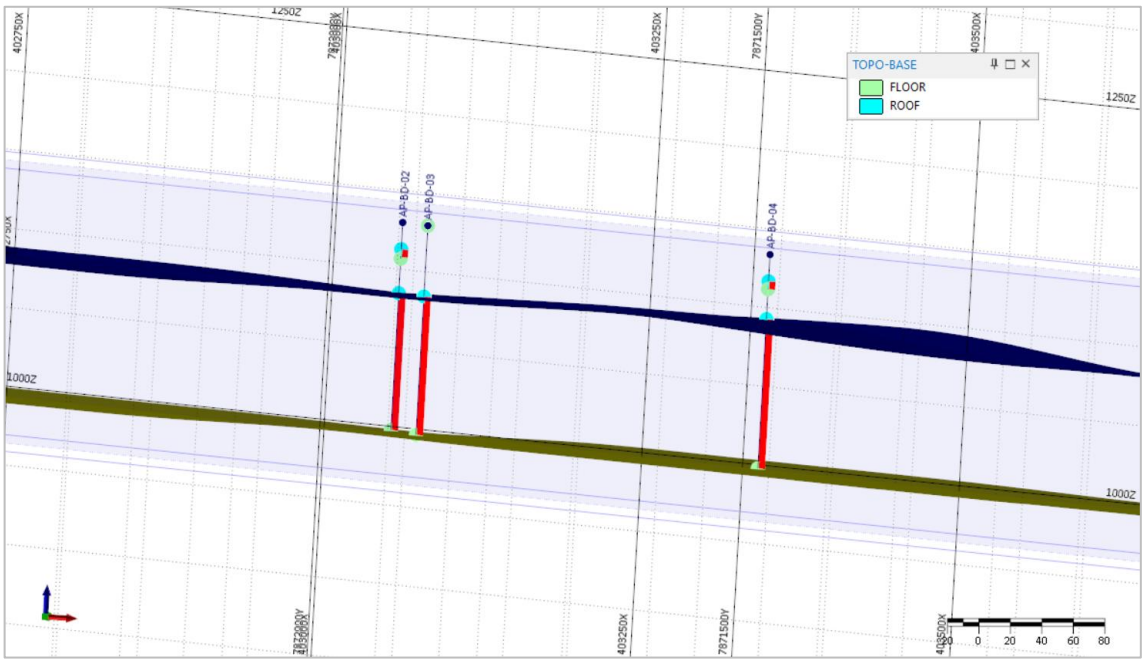



**Figure 14.10 - Digital terrain model of the Base surface of the mineralization - Balsamo and Alto da Serra targets**

The mineralization zone is located within the sedimentary rock layers of the Capacete Formation. Geological mapping data on the Capacete Formation were used to determine the continuity of the mineralization zone in plan view, as shown in Figure 14.11 to Figure 14.13.

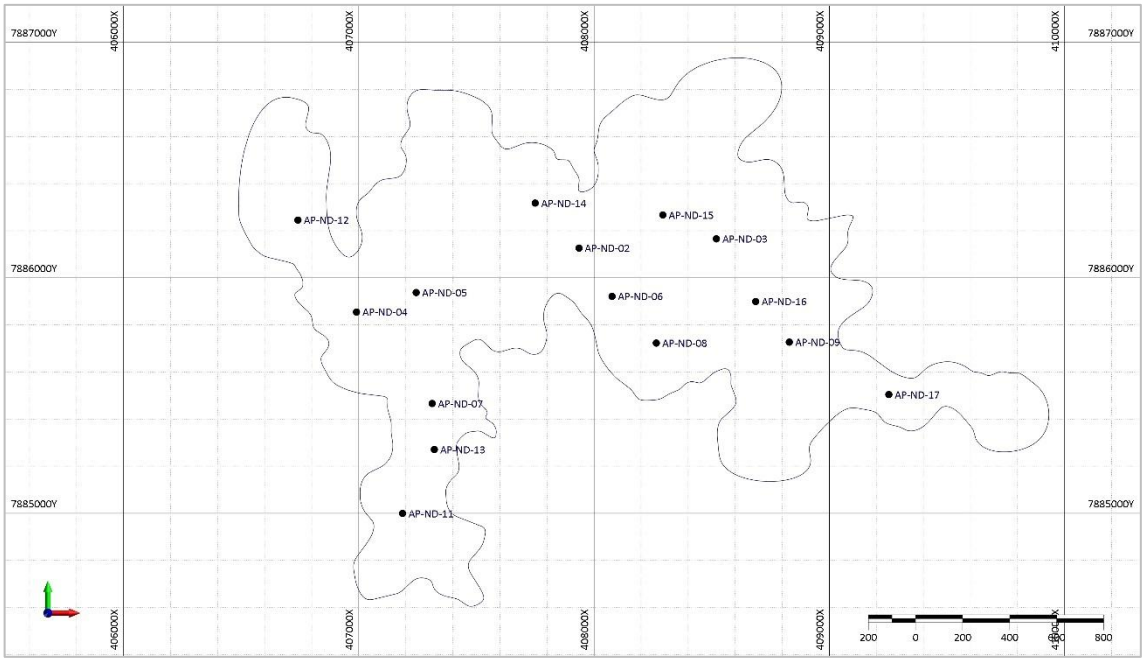



**Figure 14.11 - Geological mapping data on the Capacete Formation, Nau de Gerra target.**




**Figure 14.12 - Geological mapping data on the Capacete Formation, Alto da Serra target.**

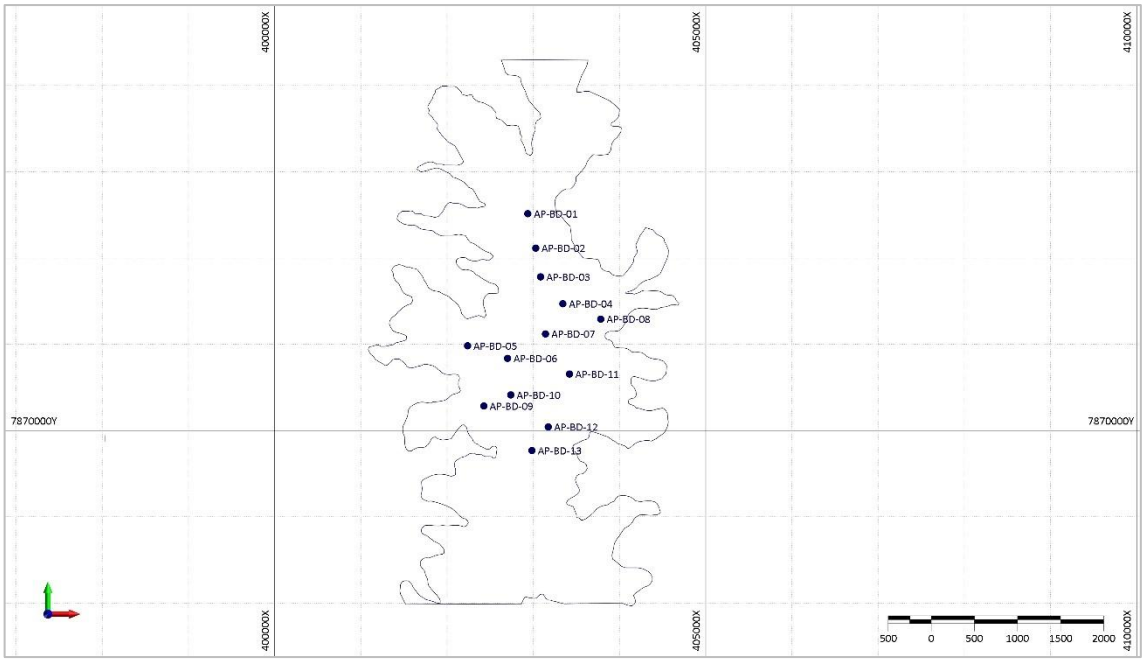



**Figure 14.13 - Geological mapping data on the Capacete Formation, Balsamo target.**

This geological boundary was used to generate a wireframe box for the mineralized zone.

Following the creation of the solid model of the orebody, a solid adjustment was performed using information from the boreholes. Geological data and chemical analyses were applied throughout the orebody wireframe, and several geological contacts were manually corrected to meet the defined interpretation criteria.

### 14.3.2 Geological Interpretation

The geological interpretation of the Nau de Guerra target, Balsamo target and Alto da Serra target orebodies was performed based on the lithological description of the boreholes. Within the Capacete Formation, four (4) lithological types were identified for clay deposits, along with four (4) lithological types for coarse clastic sedimentary rocks (sandstones and conglomerates). Additionally, the underlying rocks of the Areado Group, which do not contain mineralization, were separately identified. The **GEOLOGY.DAT** file was used for this purpose. Table 14.1 shows the codes used by target and the lithological description intervals are presented in Figure 14.14 and Figure 14.15.

**Table 14.1 - Lithological codes**

| LEGEND | | |
|---|---|---|
| **Regolith** | **Code** | **Targets** |
| soil | soi | Nau de Guerra, Balsamo e Alto da Serra |
| soil | so | Balsamo e Alto da Serra |
| saprolite | sp | Balsamo e Alto da Serra |
| laterite | la | Balsamo e Alto da Serra |
| saprolite sandstone | sar | Nau de Guerra |
| saprolite conglomeratic sandstone | sac | Nau de Guerra |
| saprolite conglomerate | scg | Nau de Guerra |
| saprolite siltstone | ssi | Nau de Guerra |
| **Litologia/Lithology** | **Code** | **Targets** |
| siltstone | si | Nau de Guerra |
| sandstone | ar | Nau de Guerra |
| conglomeratic sandstone | ac | Nau de Guerra |
| conglomerate | cg | Nau de Guerra |
| Areado Group | aa | Nau de Guerra |
| grauvaca (gv) + Kamafungitica (k) | kgv | Balsamo e Alto da Serra |
| conglomerado(cg) + Kamafungitica (k) | kcg | Balsamo e Alto da Serra |
| arenito areado (ar) + grupo areado (a) | aar | Balsamo e Alto da Serra |

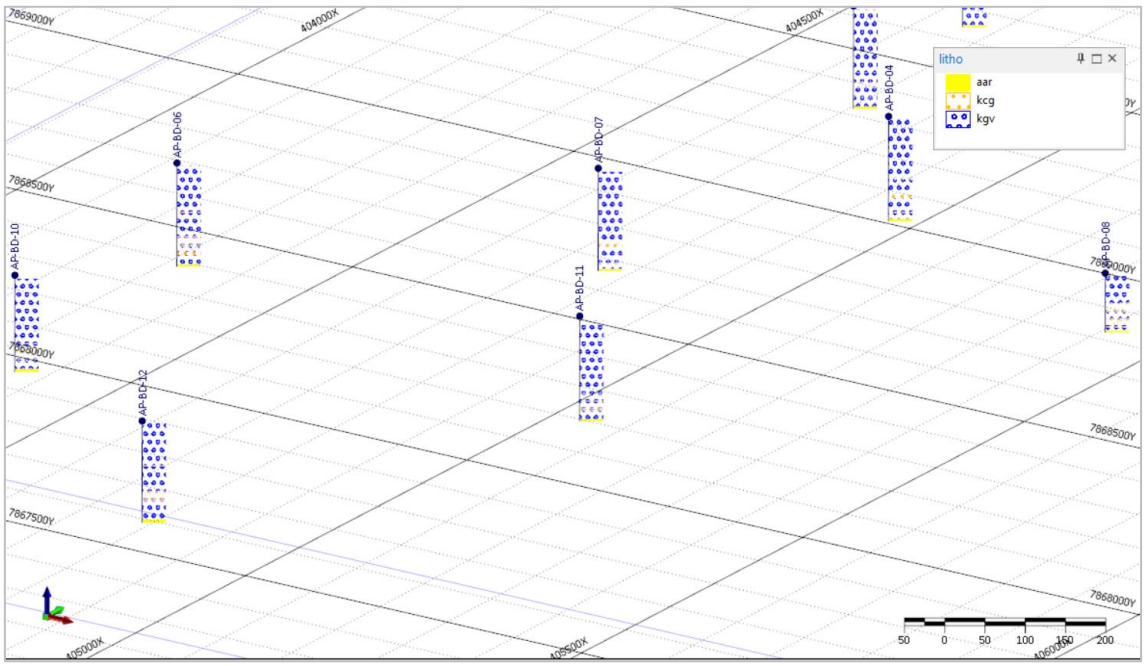



**Figure 14.14 - Lithological description intervals along the drill holes (Vertical Exaggeration *3), Balsamo and Alto da Serra targets**

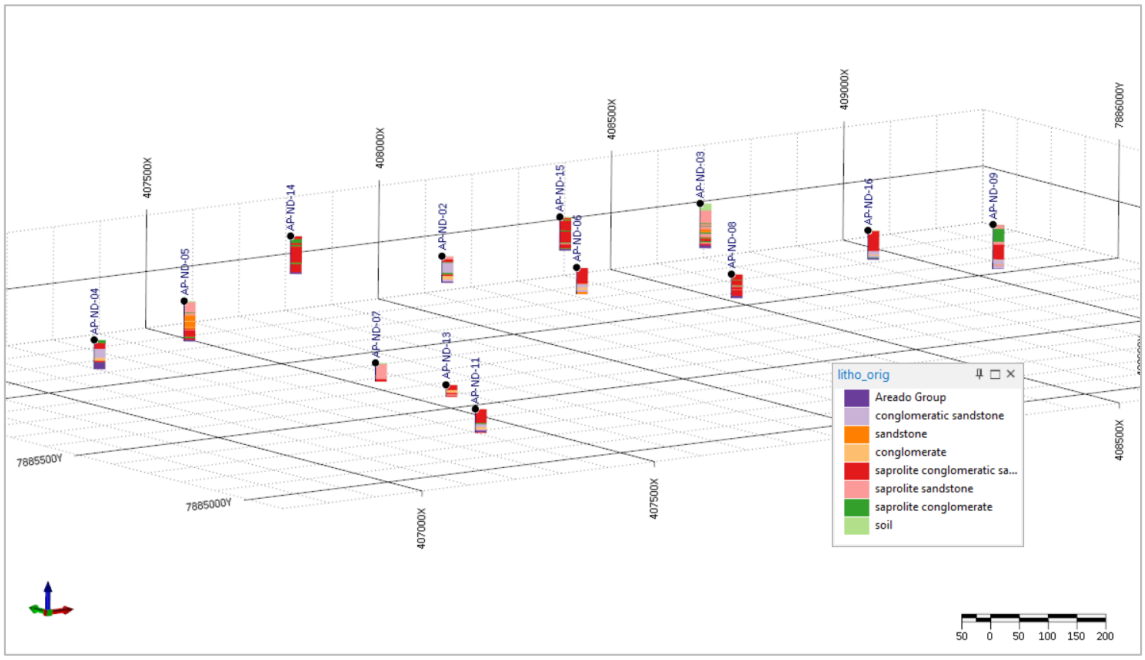



**Figure 14.15 - Lithological description intervals along the drill holes (Vertical Exaggeration *3), Nau de Guerra target**

For the Nau de Guerra target, following an analysis of the distribution of lithological types within the Capacete Formation and an examination of the relationship between lithological type and rock density, it was decided to group all fine-grained clay types under the lithological code REG. All coarse clastic sedimentary rocks (sandstones and conglomerates) were grouped and assigned the lithological code CONG. The soil layer was assigned the lithological code SOIL.

For the Balsamo and Alto da Serra targets, following an analysis of the distribution of lithological types within the Capacete Formation and an examination of the relationship between lithological type and rock density, it was decided to group all fine-grained clay types under the lithological code SAP. The soil layer was assigned the lithological code SOIL.

From the **GEOLOGY.DAT** file, **SEAM_SOIL.DAT**, and **SEAM_SAP.DAT** files were generated for each target. These contain the coordinates of each lithological interval, and new codes: ROOF for the top of the mineralized zone and FLOOR for the base of the zone. See Figure 14.16.

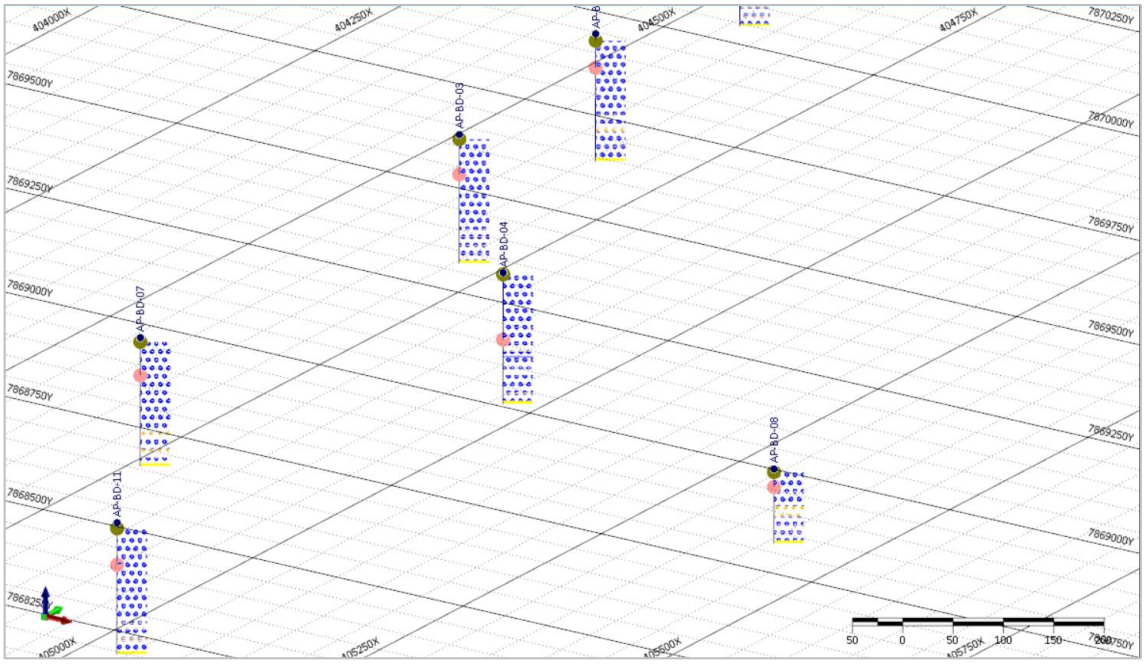



**Figure 14.16 - Points in the lithological zone**

From the **SEAM_*.DAT** file, which was corrected manually, top and base surfaces for each lithological type were created. This grid creation method was used with the IDW2 interpolation method. The cell size is 5 × 5 meters. The grids were converted into DTM (Digital Terrain Model) surfaces, as shown in Figure 14.17 and Figure 14.18.

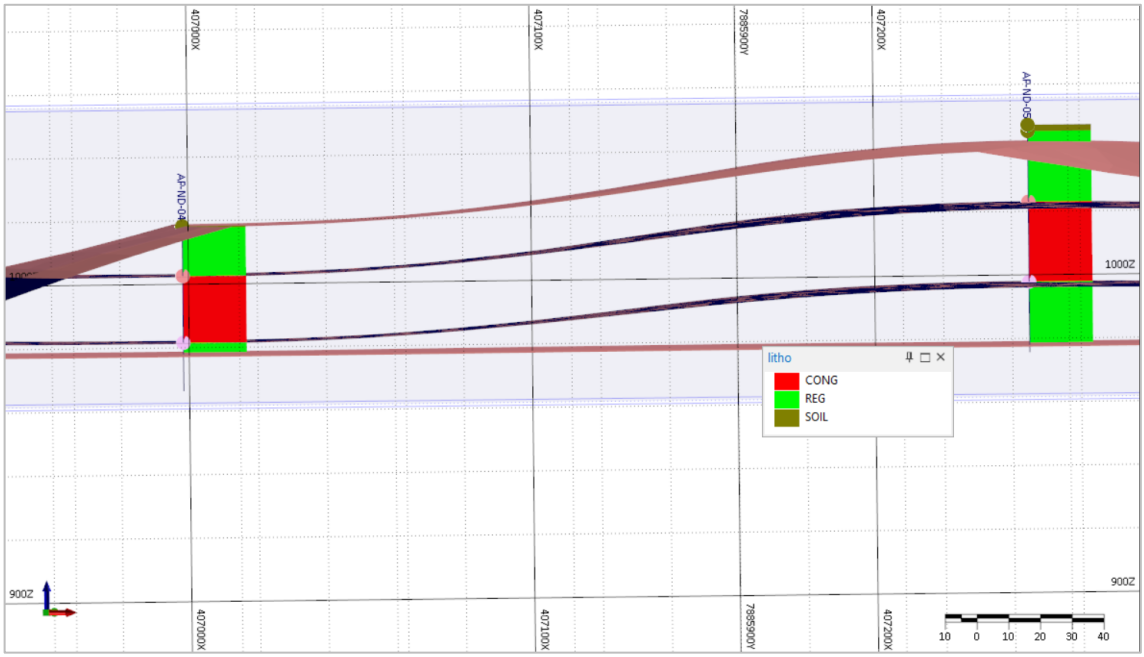



**Figure 14.17 - Digital terrain model of the base surface of the lithological types, Nau de Guerra target**

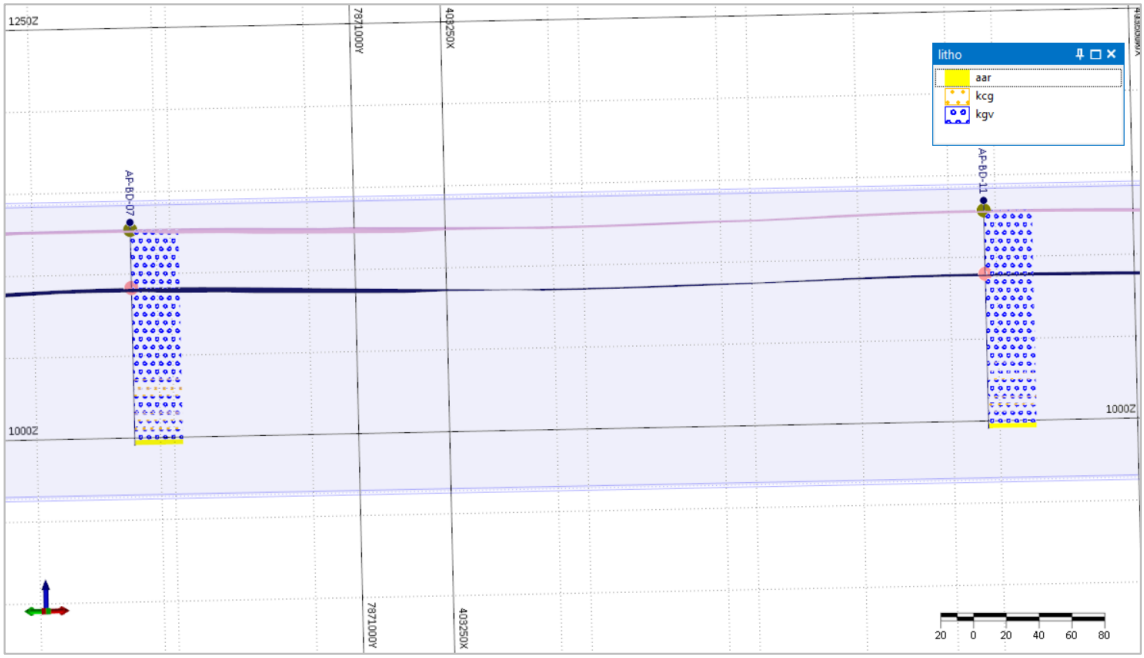



**Figure 14.18 - Digital terrain model of the base surface of lithological types, Balsamo and Alto da Serra targets**

## 14.4 Triangulation

A grid was created using the interpretation points (ROOF/FLOOR). The Inverse Distance Weighting method, with a weight equal to 2 (IDW2), was chosen for the creation of this grid. The grid was transformed into a Digital Surface Model (DSM). This method was chosen because the body is sub-

horizontal and is in the form of a layer. An example of the surfaces generated is shown in Figure 14.19 and Figure 14.20.

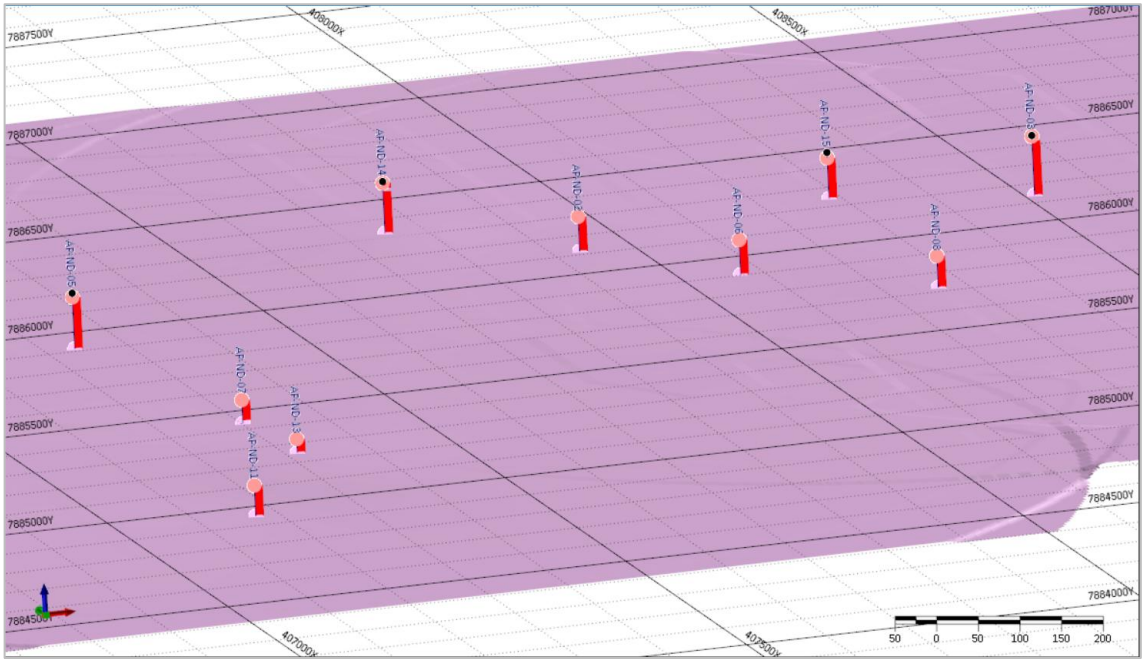



**Figure 14.19 - Digital Roof Surface Model of the mineralization zone, Nau de Guerra target**

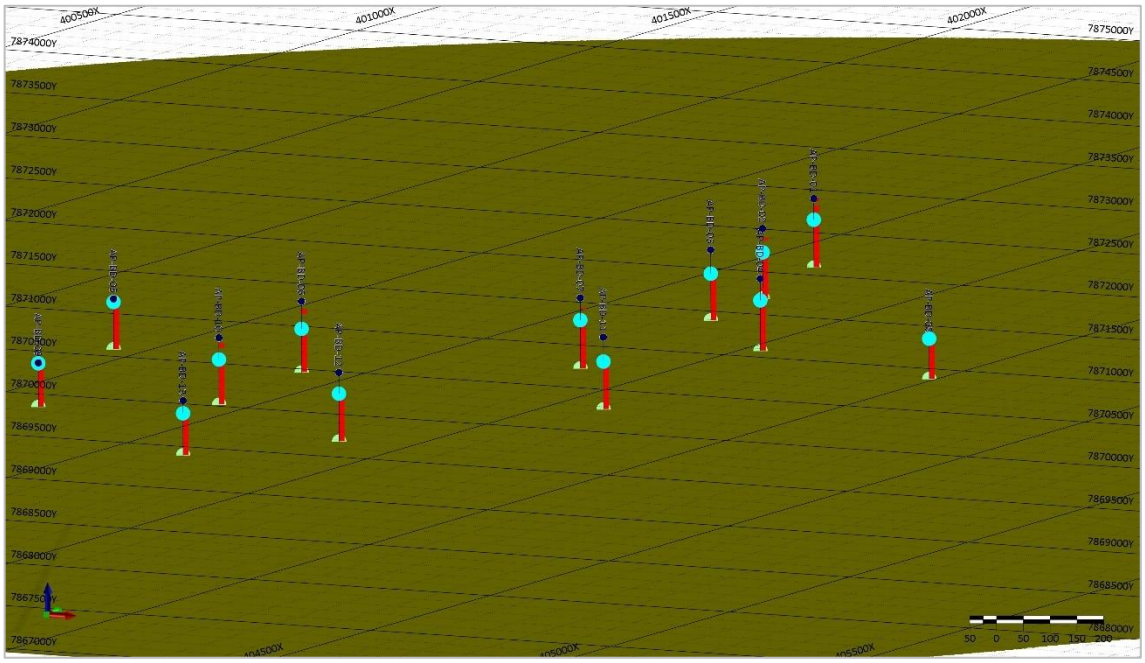



**Figure 14.20 - Digital Roof Surface Model of the mineralization zone, Balsamo and Alto da Serra targets**

Boolean Operations[3] were used to build the orebody solid. First, a solid ("box") was built within the geological limits of the mineralization zone. Then, this box was cut from the base surface, the top surface and the topographic surface (Figure 14.21 to Figure 14.23). The result obtained is the exact solid of the lithological body (Figure 14.24 to Figure 14.26).

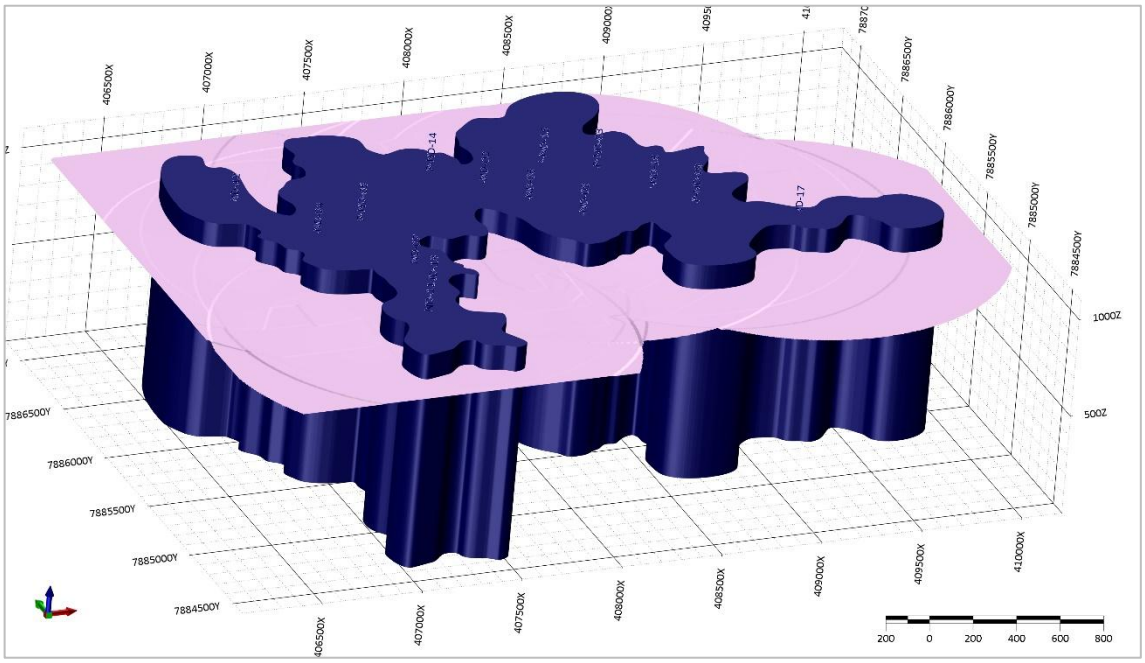



**Figure 14.21 - Boolean operations to build the mineralization body solid, Nau de Guerra target**

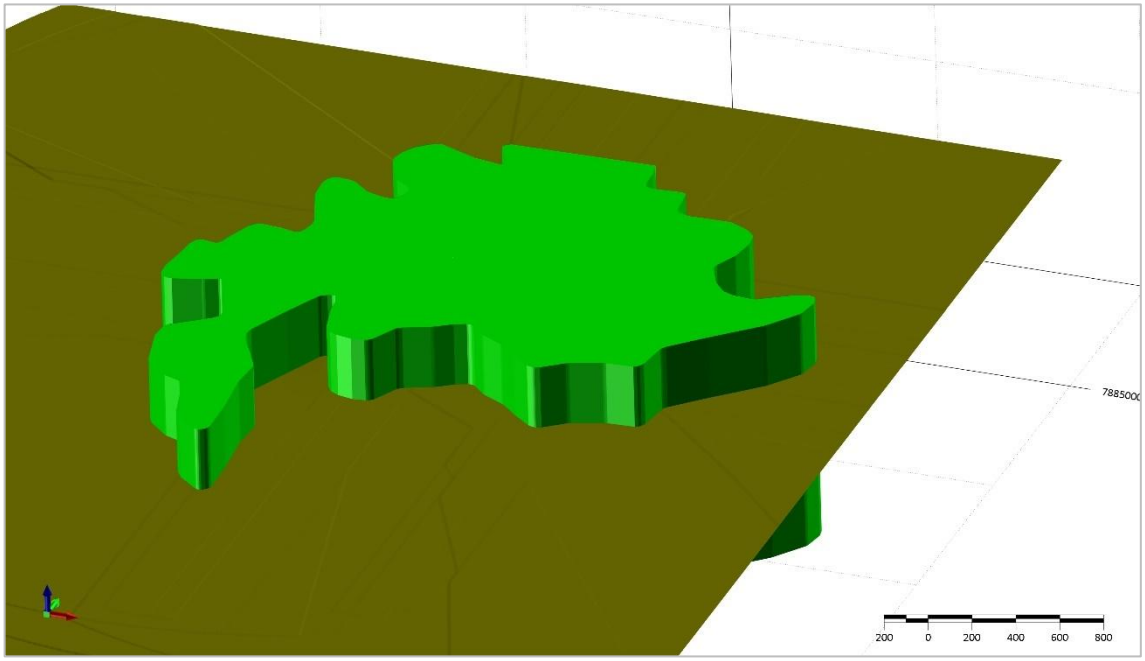



**Figure 14.22 - Boolean operations to build the mineralization body solid, Alto da Serra target**

[3] Cutting operations between surfaces and/or triangularized solids.

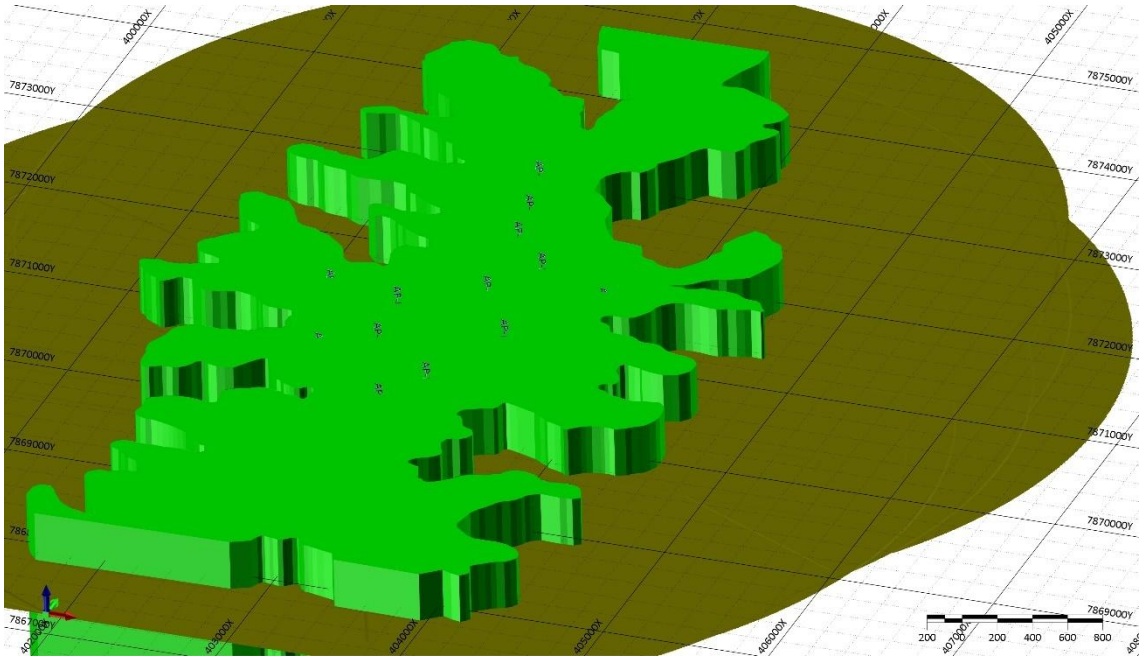



**Figure 14.23 - Boolean operations to build the mineralization body solid, Balsamo target**

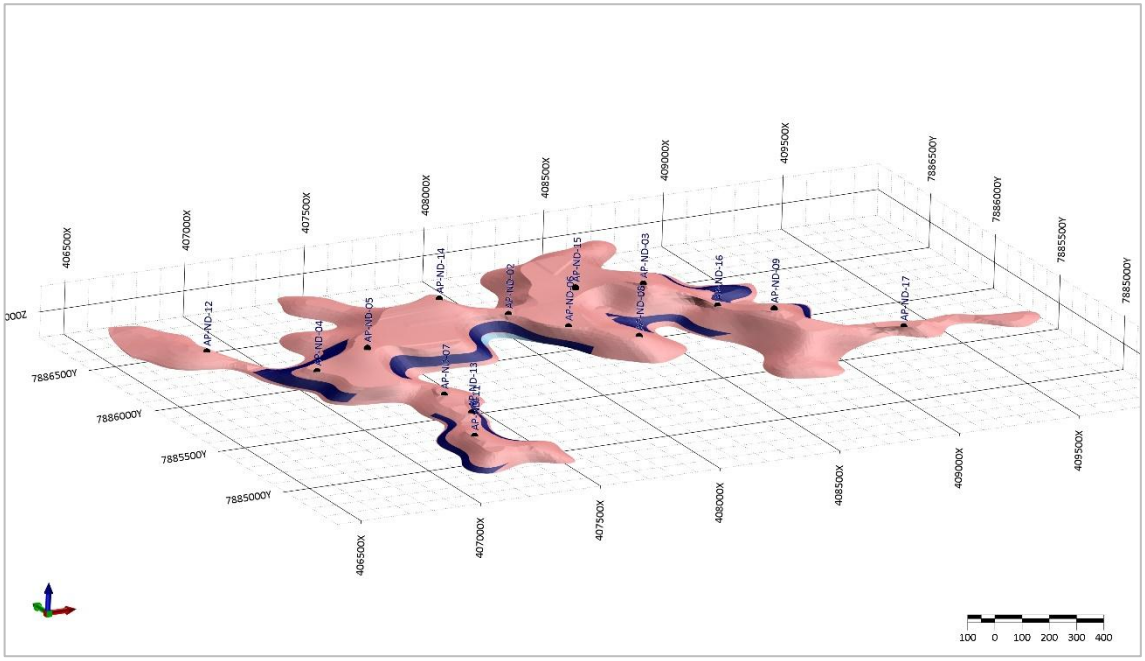



**Figure 14.24 - Lithological Solids, Nau de Guerra target**

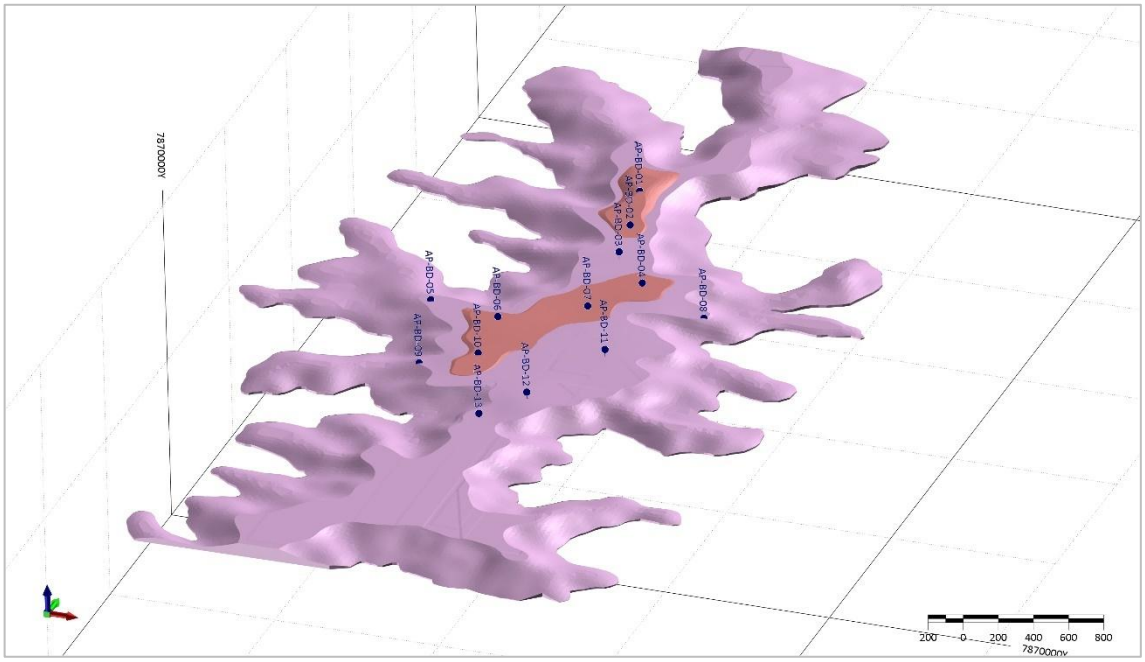



**Figure 14.25 - Mineralization body solids, Balsamo target**

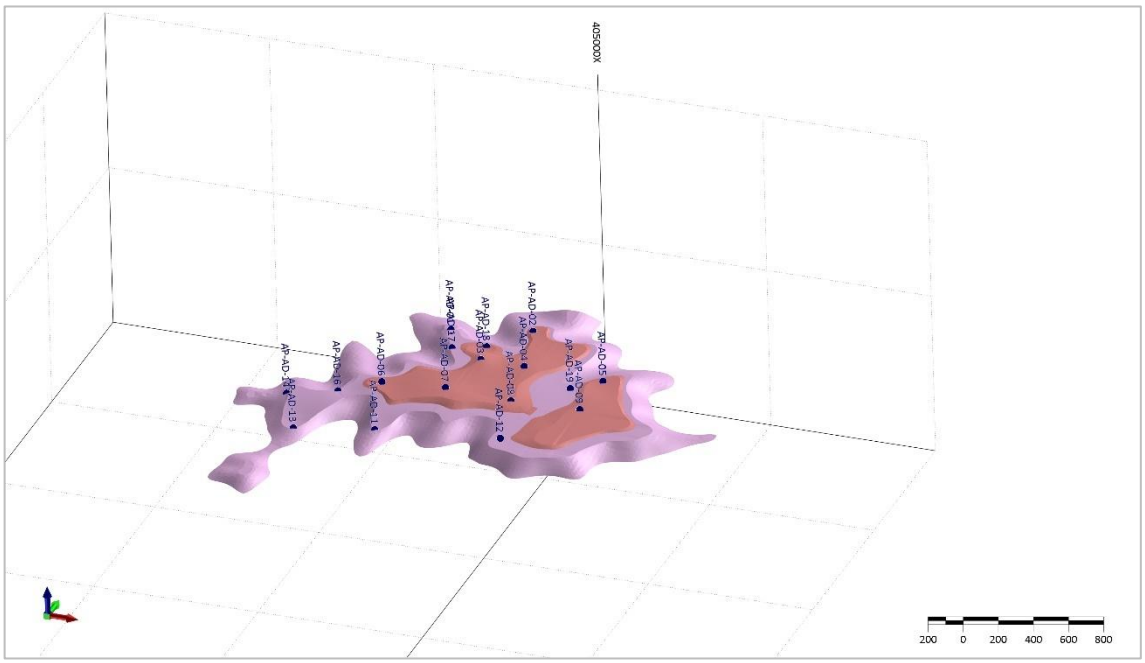


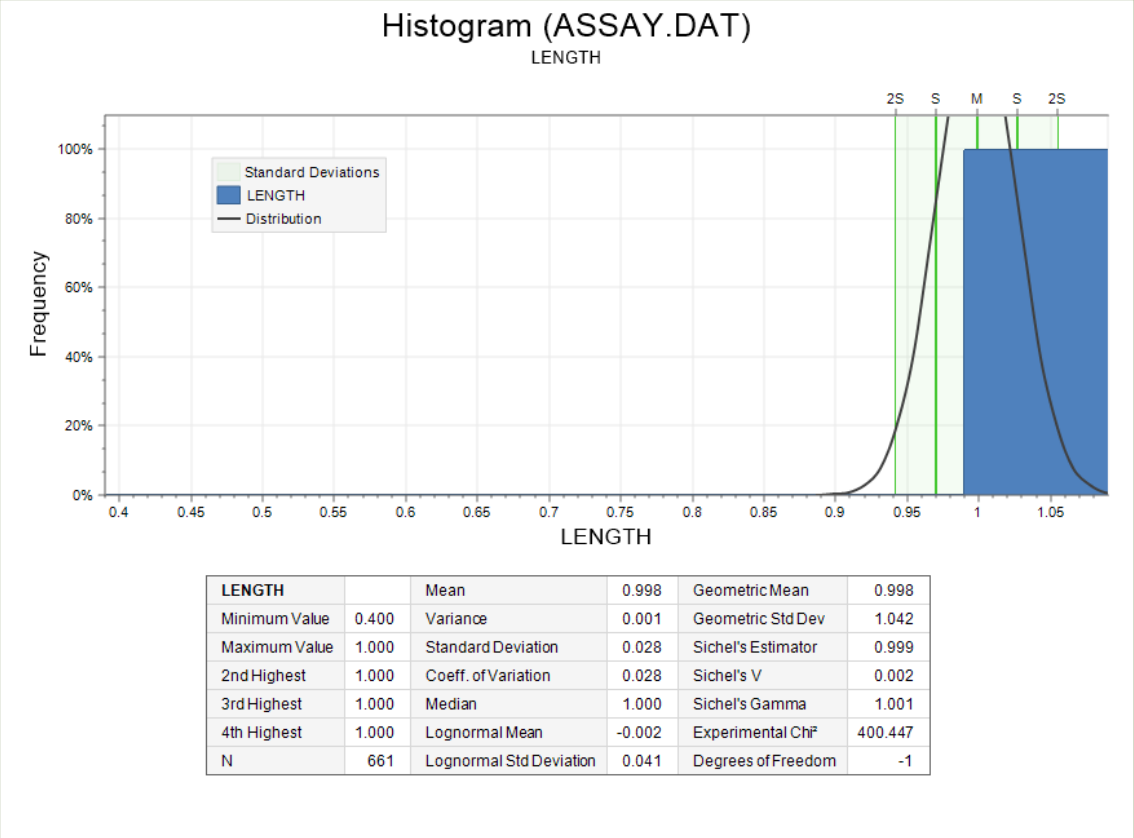

**Figure 14.26 - Mineralization body solids, Alto da Serra target**

Finally, orebodies were created for the regolith and coarse clastic sedimentary rocks in the rare earth mineralization zone.

## 14.5 Data Selection

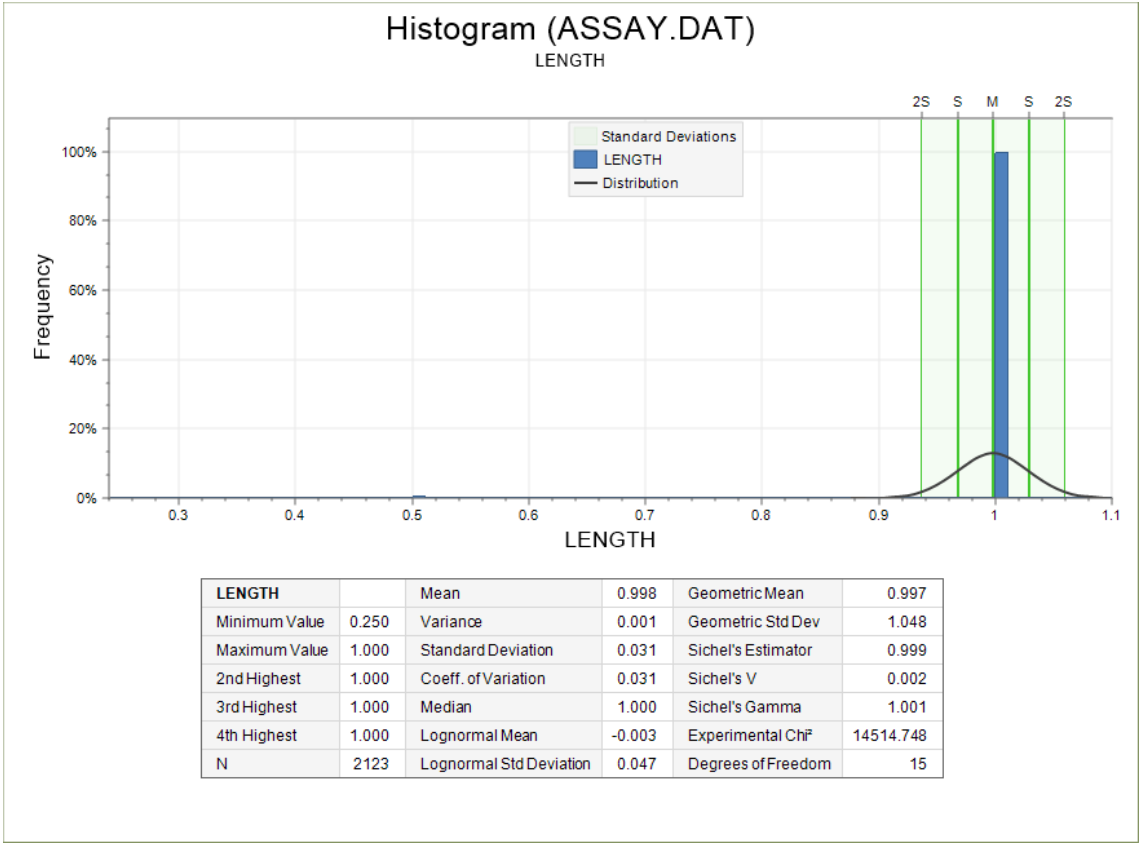
The selection of drill hole data is done via a standard certification procedure. It is essential that, during the classical statistical analysis, geostatistics and grade interpolation process, the correct samples are used. The solids of the element to be analyzed were used for drill hole sample selection.

During the analysis of samples internal to the ore body, it was noted that most of the samples collected and analyzed (approximately 99% of the samples) had a length of 1 m. A graph of sampling length distribution for the Nau de Guerra target is shown in Figure 14.27 and a graph of sampling length distribution for the Balsamo and Alto da Serra targets is show in Figure 14.28.




| LENGTH | | Mean | 0.998 | Geometric Mean | 0.998 |
| --- | --- | --- | --- | --- | --- |
| Minimum Value | 0.400 | Variance | 0.001 | Geometric Std Dev | 1.042 |
| Maximum Value | 1.000 | Standard Deviation | 0.028 | Sichel's Estimator | 0.999 |
| 2nd Highest | 1.000 | Coeff. of Variation | 0.028 | Sichel's V | 0.002 |
| 3rd Highest | 1.000 | Median | 1.000 | Sichel's Gamma | 1.001 |
| 4th Highest | 1.000 | Lognormal Mean | -0.002 | Experimental Chi² | 400.447 |
| N | 661 | Lognormal Std Deviation | 0.041 | Degrees of Freedom | -1 |

**Figure 14.27 - Histogram of sample size distribution, Nau de Guerra target**




| LENGTH | | Mean | 0.998 | Geometric Mean | 0.997 |
|---|---|---|---|---|---|
| Minimum Value | 0.250 | Variance | 0.001 | Geometric Std Dev | 1.048 |
| Maximum Value | 1.000 | Standard Deviation | 0.031 | Sichel's Estimator | 0.999 |
| 2nd Highest | 1.000 | Coeff. of Variation | 0.031 | Sichel's V | 0.002 |
| 3rd Highest | 1.000 | Median | 1.000 | Sichel's Gamma | 1.001 |
| 4th Highest | 1.000 | Lognormal Mean | -0.003 | Experimental Chi² | 14514.748 |
| N | 2123 | Lognormal Std Deviation | 0.047 | Degrees of Freedom | 15 |

**Figure 14.28 - Histogram of sample size distribution, Balsamo and Alto da Serra target**

Thus, a length of 1 m was adopted for the composite samples, and all the samples were converted into 1 meter sections. The process of creating the composite intervals started at the hole collar and proceeded in the direction of the drilling (downwards). Intervals below 0.80 m were excluded.

The descriptive statistics for composite samples for regolith and saprolite are presented in Table 14.2.

**Table 14.2 - Descriptive statistics for composite samples**

| Chemical analyses | Quantity | Minimum | Maximum | Average | Median | Variance | Std. Deviation |
|---|---|---|---|---|---|---|---|
| **Nau de Guerra Target** | | | | | | | |
| Y | 660 | 11.89 | 685.32 | 70.165 | 58.815 | 1974.42845 | 44.43454 |
| La | 660 | 63.6 | 2549.3 | 682.064 | 631.75 | 125321.522 | 354.0078 |
| Ce | 660 | 166.2 | 5220.3 | 1376.514 | 1278.05 | 467808.588 | 683.96534 |
| Pr | 660 | 15.73 | 649.97 | 151.634 | 136.785 | 7130.78737 | 84.44399 |
| Nd | 660 | 57.4 | 2428 | 544.692 | 489.75 | 94993.5705 | 308.21027 |
| Sm | 660 | 7.9 | 347.7 | 75.399 | 67.2 | 1878.34229 | 43.33985 |
| Eu | 660 | 1.75 | 85.33 | 18.526 | 16.48 | 115.26576 | 10.73619 |
| Gd | 660 | 4.76 | 246.29 | 45.106 | 39.715 | 697.64312 | 26.41293 |
| Tb | 660 | 0.61 | 26.49 | 4.673 | 4.11 | 7.11678 | 2.66773 |

| Chemical analyses | Quantity | Minimum | Maximum | Average | Median | Variance | Std. Deviation |
|---|---|---|---|---|---|---|---|
| Dy | 660 | 3.34 | 132.49 | 20.979 | 18.1 | 140.33741 | 11.84641 |
| Ho | 660 | 0.51 | 21.73 | 3.038 | 2.61 | 2.90669 | 1.7049 |
| Er | 660 | 1.51 | 54.75 | 6.669 | 5.58 | 14.62239 | 3.82392 |
| Tm | 660 | 0.18 | 5.92 | 0.747 | 0.62 | 0.17013 | 0.41247 |
| Yb | 660 | 1.2 | 33.2 | 4.14 | 3.4 | 5.17334 | 2.2745 |
| Lu | 660 | 0.15 | 4.55 | 0.529 | 0.44 | 0.08762 | 0.29601 |
| **Balsamo Target** | | | | | | | |
| Y | 1150 | 3.31 | 797.96 | 63.915 | 51.245 | 3132.19143 | 55.96598 |
| La | 1150 | 5.1 | 2366 | 588.8 | 540.25 | 142462.364 | 377.44187 |
| Ce | 1150 | 13.8 | 4820.7 | 1228.251 | 1152.4 | 510773.47 | 714.68418 |
| Pr | 1150 | 1.37 | 582.81 | 130.847 | 119.025 | 7611.73282 | 87.24525 |
| Nd | 1150 | 4.1 | 2186.1 | 464.681 | 421.6 | 99167.1583 | 314.90817 |
| Sm | 1150 | 0.6 | 288.1 | 62.813 | 56.55 | 1814.93502 | 42.60205 |
| Eu | 1150 | 0.29 | 69 | 15.429 | 13.93 | 112.05156 | 10.58544 |
| Gd | 1150 | 0.6 | 164.96 | 37.746 | 33.885 | 681.75463 | 26.11043 |
| Tb | 1150 | 0.11 | 17.17 | 4.02 | 3.565 | 7.35238 | 2.71153 |
| Dy | 1150 | 0.66 | 92.1 | 18.062 | 15.65 | 150.12432 | 12.25252 |
| Ho | 1150 | 0.13 | 18.89 | 2.689 | 2.25 | 3.62679 | 1.90441 |
| Er | 1150 | 0.5 | 52.01 | 6.002 | 4.83 | 19.98232 | 4.47016 |
| Tm | 1150 | 0.08 | 6.88 | 0.693 | 0.55 | 0.28475 | 0.53362 |
| Yb | 1150 | 0.5 | 40.1 | 3.863 | 3.1 | 8.96649 | 2.99441 |
| Lu | 1150 | 0.05 | 5.96 | 0.508 | 0.4 | 0.17677 | 0.42044 |
| **Alto da Serra Target** | | | | | | | |
| Y | 968 | 5.13 | 678.1 | 69.438 | 53.06 | 4397.56194 | 66.31412 |
| La | 968 | 4.7 | 3436.1 | 632.297 | 550.8 | 210605.512 | 458.91776 |
| Ce | 968 | 10.8 | 6784.9 | 1286.529 | 1110.1 | 913016.882 | 955.51917 |
| Pr | 968 | 0.82 | 896.7 | 142.917 | 117.735 | 14707.2961 | 121.27364 |
| Nd | 968 | 2.9 | 3460.2 | 516.089 | 422.8 | 204184.675 | 451.86798 |
| Sm | 968 | 0.7 | 484.6 | 70.735 | 57.3 | 3777.82324 | 61.464 |
| Eu | 968 | 0.16 | 115.67 | 17.238 | 13.985 | 228.05508 | 15.10149 |
| Gd | 968 | 0.69 | 303.82 | 42.086 | 34.065 | 1287.91635 | 35.88755 |
| Tb | 968 | 0.13 | 31.99 | 4.423 | 3.545 | 13.28581 | 3.64497 |
| Dy | 968 | 0.86 | 153.18 | 20.165 | 16.285 | 264.12884 | 16.25204 |
| Ho | 968 | 0.19 | 22.11 | 2.992 | 2.36 | 5.88415 | 2.42573 |
| Er | 968 | 0.6 | 51.65 | 6.666 | 5.125 | 30.82814 | 5.55231 |
| Tm | 968 | 0.09 | 6.16 | 0.76 | 0.57 | 0.41134 | 0.64135 |
| Yb | 968 | 0.6 | 37.1 | 4.31 | 3.3 | 12.95938 | 3.59991 |
| Lu | 968 | 0.1 | 5.89 | 0.56 | 0.43 | 0.24772 | 0.49771 |

## 14.6 Geostatistical Analysis

Geostatistical studies were carried out for the entire mineralized zone. The file containing data on the 1-meter composite sample was used for the construction of the semivariograms. Semivariograms were created based on the analysis of the following elements: TLREE (La+Ce+Pr+Nd+Sm+Eu), THREE (Dy+Er+Gd+Ho+Tm+Yb+Lu+Tb), Y, Th and U. A cross-validation process was used to verify the variograms. The results indicated a low value for statistical error in data interpolation.

The semivariograms generated for TLREE in the **Balsamo** target are presented in Figure 14.29 to Figure 14.31. Figure 14.33 to Figure 14.35 present data on the THREE elements. Table 14.3 shows the cross-validation result generated for the TLREE elements and Table 14.4 shows the cross-validation result generated for the THREE elements.

The semivariograms generated for TLREE in the **Nau de Guerra** target are presented in Figure 14.37 to Figure 14.39. Figure 14.41 to Figure 14.43 present the THREE elements. Table 14.5 shows the cross-validation result generated for the TLREE elements and Table 14.6 shows the cross-validation result generated for the THREE elements.

The semivariograms generated for TLREE in the **Alto da Serra** target are presented in Figure 14.37 to Figure 14.47. Figure 14.49 to Figure 14.51 present the THREE elements. Table 14.7 shows the cross-validation result generated for the TLREE elements and Table 14.8 shows the cross-validation result generated for the THREE elements.

A linear dependence diagram between the data from the composite samples file and the estimate of the grade obtained via the Cross-Validation process was also constructed.

Figure 14.32 shows the linear dependence diagram generated for the TLREE elements and Figure 14.36 shows the linear dependence diagram generated for the THREE elements for the Balsamo target.

The Figure 14.40 shows the linear dependence diagram generated for the TLREE elements and Figure 14.44 shows the linear dependence diagram generated for the THREE elements for the Nau de Gerra target.

The Figure 14.48 shows the linear dependence diagram generated for the TLREE elements and Figure 14.52 shows the linear dependence diagram generated for the THREE elements for the Alto da Serra target.

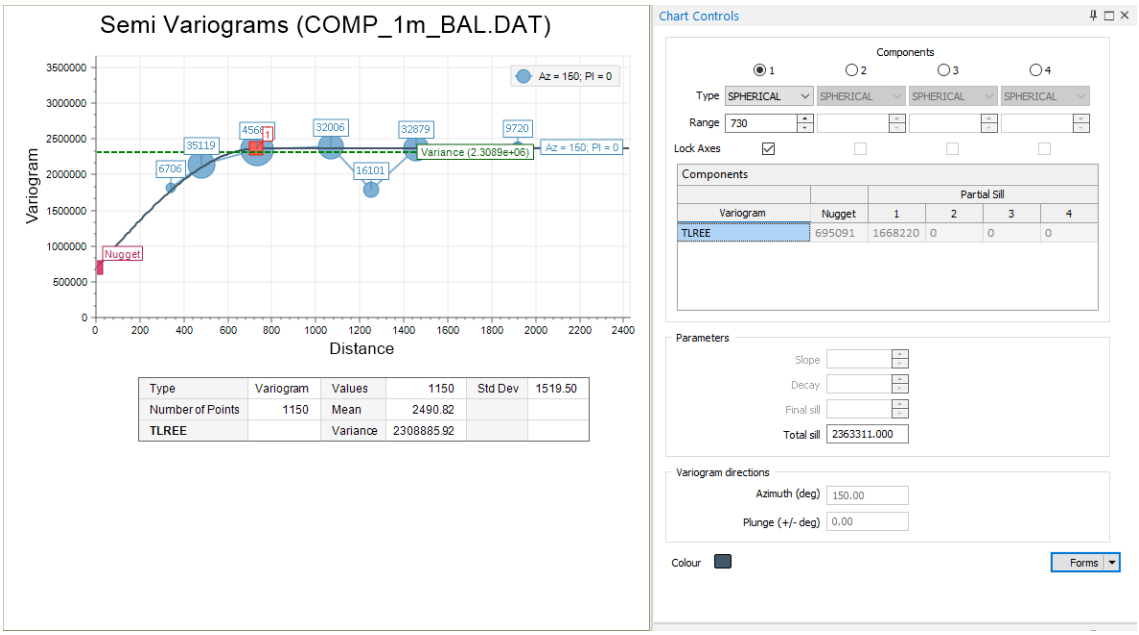



**Figure 14.29 - First axis to TLREE (ppm), Balsamo target**

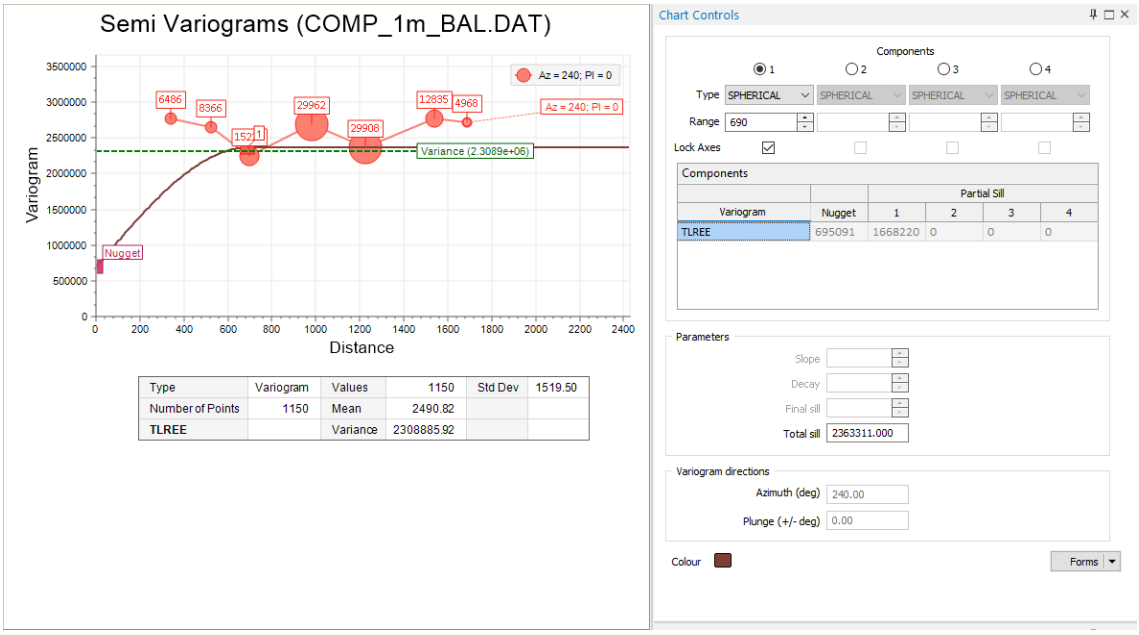



**Figure 14.30 - Second axis to TLREE (ppm), Balsamo target**

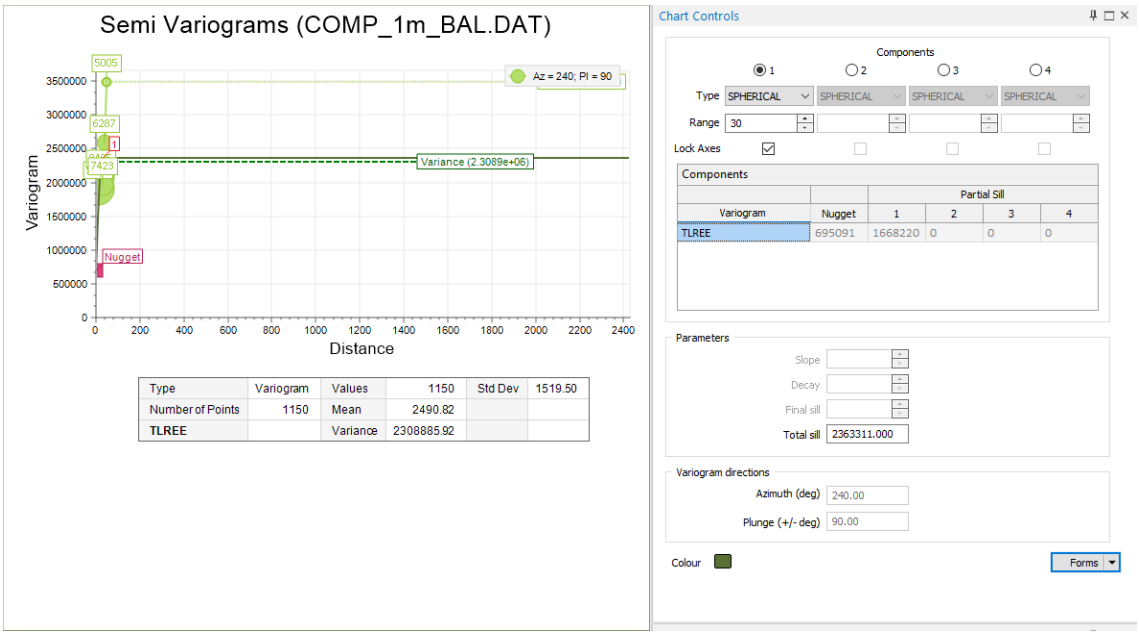
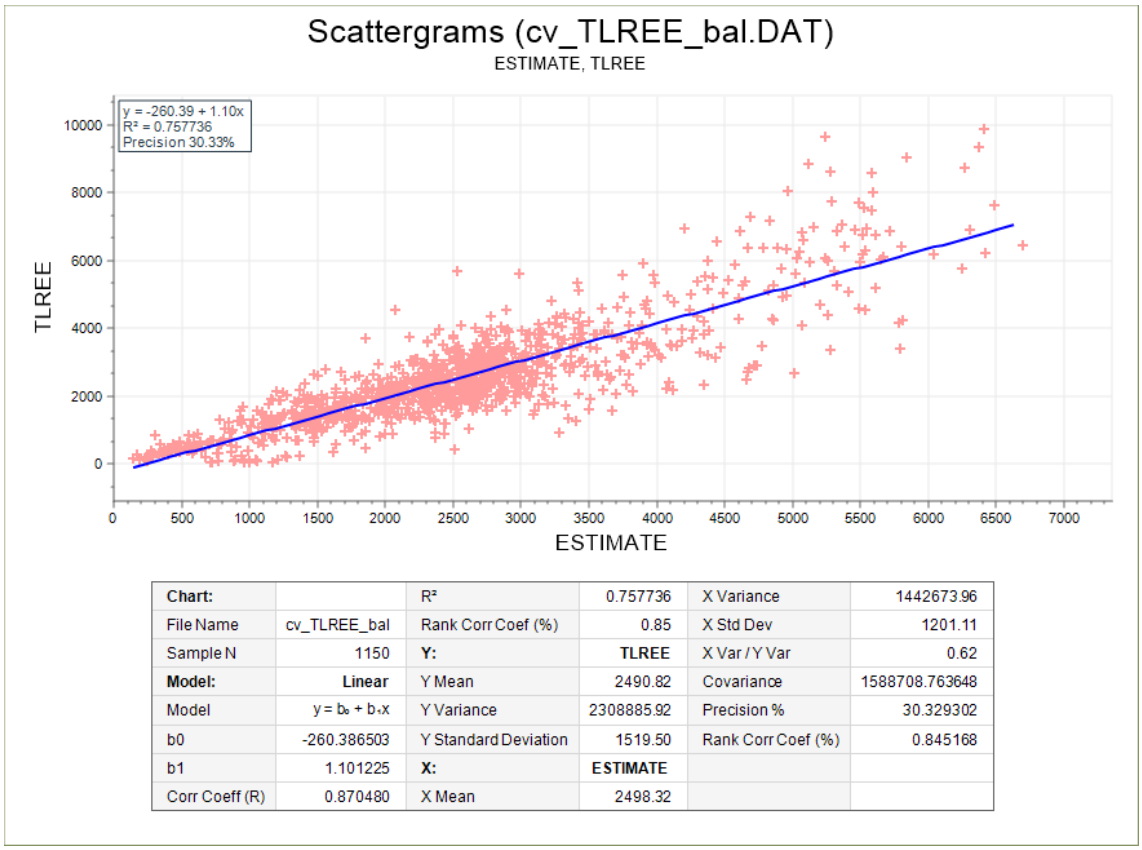



**Figure 14.31 - Third axis to TLREE (ppm), Balsamo target**

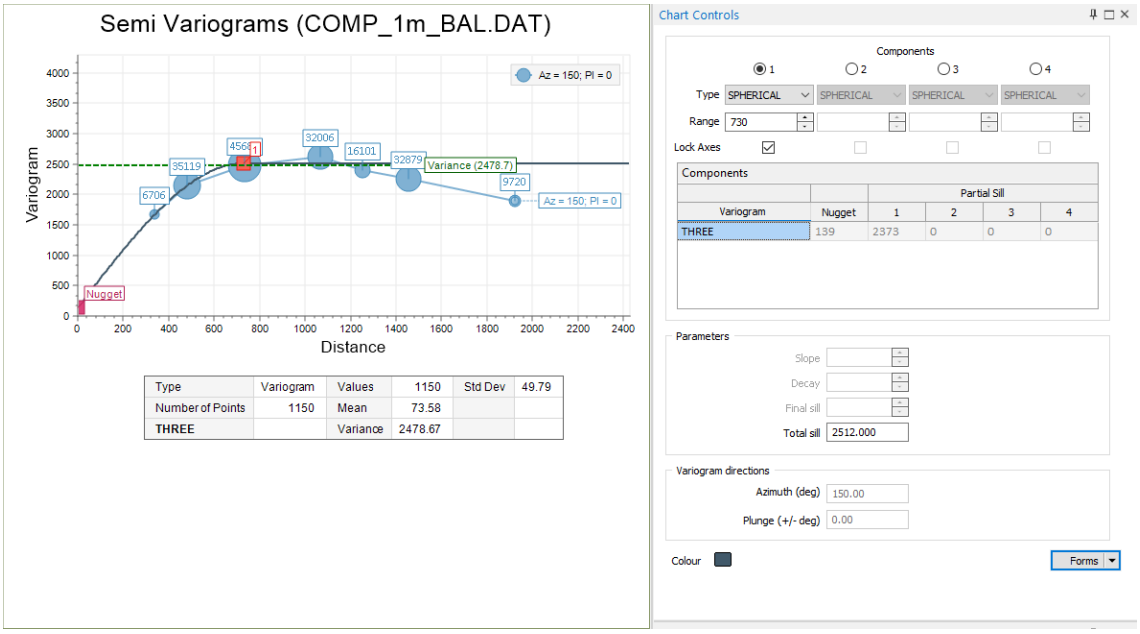
**Table 14.3 - Cross-Validation verification results for TLREE (ppm), Balsamo target**

| Metadata Label | Metadata Value | Field Name | Mean | Std Dev |
| --- | --- | --- | --- | --- |
| Output File | cv_TLREE_bal.DAT | | | |
| Input File | COMP_1m_BAL.DAT | | | |
| Analysis varb | TLREE | | | |
| Transformation | None | | | |
| Number of points | 1150 | | | |
| Raw Data | | TLREE | 2490.821852174 | 1519.501866160 |
| Standard error | | STD_ERROR | 959.830000589 | 17.373620262 |
| Estimate | | ESTIMATE | 2498.316089758 | 1201.113635238 |
| Residual | | RESIDUAL | -7.494237584 | 757.721821465 |
| Error statistic | | ERROR_STAT | -0.006201581 | 0.790260099 |
| RMSE | | | 757.429381591 | |




| Chart: | | R² | 0.757736 | X Variance | 1442673.96 |
|---|---|---|---|---|---|
| File Name | cv_TLREE_bal | Rank Corr Coef (%) | 0.85 | X Std Dev | 1201.11 |
| Sample N | 1150 | **Y:** | **TLREE** | X Var / Y Var | 0.62 |
| **Model:** | **Linear** | Y Mean | 2490.82 | Covariance | 1588708.763648 |
| Model | $y = b_0 + b_1 x$ | Y Variance | 2308885.92 | Precision % | 30.329302 |
| b0 | -260.386503 | Y Standard Deviation | 1519.50 | Rank Corr Coef (%) | 0.845168 |
| b1 | 1.101225 | **X:** | **ESTIMATE** | | |
| Corr Coeff (R) | 0.870480 | X Mean | 2498.32 | | |

**Figure 14.32 - Linear diagram of dependence between composite sample data and TLREE (ppm) grade estimates, Balsamo target**




| Type | Variogram | Values | 1150 | Std Dev | 49.79 |
|---|---|---|---|---|---|
| Number of Points | 1150 | Mean | 73.58 | | |
| **THREE** | | Variance | 2478.67 | | |

| Components | | | | | |
|---|---|---|---|---|---|
| | | Partial Sill | | | |
| Variogram | Nugget | 1 | 2 | 3 | 4 |
| THREE | 139 | 2373 | 0 | 0 | 0 |

**Figure 14.33 - First axis to THREE (ppm), Balsamo target**

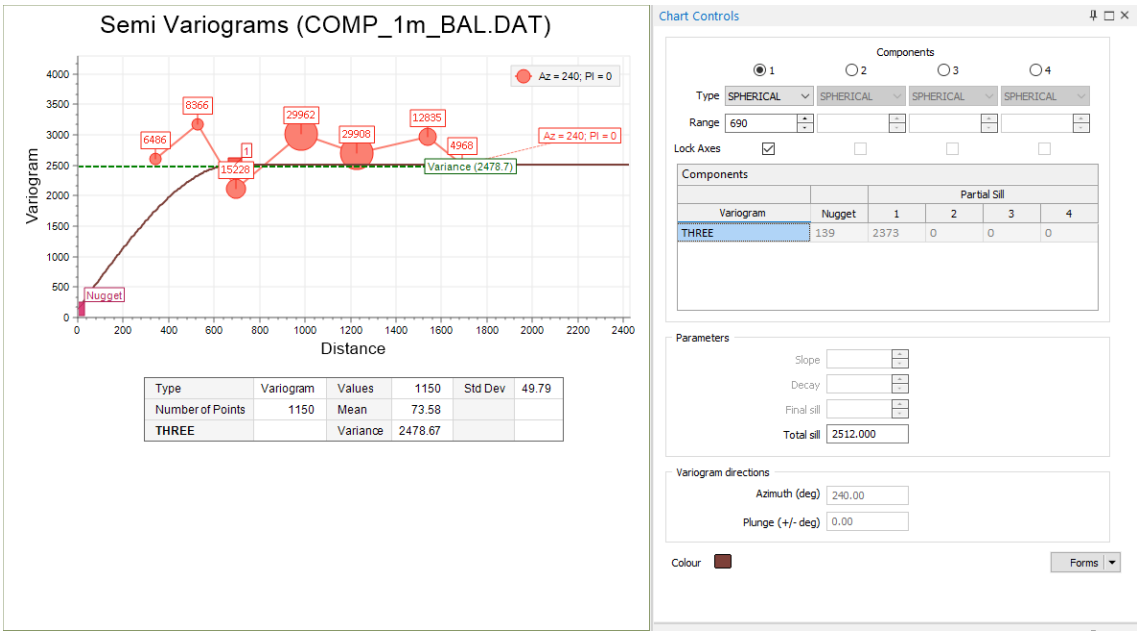



**Figure 14.34 - Second axis to THREE (ppm), Balsamo target**

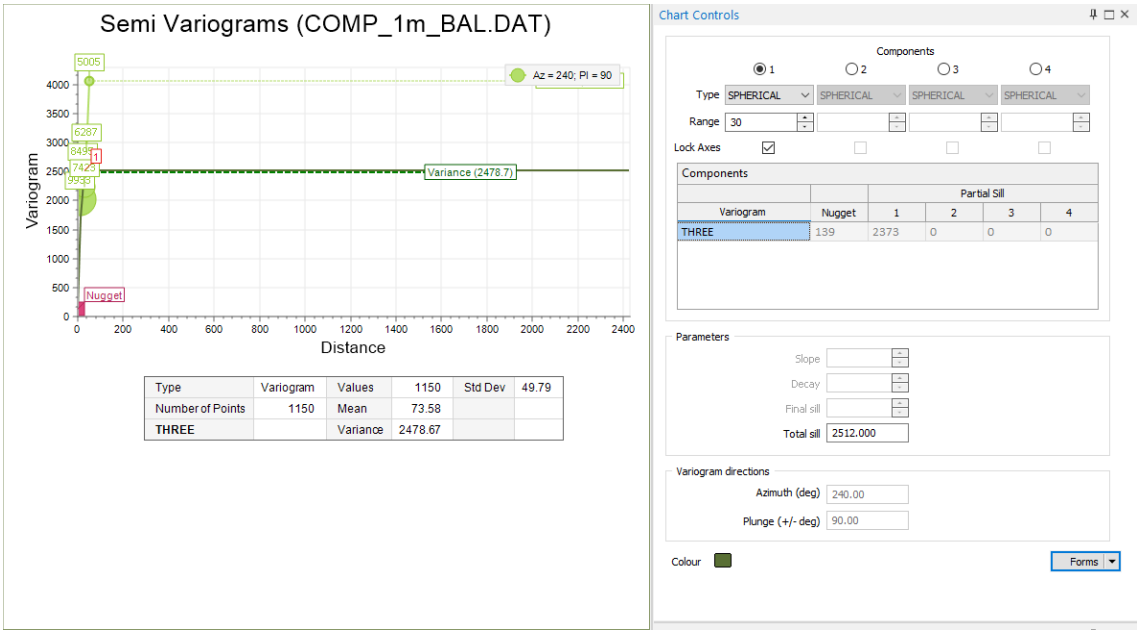
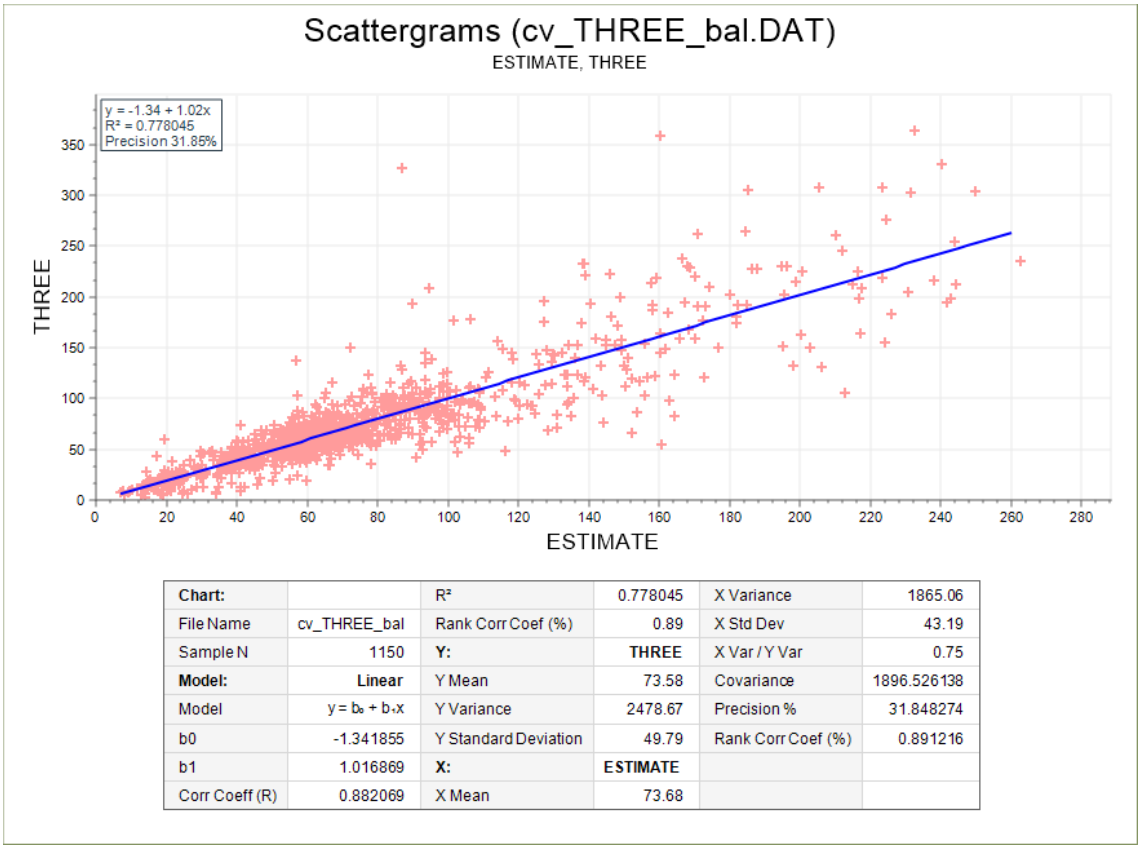



**Figure 14.35 - Third axis to THREE (ppm), Balsamo target**

**Table 14.4 - Cross-Validation verification results for THREE (ppm), Balsamo target**

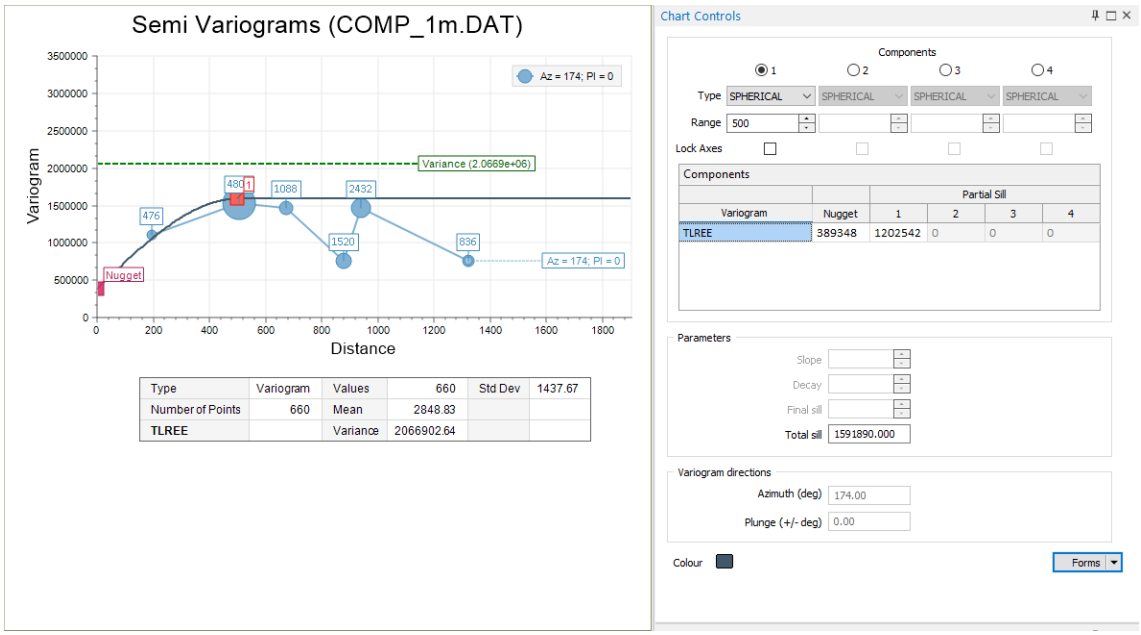
| Metadata Label | Metadata Value | Field Name | Mean | Std Dev |
|---|---|---|---|---|
| Output File | cv_THREE_bal.DAT | | | |
| Input File | COMP_1m_BAL.DAT | | | |
| Analysis varb | THREE | | | |
| Transformation | None | | | |

| Metadata Label | Metadata Value | Field Name | Mean | Std Dev |
|---|---|---|---|---|
| Number of points | 1150 | | | |
| Raw Data | | THREE | 73.583678261 | 49.786248914 |
| Standard error | | STD_ERROR | 17.656941859 | 0.695455954 |
| Estimate | | ESTIMATE | 73.682589490 | 43.186393340 |
| Residual | | RESIDUAL | -0.098911229 | 23.466633217 |
| Error statistic | | ERROR_STAT | -0.003854420 | 1.336678817 |
| RMSE | | | 23.456636658 | |



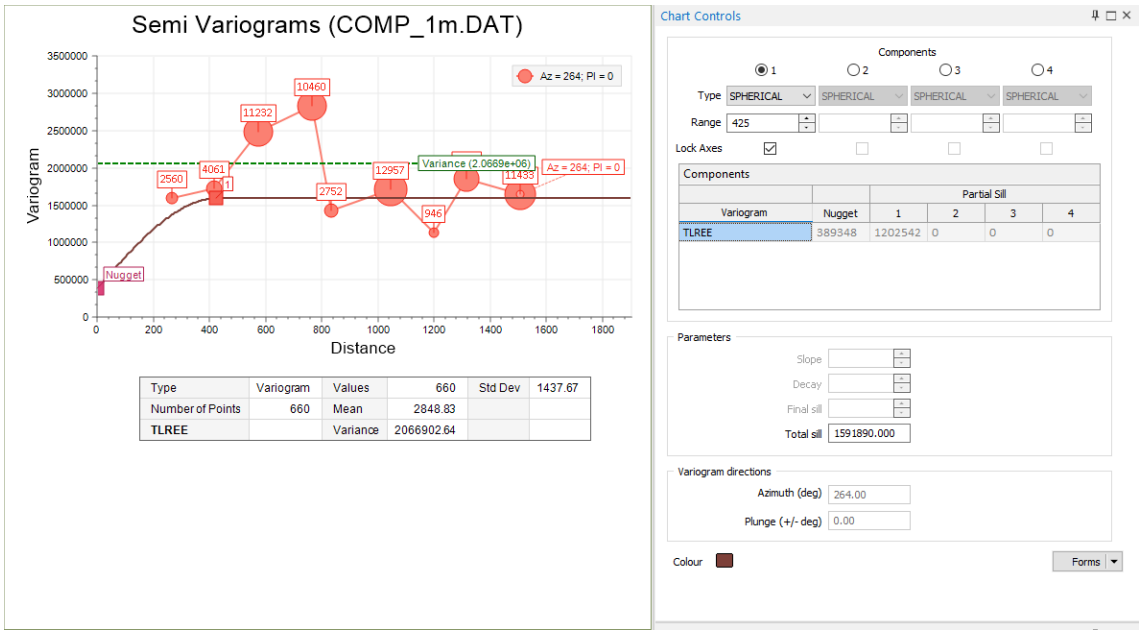

| Chart: | | R² | 0.778045 | X Variance | 1865.06 |
|---|---|---|---|---|---|
| File Name | cv_THREE_bal | Rank Corr Coef (%) | 0.89 | X Std Dev | 43.19 |
| Sample N | 1150 | **Y:** | **THREE** | X Var / Y Var | 0.75 |
| **Model:** | **Linear** | Y Mean | 73.58 | Covariance | 1896.526138 |
| Model | $y = b_0 + b_1 x$ | Y Variance | 2478.67 | Precision % | 31.848274 |
| b0 | -1.341855 | Y Standard Deviation | 49.79 | Rank Corr Coef (%) | 0.891216 |
| b1 | 1.016869 | **X:** | **ESTIMATE** | | |
| Corr Coeff (R) | 0.882069 | X Mean | 73.68 | | |

**Figure 14.36 - Linear diagram of dependence between composite samples data and THREE (ppm) grade estimates, Balsamo target**




| Type | Variogram | Values | 660 | Std Dev | 1437.67 |
| --- | --- | --- | --- | --- | --- |
| Number of Points | 660 | Mean | 2848.83 | | |
| **TLREE** | | Variance | 2066902.64 | | |

**Figure 14.37 - First axis to TLREE (ppm), Nau de Guerra target**




| Type | Variogram | Values | 660 | Std Dev | 1437.67 |
| --- | --- | --- | --- | --- | --- |
| Number of Points | 660 | Mean | 2848.83 | | |
| **TLREE** | | Variance | 2066902.64 | | |

**Figure 14.38 - Second axis to TLREE (ppm), Nau de Guerra target**

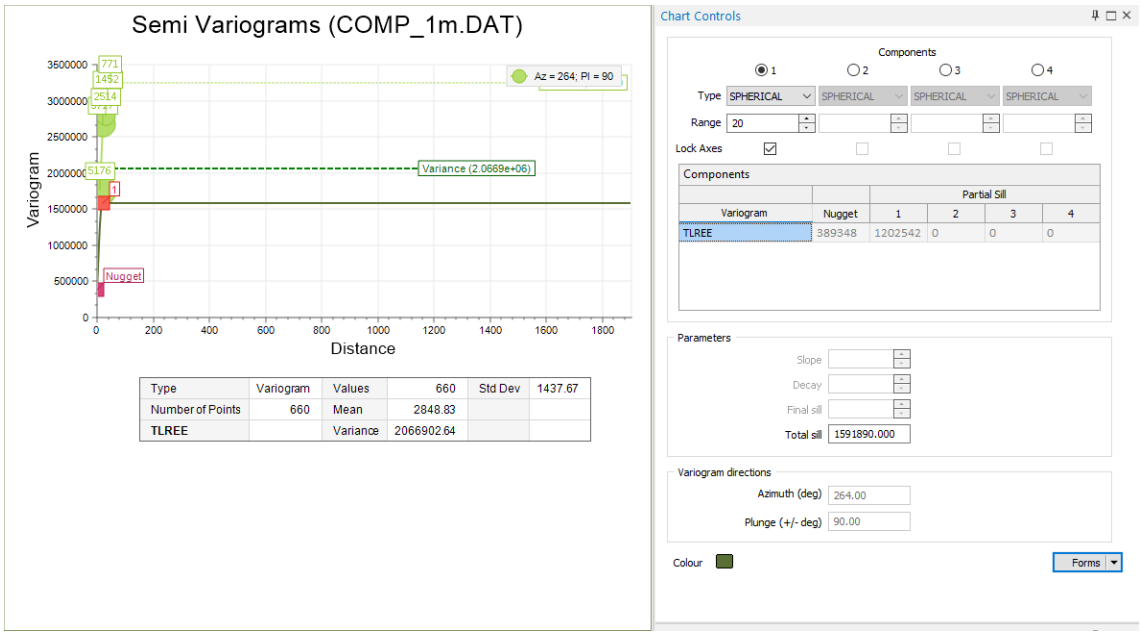
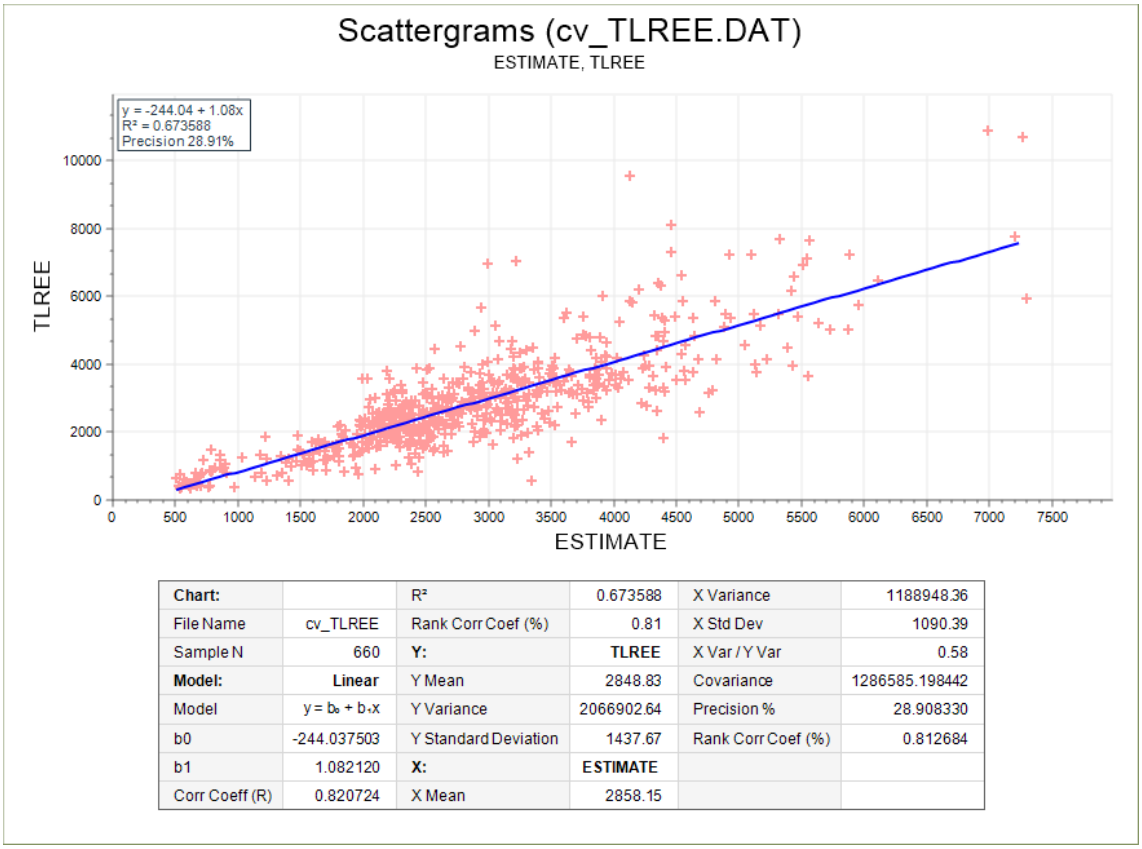



**Figure 14.39 - Third axis to TLREE (ppm), Nau de Guerra target**

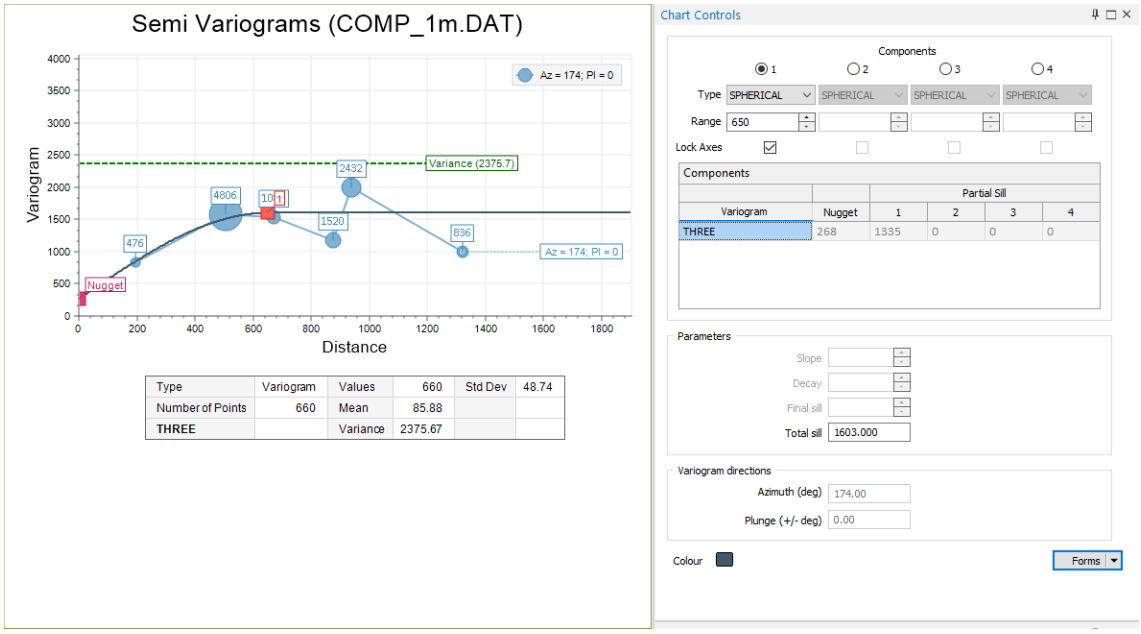
**Table 14.5 - Cross-Validation verification results for TLREE (ppm), Nau de Guerra target**

| Metadata Label | Metadata Value | Field Name | Mean | Std Dev |
| --- | --- | --- | --- | --- |
| Output File | cv_TLREE.DAT | | | |
| Input File | COMP_1m.DAT | | | |
| Analysis varb | TLREE | | | |
| Transformation | None | | | |
| Number of points | 660 | | | |
| Raw Data | | TLREE | 2848.830139394 | 1437.672646947 |
| Standard error | | STD_ERROR | 764.013182951 | 20.405825638 |
| Estimate | | ESTIMATE | 2858.154987878 | 1090.389085164 |
| Residual | | RESIDUAL | -9.324848484 | 826.244878919 |
| Error statistic | | ERROR_STAT | -0.008633994 | 1.077800115 |
| RMSE | | | 825.671356045 | |




| Chart: | | R² | 0.673588 | X Variance | 1188948.36 |
| --- | --- | --- | --- | --- | --- |
| File Name | cv_TLREE | Rank Corr Coef (%) | 0.81 | X Std Dev | 1090.39 |
| Sample N | 660 | **Y:** | **TLREE** | X Var / Y Var | 0.58 |
| **Model:** | **Linear** | Y Mean | 2848.83 | Covariance | 1286585.198442 |
| Model | $y = b_0 + b_1x$ | Y Variance | 2066902.64 | Precision % | 28.908330 |
| b0 | -244.037503 | Y Standard Deviation | 1437.67 | Rank Corr Coef (%) | 0.812684 |
| b1 | 1.082120 | **X:** | **ESTIMATE** | | |
| Corr Coeff (R) | 0.820724 | X Mean | 2858.15 | | |

**Figure 14.40 - Linear diagram of dependence between composite sample data and TLREE (ppm) grade estimates, Nau de Guerra target**




| Type | Variogram | Values | 660 | Std Dev | 48.74 |
| --- | --- | --- | --- | --- | --- |
| Number of Points | 660 | Mean | 85.88 | | |
| **THREE** | | Variance | 2375.67 | | |

**Figure 14.41 - First axis to THREE (ppm), Nau de Guerra target**

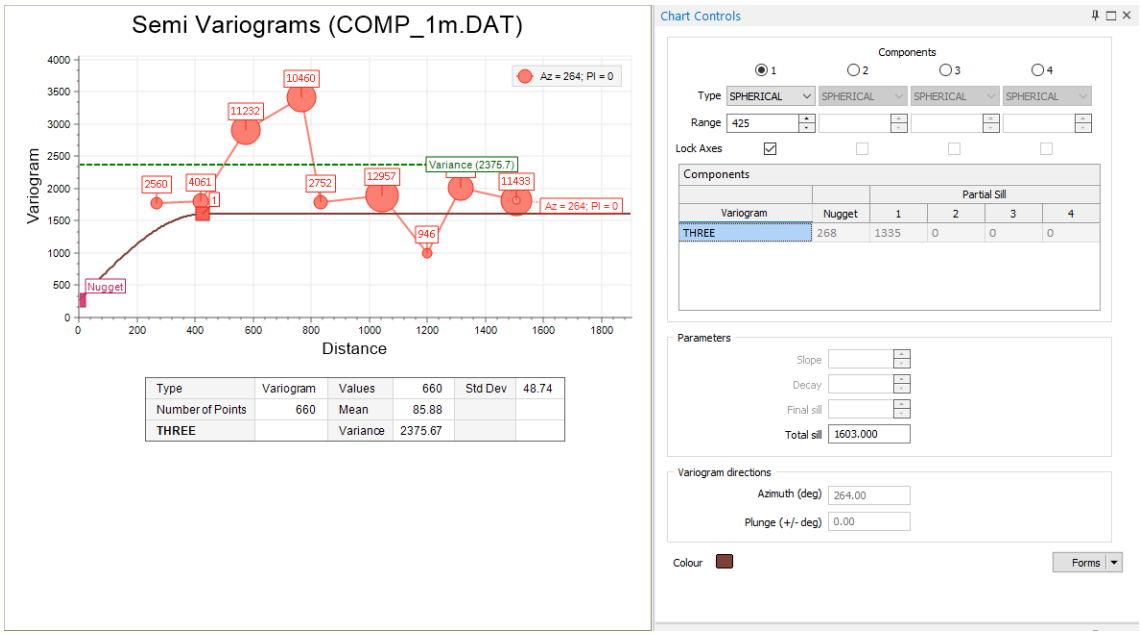



**Figure 14.42 - Second axis to THREE (ppm), Nau de Guerra target**

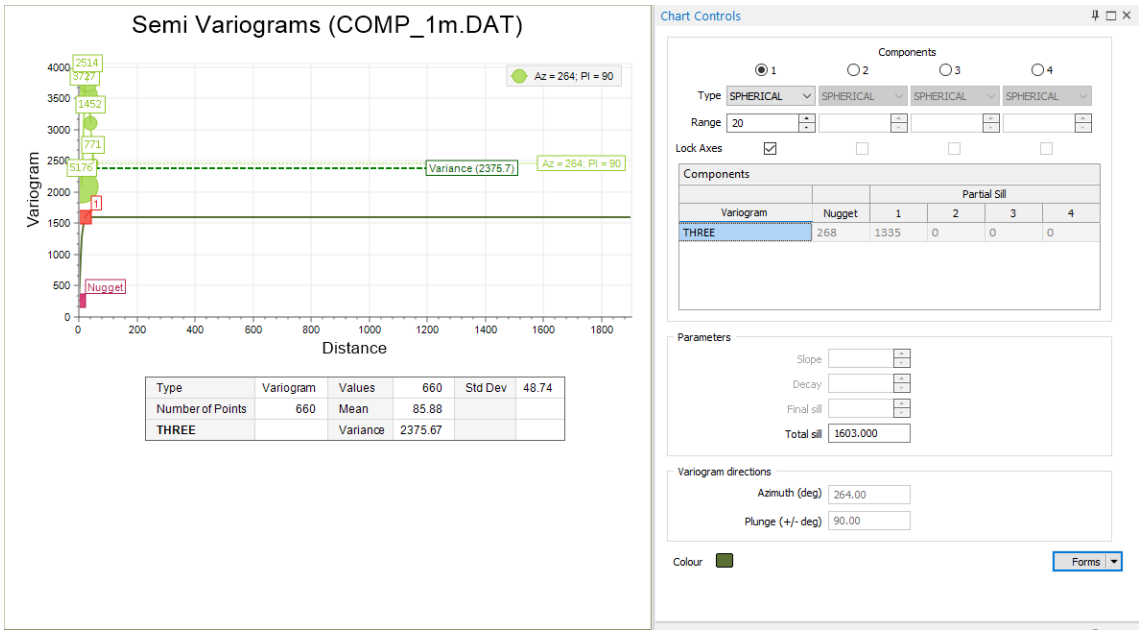
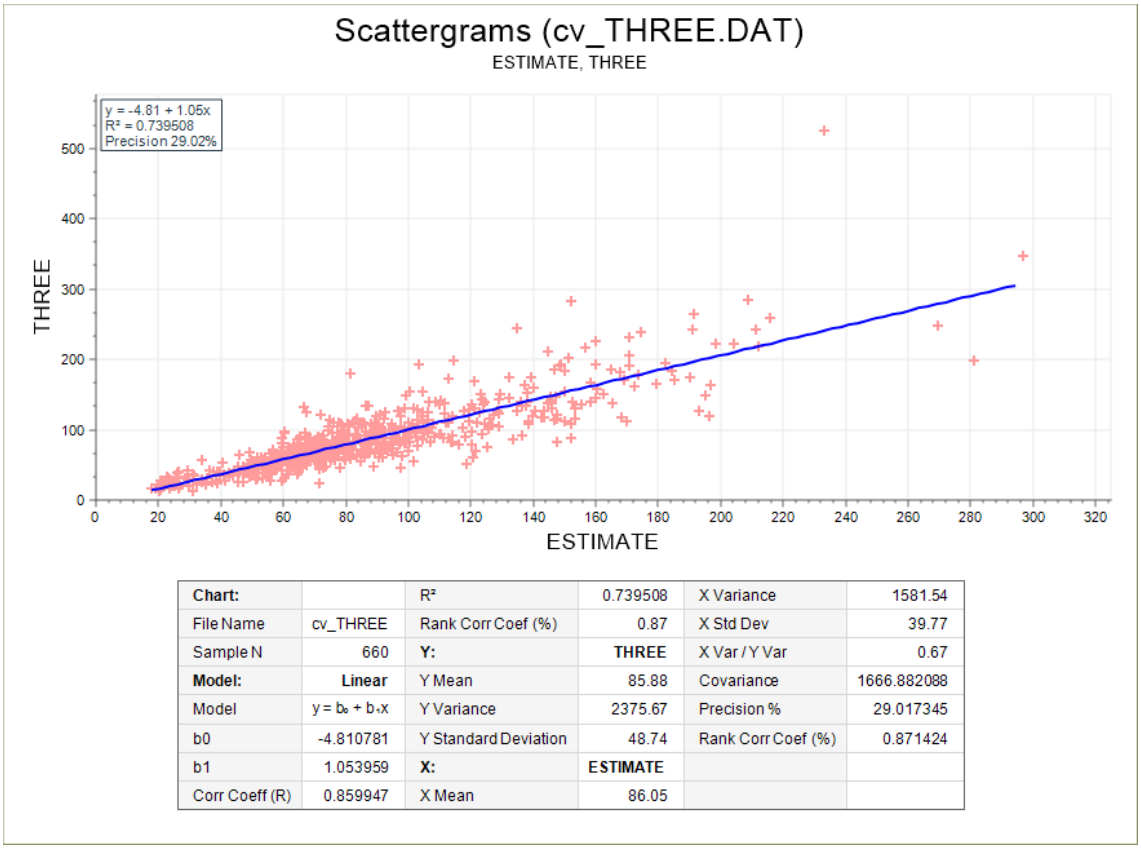



**Figure 14.43 - Third axis to THREE (ppm), Nau de Guerra target**

**Table 14.6 - Cross-Validation verification results for THREE (ppm), Nau de Guerra target**

| Metadata Label | Metadata Value | Field Name | Mean | Std Dev |
| --- | --- | --- | --- | --- |
| Output File | cv_THREE.DAT | | | |
| Input File | COMP_1m.DAT | | | |
| Analysis varb | THREE | | | |
| Transformation | None | | | |
| Number of points | 660 | | | |

| Metadata Label | Metadata Value | Field Name | Mean | Std Dev |
|---|---|---|---|---|
| Raw Data | | THREE | 85.880587879 | 48.740825456 |
| Standard error | | STD_ERROR | 21.259382404 | 0.680946828 |
| Estimate | | ESTIMATE | 86.048279488 | 39.768623293 |
| Residual | | RESIDUAL | -0.167691610 | 24.968926451 |
| Error statistic | | ERROR_STAT | -0.004701992 | 1.178216857 |
| RMSE | | | 24.950566957 | |




| Chart: | | R² | 0.739508 | X Variance | 1581.54 |
|---|---|---|---|---|---|
| File Name | cv_THREE | Rank Corr Coef (%) | 0.87 | X Std Dev | 39.77 |
| Sample N | 660 | **Y:** | **THREE** | X Var / Y Var | 0.67 |
| **Model:** | **Linear** | Y Mean | 85.88 | Covariance | 1666.882088 |
| Model | $y = b_0 + b_1 x$ | Y Variance | 2375.67 | Precision % | 29.017345 |
| b0 | -4.810781 | Y Standard Deviation | 48.74 | Rank Corr Coef (%) | 0.871424 |
| b1 | 1.053959 | **X:** | **ESTIMATE** | | |
| Corr Coeff (R) | 0.859947 | X Mean | 86.05 | | |

**Figure 14.44 - Linear diagram of dependence between composite sample data and THREE (ppm) grade estimates, Nau de Guerra target**

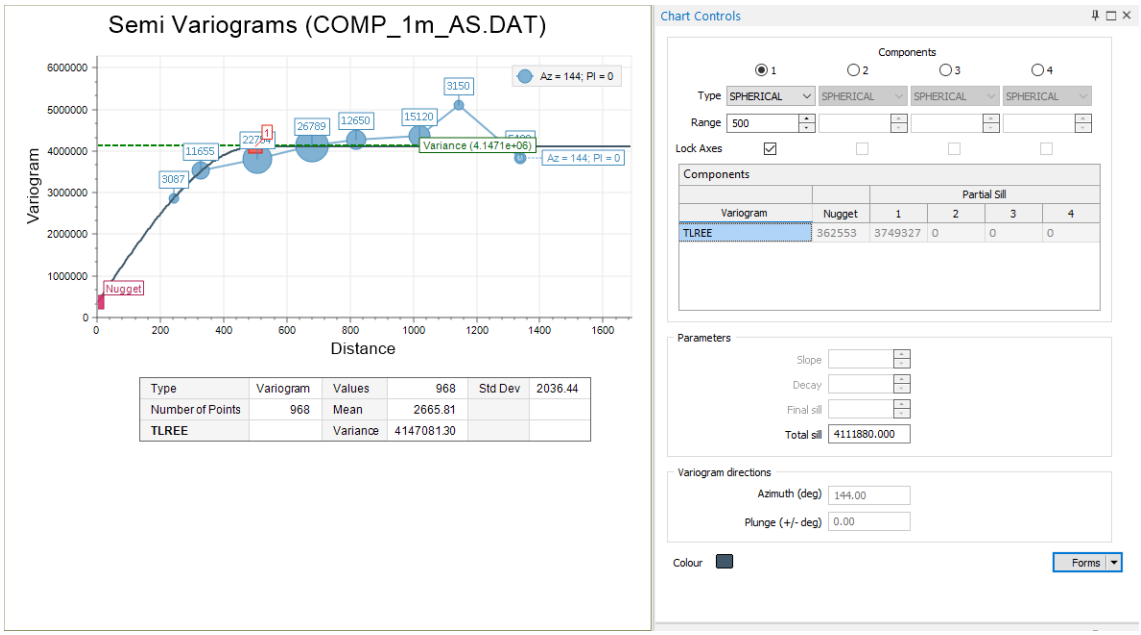



**Figure 14.45 - First axis to TLREE (ppm), Alto da Serra target**

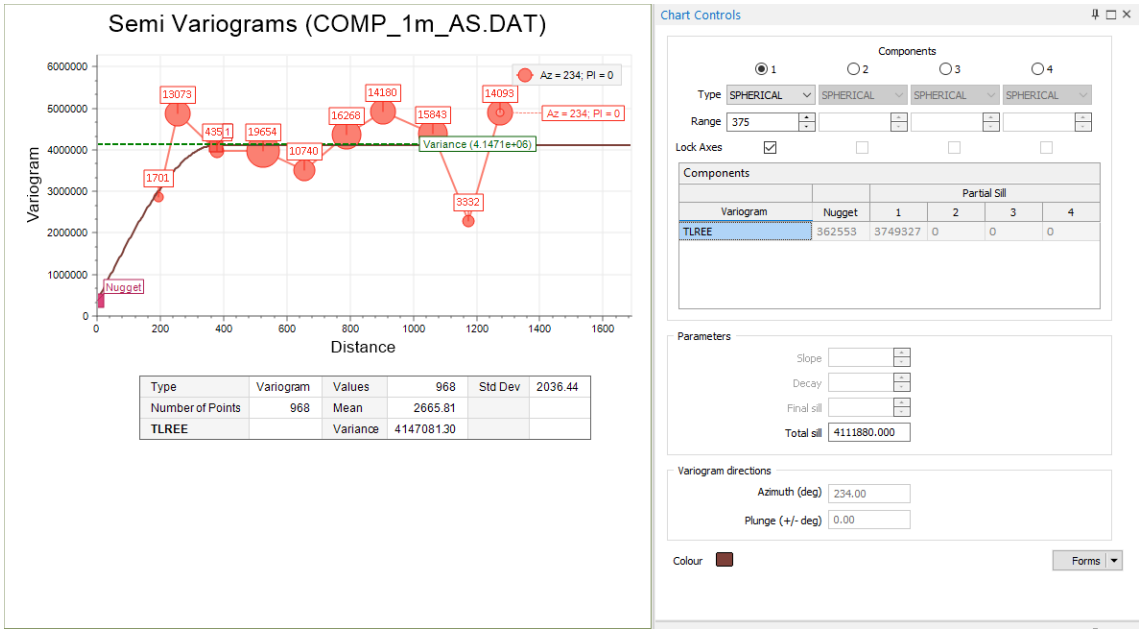



**Figure 14.46 - Second axis to TLREE (ppm), Alto da Serra target**

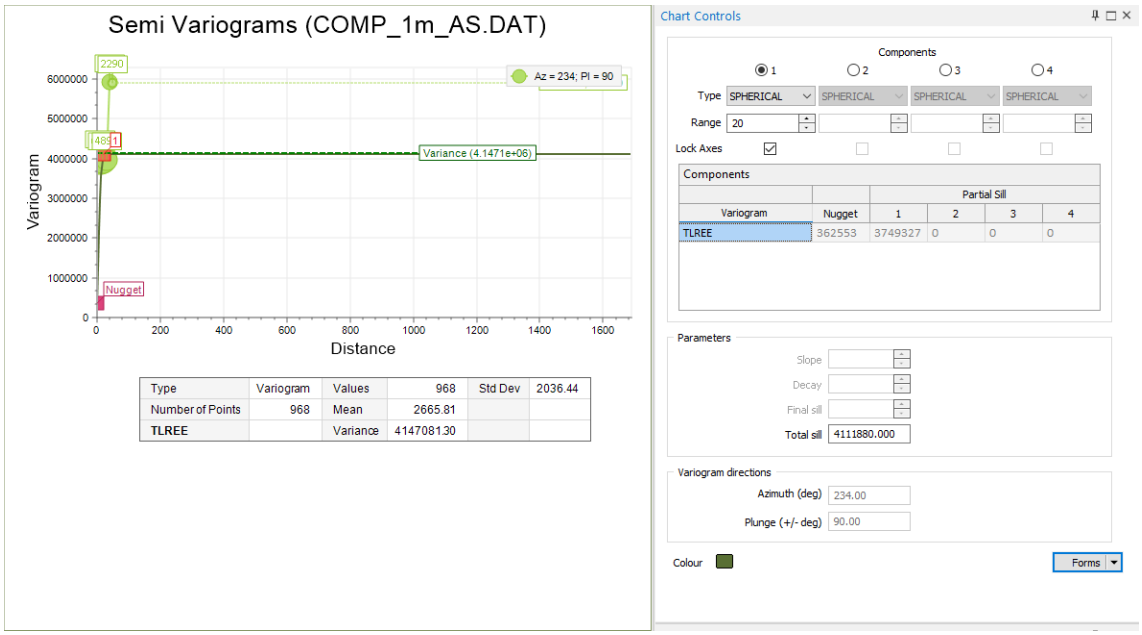
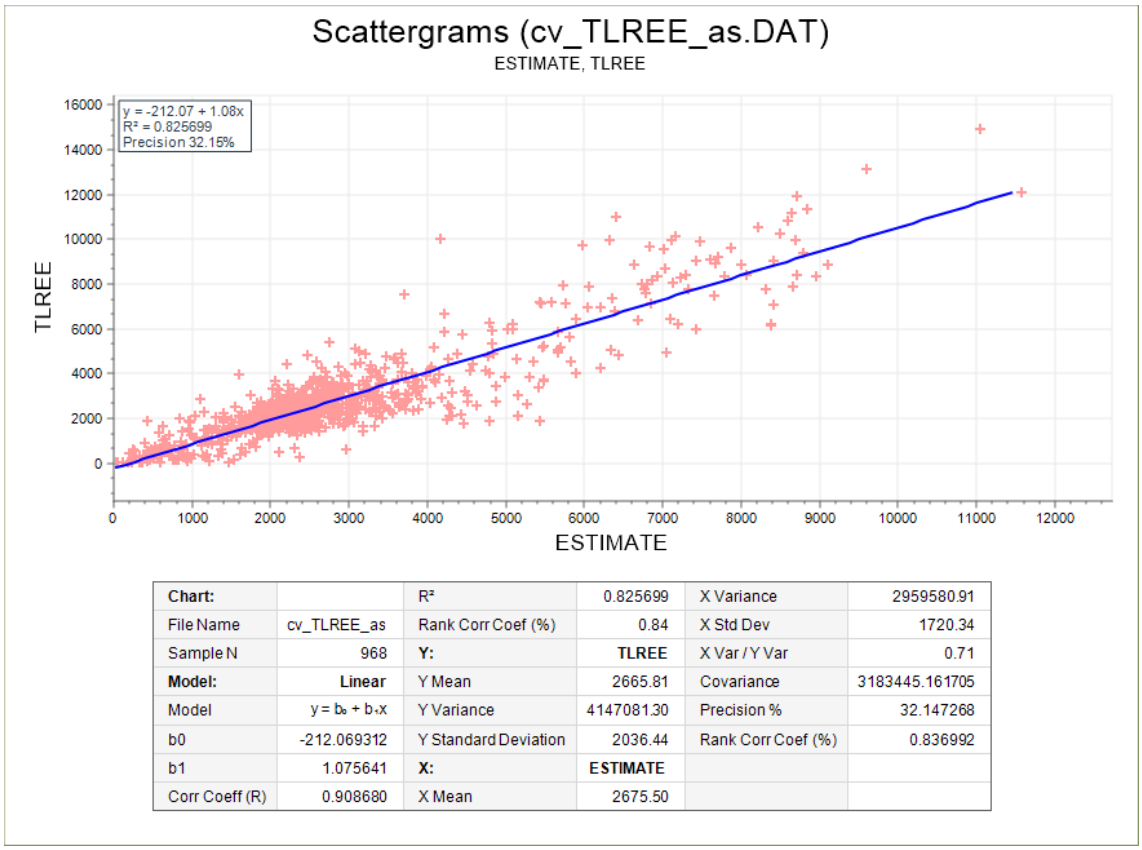



**Figure 14.47 - Third axis to TLREE (ppm), Alto da Serra target**

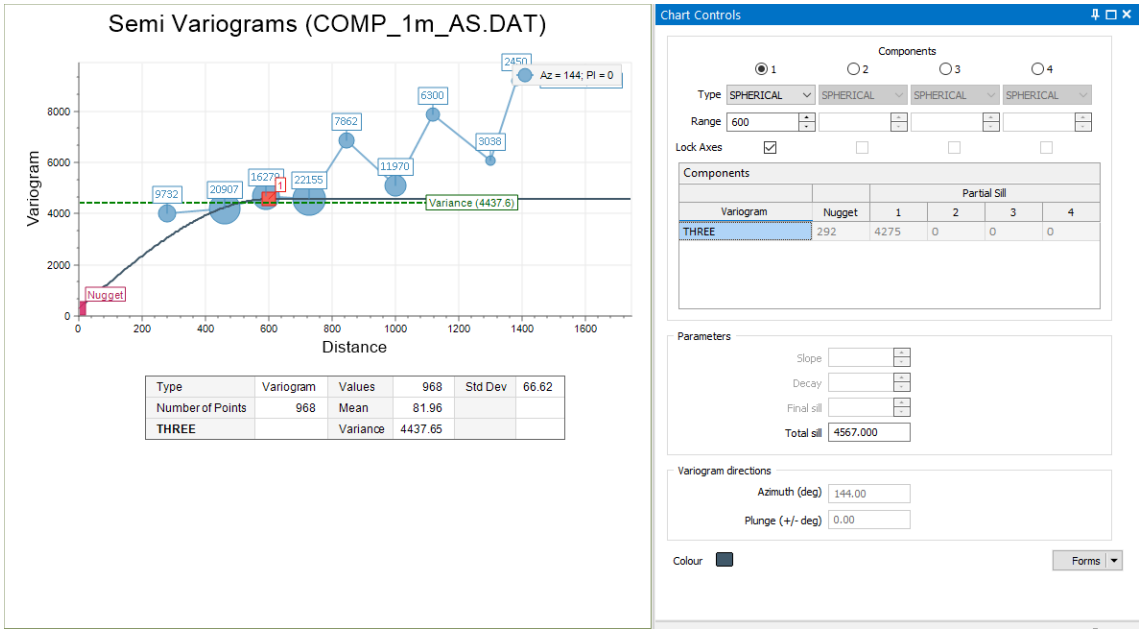
**Table 14.7 - Cross-Validation verification results for TLREE (ppm), Alto da Serra target**

| Metadata Label | Metadata Value | Field Name | Mean | Std Dev |
| --- | --- | --- | --- | --- |
| Output File | cv_TLREE_as.DAT | | | |
| Input File | COMP_1m_AS.DAT | | | |
| Analysis varb | TLREE | | | |
| Transformation | None | | | |
| Number of points | 968 | | | |
| Raw Data | | TLREE | 2665.806136364 | 2036.438386587 |
| Standard error | | STD_ERROR | 887.297580875 | 39.475161873 |
| Estimate | | ESTIMATE | 2675.499280041 | 1720.343253431 |
| Residual | | RESIDUAL | -9.693143677 | 860.099929416 |
| Error statistic | | ERROR_STAT | -0.007194846 | 0.975186597 |
| RMSE | | | 859.710194460 | |




| Chart: | | R² | 0.825699 | X Variance | 2959580.91 |
| --- | --- | --- | --- | --- | --- |
| File Name | cv_TLREE_as | Rank Corr Coef (%) | 0.84 | X Std Dev | 1720.34 |
| Sample N | 968 | **Y:** | **TLREE** | X Var / Y Var | 0.71 |
| **Model:** | **Linear** | Y Mean | 2665.81 | Covariance | 3183445.161705 |
| Model | $y = b_0 + b_1 x$ | Y Variance | 4147081.30 | Precision % | 32.147268 |
| b0 | -212.069312 | Y Standard Deviation | 2036.44 | Rank Corr Coef (%) | 0.836992 |
| b1 | 1.075641 | **X:** | **ESTIMATE** | | |
| Corr Coeff (R) | 0.908680 | X Mean | 2675.50 | | |

**Figure 14.48 - Linear diagram of dependence between composite sample data and TLREE (ppm) grade estimates, Alto da Serra target**




| Type | Variogram | Values | 968 | Std Dev | 66.62 |
| --- | --- | --- | --- | --- | --- |
| Number of Points | 968 | Mean | 81.96 | | |
| **THREE** | | Variance | 4437.65 | | |

**Figure 14.49 - First axis to THREE (ppm), Alto da Serra target**

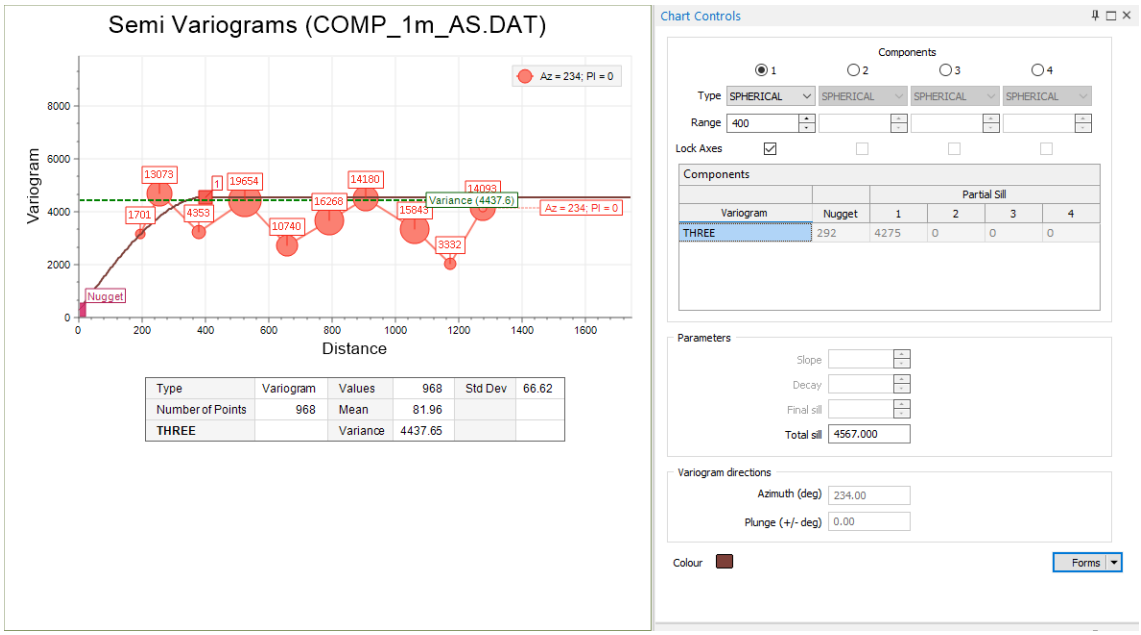



**Figure 14.50 - Second axis to THREE (ppm), Alto da Serra target**

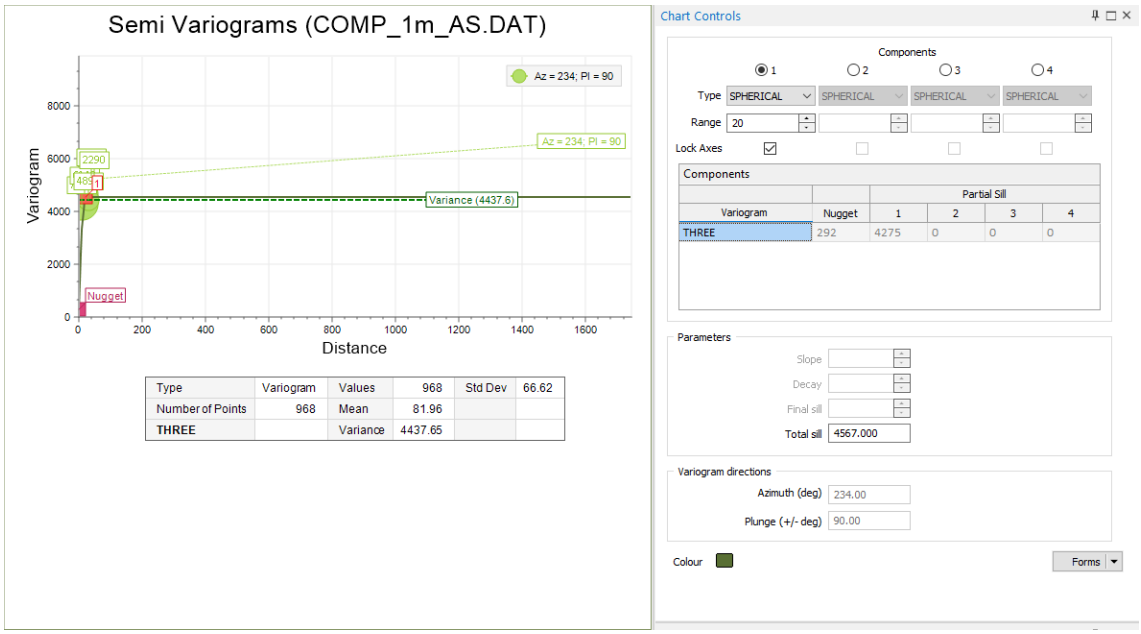
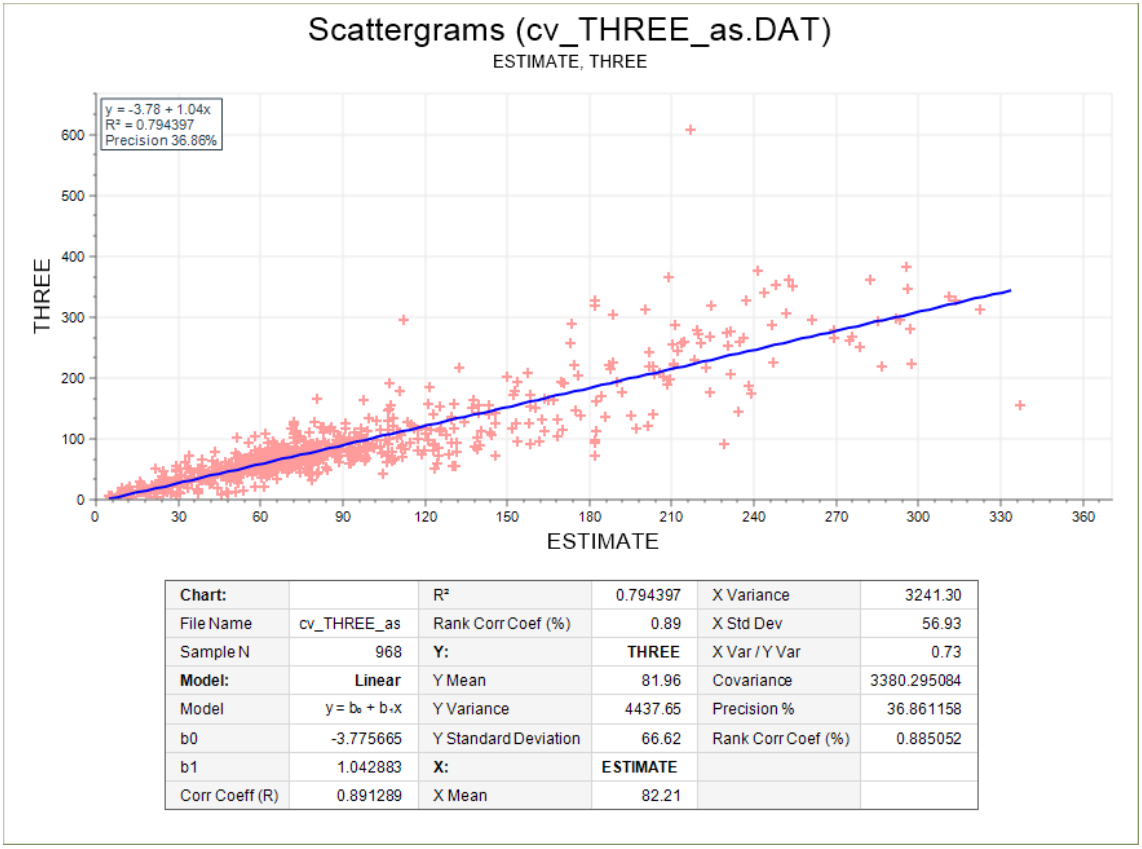



**Figure 14.51 - Third axis to THREE (ppm), Alto da Serra target**

**Table 14.8 - Cross-Validation verification results for THREE (ppm), Alto da Serra target**

| Metadata Label | Metadata Value | Field Name | Mean | Std Dev |
| --- | --- | --- | --- | --- |
| Output File | cv_THREE_as.DAT | | | |
| Input File | COMP_1m_AS.DAT | | | |
| Analysis varb | THREE | | | |
| Transformation | None | | | |
| Number of points | 968 | | | |
| Raw Data | | THREE | 81.962153926 | 66.615683542 |
| Standard error | | STD_ERROR | 27.198456922 | 1.336846511 |
| Estimate | | ESTIMATE | 82.212286566 | 56.932394980 |
| Residual | | RESIDUAL | -0.250132640 | 30.304401067 |
| Error statistic | | ERROR_STAT | -0.005965530 | 1.124107730 |
| RMSE | | | 30.289776736 | |




| Chart: | | R² | 0.794397 | X Variance | 3241.30 |
| --- | --- | --- | --- | --- | --- |
| File Name | cv_THREE_as | Rank Corr Coef (%) | 0.89 | X Std Dev | 56.93 |
| Sample N | 968 | Y: | THREE | X Var / Y Var | 0.73 |
| Model: | Linear | Y Mean | 81.96 | Covariance | 3380.295084 |
| Model | $y = b_0 + b_1 x$ | Y Variance | 4437.65 | Precision % | 36.861158 |
| b0 | -3.775665 | Y Standard Deviation | 66.62 | Rank Corr Coef (%) | 0.885052 |
| b1 | 1.042883 | X: | ESTIMATE | | |
| Corr Coeff (R) | 0.891289 | X Mean | 82.21 | | |

**Figure 14.52 - Linear diagram of dependence between composite sample data and THREE (ppm) grade estimates, Alto da Serra target**

Semivariograms and cross validation verification graphs for Y, Th and U can be found in APPENDIX IV.

## 14.7 Modelling

The block model was generated based on the discretization of the three-dimensional solids into blocks of defined dimensions. The parameters of the blocks are listed in Table 14.9 and Table 14.10.

The discretization process for the solid included the sub-blocking process. Initially, the model was filled with blocks measuring 50 (X) by 50 (Y) by 10 (Z) meters, which were divided into subunits of a smaller size, with a factor for size subdivision of 10 by 10 by 10 in contact with the surrounding three-dimensional solids.

As a result, at the limit with the solids, the size of the blocks became 5.0 (X) by 5.0 (Y) by 2.0 (Z) meters. The initial size of the blocks was chosen based on the morphology of the orebodies and the size of the exploration grid at ¼ of the main grid.

The solid was used to create a block model within the mineralized geological body. This solid was also used to encode the respective blocks. The digital model of the topographic surface was used to limit the block models along the vertical axis. The blocks were generated with faces parallel to the North/South and East/West axes.

**Table 14.9 - Block model parameters, Nau de Guerra target**

| Directions | Length (m) | | Grade Models | | |
|---|---|---|---|---|---|
| | Minimum | Maximum | Block Size (m) | Minimum sub-block size (m) | Number of primary blocks |
| East | 406489 | 409839 | 50 | 5.0 | 68 |
| North | 7884679 | 7886879 | 50 | 5.0 | 45 |
| RL - Elevation | 972 | 1052 | 10 | 2.0 | 9 |

**Table 14.10 - Block model parameters, Balsamo and Alto da Serra targets**

| Directions | Length (m) | | Grade Models | | |
|---|---|---|---|---|---|
| | Minimum | Maximum | Block Size (m) | Minimum sub-block size (m) | Number of primary blocks |
| East | 401086 | 409839 | 406436 | 5.0 | 108 |
| North | 7867910 | 7886879 | 7884160 | 5.0 | 326 |
| RL - Elevation | 981 | 1052 | 1121 | 2.0 | 15 |

## 14.8 Grade Interpolation and Mineral Resource Classification

### 14.8.1 Grade Interpolation

All analyzed elements were interpolated to the empty block model using the Ordinary Kriging (OK) and IDW3 (Inverse Distance Weighting with weight 3) methods. The parameters used for all three methods were the same and are described below.

The grade estimation was performed in four consecutive steps (rounds) using different search radii, numbers of composite sample criteria and numbers of holes.

The search ellipse parameters were defined based on the geostatistical analysis performed for each of the elements analyzed: La, Ce, Pr, Nd, Sm, Eu, Gd, Tb, Dy, Ho, Er, Tm, Yb, Lu, Y, Th and U.

The search ellipse parameters obtained for the TLREE elements (La+Ce+Pr+Nd+Sm+Eu), THREE elements (Dy+Er+Gd+Ho+Tm+Yb+Lu+Tb), Y, Th and U were used for the interpolation of the rare earth elements. The search ellipsoid was divided into four sectors. The search radii were determined based on the range of the variograms. The orientation of the search ellipsoid and the sizes of the axes for all the interpolated elements are described in Table 14.11 and Table 14.2. The search ellipse radii parameters and interpolation parameters for each step (round) of the grade estimation are described in Table 14.13.

**Table 14.11 - Direction of the search ellipsoid axes for all interpolated elements, all targets**

| Element | First axis azimuth | First axis dip | Second axis dip |
|---|---|---|---|
| **Nau de Guerra** | | | |
| TLREE (ppm) | 174 | 0 | 0 |
| THREE (ppm) | 174 | 0 | 0 |
| Y (ppm) | 174 | 0 | 0 |

| Element | First axis azimuth | First axis dip | Second axis dip |
|---|---|---|---|
| Th (ppm) | 168 | 0 | 0 |
| U (ppm) | 168 | 0 | 0 |
| **Alto da Serra Target** | | | |
| TLREE (ppm) | 144 | 0 | 0 |
| THREE (ppm) | 144 | 0 | 0 |
| Y (ppm) | 144 | 0 | 0 |
| Th (ppm) | 36 | 0 | 0 |
| U (ppm) | 36 | 0 | 0 |
| **Balsamo Target** | | | |
| TLREE (ppm) | 150 | 0 | 0 |
| THREE (ppm) | 150 | 0 | 0 |
| Y (ppm) | 150 | 0 | 0 |
| Th (ppm) | 150 | 0 | 0 |
| U (ppm) | 150 | 0 | 0 |

**Table 14.12 - Direction of the search ellipsoid axes and search ellipse parameters for each interpolated element, Nau de Guerra, Balsamo and Alto da Serra targets**

| Element | Axis | Length (meters) |
|---|---|---|
| **Nau de Guerra** | | |
| TLREE (ppm) | 1 | 500 |
| | 2 | 425 |
| | 3 | 20 |
| THREE (ppm) | 1 | 650 |
| | 2 | 425 |
| | 3 | 20 |
| Y (ppm) | 1 | 670 |
| | 2 | 500 |
| | 3 | 20 |
| Th (ppm) | 1 | 500 |
| | 2 | 500 |
| | 3 | 20 |
| U (ppm) | 1 | 500 |
| | 2 | 500 |
| | 3 | 20 |
| **Alto da Serra Target** | | |
| TLREE (ppm) | 1 | 500 |
| | 2 | 375 |
| | 3 | 20 |
| THREE (ppm) | 1 | 600 |
| | 2 | 400 |
| | 3 | 20 |
| Y (ppm) | 1 | 600 |
| | 2 | 525 |
| | 3 | 20 |
| Th (ppm) | 1 | 470 |
| | 2 | 470 |
| | 3 | 20 |
| U (ppm) | 1 | 470 |
| | 2 | 470 |
| | 3 | 20 |
| **Balsamo Target** | | |
| TLREE (ppm) | 1 | 730 |
| | 2 | 690 |
| | 3 | 30 |
| THREE (ppm) | 1 | 730 |
| | 2 | 690 |
| | 3 | 30 |
| Y (ppm) | 1 | 730 |
| | 2 | 560 |
| | 3 | 20 |

| Element | Axis | Length (meters) |
|---|---|---|
| Th (ppm) | 1 | 730 |
| | 2 | 700 |
| | 3 | 30 |
| U (ppm) | 1 | 730 |
| | 2 | 700 |
| | 3 | 30 |

**Table 14.13 - Search radius and interpolation parameters for all elements and interpolation methods**

| Round | Search ellipse size factor | Minimum composites | Maximum composites | Minimum hole number |
|---|---|---|---|---|
| 1 | 0.667 | 3 | 4 | 2 |
| 2 | 1 | 2 | 4 | 2 |
| 3 | 2 | 2 | 4 | 1 |
| 4 | 100 | 1 | 4 | 1 |

The blocks for each zone of the ore body were interpolated using only composite samples belonging to the corresponding part of the mineralized body, i.e., the waste rock samples were not used. During the interpolation, the discretization process for each block, evaluated using the X, Y axes with a factor of 4 and Z with a factor of 2, was used. This made it possible to evaluate each block in thirty-two (32) positions and assign to the center of the block an average of these evaluations. This increased the precision of the grade estimation in each block.

The limitations presented by each sector of a search ellipse were: the maximum number of points in the sector and the minimum total number of points in the interpolation, which varies, depending on the size of the ellipse, from 3 to 1. Thus, the maximum total number of samples involved in the interpolation was 16 samples.

To evaluate the influence of the nugget effect on the estimation of geological resources, the following elements were interpolated Y_cut, La_cut, Ce_cut, Pr_cut, Nd_cut, Sm_cut, Eu_cut, Gd_cut, Tb_cut, Dy_cut, Ho_cut, Er_cut, Tm_cut, Yb_cut and Lu_cut with the application of cut-off grades (capping). The 97.7$^{th}$ percentile (+2 SD) was chosen as a capping grade definition criterion. Table 14.14 shows the capping values.

**Table 14.14 - Capping grade values for the Nau de Guerra, Balsamo and Alto da Serra targets**

| Element | Cut-off Grade ppm |
|---|---|
| **Nau de Guerra Targets** | |
| Y | 176.766 |
| La | 1591.673 |
| Ce | 3213.922 |
| Pr | 388.929 |
| Nd | 1395.318 |
| Sm | 193.356 |
| Eu | 46.52 |
| Gd | 115.16 |
| Tb | 11.904 |
| Dy | 52.766 |
| Ho | 7.788 |
| Er | 16.636 |
| Tm | 1.87 |
| Yb | 10 |
| Lu | 1.3 |
| **Balsamo and Alto da Serra Targets** | |
| Y | 217.461 |
| La | 1874.843 |
| Ce | 3704.049 |
| Pr | 457.23 |
| Nd | 1667.342 |
| Sm | 222.197 |
| Eu | 56.05 |
| Gd | 139.425 |
| Tb | 14.45 |
| Dy | 63.698 |
| Ho | 9.242 |
| Er | 19.921 |
| Tm | 2.164 |
| Yb | 11.9 |
| Lu | 1.514 |

### 14.8.2 CAPPING

To assess the impact on the estimation of geological Resources of samples with abnormally high grades, capped grades were interpolated into the block model. The values used for this capping are listed in the previous section. Table 14.15 shows the results of the comparison of the average grades of the components interpreted with and without capping.

It can thus be concluded that samples with abnormally high grades do not affect the calculation of geological resources.

**Table 14.15 - Comparison of the average grades of components interpreted with and without capping**

| | Y ppm | La ppm | Ce ppm | Pr ppm | Nd ppm | Sm ppm | Eu ppm | Gd ppm | Tb ppm | Dy ppm | Ho ppm | Er ppm | Tm ppm | Yb ppm | Lu ppm |
|---|---|---|---|---|---|---|---|---|---|---|---|---|---|---|---|
| **Nau de Guerra Target** | | | | | | | | | | | | | | | |
| Regular samples | 68.35033 | 683.4253 | 1388.154 | 150.8494 | 540.6902 | 74.51802 | 18.28146 | 44.51327 | 4.600994 | 20.59855 | 2.974479 | 6.511294 | 0.726062 | 4.040855 | 0.51641 |
| Capping samples | 65.14067 | 678.2239 | 1368.143 | 149.3815 | 534.6529 | 73.59134 | 18.03438 | 43.76183 | 4.521344 | 20.16731 | 2.901846 | 6.299038 | 0.703789 | 3.909482 | 0.498098 |
| Relative difference % | ***4.7*** | ***0.76*** | ***1.44*** | ***0.97*** | ***1.12*** | ***1.24*** | ***1.35*** | ***1.69*** | ***1.73*** | ***2.09*** | ***2.44*** | ***3.26*** | ***3.07*** | ***3.25*** | ***3.55*** |
| **Alto da Serra Target** | | | | | | | | | | | | | | | |
| Regular samples | 653.9528 | 1336.215 | 147.8496 | 535.1616 | 73.59501 | 18.0669 | 44.40024 | 4.665921 | 21.29373 | 3.167779 | 7.049294 | 0.800777 | 4.515716 | 0.583424 | 653.9528 |
| Capping samples | 645.5108 | 1314.489 | 144.1887 | 519.4825 | 71.16818 | 17.50405 | 43.28224 | 4.550189 | 20.62528 | 3.036103 | 6.684872 | 0.751943 | 4.248173 | 0.542159 | 645.5108 |
| Relative difference % | ***1.29*** | ***1.63*** | ***2.48*** | ***2.93*** | ***3.3*** | ***3.12*** | ***2.52*** | ***2.48*** | ***3.14*** | ***4.16*** | ***5.17*** | ***6.1*** | ***5.92*** | ***7.07*** | ***1.29*** |
| **Balsamo Target** | | | | | | | | | | | | | | | |
| Regular samples | 61.78021 | 607.2356 | 1292.579 | 135.4171 | 480.6751 | 64.17742 | 15.63937 | 38.04704 | 4.058151 | 18.02212 | 2.629517 | 5.804262 | 0.662455 | 3.6416 | 0.473134 |
| Capping samples | 60.99148 | 606.6442 | 1290.948 | 135.4171 | 480.6751 | 64.17742 | 15.63937 | 38.04704 | 4.055705 | 17.97815 | 2.614582 | 5.754831 | 0.655021 | 3.59666 | 0.466254 |
| Relative difference % | ***1.28*** | ***0.1*** | ***0.13*** | ***0*** | ***0*** | ***0*** | ***0*** | ***0*** | ***0.06*** | ***0.24*** | ***0.57*** | ***0.85*** | ***1.12*** | ***1.23*** | ***1.45*** |

## 14.9 Density Values for the Block Model

The assignment of density values to the block model was done via direct assignment for each block. The density value was obtained based on the average of 175 density measurements for the Nau de Guerra target and 470 density measurements for the Balsamo and Alto da Serra targets, as shown in Table 14.16. It should be noted that the average density calculated is below what was expected. It is recommended that the number of density samples be increased to obtain a data set that better represents the regolith and the saprolite rock density.

**Table 14.16 - Average density used for the mineralization zone**

| Type of rock | Dry Density (g/cm3) |
|---|---|
| **Nau de Guerra Target** | |
| Soil | 1.65 |
| Regolith | 1.81 |
| Clastic sedimentary rocks | 1.96 |
| **Balsamo and Alto da Serra Target** | |
| Soil | 1.56 |
| Regolith/saprolite | 1.74 |
| Frech rocks | 1.79 |

## 14.10 Verification of The Block Model

The block model with interpolated grades underwent visual and statistical verification. Histograms and probability graphs for the interpolated grades were built. Then, the interpolated grades from the block model were compared with the same histograms and probability graphs of the composite samples. The histograms and graphs for the interpolated grades and composite samples were similar, and the block model histograms were smoother than the composite histograms. These comparisons confirmed the validity and consistency of the block model that had been built. The comparison histograms are shown in Figure 14.53 to Figure 14.55.

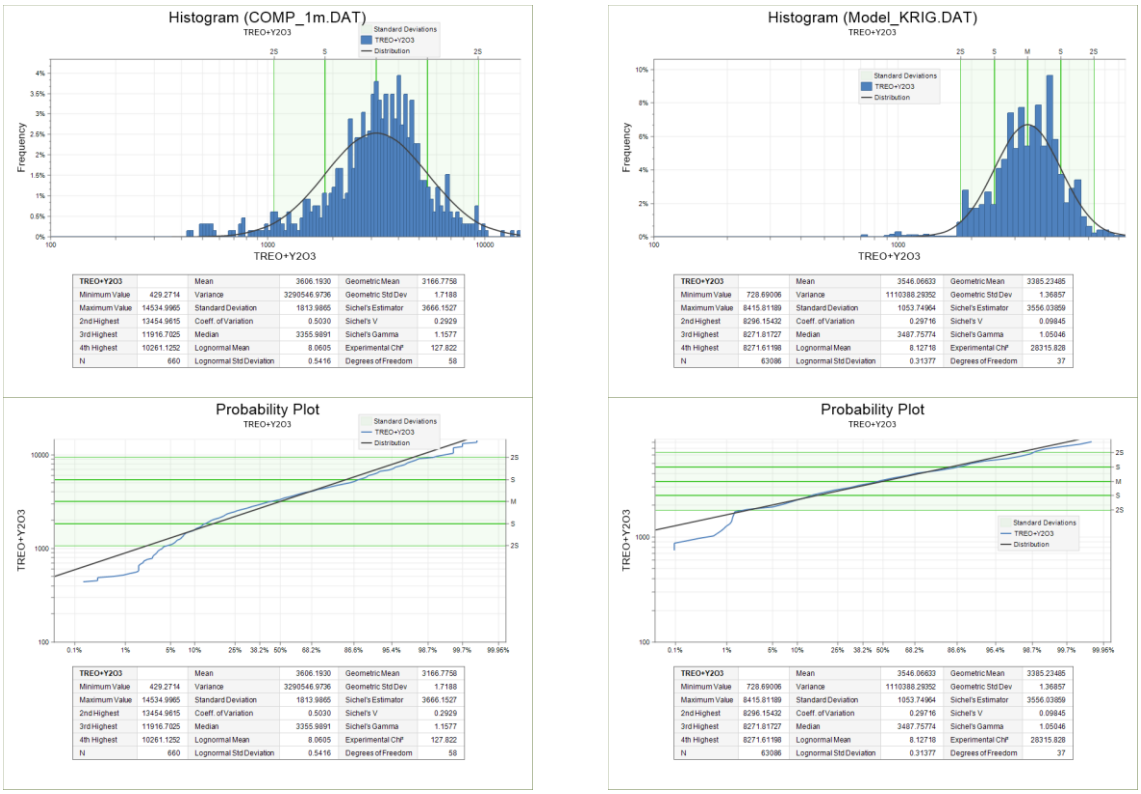



**Figure 14.53 - Histogram and graph of TREE + $Y_2O_3$ distribution probability in composite samples (left) and a block model interpolated using the Ordinary Kriging method (right) for regolith rock, Nau de Guerra target**

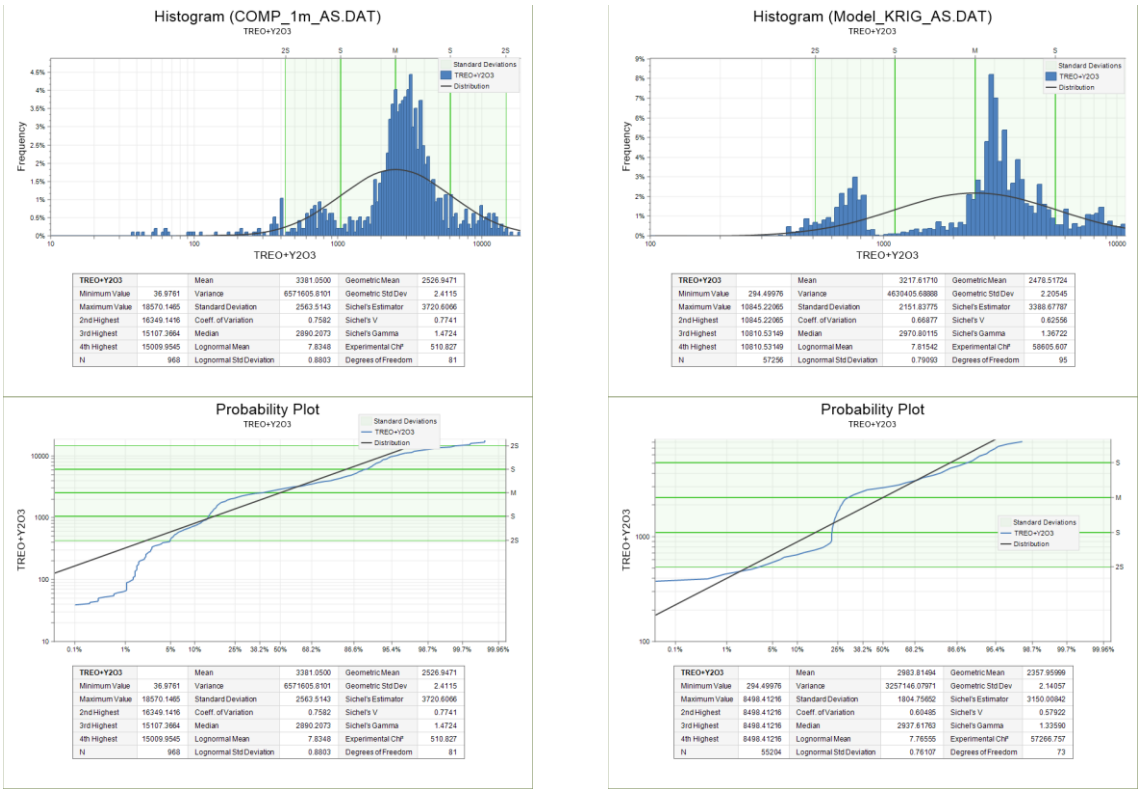


**Figure 14.54 - Histogram and graph of TREE + $Y_2O_3$ distribution probability in composite samples (left) and block model interpolated using the Ordinary Kriging method (right), Alto da Serra target**

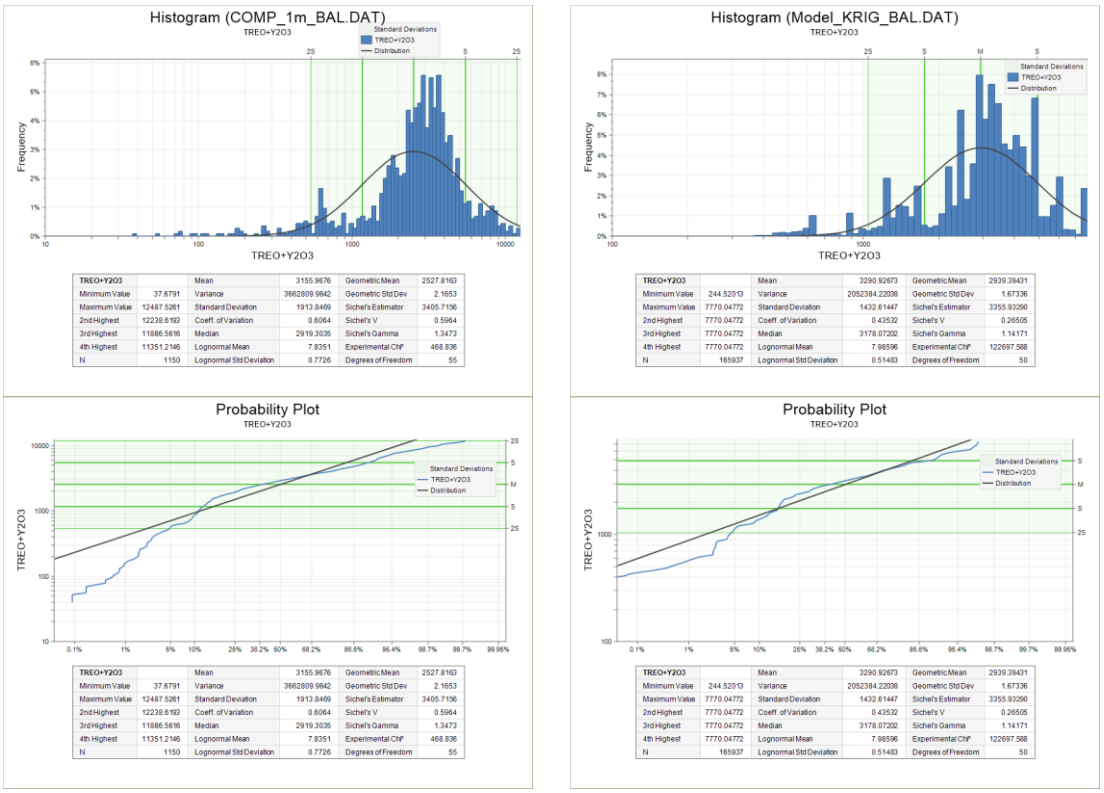



**Figure 14.55 - Histogram and graph of TREE + $Y_2O_3$ distribution probability in composite samples (left) and block model interpolated using the Ordinary Kriging method (right), Balsamo target**

In addition, the interpolated grades were visually compared with the actual sample grades. A comparison between the actual samples and interpolated grades shows an approximate relation, which indicates the level of precision of the estimated grades in the block model. Several sections were constructed showing the grades in the block model and the grades along the drill holes. The visual comparison is shown in the following figures (Figure 14.56 to Figure 14.63).

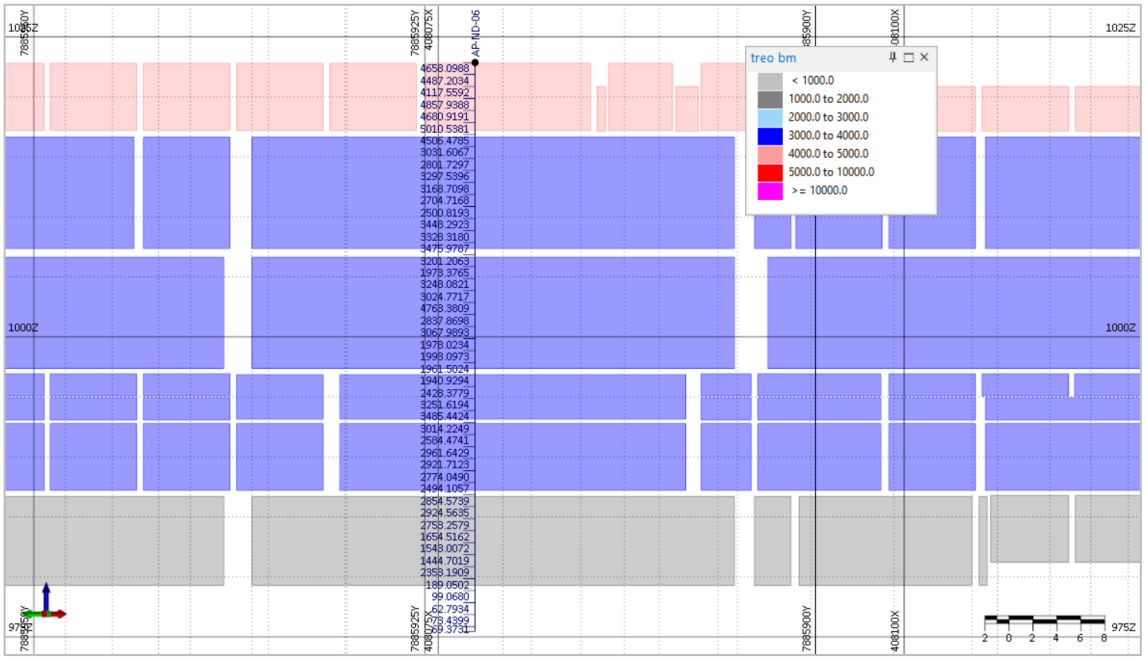



**Figure 14.56 - Visualization TREO +$Y_2O_3$ with Block Model, Nau de Guerra target**

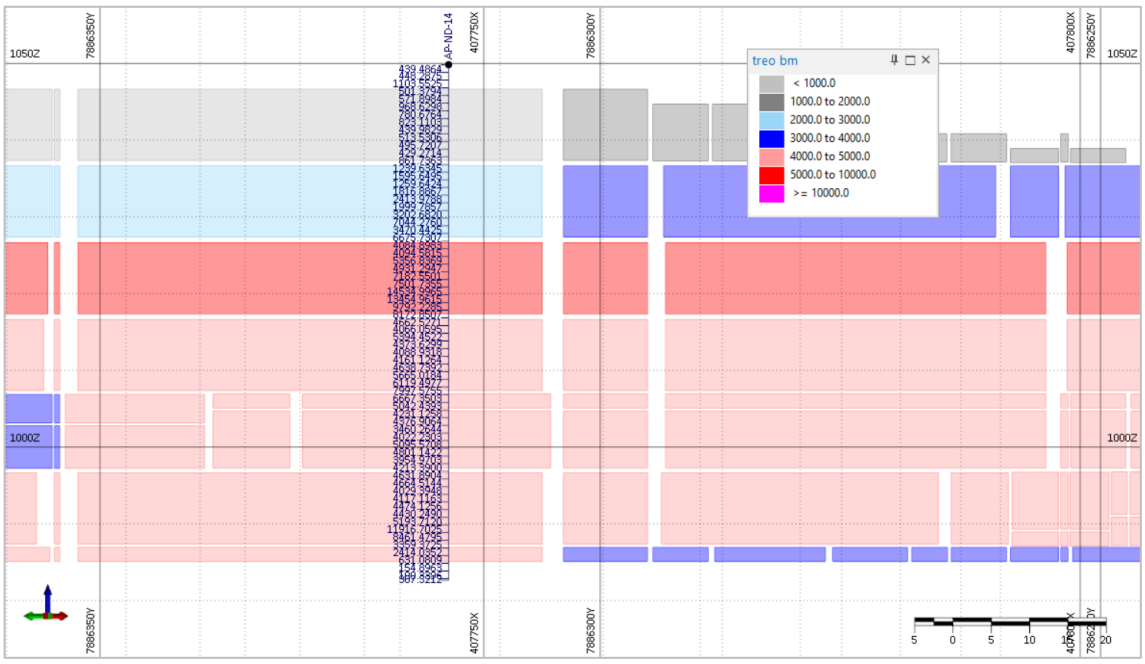



**Figure 14.57 - Visualization TREO + $Y_2O_3$ with Block Model, Nau de Guerra target**

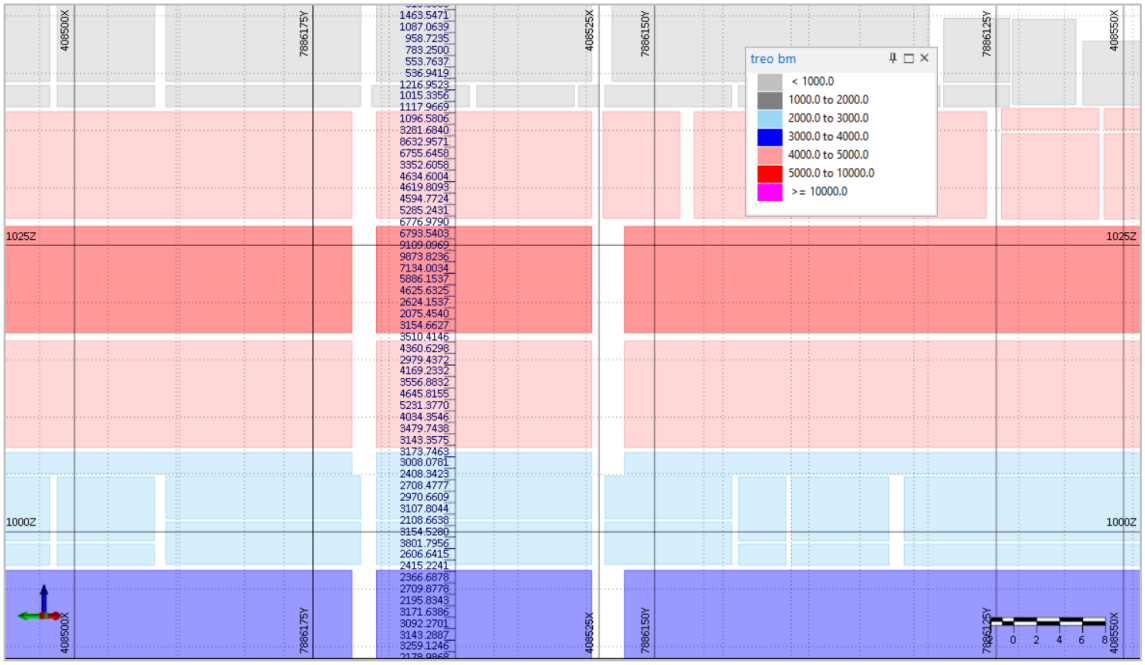



**Figure 14.58 - Visualization TREO + $Y_2O_3$ with Block Model, Nau de Guerra target**

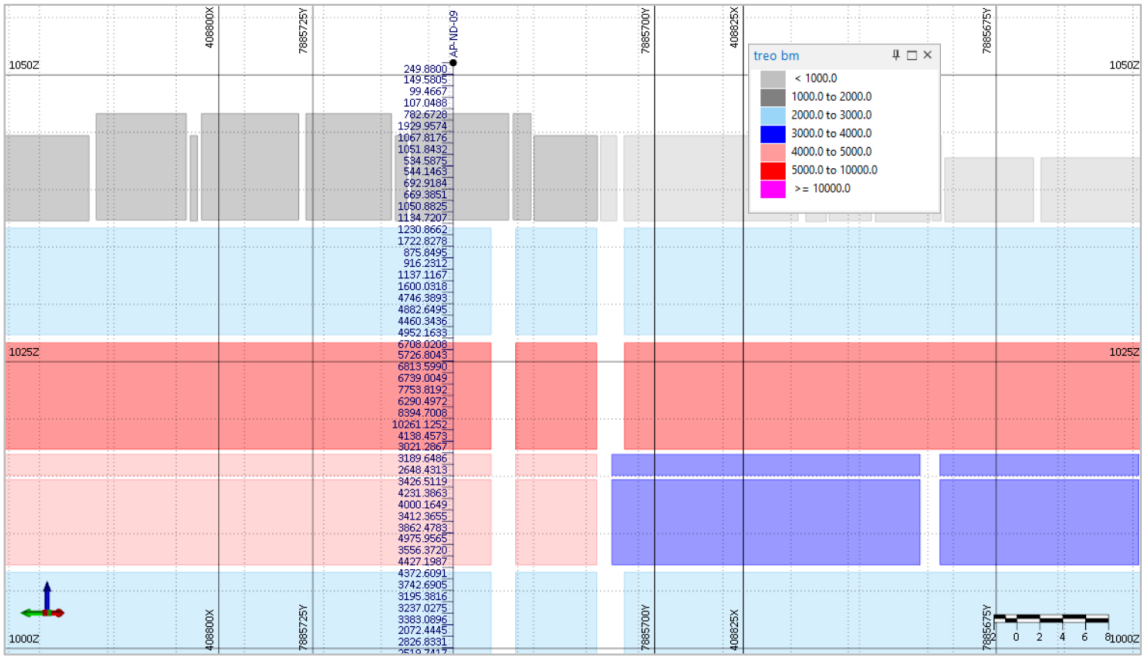



**Figure 14.59 - Visualization TREO + $Y_2O_3$ with Block Model, Nau de Guerra target**

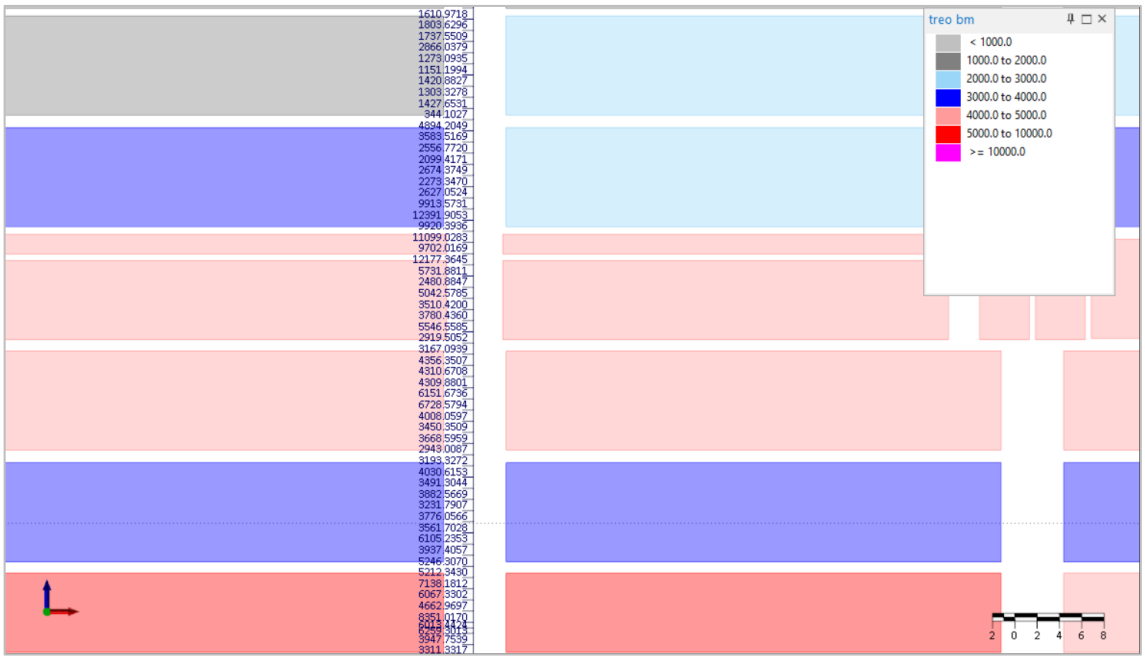



**Figure 14.60 - Visualization TREO +$Y_2O_3$ with Block Model, Alto da Serra target**

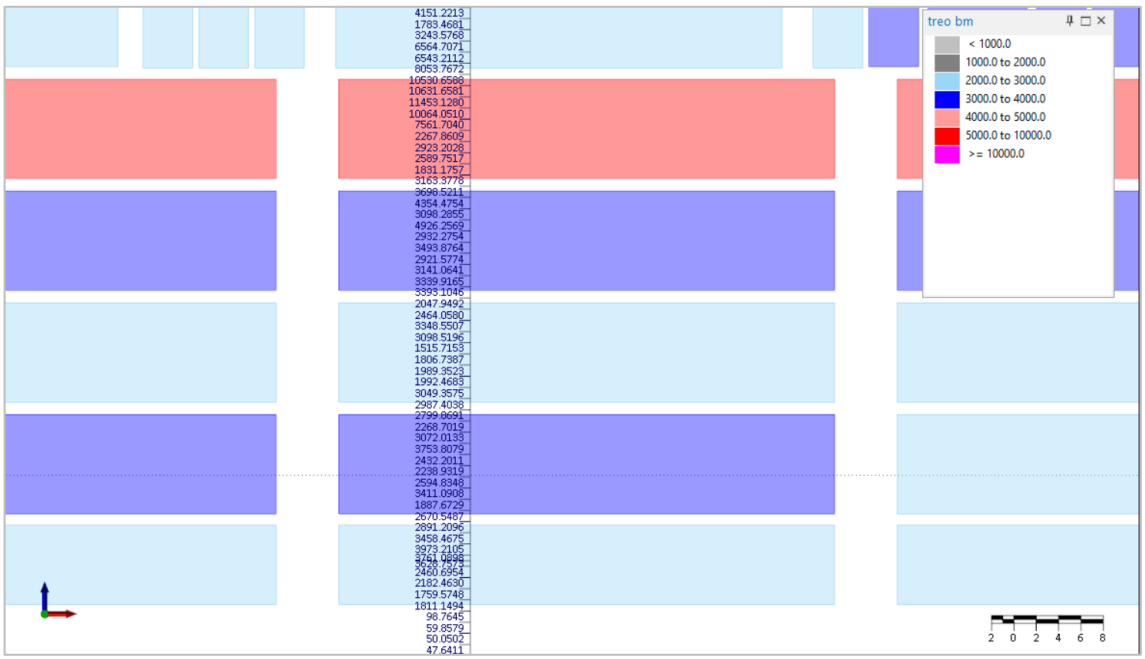



**Figure 14.61 – Visualization TREO + $Y_2O_3$ with Block Model, Alto da Serra target**

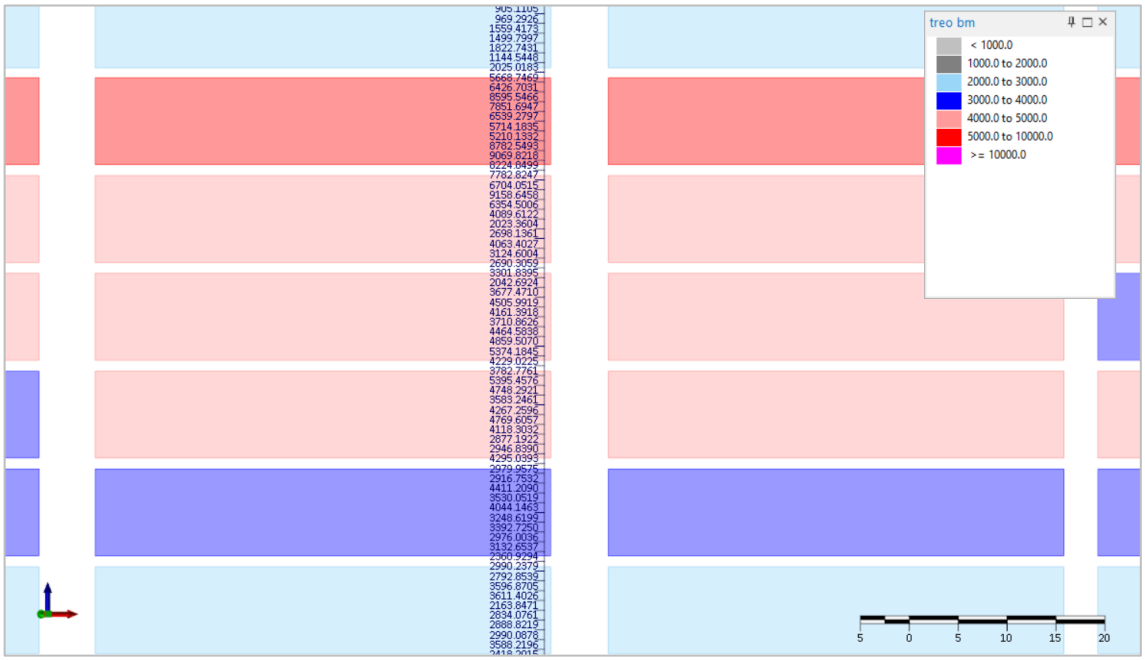



**Figure 14.62 - Visualization TREO + $Y_2O_3$ with Block Model, Balsamo target**

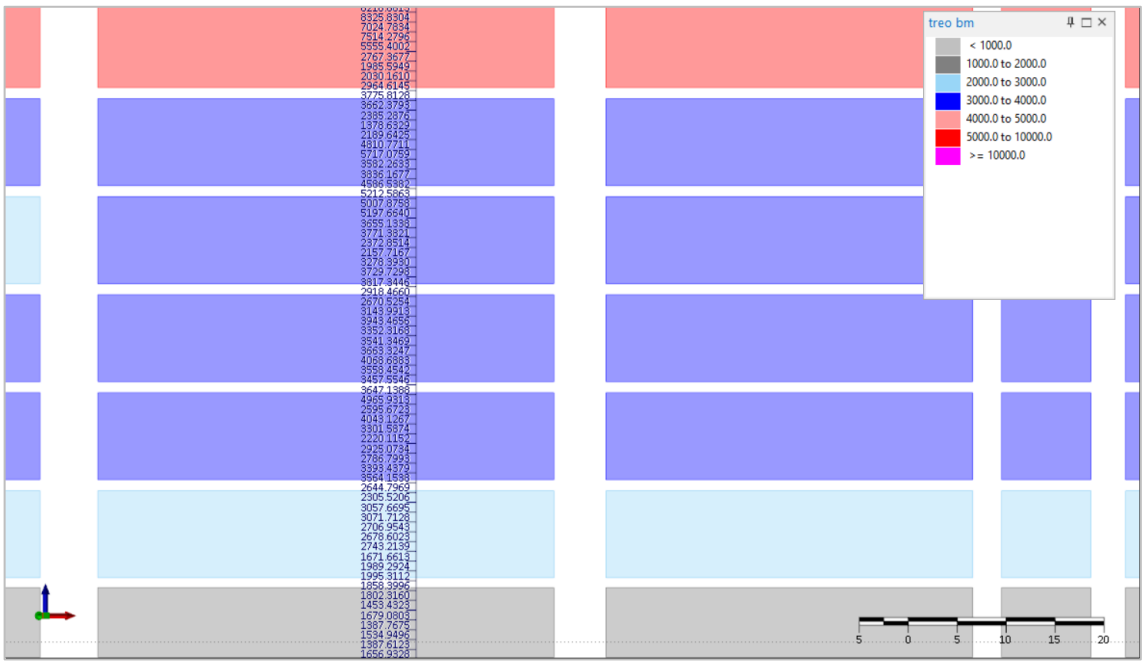



**Figure 14.63 - Visualization TREO + $Y_2O_3$ with Block Model, Balsamo target**

The average grade of the chemical variable from the model was compared with the average grade of the chemical variable from the sampling interval file for all elements interpolated using the three methods employed. This comparison produced a highly satisfactory result.

A comparison was made between a provisional polygonal estimate using the "interval" weighting method and the interpolation data from the Kriging and IDW3 methods for rare earth orebodies. This comparison is presented in Table 14.17.

The difference between the volumes of the solid and of the block model is 0.15%. The difference between the average grades of TREO ppm for ore is, in relative percentages, 0.42%. These results confirm the good convergence and high reliability of the estimated block model data. The analysis performed for the other elements was also satisfactory.

The difference in the average grades of TREO ppm between the block model estimated using IDW3 and the block model estimated using Kriging of -0.27% (relative percent) was expected and is satisfactory.

**Table 14.17 - Data comparison between different estimation methods for TREO + $Y_2O_3$**

| ESTIMATION METHOD | VOLUME | TREO + $Y_2O_3$ | TREO |
|---|---|---|---|
| | $m^3$ | % | % |
| **Nau de Guerra Target** | | | |
| Block Model Kriging (Reg) | 65,428,450.00 | 3,618.83 | 3,531.79 |

| ESTIMATION METHOD | VOLUME | TREO + $Y_2O_3$ | TREO |
|---|---|---|---|
| | $m^3$ | % | % |
| Block Model IDW3 (Reg) | 65,428,450.00 | 3,627.43 | 3,541.40 |
| Relative difference % | 0 | -0.24 | -0.27 |
| Block Model Kriging | 65,428,450.00 | 3.618,83 | 3.531,79 |
| Solid | 65,524,769.56 | 3,606.19 | 3,517.09 |
| Relative difference % | -0.15 | 0.35 | 0.42 |
| **Alto da Serra Target** | | | |
| Block Model Kriging | 137,644,100.00 | 3,510.09 | 3,416.98 |
| Block Model IDW3 | 137,644,100.00 | 3,550.14 | 3,454.87 |
| Relative difference % | 0 | -1.14 | -1.11 |
| Block Model Kriging | 142,053,400.00 | 3,543.80 | 3,449.33 |
| Solid | 142,121,839.59 | 3,451.93 | 3,362.23 |
| Relative difference % | -0.05 | 2.59 | 2.53 |
| **Balsamo Target** | | | |
| Block Model Kriging (Reg) | 661,522,500.00 | 3,279.62 | 3,201.17 |
| Block Model IDW3 (Reg) | 661,522,500.00 | 3,268.24 | 3,190.87 |
| Relative difference % | 0 | 0.35 | 0.32 |
| Block Model Kriging | 698,311,800.00 | 3,268.36 | 3,190.53 |
| Solid | 698,253,888.31 | 3,273.51 | 3,190.11 |
| Relative difference % | 0.01 | -0.16 | 0.01 |

## 14.11 Mineral Resource Classification

The mineral resources at the Man of War Project have been classified as **Inferred** due to limitations in the hole spacing. The parameters used to determine the mineral resource classification include, but are not limited to, drilling density, estimation pass number and the number of samples used to produce a block estimate, as well as the average distance to find samples to produce a block estimate.

BNA have estimated Inferred Mineral Resources for the oxide portion of the Man of War Prospect in accordance with the CIM guidelines (CIM 2014), which have been adopted as part of NI 43-101.

## 14.12 Results of the Resource Evaluation

The block model of Nau de Guerra target was cut by the ANM mining rights limits (832.543/2016), as shown in Figure 14.64. The block model of Alto da Serra target was cut by the ANM mining rights limits (832,544/2016), as shown in Figure 14.65, and the block model of the Balsamo

target was cut by the ANM mining rights limits (830.794/2010 and 830.796/2010), as shown in Figure 14.66.

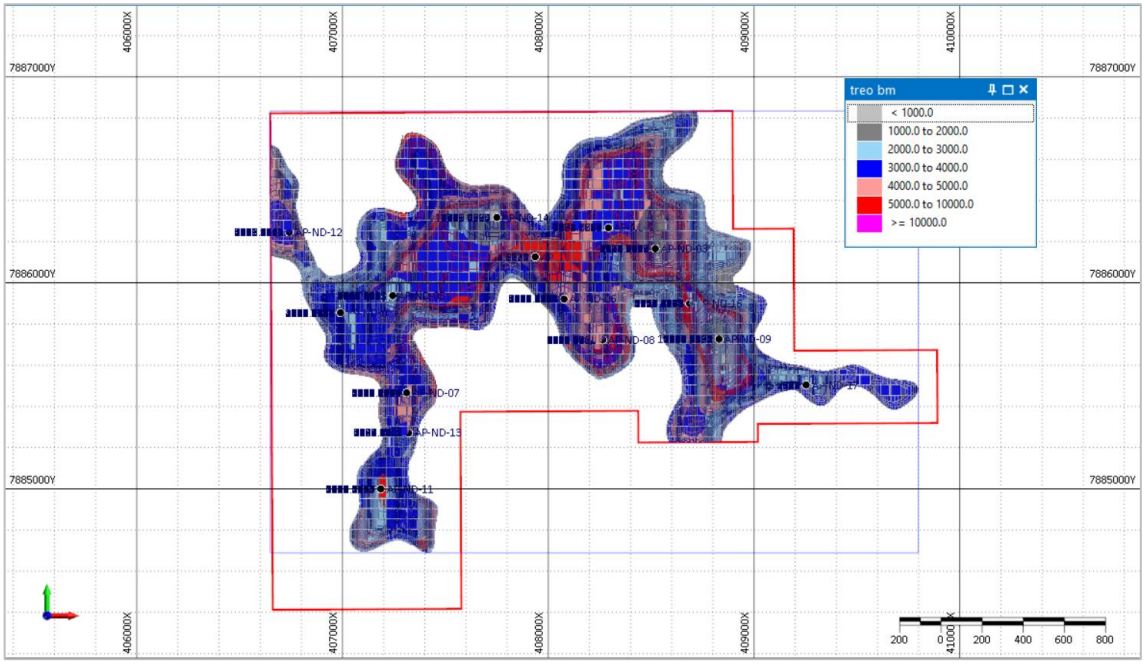



**Figure 14.64 - ANM mining rights limits, Nau de Guerra target**

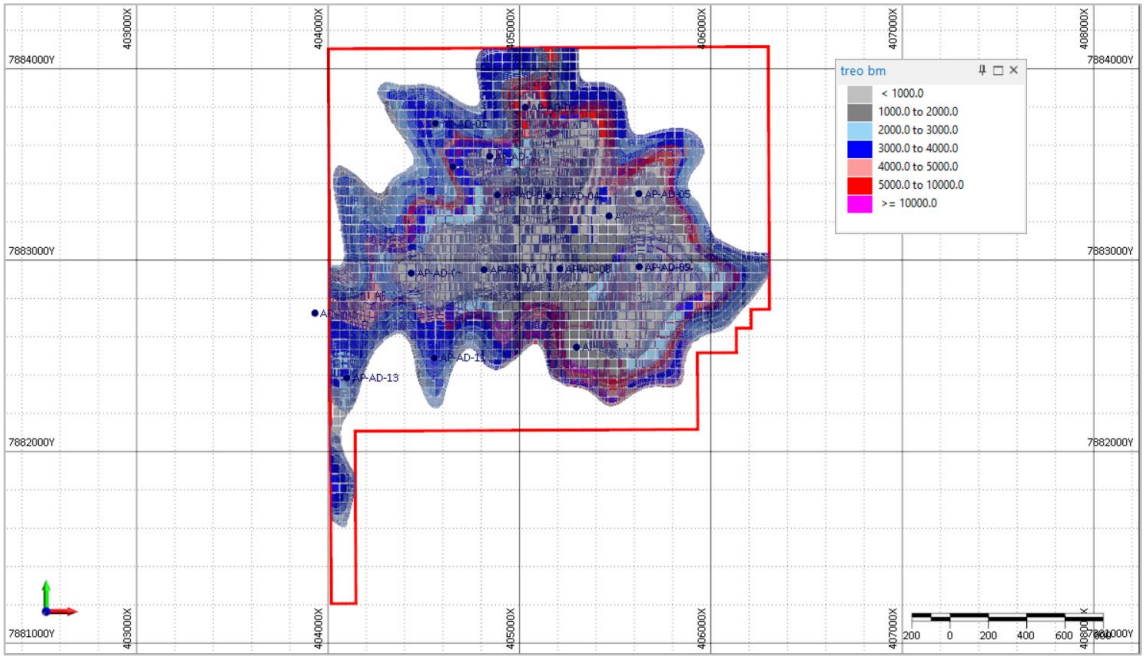



**Figure 14.65 - ANM mining rights limits, Balsamo and Alto da Serra targets**

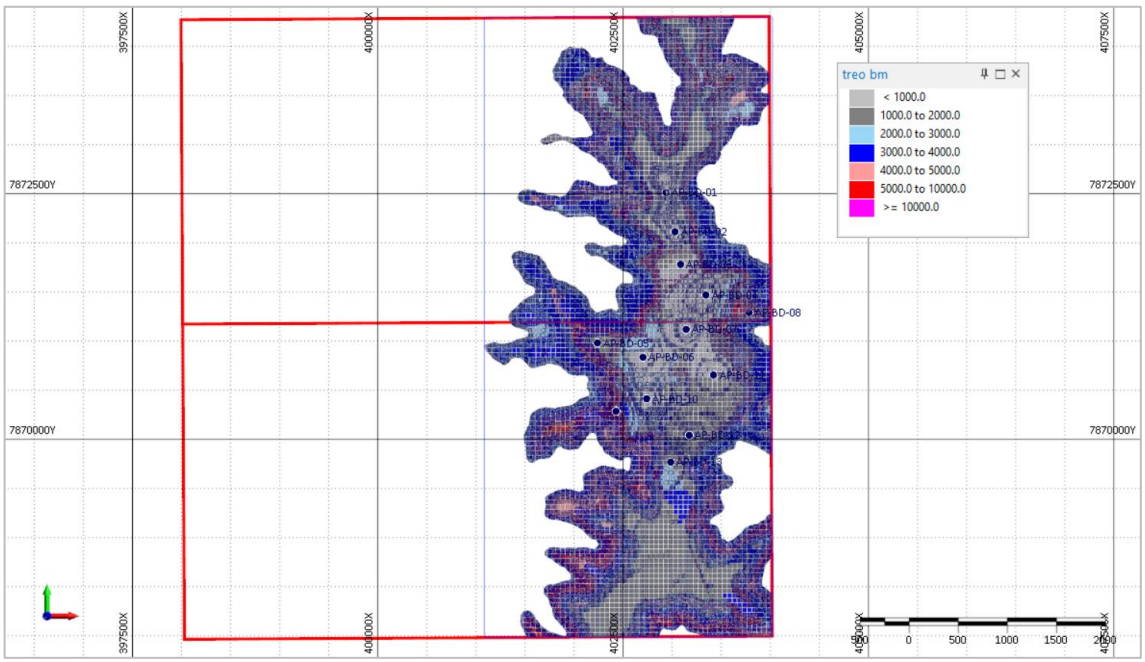



**Figure 14.66 - ANM mining rights limits, Balsamo and Alto da Serra targets**

The results of the resource evaluation, based on the block model interpolated using the Ordinary Kriging (OK) method, of rare earth ore of the Nau de Guerra, Balsamo and Alto da Serra targets are presented in Table 14.18. The resources presented for rare earth chemical element grades with the application of several Cut Off grades are presented in APPENDIX V.

**Table 14.18 - Geological resources in situ with a Cut-off of 1000 ppm TREO on a dry basis**

| CUT-OFF<br>TREO+$Y_2O_3$ (ppm) | VOLUME<br>m3 | TONNES<br>t | DENSITY<br>(t / $m^3$) | TREO<br>ppm | TREO less $Y_2O_3$<br>ppm | $Y_2O_3$<br>ppm | HREO<br>ppm | LREO<br>ppm | MREO<br>ppm | $Pr_6O_{11}$<br>ppm | $Nd_2O_3$<br>ppm | $Tb_4O_7$<br>ppm | $Dy_2O_3$<br>ppm |
|---|---|---|---|---|---|---|---|---|---|---|---|---|---|
| **Nau de Guerra Target** | | | | | | | | | | | | | |
| 1000 | 65,205,750.00 | 120,093,635.00 | 1.84 | 3,627.61 | 3,540.39 | 87.22 | 97.73 | 3,442.66 | 846.04 | 183.13 | 633.70 | 5.44 | 23.76 |
| **Alto da Serra Target** | | | | | | | | | | | | | |
| 1000 | 129,109,800.00 | 230,213,682.00 | 1.78 | 3,683.52 | 3,586.57 | 96.95 | 104.06 | 3,482.51 | 874.57 | 187.54 | 655.73 | 5.75 | 25.55 |
| **Balsamo Target** | | | | | | | | | | | | | |
| 1000 | 640,828,400.00 | 1,145,624,208.50 | 1.79 | 3,357.88 | 3,278.31 | 79.57 | 85.99 | 3,192.32 | 768.70 | 167.82 | 574.98 | 4.87 | 21.04 |

**Table 14.19 - Resource Estimate Summary***

| Target | Tons | TREO[4] | MREO[5] | $Pr_6O_{11}$ | $Nd_2O_3$ | $Tb_4O_7$ | $Dy_2O_3$ |
|---|---|---|---|---|---|---|---|
| | | *ppm* | *ppm* | *ppm* | *ppm* | *ppm* | *ppm* |
| Nau de Guerra | 120,093,635 | 3,628 | 846 | 183 | 634 | 5 | 24 |
| Alto da Serra | 230,213,682 | 3,684 | 875 | 188 | 656 | 6 | 26 |
| Balsamo | 1,145,624,209 | 3,358 | 769 | 168 | 575 | 5 | 21 |
| **TOTAL** | **1,495,931,526** | **3,430** | **791** | **172** | **592** | **5** | **22** |

**Values are rounded*

[4] Total Rare Earth Oxides (TREO) refers to the sum of the oxides of rare earth elements, which include: Lanthanum Oxide ($La_2O_3$), Cerium Oxide ($CeO_2$), Praseodymium Oxide ($Pr_6O_{11}$), Neodymium Oxide ($Nd_2O_3$), Samarium Oxide ($Sm_2O_3$), Europium Oxide ($Eu_2O_3$), Gadolinium Oxide ($Gd_2O_3$), Terbium Oxide ($Tb_4O_7$), Dysprosium Oxide ($Dy_2O_3$), Holmium Oxide ($Ho_2O_3$), Erbium Oxide ($Er_2O_3$), Thulium Oxide ($Tm_2O_3$), Ytterbium Oxide ($Yb_2O_3$), Lutetium Oxide ($Lu_2O_3$), and Yttrium Oxide ($Y_2O_3$).

[5] Magnetic Rare Earth Oxides (MREO) refers to the sum of the oxides of rare earth elements with magnetic properties, which include: Praseodymium Oxide ($Pr_6O_{11}$), Neodymium Oxide ($Nd_2O_3$), Terbium Oxide ($Tb_4O_7$), and Dysprosium Oxide ($Dy_2O_3$).

## 14.13 Reasonable Prospects for Eventual Economic Extraction

Mineral Resources that are not Mineral Reserves do not have demonstrated economic viability. There is no certainty that all or any part of the Mineral Resources will be converted into Mineral Reserves. The estimation of Mineral Resources is subject to inherent uncertainties, and the results of further exploration or feasibility studies may materially affect the estimates.

The CIM Definition Standards on Mineral Resources and Mineral Reserves require that an estimated mineral resource have reasonable prospects for eventual economic extraction. The Mineral Resource estimate discussed herein has been constrained by reasonable potential open pit mine design parameters, using economic and technical assumptions appropriate for an open pit mining scenario. The potential open pit mining shells described below are preliminary and conceptual in nature.

BNA has based the resource categories and cut-off grades of the deposit in the resource estimate stated herein on the requirement of “reasonable prospects for eventual economic extraction”, assuming an open pit mining production method scenario.

A preliminary economic analysis was performed on the targets to define the economically mineable resource. To this end, a pit optimization exercise was performed using the parameters listed in Table 14.20 and Table 14.21.

**Table 14.20 - Optimization Parameters**

| Parameters | | Valor | |
|---|---|---|---|
| Ore Density | | Default 1.79 (block model) | t/m$^3$ |
| Waste Density | | 1.78 | t/m$^3$ |
| Mining Cost | Ore | 1.96 | US$/t ROM |
| | Waste | 1.96 | US$/t moved |
| Bench face angle | | 45.00 | degrees |
| Bench height | | 10.00 | m |
| Berm width | | 3.00 | m |
| Process Cost | | 7.65 | US$/t ROM |
| CFEM cost | | 0.95 | US$/t ROM |
| Royalties | | 0.47 | US$/t ROM |
| CutOff | | 1000 | ppm TREO (TREO + Yb) |
| Mass Recovery | | 100.00 | % |
| Mining Recovery | | 95.00 | % |

| Parameters | Valor | |
|---|---|---|
| Mining Dilution | 0.00 | |
| Production Rate | 25Mtpa | Mt Feed / Year |
| Discount Rate | 8.00 | % by year |
| Payabillity | 92 | % |
| Block Model Files: | BM_KRIG_AS | |
| | BM_KRIG | |
| | BM_KRIG_BAL | |

**Table 14.21 - Price and Recovery**

| Element | Argus (Aclara Scoping Study) | Recovery |
|---|---|---|
| | *US$/kg* | *%* |
| $CeO_2$ | 0.69 | 11.20% |
| $Dy_2O_3$ | 477.25 | 35.30% |
| $Er_2O_3$ | 59.1 | 36.30% |
| $Eu_2O_3$ | 27.45 | 34.40% |
| $Gd_2O_3$ | 71.55 | 35.60% |
| $Ho_2O_3$ | 137.25 | 36.10% |
| $La_2O_3$ | 0.68 | 28.60% |
| $Lu_2O_3$ | 834.75 | 38.90% |
| $Nd_2O_3$ | 150.75 | 33.70% |
| $Pr_6O_{11}$ | 144.18 | 33.00% |
| $Sm_2O_3$ | 2.39 | 33.80% |
| $Tb_4O_7$ | 1,789.25 | 34.30% |
| $Tm_2O_3$ | 0.01 | 39.00% |
| $Y_2O_3$ | 2.86 | 39.30% |
| $Yb_2O_3$ | 19.85 | 34.70% |

The results are presented in Table 14.22 and Figure 14.67.

**Table 14.22 - Reasonable Prospects for Eventual Economic Extraction**

| CUT-OFF TREO+$Y_2O_3$ (ppm) | TARGET | Tonnes | | In Situ Grades (PPM) | | | | | |
|---|---|---|---|---|---|---|---|---|---|
| | | RPEE RESOURCE | Waste | TREO | MREO | $Pr_6O_{11}$ | $Nd_2O_3$ | $Tb_4O_7$ | $Dy_2O_3$ |
| 1000 | Nau De Guerra | 104,803,251 | 36,820,399 | 3,618.33 | 843.46 | 182.57 | 631.75 | 5.43 | 23.71 |
| 1000 | Alto da Serra | 210,776,735 | 97,575,737 | 3,679.68 | 873.29 | 187.26 | 654.75 | 5.75 | 25.53 |
| 1000 | Balsamo | 1,034,240,886 | 291,327,544 | 3,369.70 | 772.04 | 168.59 | 577.48 | 4.88 | 21.10 |
| **1000** | **TOTAL** | **1,349,820,872** | **425,723,680** | **3,437.41** | **793.39** | **172.59** | **593.76** | **5.06** | **21.99** |

**Table 14.23 - Reasonable Prospects for Eventual Economic Extraction Summary**

| Tonnes | In Situ Grades (PPM)* | | | | | |
|---|---|---|---|---|---|---|
| RPEE RESOURCE | TREO | MREO | Pr6O11 | Nd2O3 | Tb4O7 | Dy2O3 |
| **1,349,820,872** | **3,437** | **793** | **173** | **594** | **5** | **22** |

**Values are rounded*

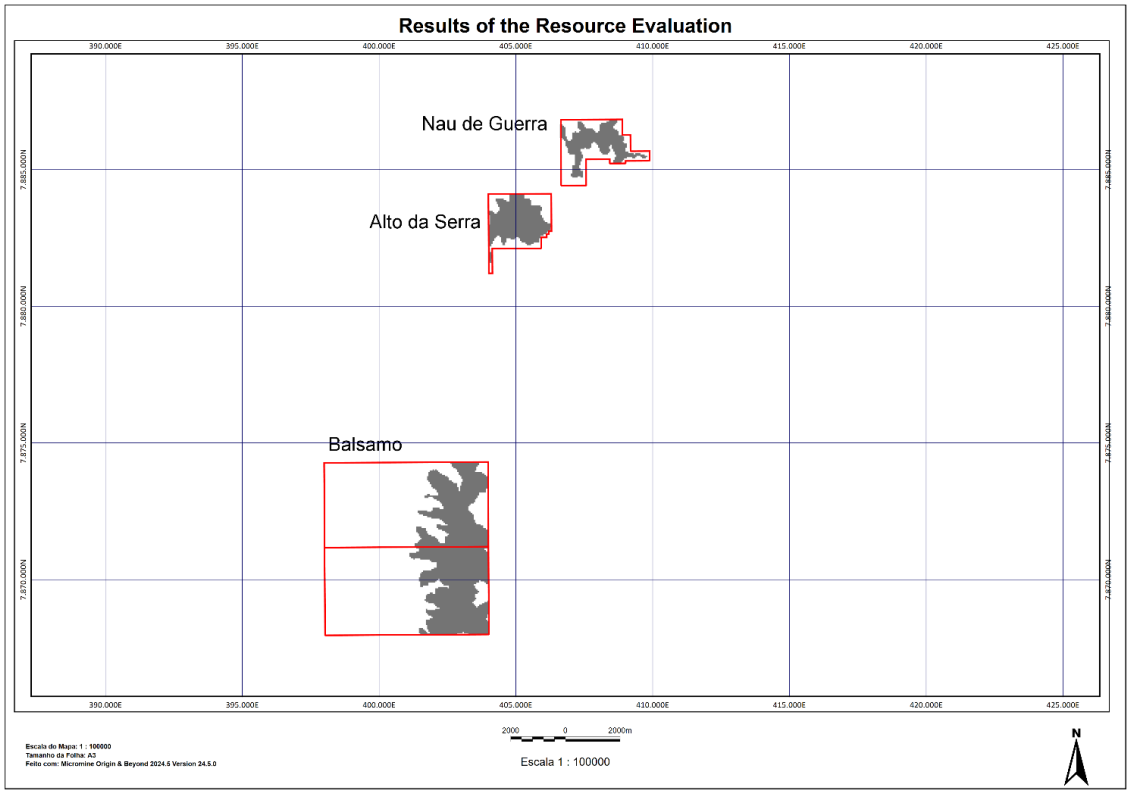



**Figure 14.67 - Reasonable Prospects for Eventual Economic Extraction**

## 14.14 Comments on Mineral Resources

Mineral Resource estimation involves a degree of uncertainty and risk. The primary risks are associated with rare earth price fluctuations, increases in operating costs, or increases in the cost of important operating consumables, such as fuel and chemical reagents. Other potential risks could include mining factors such as pit wall stability, mining dilution and processing factors such as recovery estimates. Political factors such as changes to mining laws, tax structures, or government policies, could potentially affect the Mineral Resource estimates, as could environmental factors such as changes to regulations or permits.

While certain factors may present risks, these also present potential opportunities. Higher rare earth prices or lower operating costs would present a huge opportunity for the project and thus the overall resources.

# 15 Mineral Reserve Estimate

Not included in this report.

# 16 Mining Methods

Not included in this report.

# 17 Recovery Methods

Not included in this report.

# 18 Project Infrastructure

Not included in this report.

# 19 Market Studies and Contracts

Not included in this report.

# 20 Environmental Studies, Permitting and Social or Community Impact

Not included in this report.

# 21 Capital and Operating Costs

Not included in this report.

# 22 Adjacent Properties

The current mining tenements 830.543/2016 and 832.544/2016 (Nau de Guerra and Alto da Serra targets) originated from subdivisions of the original tenements 833.324/2008 and 833.326/2008, with the exploration permits numbered 14.084 and 11.928, respectively. Verde AgriTech Ltd, through its subsidiary FVS Mineração Ltda., holds these tenements.

Tenements 833.324/2008 and 833.326/2008 are part of a broader regional research initiative for potassic rocks, known as the Cerrado Verde Project. This project, led by Verde AgriTech Ltd, aims to utilize glauconitic siltstone for the production of simple mineral fertilizers from a potassium source.

The Cerrado Verde Project encompasses the following tenements: 833.306/2008, 833.295/2008, 833.323/2008, 833.270/2008, 830.383/2008, 833.280/2008, 833.263/2008, 833.268/2008, 833.276/2008, 833.272/2008, 833.324/2008, and 833.326/2008. These tenements are associated with exploration permits numbered 11.929, 11.931, 11.924, 12.464, 8.470, 11.932, 11.927, 1.841, 13.151, 14.088, 14.084, and 11.928. They collectively cover an area of 19,040 hectares in the municipalities of São Gotardo, Matutina, Tiros, and Quartel Geral in the state of Minas Gerais, and have received approval for the Final Research Report on potassic rock.

For the Balsamo target, Verde AgriTech Ltd, through its subsidiary Verde Fertilizantes Ltda., holds exploration permits Nos. 8461 and 8462 for tenements 830.794/2010 and 830.796/2010, respectively.

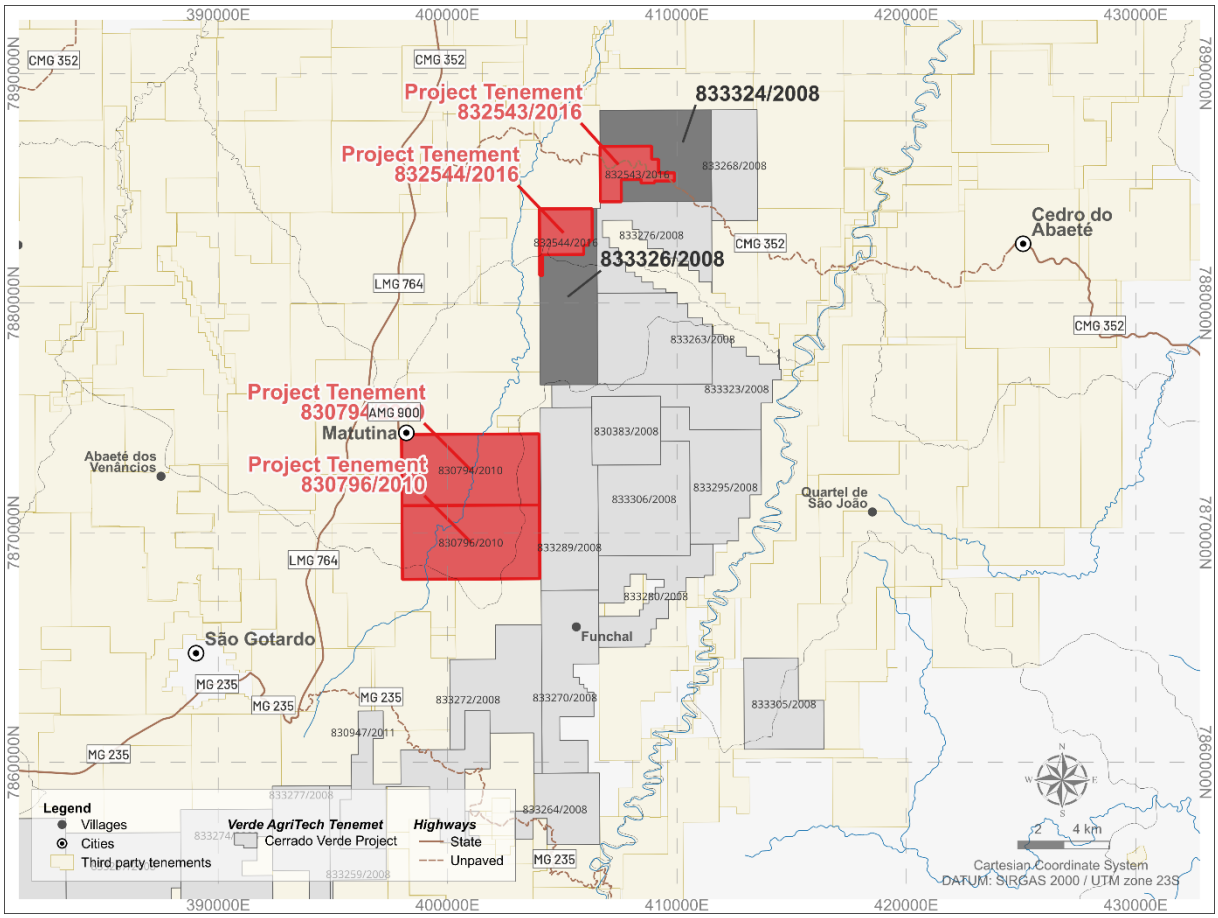



**Figure 22.1 - Adjacent Properties to the Man of War Project**

# 23 Other Relevant Data and Information

No other relevant information available.

# 24 Interpretation and Conclusions

BNA conducted an evaluation of the mineral resources of the Nau de Guerra Project - Rare Earth, belonging to Verde, in compliance with the Canadian Institute of Mining, Metallurgy and Petroleum Standards on Mineral Resources and Reserves: Definitions and Guidelines, May 19, 2014 (https://mrmr.cim.org/media/1128/cim-definition-standards_2014.pdf). The main activities undertaken by BNA were:

- Verification of the status of the mining rights belonging to the project;
- Site visit, discussions with the technical staff from Verde, gaining an understanding of the geology and mineralization of the deposit, and verification of the geological work performed by Verde and contractors on site, as well as verification of the materiality of the results achieved;
- Validation of the drilling database and the topographical information;
- Verification of the QA/QC program established by Verde for geological work and of its implementation, especially during the drilling work;
- Verification of the Verde Agritech – Declaração SGSGeosol.pdf document demonstrating the recovery of rare earth elements for the ionic clay mineralization of the Man of War project;
- Selection of the drilling data used in the definition of mineral resources;
- Interpretation of the geological model;
- Performance of statistical and geostatistical studies;
- Estimation of mineral resources, as well as their quantification and classification;
- Disclosure of the mineral resources from the Man of War Project in accordance with the Canadian Institute of Mining, Metallurgy and Petroleum Standards on Mineral Resources and Reserves: Definitions and Guidelines, May 19, 2014 (https://mrmr.cim.org/media/1128/cim-definition-standards_2014.pdf).

The materiality of the work undertaken by Verde, as well as the materiality of the deposit and the studies performed, are sufficient to support the declaration of mineral resources and mineral reserves for the Nau de Guerra Project.

Furthermore, the work conducted revealed notable concentrations of Nb, Sc, Hf, Ga, Rb, V and Co, highlighting the need for studies on these elements.

# 25 Recommendations

## 25.1 Work Program

BNA, based on the studies and work carried out on the mineral resources of the Man of War Prospect, owned by Verde, makes the following recommendations:

- Perform cross-validation between the geological description and the chemical analysis results;
- Perform interlaboratory verification of the analysis results
- Designate a professional or team to be responsible for the database feed and handling;
- Densify and regularize the exploratory drill grid;
- Standardize lithological codes in the geological descriptions;
- Conduct a detailed topographic survey of the site;
- Perform detailed geological mapping of the Capacete Formation;
- Perform additional metallurgical test work for rare earth elements as a critical component in advancing the project;
- Perform metallurgical test work for additional elements (Nb, Sc, Hf, Ga, Rb, V and Co), to verify their potential for economic exploitation.

## 25.2 Potential of Additional Elements for the Project

The identification of additional elements within the Man of War Project underscores its strategic significance and economic potential. In addition to the confirmed rare earth elements (REE), the discovery of niobium (Nb), scandium (Sc), hafnium (Hf), gallium (Ga), rubidium (Rb), vanadium (V) and cobalt (Co) in potentially economically recoverable concentrations could substantially enhance the project's value. This section summarizes preliminary information on the concentrations and distributions of these elements as potential co-products.

The presence of these elements within the same geological targets as REEs suggests valuable synergies that could expand the project's scope and market appeal. Given the increasing global demand for critical materials, further studies are warranted to assess their economic potential and strategic integration within the Man of War Project.

### 25.2.1 Estimated Average Grade

Within the same modelled domains defined for rare earths in this NI 43-101 report, the block model also provided estimated concentrations of niobium pentoxide ($Nb_2O_5$), vanadium pentoxide ($V_2O_5$), cobalt oxide (CoO), hafnium dioxide ($HfO_2$), molybdenum trioxide ($MoO_3$), and rubidium oxide ($Rb_2O$). Although these elements have not yet been classified as NI 43-101 resources—having not undergone the same rigorous evaluation process as the rare earth elements—they serve as strong indicators of the deposit's potential.

The Table 25.1 presents average grade estimated for key targets within the Man of War (MoW) Project, using a 1,000 ppm TREO cutoff.

**Table 25.1 – Estimated Average Grades**

| Target | TREO | CoO | $HfO_2$ | $Nb_2O_5$ | $V_2O_5$ | $Rb_2O$ |
|---|---|---|---|---|---|---|
| | *ppm* | *ppm* | *ppm* | *ppm* | *ppm* | *ppm* |
| Nau de Guerra | 3,628 | 89 | 23 | 685 | 684 | 173 |
| Alto da Serra | 3,684 | 88 | 24 | 678 | 805 | 167 |
| Balsamo | 3,358 | 39 | 20 | 611 | 650 | 146 |
| **TOTAL** | **3,430** | **51** | **21** | **627** | **677** | **152** |

*Cutoff 1,000 ppm TREO

### 25.2.2 Highlights assays

Beyond the average grade estimates derived from the block model, individual drill hole results for elements such as Hf, Nb, V, Ga, Rb, Co, Mo, and Sc demonstrate notable variability across the deposit profile. While these elements are generally contained within the same mineralized domain as the rare earths, their distribution patterns often exhibit unique spatial trends with varying starting and ending elevations.

In some instances, specific elemental domains extend beyond or fall within different boundaries compared to the rare earth-bearing zones. These geological distinctions emphasize the potential for refining resource models and optimizing selective mining strategies to target zones with higher concentrations of key elements, ultimately enhancing the project's economic outlook.

The following sections will present drilling highlights from each of the three key deposits, showcasing high-grade intervals and reinforcing the deposit's complexity and potential for maximizing resource utilization.

**Niobium**

Niobium (Nb) is a strategic metal widely used in high-strength steel alloys, superconductors, and aerospace components due to its unique properties of enhancing strength and corrosion resistance. Its synergy with REEs is particularly notable in advanced materials, where both are used to develop cutting-edge technologies. The current market price of niobium pentoxide ($Nb_2O_5 \geq 99.5\%$) stands at $48 to $50 USD/kg[6].

Drilling assays confirm the presence of significant niobium mineralization across multiple targets. The highest recorded grade for a one-metre interval is 2,274 ppm $Nb_2O_5$ in the Alto da Serra target. Additionally, the Balsamo target presented substantial intercepts, such as a 33-meter thick interval grading 895 ppm $Nb_2O_5$. See Table 25.2 for detail.

**Table 25.2 – Highlighted Drill Hole Intersections and Niobium Oxide ($Nb_2O_5$) Concentrations for the Man of War Project**

| Target | Hole | From (m) | To (m) | Thickness (m) | $Nb_2O_5$ (ppm) |
|---|---|---|---|---|---|
| Nau de Guerra | AP-ND-05 | 9 | 26 | 17 | 836 |
| | | 22 | 23 | 1 | 1,430 |
| | AP-ND-09 | 20 | 34 | 14 | 1,107 |
| | | 28 | 29 | 1 | 1,481 |
| | AP-ND-14 | 20 | 50 | 30 | 964 |
| | | 29 | 30 | 1 | 1,877 |
| Balsamo | AP-BD-01 | 53 | 86 | 33 | 895 |
| | | 65 | 66 | 1 | 2,227 |
| | AP-BD-09 | 11 | 60 | 49 | 772 |
| | | 20 | 21 | 1 | 1,749 |
| | AP-BD-10 | 58 | 92 | 34 | 822 |
| | | 64 | 65 | 1 | 1,757 |
| Alto da Serra | AP-AD-06 | 28 | 70 | 42 | 744 |
| | | 38 | 39 | 1 | 2,167 |
| | AP-AD-16 | 0 | 52 | 52 | 767 |
| | | 7 | 8 | 1 | 2,274 |
| | AP-AD-17 | 6 | 48 | 42 | 768 |
| | | 13 | 14 | 1 | 2,042 |

**Vanadium**

Vanadium (V) is an important element in energy storage technologies, primarily used in vanadium redox flow batteries (VRFBs) for grid-scale energy storage, as well as in steel production to

[6] Available at https://www.metal.com/Niobium-Tantalum/202107260001 accessed on 01/20/2025

improve hardness and wear resistance. Its market demand is driven by the global transition to renewable energy, positioning vanadium as a strategic resource. Vanadium pentoxide ($V_2O_5 \geq 98\%$) is currently valued at $8,680 to $9,040 USD/mt[7], reflecting its high market demand and strategic importance.

Exploration results within the Man of War Project indicate consistent vanadium mineralization, with concentrations between 1200ppm and 2000ppm over widths of 10 to 16 metres, with one-metre interval grades up to 4,223 ppm $V_2O_5$ at the Alto da Serra target. See Table 25.3 for detail.

**Table 25.3 – Highlighted Drill Hole Intersections and Vanadium Oxide ($V_2O_5$) Concentrations for the Man of War Project**

| Target | Hole | From (m) | To (m) | Thickness (m) | $V_2O_5$ (ppm) |
|---|---|---|---|---|---|
| Nau de Guerra | AP-ND-09 | 21 | 32 | 11 | 1,378 |
| | | 21 | 22 | 1 | 1,847 |
| | AP-ND-14 | 18 | 34 | 16 | 1,198 |
| | | 25 | 26 | 1 | 1,483 |
| | AP-ND-15 | 9 | 14 | 5 | 1,344 |
| | | 12 | 13 | 1 | 1,482 |
| Balsamo | AP-BD-01 | 55 | 67 | 12 | 1,609 |
| | | 60 | 61 | 1 | 2,165 |
| | AP-BD-06 | 59 | 68 | 9 | 2,030 |
| | | 62 | 63 | 1 | 2,763 |
| | AP-BD-09 | 11 | 24 | 13 | 1,406 |
| | | 58 | 59 | 1 | 1,969 |
| Alto da Serra | AP-AD-03 | 40 | 54 | 14 | 1,541 |
| | | 48 | 49 | 1 | 4,223 |
| | AP-AD-12 | 18 | 30 | 12 | 1,436 |
| | | 11 | 12 | 1 | 3,845 |
| | AP-AD-19 | 10 | 23 | 13 | 1,312 |
| | | 10 | 11 | 1 | 3,657 |

**Rubidium**

Rubidium is a valuable alkali metal used in advanced technologies such as quantum computing, telecommunications, and atomic clocks. Its applications in niche markets with high market value, with

[7] Available at https://www.metal.com/Other-Minor-Metals/202110220002 accessed on 01/20/2025

rubidium oxide (Rb2O3≥99%) currently priced at around $1,000USD/kg[8], position it as an attractive co-product within the Man of War Project.

Significant rubidium concentrations have been identified across the project's targets, with grades peaking at 426 ppm $Rb_2O$ in the Alto da Serra target (see Table 25.4). Assays over 200ppm over 20 to 50m intersections are promising.

**Table 25.4 – Highlighted Drill Hole Intersections and Rubidium Oxide ($Rb_2O$) Concentrations for the Man of War Project**

| Target | Hole | From (m) | To (m) | Thickness (m) | $Rb_2O$ (ppm) |
|---|---|---|---|---|---|
| Nau de Guerra | AP-ND-03 | 25 | 58 | 33 | 230 |
| | | 29 | 30 | 1 | 386 |
| | AP-ND-07 | 22 | 29 | 7 | 314 |
| | | 27 | 28 | 1 | 404 |
| | AP-ND-08 | 34 | 39 | 5 | 300 |
| | | 37 | 38 | 1 | 430 |
| Balsamo | AP-BD-05 | 27 | 50 | 23 | 232 |
| | | 94 | 95 | 1 | 355 |
| | AP-BD-10 | 66 | 87 | 21 | 209 |
| | | 121 | 122 | 1 | 350 |
| | AP-BD-13 | 49 | 103 | 54 | 222 |
| | | 102 | 103 | 1 | 358 |
| Alto da Serra | AP-AD-01 | 9 | 50 | 41 | 240 |
| | | 44 | 45 | 1 | 353 |
| | AP-AD-03 | 48 | 89 | 41 | 226 |
| | | 53 | 54 | 1 | 377 |
| | AP-AD-07 | 68 | 113 | 45 | 265 |
| | | 106 | 107 | 1 | 426 |

**Hafnium**

Hafnium is a strategic element primarily used in aerospace technologies and nuclear reactor control rods due to its exceptional ability to absorb neutrons. The hafnium dioxide (Hf+Zr min. 99,9%, Zr < 0,2%) commands a premium market value of $1,200 USD/kg[9], making it a valuable addition to the project.

[8] Available at https://www.metal.com/Other-Minor-Metals/202012250004 accessed on 01/20/2025
[9] Available at https://strategicmetalsinvest.com/hafnium-prices/ accessed on 01/20/2025

Drill intersections of 10 to 15 m averaging 45 to 50ppm in each target could add significant value. See Table 25.5 for detail.

**Table 25.5 – Highlighted Drill Hole Intersections and Hafnium Oxide ($HfO_2$) Concentrations for the Man of War Project**

| Target | Hole | From (m) | To (m) | Thickness (m) | $HfO_2$ (ppm) |
|---|---|---|---|---|---|
| Nau de Guerra | AP-ND-09 | 20 | 33 | 13 | 45 |
| | | 21 | 22 | 1 | 71 |
| | AP-ND-14 | 18 | 34 | 16 | 49 |
| | | 31 | 32 | 1 | 59 |
| | AP-ND-15 | 7 | 17 | 10 | 42 |
| | | 13 | 14 | 1 | 54 |
| Balsamo | AP-BD-04 | 59 | 71 | 12 | 50 |
| | | 68 | 69 | 1 | 68 |
| | AP-BD-05 | 19 | 30 | 11 | 45 |
| | | 21 | 22 | 1 | 66 |
| | AP-BD-09 | 11 | 24 | 13 | 49 |
| | | 13 | 14 | 1 | 67 |
| Alto da Serra | AP-AD-08 | 41 | 55 | 14 | 50 |
| | | 42 | 43 | 1 | 72 |
| | AP-AD-12 | 19 | 30 | 11 | 48 |
| | | 23 | 24 | 1 | 63 |
| | AP-AD-16 | 4 | 13 | 9 | 54 |
| | | 6 | 7 | 1 | 68 |

**Gallium**

Gallium is critical in semiconductor manufacturing, LED technology, and solar panels, ensuring a strong demand trajectory due to the global shift towards renewable energy. Gallium oxide (Ga2O3 ≥99.99%) is currently valued at around $300 USD/kg[10].

The most notable drill intercepts include a 27-meter interval from surface at Balsamo, grading 65 ppm $Ga_2O_3$, with a peak of 79 ppm. At Alto da Serra, a 17-meter intercept from surface returned 58 ppm, with a peak of 66 ppm. See Table 25.6 for detail.

[10] Available at https://www.metal.com/Indium-Germanium-Gallium/202209070002 accessed on 01/20/2025

**Table 25.6 – Highlighted Drill Hole Intersections and Gallium Oxide ($Ga_2O_3$) Concentrations for the Man of War Project**

| Target | Hole | From (m) | To (m) | Thickness (m) | $Ga_2O_3$ (ppm) |
|---|---|---|---|---|---|
| Balsamo | AP-BD-04 | 0 | 27 | 27 | 65 |
| | | 4 | 5 | 1 | 79 |
| | AP-BD-07 | 0 | 27 | 27 | 58 |
| | | 8 | 9 | 1 | 75 |
| | AP-BD-11 | 0 | 33 | 33 | 55 |
| | | 6 | 7 | 1 | 71 |
| Alto da Serra | AP-AD-04 | 0 | 17 | 17 | 58 |
| | | 6 | 7 | 1 | 66 |
| | AP-AD-07 | 0 | 27 | 27 | 55 |
| | | 20 | 21 | 1 | 72 |
| | AP-AD-09 | 0 | 19 | 19 | 50 |
| | | 3 | 4 | 1 | 65 |

**Cobalt**

Cobalt is an essential element in the production of high-performance alloys, rechargeable batteries, and magnets, with significant demand in the electric vehicle and renewable energy sectors. With a market value of around $12,000 USD/mt[11] for cobalt oxide (Co≥72%), it is a potentially valuable co-product in the Man of War Project.

The project has identified cobalt mineralization with grades reaching up to 938 ppm CoO, and with 20m to 58m thick intersections averaging over 140ppm in the three targets. See Table 25.7 for detail.

**Table 25.7 – Highlighted Drill Hole Intersections and Cobalt Oxide (CoO) Concentrations for the Man of War Project**

| Target | Hole | From (m) | To (m) | Thickness (m) | CoO (ppm) |
|---|---|---|---|---|---|
| Nau de Guerra | AP-ND-09 | 22 | 54 | 32 | 140 |
| | | 53 | 54 | 1 | 382 |
| | AP-ND-14 | 30 | 44 | 14 | 280 |
| | | 35 | 36 | 1 | 938 |
| | AP-ND-16 | 8 | 35 | 27 | 119 |
| | | 8 | 9 | 1 | 492 |
| Balsamo | AP-BD-04 | 61 | 80 | 19 | 128 |
| | | 79 | 80 | 1 | 520 |
| | AP-BD-06 | 62 | 96 | 34 | 154 |

[11] Available at https://www.metal.com/Chemical-compound/201102250301 accessed on 01/20/2025

| | | | | | |
|---|---|---|---|---|---|
| | | 68 | 69 | 1 | 647 |
| | AP-BD-13 | 39 | 97 | 58 | 124 |
| | | 55 | 56 | 1 | 405 |
| Alto da Serra | AP-AD-01 | 5 | 51 | 46 | 114 |
| | | 14 | 15 | 1 | 632 |
| | AP-AD-07 | 61 | 113 | 52 | 145 |
| | | 101 | 102 | 1 | 689 |
| | AP-AD-09 | 43 | 96 | 53 | 123 |
| | | 76 | 77 | 1 | 601 |

**Scandium**

Scandium, an essential component in aluminum-scandium alloys for aerospace and fuel cell technologies, represents a high-value opportunity with scandium oxide (Sc2O5 >= 99.99%) priced at around $740 USD/kg[12]. Its synergistic potential with REEs enhances metallurgical recovery processes.

The Man of War samples were analyzed by SGS laboratories using the ICP95A/IMS95A methods, covering 47 parameters, excluding scandium. Recognizing scandium's industrial relevance, the Company conducted a reanalysis of 30 core samples across three drill holes using the ICM40B method to Scandium levels specifically.

Following targeted reanalysis, notable scandium results include a 16-meter intercept at Nau de Guerra from 18 meters depth, grading 49 ppm $Sc_2O_3$, with a peak of 59 ppm. Additionally, a 10-meter intercept from just 7 meters depth returned 42 ppm, with a peak of 54 ppm. See Table 25.8 for detail.

**Table 25.8 – Highlighted Drill Hole Intersections and Scandium Oxide ($Sc_2O_3$) Concentrations for the Man of War Project**

| Target | Hole | From (m) | To (m) | Thickness (m) | $Sc_2O_3$ (ppm) |
|---|---|---|---|---|---|
| Nau de Guerra | AP-ND-09 | 20 | 33 | 13 | 45 |
| | | 21 | 22 | 1 | 71 |
| | AP-ND-14 | 18 | 34 | 16 | 49 |
| | | 31 | 32 | 1 | 59 |
| | AP-ND-15 | 7 | 17 | 10 | 42 |
| | | 13 | 14 | 1 | 54 |

[12] Available at https://www.metal.com/Rare-Earth-Oxides/202104090003 accessed on 01/20/2025

### 25.2.3 Future Studies and Exploration Directions

As the exploration phase of the Man of War Project advances, the identification of niobium, scandium, hafnium, gallium, rubidium, vanadium and cobalt opens up opportunities for further research and development. These elements not only enhance the project's economic potential but also position it as a significant contributor to the global supply of critical materials. To fully realize the potential of these elements, several future studies are being prioritized, focusing on refining resource models, optimizing extraction methods, and evaluating market integration strategies.

- **Geological and Mineralogical Characterization:** Further geological mapping and mineralogical analysis will better define the distribution of these elements across the deposit. Focus will be on mineralization patterns and geochemical associations to optimize extraction and processing strategies.
- **Resource Estimation and Classification:** A comprehensive resource estimation will classify niobium, scandium, vanadium, and other critical elements into NI 43-101 categories. This will involve additional drilling, sampling, and lab analyses to increase confidence and integrate these elements into economic models.
- **Metallurgical Testing and Processing Optimization:** Metallurgical tests will assess the feasibility of extracting these elements with REEs. Pilot-scale and bench tests will optimize processing methods for multi-element recovery, focusing on cost-effectiveness and environmental sustainability.
- **Market Analysis and Strategic Integration:** An in-depth market analysis will evaluate demand, pricing, and supply chains for these elements, guiding their integration into the Man of War Project's business model. Efforts will include exploring off-take agreements and strategic partnerships.

## 25.3 Budget

**Recommendations for Future Investments in the Man of War Project**

The Man of War rare earths project has demonstrated significant potential for further development through strategic investments in exploration and resource evaluation. The current data suggests that the deposit contains a substantial rare earth element resource with promising economic prospects. It is recommended to advance the project towards the Preliminary Economic Assessment (PEA) stage by implementing a comprehensive work program. This program should focus on infill drilling, exploration of new targets, resource estimation updates, and economic viability studies.

To enhance the confidence level in the existing resource, an infill drilling campaign is recommended. This will aid in converting Inferred Mineral Resources into Indicated or Measured categories, thereby improving the reliability of future feasibility studies. In addition, drilling new targets, specifically the Fragata and Caravela targets, will provide valuable insights into the lateral and depth extensions of the mineralization, ensuring a more comprehensive understanding of the deposit's potential.

An updated NI 43-101 compliant resource estimate is necessary to incorporate new geological data and ensure that the project aligns with industry standards. This updated estimate will serve as a foundation for further economic evaluations and decision-making processes. Additionally, it is crucial to initiate a PEA to assess the project's economic feasibility, including mining methods, processing options, environmental considerations, and market analysis. The PEA will provide essential inputs to guide future investments and strategic planning.

Metallurgical test work is also a critical component in advancing the project. Future studies with specialized companies will focus on advanced leaching processes, impurity treatment methodologies, and recovery optimization. These efforts are expected to significantly enhance recovery rates and contribute to the overall economic potential of the project. Additionally, other elements identified in the deposit will require preliminary metallurgical studies to better understand their processing requirements and economic viability.

Overall, the recommended investment plan aims to position the Man of War project for future development and value realization. By conducting targeted exploration, resource assessment, and economic evaluation, the project will move closer to achieving its objectives and attracting potential investors. It is advised to secure adequate funding and resources to successfully implement the proposed work plan and advance the project to the next stage of development.

The estimated budget for this work program is shown in Table 25.9.

**Table 25.9 - Estimated Investment Breakdown**

| Description | Value (CAD) | Value (BRL) |
|---|---|---|
| Infill Drilling | $4,004,854 | R$ 16,500,000 |
| Drilling New Targets | $485,437 | R$ 2,000,000 |
| NI 43-101 Resource Update | $145,631 | R$ 600,000 |
| Preliminary Economic Assessment (PEA) | $533,981 | R$ 2,200,000 |
| Metallurgical Flowsheet Design | $121,359 | R$ 500,000 |
| Initial Environmental Studies (EIS/PCA) | $266,990 | R$ 1,100,000 |
| **Total Investment** | **$5,558,252** | **R$ 22,900,000** |

# 26 References

Agência Nacional de Mineração [National Mining Agency of Brazil] (ANM). 2023. https://www.gov.br/anm.

ALMEIDA, F. F. M. 1977. O Cráton São Francisco. Revista Brasileira de Geociências. 7: 285-295.

BARBOSA, A.R. & CARVALHO MATOS, H., 1997. O Novo Código de Mineração. Editora Signus, São Paulo - SP.

Canadian Institute of Mining, Metallurgy and Petroleum (CIM), 2014. CIM Standards for Mineral Resources and Mineral Reserves, Definitions and Guidelines: Canadian Institute of Mining, Metallurgy and Petroleum, May 10, 2014.

Guimarães D. 1967. Ocorrências de fosforita no município de Abaeté. Rio de Janeiro: DNPM-DGM, 18 p.

Ionic Rare Earths, 2021, "Mineral Resource Estimate Increased Threefold At Makuutu", March 3, 2021.

https://wcsecure.weblink.com.au/clients/ionicre/headline.aspx?headlineid=61022919

Instituto Brasileiro de Geografia e Estatística. 2023.

King, L.C. 1956. A geomorfologia do Brasil oriental. Rev. Bras. Geogr.,18(2): 147-265.

LIMA, O.N.B., 2005. Grupo Bambuí: Estratigrafia regional no Alto Rio São Francisco e geologia dos depósitos fosfáticos da Serra da Saudade. 142 f.. Dissertação (Mestrado) – Instituto de Geociências, Universidade Federal de Minas Gerais – Belo Horizonte, Brasil.

Lima O.N.B., Uhlein A., Britto W. 2007. Estratigrafia do Grupo Bambuí na Serra da Saudade e geologia do depósito fosfático de Cedro do Abaeté, Minas Gerais. Revista Brasileira de Geociências, 37(4 Suppl.):204-215.

Moreira, D. S. et al. Ediacaran/Early Cambrian Serra da Saudade Formation, Bambuí Group: the sedimentary record of a foreland basin in Southeastern Brazil. Brazilian Journal of Geology, v. 51 (03), 2021.

Sanematsu, K. & Watanabe, Y. 2016. Characteristics and genesis of ion adsorption-type rare earth element deposits. In P.L. Verplanck and M.W. Hitzman (Eds.), Rare Earth and Critical Elements in Ore Deposits. Reviews in Economic Geology, 18, 55–79. https://doi.org/10.5382/Rev.18.03.

TULLER, M. P. & E SILVA, P. C. S. Carta Geológica Folha Se.23-Y-D – Bom Despacho, MG – Escala 1:250.000. Convênio COMIG/CPRM, 2003.

Yang, M., Liang, X., Ma, L., Huang, J., He, H., & Zhu, J. 2019. Adsorption of REEs on kaolinite and halloysite: A link to the REE distribution on clays in the weathering crust of granite. Chemical Geology, 525, 210–217. https://doi.org/10.1016/j.chemgeo.2019.07.024.

# 27 Date and Signature Page

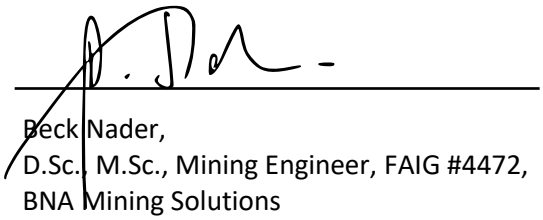
**NI 43-101 Technical Report, Mineral Resources for the Man of War Project**

**Targets: Nau de Guerra, Alto da Serra and Balsamo**

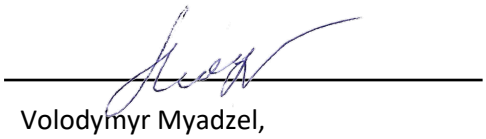
**Prepared for:**
Verde Agritech Ltd
16 Collyer Quay
#17-00
Income at Raffles
Singapore (049318)

**Prospect Location:**
São Gotardo and Matutina, Minas Gerais, Brazil

Signed in Belo Horizonte on January, 31, 2025



Beck Nader,
D.Sc., M.Sc., Mining Engineer, FAIG #4472,
BNA Mining Solutions
Belo Horizonte, Minas Gerais (Brazil)



Volodymyr Myadzel,
PhD in Geology, MAIG #3974,
BNA Mining Solutions
Belo Horizonte, Minas Gerais (Brazil)

# 28 Certificates of Qualified Persons

**CONSENT OF QUALIFIED PERSON**

Filed by SEDAR

TO: VerdeAgritech Ltd
British Columbia Securities Commission
Alberta Securities Commission
Saskatchewan Financial Services Commission
The Manitoba Securities Commission
Ontario Securities Commission
Nova Scotia Securities Commission
Financial and Consumer Services Commission, New Brunswick
Office of the Superintendent of Securities, Prince Edward Island
Office of the Superintendent of Securities, Government of Newfoundland and Labrador
Office of the Yukon Superintendent of Securities
Office of the Superintendent of Securities, Government of the Northwest Territories
Office of the Superintendent of Securities, Nunavut

**RE:** VerdeAgritech - NI 43-101 Technical Report Mineral Resources for the Man of War Project, dated Jan 31, 2025

This letter is being filed as the consent of Dr. Beck Nader to being named in the Disclosure and to the use and public filing of the report titled "*NI 43-101 Technical Report Mineral Resources for the Man of War Project*" dated Jan 31, 2025 (the "Technical Report") by VerdeAgritech Ltd in connection with the filing of the Disclosure and to the inclusion of the written disclosure of the Technical Report and of extracts from or a summary of the Technical Report in the written disclosure contained in the Disclosure or incorporated by reference therein.

I hereby confirm that I have read the Technical Report, including the written disclosure and extracts from or a summary of the Technical Report contained in the Disclosure or incorporated by reference therein and that it fairly and accurately represents the information in the Technical Report.

Dated this 31st day of January 2025.

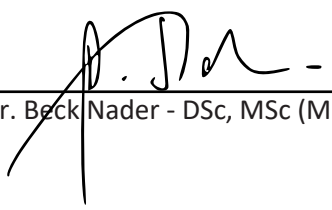
Dr. Beck Nader - DSc, MSc (Mining Engineer); FAIG #4472

**CERTIFICATE OF AUTHOR – Dr. Beck Nader**

I, Beck Nader, FAIG #4472, do hereby certify that:

1. I am the Principal Mining Consultant of: BNA Mining Solutions Ltda.
   R. Desembargador Leão Starling, 200, Ouro Preto, Belo Horizonte – MG – Brazil. 31310-370
2. I graduated with a degree in Mining Engineering from Escola Politécnica of the Universidade of São Paulo - USP, SP, Brazil in 1981. In addition, I obtained a Mineral Technology MSc title from the Universidade Federal de Minas Gerais (2004) and a DSc title from the Universidade de São Paulo in Mineral Engineering (2012).
3. I am a fellow of the Australian Institute of Geoscientists (FAIG #4472) and a registered member of CREA-MG, the Regional Council of Engineering and Agronomy of the Minas Gerais State.
4. I have worked as a Mining Engineer for a total of more than 43 years since my graduation from university. My relevant experience includes mineral resource and reserve estimation of deposits, including economical evaluation of mineral projects, risk assessment and multidisciplinary coordination and integration.
5. I have read the definition of “qualified person” set out in National Instrument 43-101 (NI 43-101) and certify that by reason of my education, affiliation with a professional association (as defined in NI 43-101) and past relevant work experience, I fulfill the requirements to be a “qualified person” for the purposes of NI 43-101.
6. I have supervised the preparation of the Technical Report. I am responsible for item 1.8 of Chapter 1, for item 14.13 of Chapter 14, and jointly to responsible for items 1.1, 1.9 and 1.10 of Chapter 1 and jointly responsible for Chapters 3, 4, 5, 6, 7, 8, 9, 10, 11, 13,15, 16, 17, 18, 19, 20, 21, 22, 23, 25 and 26 of the Technical Report “NI 43-101 TECHNICAL REPORT Man of War Project Rare Earths”, dated January 31, 2025, relating to the Man of War Project.
7. I have not had any prior involvement with the property that is the subject of the Technical Report on Resources.
8. I am independent of the issuer applying all of the tests in section 1.5 of National Instrument 43-101.
9. I have read NI 43-101 and Form 43-101F1, and the technical report on resources has been prepared in compliance with that instrument and form.
10. I consent to the filing of the Technical Report on Resources with any stock exchange and other regulatory authority and any publication by them for regulatory purposes, including electronic publication in the public company files on their websites accessible by the public, of the Technical Report on Resources.
11. As of the effective date of the Technical Report on Resources, to the best of my knowledge, information and belief, the Technical Report on Resources, or part that the qualified person is responsible for, contains all the scientific and technical information that is required to be disclosed to ensure that the technical report is not misleading.

Signed this 31st day of January, 2025, in Belo Horizonte, Minas Gerais, Brazil.



Dr. Beck Nader - DSc, MSc (Mining Engineer); FAIG #4472

## CONSENT OF QUALIFIED PERSON

Filed by SEDAR

TO: VerdeAgritech Ltd
British Columbia Securities Commission
Alberta Securities Commission
Saskatchewan Financial Services Commission
The Manitoba Securities Commission
Ontario Securities Commission
Nova Scotia Securities Commission
Financial and Consumer Services Commission, New Brunswick
Office of the Superintendent of Securities, Prince Edward Island
Office of the Superintendent of Securities, Government of Newfoundland and Labrador
Office of the Yukon Superintendent of Securities
Office of the Superintendent of Securities, Government of the Northwest Territories
Office of the Superintendent of Securities, Nunavut

**RE:** VerdeAgritech - NI 43-101 Technical Report Mineral Resources for the Man of War Project, dated Jan 31, 2025

This letter is being filed as the consent of Dr. Volodymyr Myadzel to being named in the Disclosure and to the use and public filing of the report titled "*NI 43-101 Technical Report Mineral Resources for the Man of War Project*" dated Jan 31, 2025 (the "Technical Report") by VerdeAgritech Ltd in connection with the filing of the Disclosure and to the inclusion of the written disclosure of the Technical Report and of extracts from or a summary of the Technical Report in the written disclosure contained in the Disclosure or incorporated by reference therein.

I hereby confirm that I have read the Technical Report, including the written disclosure and extracts from or a summary of the Technical Report contained in the Disclosure or incorporated by reference therein and that it fairly and accurately represents the information in the Technical Report.

Dated this 31st day of January 2025.

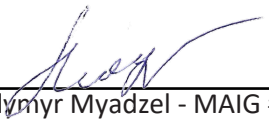
Dr. Volodymyr Myadzel - PhD; MAIG #3974

**CERTIFICATE OF AUTHOR – Dr. Volodymyr Myadzel**

I, Volodymyr Myadzel, MAIG #3974, do hereby certify that:

1. I am the Principal Geologist of: BNA Mining Solutions Ltda.
   R. Desembargador Leão Starling, 200, Ouro Preto, Belo Horizonte – MG – Brazil. 31310-370
2. I graduated with a degree in Geology from Kryvyi Rih National University, Kryvyi Rih, Ukraine in 1999. In addition, I obtained a PhD in Geology from Kryvyi Rih National University, Kryvyi Rih, Ukraine in 2004.
3. I am Member #3974 of the Australasian Institute of Geoscientists.
4. I have worked as a Geologist for a total of 25 years since my graduation from university. My relevant experience includes modeling and resource and reserve estimation of deposits, prospecting and surveying, geological mapping, mineralogy and petrology of metamorphic rocks and ore deposits.
5. I have read the definition of “qualified person” set out in National Instrument 43-101 (NI 43-101) and certify that by reason of my education, affiliation with a professional association (as defined in NI 43-101) and past relevant work experience, I fulfill the requirements to be a “qualified person” for the purposes of NI 43-101.
6. I am responsible for the preparation of items 1.2 to 1.7 of Chapter 1 and Chapters 2, 12, 14, 24, 25 and jointly responsible for items 1.1, 1.9 and 1.10 and Chapters 3, 4, 5, 6, 7, 8, 9, 10, 11, 13,15, 16, 17, 18, 19, 20, 21, 22, 23 and 26 of the Technical Report “NI 43-101 TECHNICAL REPORT Man of War Project Rare Earths”, dated January 31, 2025, relating to the Man of War Project. I visited the Man of War Prospect on July 1 and 2 and August 13, 2024.
7. I have not had any prior involvement with the property that is the subject of the Technical Report on Resources.
8. I am independent of the issuer applying all of the tests in section 1.5 of National Instrument 43-101.
9. I have read NI 43-101 and Form 43-101F1, and the technical report on resources has been prepared in compliance with that instrument and form.
10. I consent to the filing of the Technical Report on Resources with any stock exchange and other regulatory authority and any publication by them for regulatory purposes, including electronic publication in the public company files on their websites accessible by the public, of the Technical Report on Resources.
11. As of the effective date of the Technical Report on Resources, to the best of my knowledge, information and belief, the Technical Report on Resources, or part that the qualified person is responsible for, contains all the scientific and technical information that is required to be disclosed to ensure that the technical report is not misleading.

Signed this 31st day of January, 2025, in Belo Horizonte, Minas Gerais, Brazil.



Dr. Volodymyr Myadzel - MAIG #3974, PhD

# APPENDIX I – Standards Certificates

# LIST OF CERTIFICATES

Appendix I - Certificate I – MULTIELEMENT GEOCHEMICAL MATERIAL – CERTIFIED REFERENCE MATERIAL – SG-142

Appendix I - Certificate II – CARBONATITE SUPERGENE REE-Nb ORE (TREO 0.53%) CERTIFIED REFERENCE MATERIAL – OREAS 460

Appendix I - Certificate III – CARBONATITE SUPERGENE REE-Nb ORE (TREO 1.06%) – CERTIFIED REFERENCE MATERIAL – OREAS 461

# APPENDIX II – Chemical Analysis Certificates

# LIST OF CERTIFICATES ALTO DA SERRA

Appendix II – Analysis Certificate I – GQ2409239.PDF

Appendix II – Analysis Certificate II – GQ2409240.PDF

Appendix II – Analysis Certificate III – GQ2409241.PDF

Appendix II – Analysis Certificate IV – GQ2409242.PDF

Appendix II – Analysis Certificate V – GQ2409243.PDF

Appendix II – Analysis Certificate VI – GQ2409244.PDF

Appendix II – Analysis Certificate VII – GQ2409245.PDF

Appendix II – Analysis Certificate VIII – GQ2409246.PDF

Appendix II – Analysis Certificate IX – GQ2409247.PDF

Appendix II – Analysis Certificate X – GQ2409248.PDF

Appendix II – Analysis Certificate XI – GQ2409249.PDF

Appendix II – Analysis Certificate XII – GQ2409250.PDF

Appendix II – Analysis Certificate XIII – GQ2409251.PDF

Appendix II – Analysis Certificate XIV – GQ2409252.PDF

Appendix II – Analysis Certificate XV – GQ2409253.PDF

Appendix II – Analysis Certificate XVI – GQ2409254.PDF

Appendix II – Analysis Certificate XVII – GQ2409255.PDF

Appendix II – Analysis Certificate XVIII – GQ2409256.PDF

Appendix II – Analysis Certificate XIX –GQ2409257.PDF

Appendix II – Analysis Certificate XX – GQ2409258.PDF

Appendix II – Analysis Certificate XXI – GQ2409259.PDF

Appendix II – Analysis Certificate XXII – GQ2409260.PDF

Appendix II – Analysis Certificate XXIII – GQ2409261.PDF

Appendix II – Analysis Certificate XXIV – GQ2409262.PDF

# LIST OF CERTIFICATES BALSAMO

Appendix II – Analysis Certificate I – GQ2408270.PDF

Appendix II – Analysis Certificate II – GQ2408272.PDF

Appendix II – Analysis Certificate III – GQ2408273.PDF

Appendix II – Analysis Certificate IV – GQ2408274.PDF

Appendix II – Analysis Certificate V – GQ2408275.PDF

Appendix II – Analysis Certificate VI – GQ2408276.PDF

Appendix II – Analysis Certificate VII – GQ2408277.PDF

Appendix II – Analysis Certificate VIII – GQ2408279.PDF

Appendix II – Analysis Certificate IX – GQ2408280.PDF

Appendix II – Analysis Certificate X – GQ2408281.PDF

Appendix II – Analysis Certificate XI – GQ2408282.PDF

Appendix II – Analysis Certificate XII – GQ2408283.PDF

Appendix II – Analysis Certificate XIII – GQ2408284.PDF

Appendix II – Analysis Certificate XIV – GQ2408285.PDF

Appendix II – Analysis Certificate XV – GQ2408286.PDF

Appendix II – Analysis Certificate XVI – GQ2408287.PDF

Appendix II – Analysis Certificate XVII – GQ2408288.PDF

Appendix II – Analysis Certificate XVIII – GQ2408289.PDF

Appendix II – Analysis Certificate XIX – GQ2408290.PDF

Appendix II – Analysis Certificate XX – GQ2408291.PDF

Appendix II – Analysis Certificate XXI – GQ2408293.PDF

Appendix II – Analysis Certificate XXII – GQ2408294.PDF

Appendix II – Analysis Certificate XXIII – GQ2408295.PDF

Appendix II – Analysis Certificate XXIV – GQ2408296.PDF

Appendix II – Analysis Certificate XXV – GQ2408298.PDF

Appendix II – Analysis Certificate XXVI – GQ2408299.PDF

Appendix II – Analysis Certificate XXVII – GQ2408300.PDF

Appendix II – Analysis Certificate XXVIII – GQ2408301.PDF

Appendix II – Analysis Certificate XXIX – GQ2408303.PDF

Appendix II – Analysis Certificate XXX – GQ2408304.PDF

Appendix II – Analysis Certificate XXXI – GQ2408305.PDF

Appendix II – Analysis Certificate XXXII – GQ2410696.PDF

Appendix II – Analysis Certificate XXXIII – GQ2410699.PDF

# LIST OF CERTIFICATES NAU DE GUERRA

Appendix II – Analysis Certificate I – GQ2403712.PDF

Appendix II – Analysis Certificate II – GQ2403713.PDF

Appendix II – Analysis Certificate III – GQ2407376.PDF

Appendix II – Analysis Certificate IV – GQ2407378.PDF

Appendix II – Analysis Certificate V – GQ2407379.PDF

Appendix II – Analysis Certificate VI – GQ2407380.PDF

Appendix II – Analysis Certificate VII – GQ2407381.PDF

Appendix II – Analysis Certificate VIII – GQ2407382.PDF

Appendix II – Analysis Certificate IX – GQ2407383.PDF

Appendix II – Analysis Certificate X – GQ2407385.PDF

Appendix II – Analysis Certificate XI – GQ2407386.PDF

Appendix II – Analysis Certificate XII – GQ2407387.PDF

Appendix II – Analysis Certificate XIII – GQ2407388.PDF

Appendix II – Analysis Certificate XIV – GQ2407389.PDF

Appendix II – Analysis Certificate XV – GQ2407390.PDF

Appendix II – Analysis Certificate XVI – GQ2409649.PDF

Appendix II – Analysis Certificate XVII – GQ2409652.PDF

Appendix II – Analysis Certificate XVIII – GQ2409653.PDF

# APPENDIX III – Qa/Qc

# LIST OF FIGURES

Appendix III - Figure 1 – Standard OREAS 460, element La, Nau de Guerra Target. ..... 194

Appendix III - Figure 2 – Standard OREAS 461, element La, Nau de Guerra Target. ..... 194

Appendix III - Figure 3 – Standard SG-142, element La, Nau de Guerra Target..... 195

Appendix III - Figure 4 – Standard OREAS 460, element La, Balsamo e Alto da Serra Target..... 195

Appendix III - Figure 5 – Standard OREAS 461, element La, Balsamo e Alto da Serra Target..... 196

Appendix III - Figure 6 – Standard SG-142, element La, Balsamo e Alto da Serra Target. ..... 196

Appendix III - Figure 7 – Standard OREAS 460, element Ce, Nau de Guerra Target. ..... 197

Appendix III - Figure 8 – Standard OREAS 461, element Ce, Nau de Guerra Target. ..... 197

Appendix III - Figure 9 – Standard SG-142, element Ce, Nau de Guerra Target. ..... 198

Appendix III - Figure 10 – Standard OREAS 460, element Ce, Balsamo e Alto da Serra Target. ..... 198

Appendix III - Figure 11 – Standard OREAS 461, element Ce, Balsamo e Alto da Serra Target. ..... 199

Appendix III - Figure 12 – Standard SG-142, element Ce, Balsamo e Alto da Serra Target. ..... 199

Appendix III - Figure 13 – Standard OREAS 460, element Y, Nau de Guerra Target. ..... 200

Appendix III - Figure 14 – Standard OREAS 461, element Y, Nau de Guerra Target. ..... 200

Appendix III - Figure 15 – Standard SG-142, element Yb, Nau de Guerra Target. ..... 201

Appendix III - Figure 16 – Standard OREAS 460, element Y, Balsamo e Alto da Serra Target. ..... 201

Appendix III - Figure 17 – Standard OREAS 461, element Y, Balsamo e Alto da Serra Target. ..... 202

Appendix III - Figure 18 – Standard SG-142, element Yb, Balsamo e Alto da Serra Target. ..... 202

Appendix III - Figure 19 – Linear Regression Diagram for Y ppm, field duplicate, class: Diamond Drilling, internal control results Nau de Guerra Target. ..... 203

Appendix III - Figure 20 – Quantis plotting for Y ppm, field duplicate, class: Diamond Drilling, internal control results Nau de Guerra Target. ..... 204

Appendix III - Figure 21 – Linear Regression Diagram for Y ppm, field duplicate, class: Diamond Drilling, internal control results Balsamo and Alto da Serra Target. ..... 204

Appendix III - Figure 22 – Quantis plotting for Y ppm, field duplicate, class: Diamond Drilling, internal control results Balsamo and Alto da Serra Target. ..... 205

Appendix III - Figure 23 – Linear Regression Diagram for Ce ppm, field duplicate, class: Diamond Drilling, internal control results Nau de Guerra Target. ..... 206

Appendix III - Figure 24 – Quantis plotting for Ce ppm, field duplicate, class: Diamond Drilling, internal control results Nau de Guerra Target. ..... 207

Appendix III - Figure 25 – Linear Regression Diagram for Ce ppm, field duplicate, class: Diamond Drilling, internal control results Balsamo and Alto da Serra Target. ..... 207

Appendix III - Figure 26 – Quantis plotting for Ce ppm, field duplicate, class: Diamond Drilling, internal control results Balsamo and Alto da Serra Target. ..... 208

Appendix III - Figure 27 – Linear Regression Diagram for Tb ppm, field duplicate, class: Diamond Drilling, internal control results Nau de Guerra Target. ..... 209

Appendix III - Figure 28 – Quantis plotting for Tb ppm, field duplicate, class: Diamond Drilling, internal control results Nau de Guerra Target. ..... 210

Appendix III - Figure 29 – Linear Regression Diagram for Tb ppm, field duplicate, class: Diamond Drilling, internal control results Balsamo and Alto da Serra Target. ..... 210

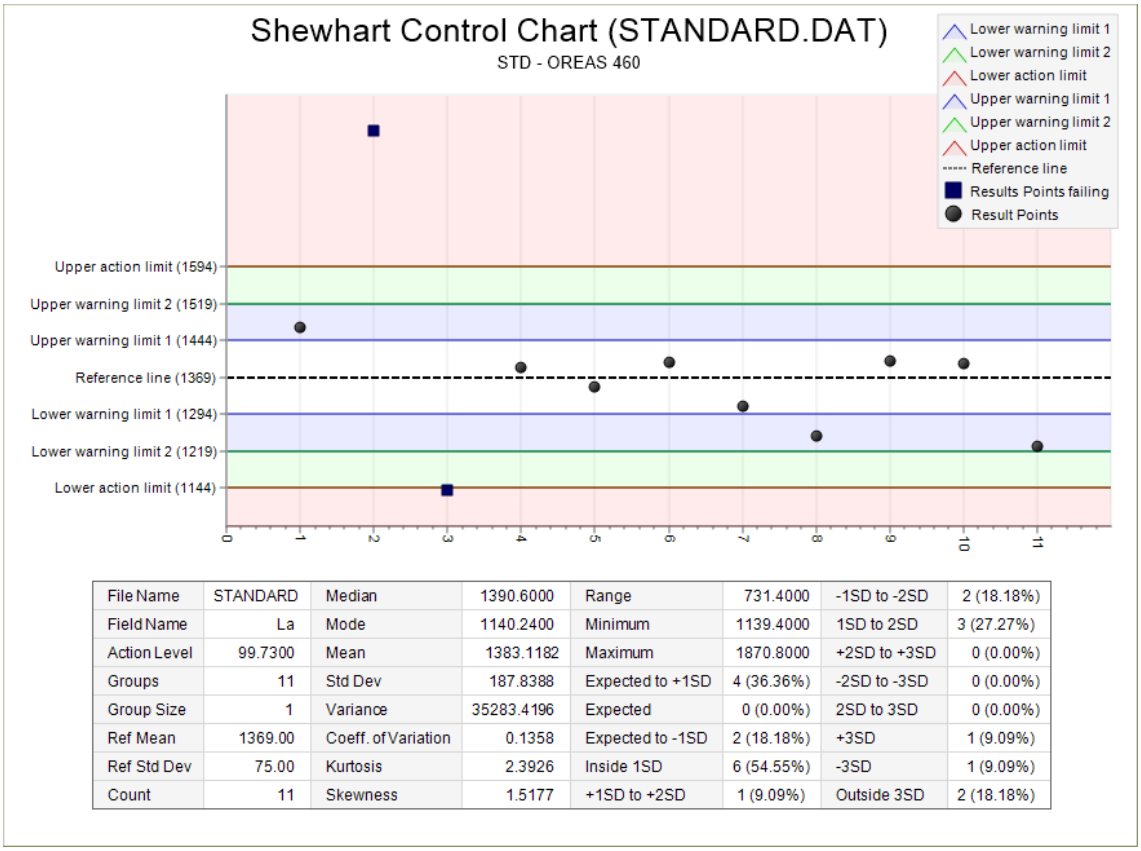
Appendix III - Figure 30 – Quantis plotting for Tb ppm, field duplicate, class: Diamond Drilling, internal control results Balsamo and Alto da Serra Target. ..... 211

Appendix III - Figure 31 – Linear Regression Diagram for Pr ppm, field duplicate, class: Diamond Drilling, internal control results Nau de Guerra Target. ..... 211

Appendix III - Figure 32 – Quantis plotting for Pr ppm, field duplicate, class: Diamond Drilling, internal control results Nau de Guerra Target. ..... 212

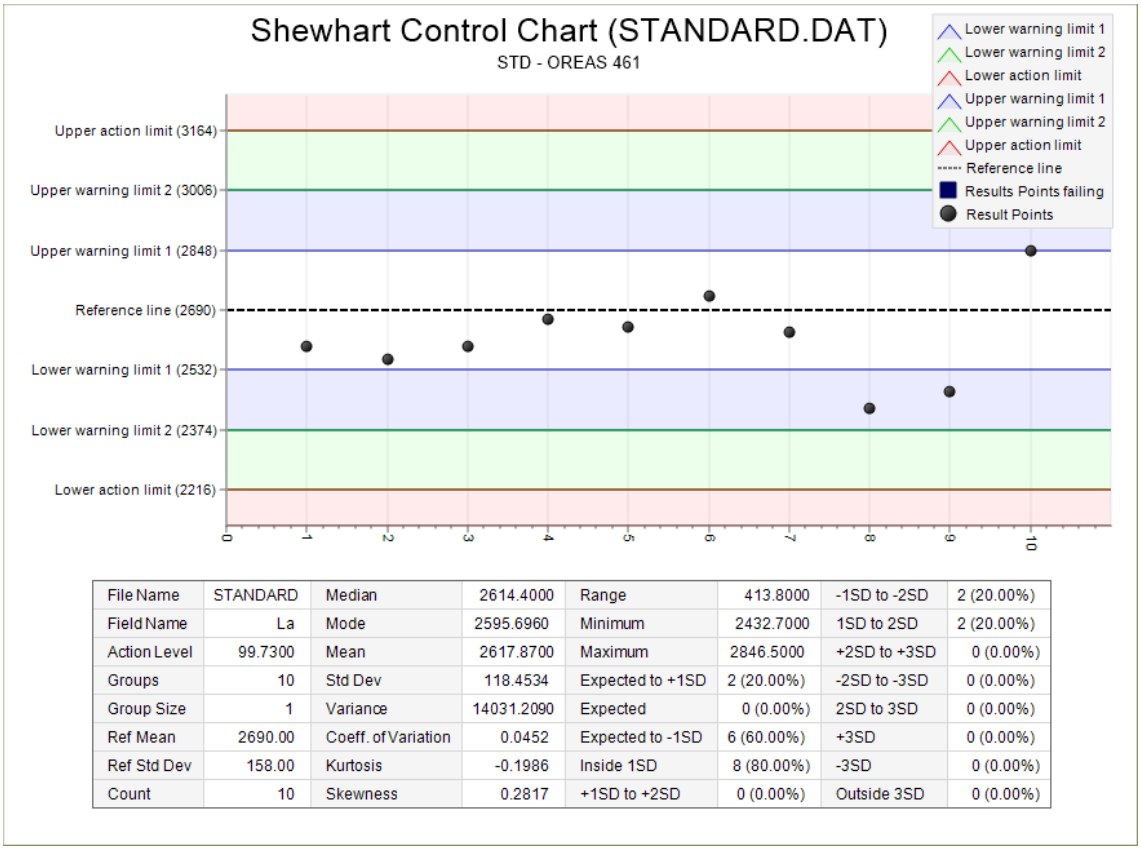
Appendix III - Figure 33 – Linear Regression Diagram for Pr ppm, field duplicate, class: Diamond Drilling, internal control results Balsamo and Alto da Serra Target. ..... 212

Appendix III - Figure 34 – Quantis plotting for Pr ppm, field duplicate, class: Diamond Drilling, internal control results Balsamo and Alto da Serra Target. ..... 213



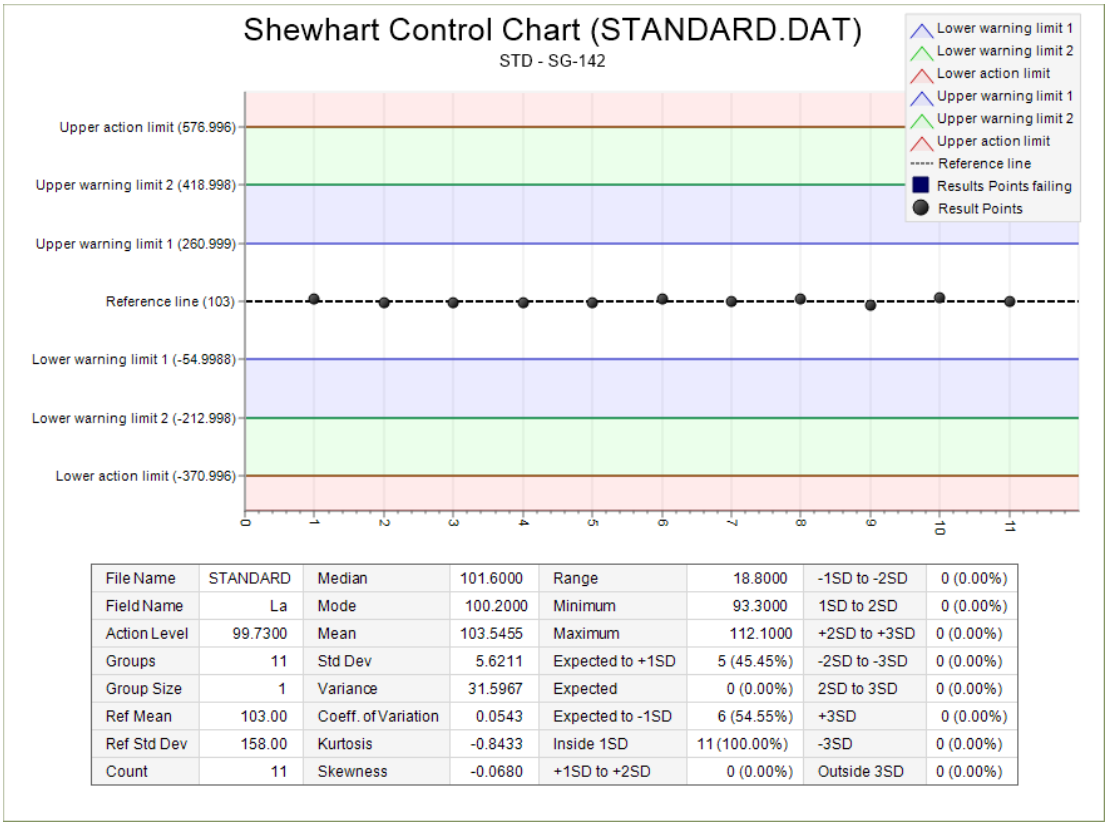

| File Name | STANDARD | Median | 1390.6000 | Range | 731.4000 | -1SD to -2SD | 2 (18.18%) |
| --- | --- | --- | --- | --- | --- | --- | --- |
| Field Name | La | Mode | 1140.2400 | Minimum | 1139.4000 | 1SD to 2SD | 3 (27.27%) |
| Action Level | 99.7300 | Mean | 1383.1182 | Maximum | 1870.8000 | +2SD to +3SD | 0 (0.00%) |
| Groups | 11 | Std Dev | 187.8388 | Expected to +1SD | 4 (36.36%) | -2SD to -3SD | 0 (0.00%) |
| Group Size | 1 | Variance | 35283.4196 | Expected | 0 (0.00%) | 2SD to 3SD | 0 (0.00%) |
| Ref Mean | 1369.00 | Coeff. of Variation | 0.1358 | Expected to -1SD | 2 (18.18%) | +3SD | 1 (9.09%) |
| Ref Std Dev | 75.00 | Kurtosis | 2.3926 | Inside 1SD | 6 (54.55%) | -3SD | 1 (9.09%) |
| Count | 11 | Skewness | 1.5177 | +1SD to +2SD | 1 (9.09%) | Outside 3SD | 2 (18.18%) |

**Appendix III - Figure 1 – Standard OREAS 460, element La, Nau de Guerra Target.**



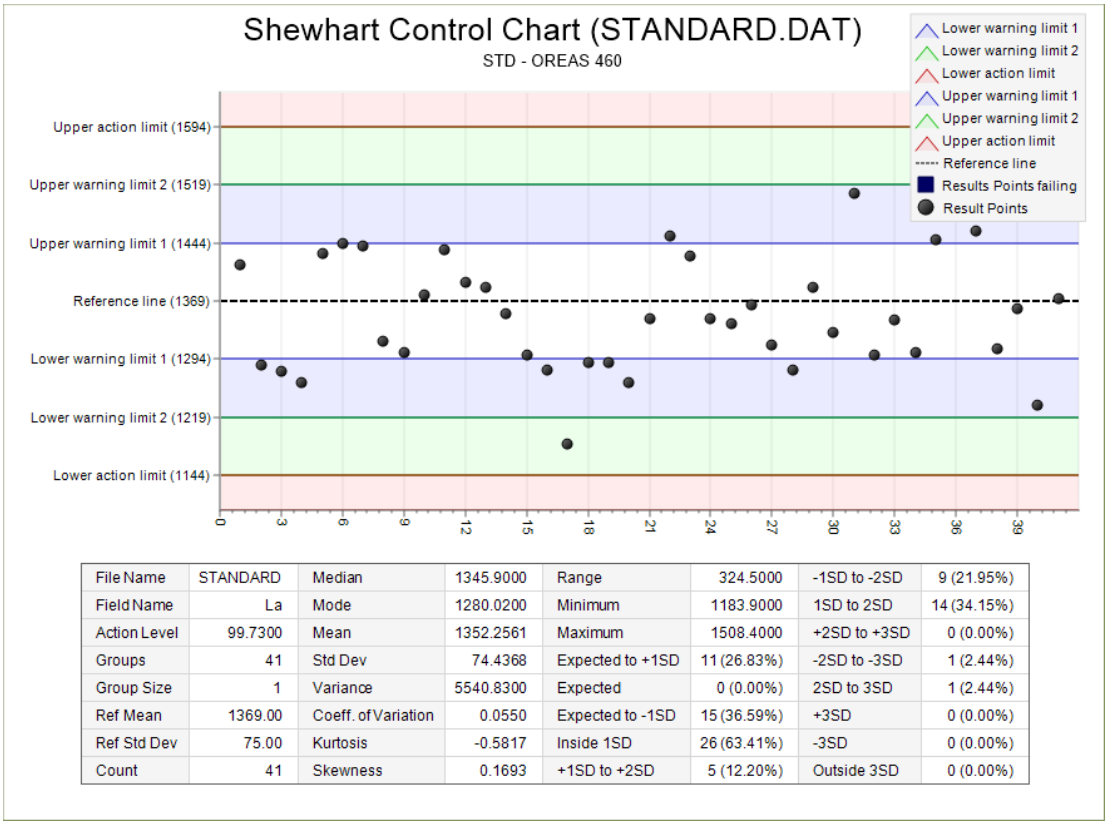

| File Name | STANDARD | Median | 2614.4000 | Range | 413.8000 | -1SD to -2SD | 2 (20.00%) |
| --- | --- | --- | --- | --- | --- | --- | --- |
| Field Name | La | Mode | 2595.6960 | Minimum | 2432.7000 | 1SD to 2SD | 2 (20.00%) |
| Action Level | 99.7300 | Mean | 2617.8700 | Maximum | 2846.5000 | +2SD to +3SD | 0 (0.00%) |
| Groups | 10 | Std Dev | 118.4534 | Expected to +1SD | 2 (20.00%) | -2SD to -3SD | 0 (0.00%) |
| Group Size | 1 | Variance | 14031.2090 | Expected | 0 (0.00%) | 2SD to 3SD | 0 (0.00%) |
| Ref Mean | 2690.00 | Coeff. of Variation | 0.0452 | Expected to -1SD | 6 (60.00%) | +3SD | 0 (0.00%) |
| Ref Std Dev | 158.00 | Kurtosis | -0.1986 | Inside 1SD | 8 (80.00%) | -3SD | 0 (0.00%) |
| Count | 10 | Skewness | 0.2817 | +1SD to +2SD | 0 (0.00%) | Outside 3SD | 0 (0.00%) |

**Appendix III - Figure 2 – Standard OREAS 461, element La, Nau de Guerra Target.**



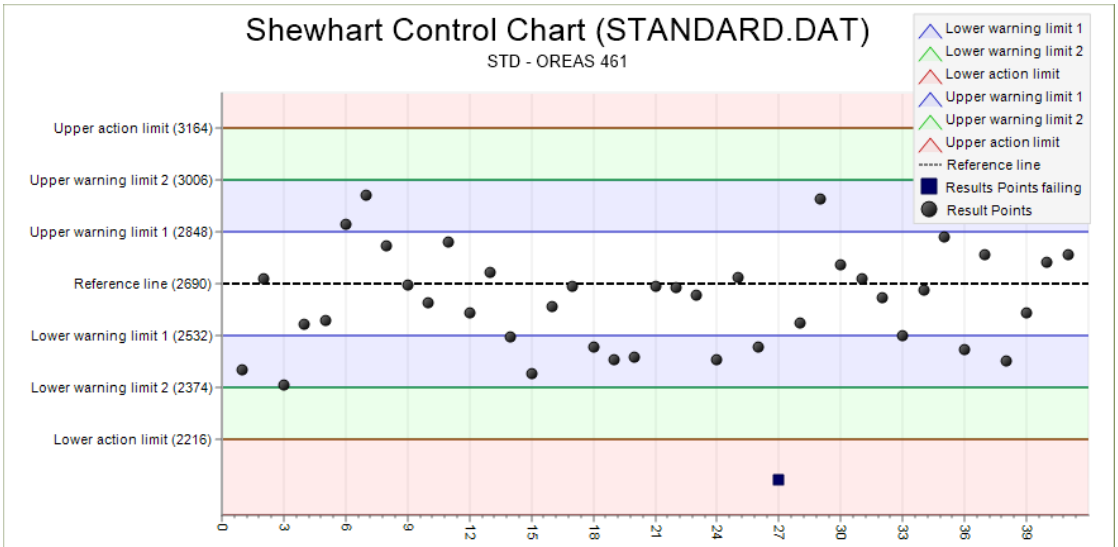

| File Name | STANDARD | Median | 101.6000 | Range | 18.8000 | -1SD to -2SD | 0 (0.00%) |
| --- | --- | --- | --- | --- | --- | --- | --- |
| Field Name | La | Mode | 100.2000 | Minimum | 93.3000 | 1SD to 2SD | 0 (0.00%) |
| Action Level | 99.7300 | Mean | 103.5455 | Maximum | 112.1000 | +2SD to +3SD | 0 (0.00%) |
| Groups | 11 | Std Dev | 5.6211 | Expected to +1SD | 5 (45.45%) | -2SD to -3SD | 0 (0.00%) |
| Group Size | 1 | Variance | 31.5967 | Expected | 0 (0.00%) | 2SD to 3SD | 0 (0.00%) |
| Ref Mean | 103.00 | Coeff. of Variation | 0.0543 | Expected to -1SD | 6 (54.55%) | +3SD | 0 (0.00%) |
| Ref Std Dev | 158.00 | Kurtosis | -0.8433 | Inside 1SD | 11 (100.00%) | -3SD | 0 (0.00%) |
| Count | 11 | Skewness | -0.0680 | +1SD to +2SD | 0 (0.00%) | Outside 3SD | 0 (0.00%) |

**Appendix III - Figure 3 – Standard SG-142, element La, Nau de Guerra Target.**



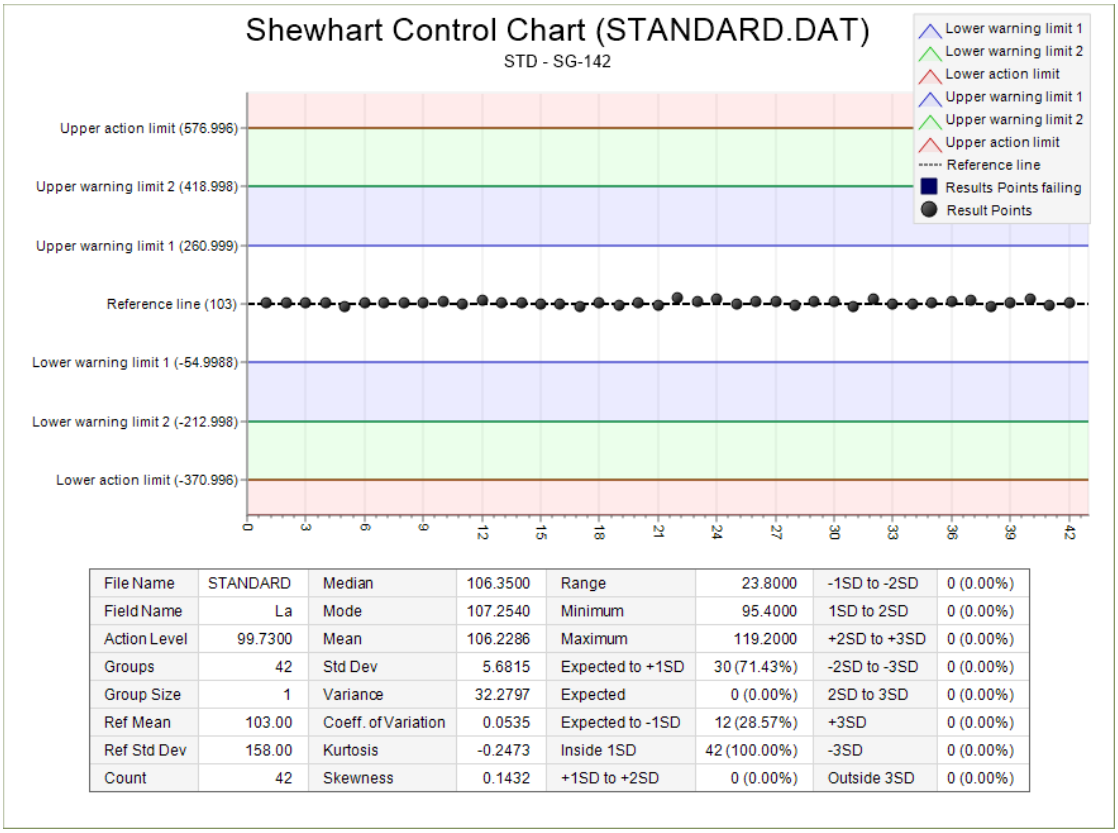

| File Name | STANDARD | Median | 1345.9000 | Range | 324.5000 | -1SD to -2SD | 9 (21.95%) |
| --- | --- | --- | --- | --- | --- | --- | --- |
| Field Name | La | Mode | 1280.0200 | Minimum | 1183.9000 | 1SD to 2SD | 14 (34.15%) |
| Action Level | 99.7300 | Mean | 1352.2561 | Maximum | 1508.4000 | +2SD to +3SD | 0 (0.00%) |
| Groups | 41 | Std Dev | 74.4368 | Expected to +1SD | 11 (26.83%) | -2SD to -3SD | 1 (2.44%) |
| Group Size | 1 | Variance | 5540.8300 | Expected | 0 (0.00%) | 2SD to 3SD | 1 (2.44%) |
| Ref Mean | 1369.00 | Coeff. of Variation | 0.0550 | Expected to -1SD | 15 (36.59%) | +3SD | 0 (0.00%) |
| Ref Std Dev | 75.00 | Kurtosis | -0.5817 | Inside 1SD | 26 (63.41%) | -3SD | 0 (0.00%) |
| Count | 41 | Skewness | 0.1693 | +1SD to +2SD | 5 (12.20%) | Outside 3SD | 0 (0.00%) |

**Appendix III - Figure 4 – Standard OREAS 460, element La, Balsamo e Alto da Serra Target.**



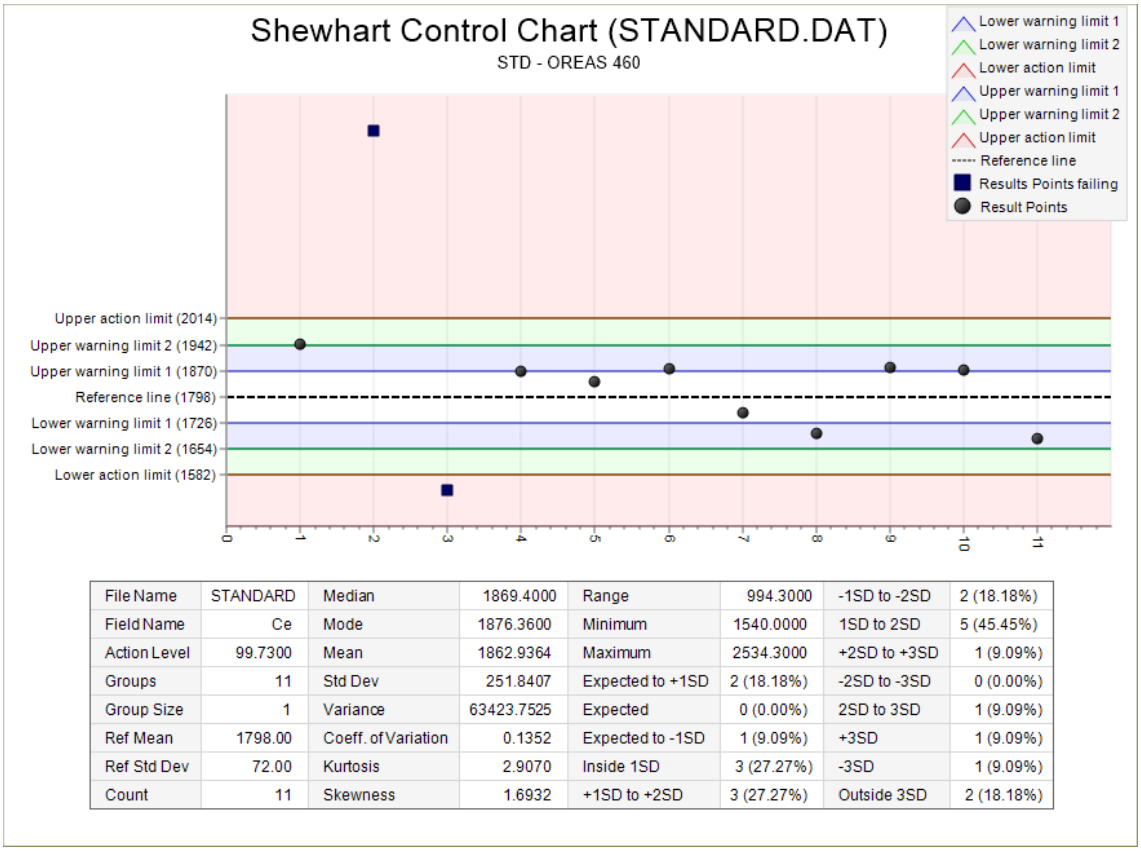

| | | | | | | | |
|---|---|---|---|---|---|---|---|
| File Name | STANDARD | Median | 2648.7000 | Range | 867.5000 | -1SD to -2SD | 12 (29.27%) |
| Field Name | La | Mode | 2457.1800 | Minimum | 2091.0000 | 1SD to 2SD | 15 (36.59%) |
| Action Level | 99.7300 | Mean | 2626.4293 | Maximum | 2958.5000 | +2SD to +3SD | 0 (0.00%) |
| Groups | 41 | Std Dev | 167.9898 | Expected to +1SD | 11 (26.83%) | -2SD to -3SD | 0 (0.00%) |
| Group Size | 1 | Variance | 28220.5636 | Expected | 0 (0.00%) | 2SD to 3SD | 0 (0.00%) |
| Ref Mean | 2690.00 | Coeff. of Variation | 0.0640 | Expected to -1SD | 14 (34.15%) | +3SD | 0 (0.00%) |
| Ref Std Dev | 158.00 | Kurtosis | 1.0441 | Inside 1SD | 25 (60.98%) | -3SD | 1 (2.44%) |
| Count | 41 | Skewness | -0.5050 | +1SD to +2SD | 3 (7.32%) | Outside 3SD | 1 (2.44%) |

**Appendix III - Figure 5 – Standard OREAS 461, element La, Balsamo e Alto da Serra Target.**



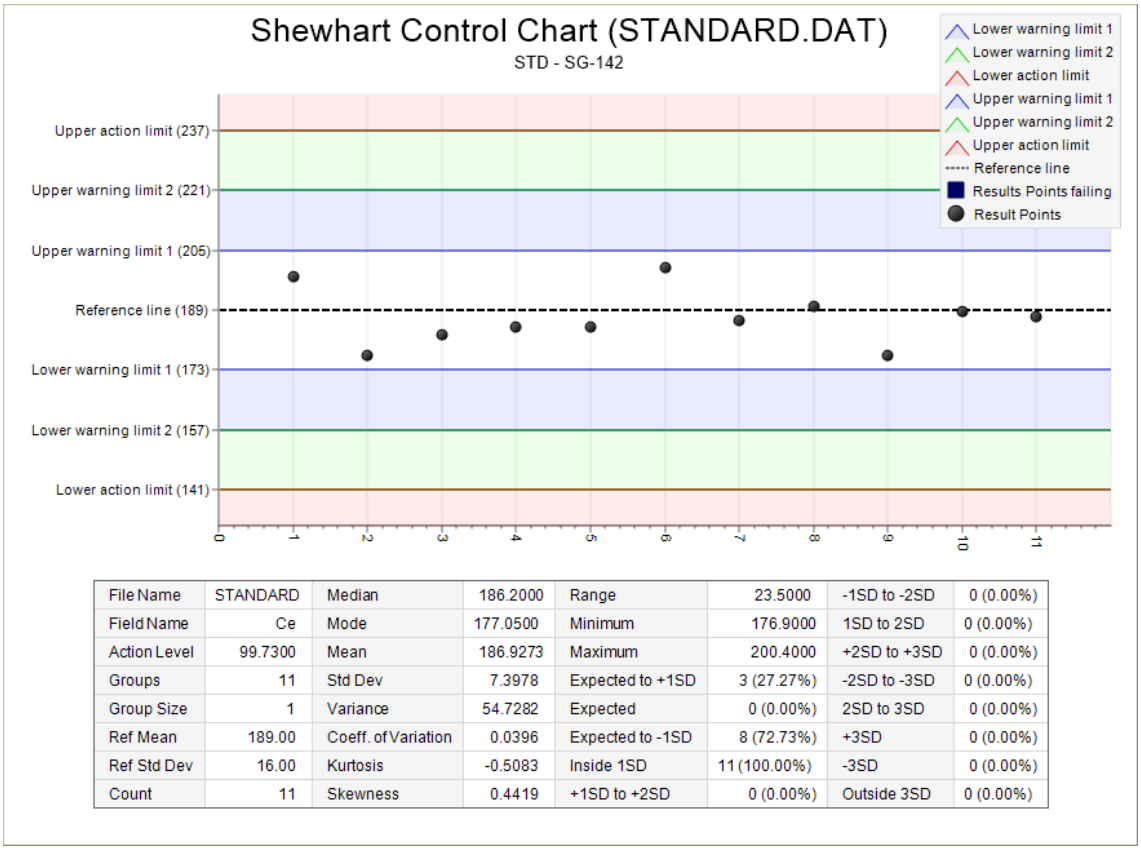

| | | | | | | | |
|---|---|---|---|---|---|---|---|
| File Name | STANDARD | Median | 106.3500 | Range | 23.8000 | -1SD to -2SD | 0 (0.00%) |
| Field Name | La | Mode | 107.2540 | Minimum | 95.4000 | 1SD to 2SD | 0 (0.00%) |
| Action Level | 99.7300 | Mean | 106.2286 | Maximum | 119.2000 | +2SD to +3SD | 0 (0.00%) |
| Groups | 42 | Std Dev | 5.6815 | Expected to +1SD | 30 (71.43%) | -2SD to -3SD | 0 (0.00%) |
| Group Size | 1 | Variance | 32.2797 | Expected | 0 (0.00%) | 2SD to 3SD | 0 (0.00%) |
| Ref Mean | 103.00 | Coeff. of Variation | 0.0535 | Expected to -1SD | 12 (28.57%) | +3SD | 0 (0.00%) |
| Ref Std Dev | 158.00 | Kurtosis | -0.2473 | Inside 1SD | 42 (100.00%) | -3SD | 0 (0.00%) |
| Count | 42 | Skewness | 0.1432 | +1SD to +2SD | 0 (0.00%) | Outside 3SD | 0 (0.00%) |

**Appendix III - Figure 6 – Standard SG-142, element La, Balsamo e Alto da Serra Target.**



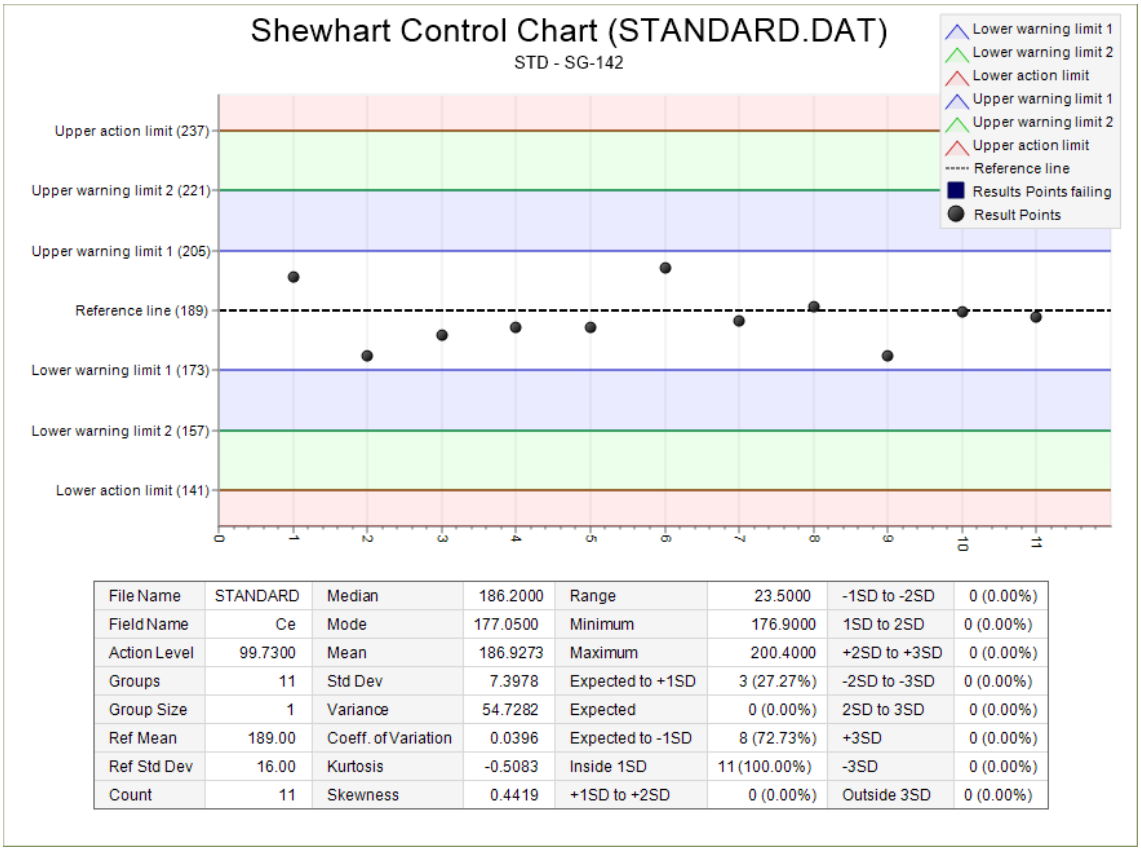

| File Name | STANDARD | Median | 1869.4000 | Range | 994.3000 | -1SD to -2SD | 2 (18.18%) |
| --- | --- | --- | --- | --- | --- | --- | --- |
| Field Name | Ce | Mode | 1876.3600 | Minimum | 1540.0000 | 1SD to 2SD | 5 (45.45%) |
| Action Level | 99.7300 | Mean | 1862.9364 | Maximum | 2534.3000 | +2SD to +3SD | 1 (9.09%) |
| Groups | 11 | Std Dev | 251.8407 | Expected to +1SD | 2 (18.18%) | -2SD to -3SD | 0 (0.00%) |
| Group Size | 1 | Variance | 63423.7525 | Expected | 0 (0.00%) | 2SD to 3SD | 1 (9.09%) |
| Ref Mean | 1798.00 | Coeff. of Variation | 0.1352 | Expected to -1SD | 1 (9.09%) | +3SD | 1 (9.09%) |
| Ref Std Dev | 72.00 | Kurtosis | 2.9070 | Inside 1SD | 3 (27.27%) | -3SD | 1 (9.09%) |
| Count | 11 | Skewness | 1.6932 | +1SD to +2SD | 3 (27.27%) | Outside 3SD | 2 (18.18%) |

**Appendix III - Figure 7 – Standard OREAS 460, element Ce, Nau de Guerra Target.**



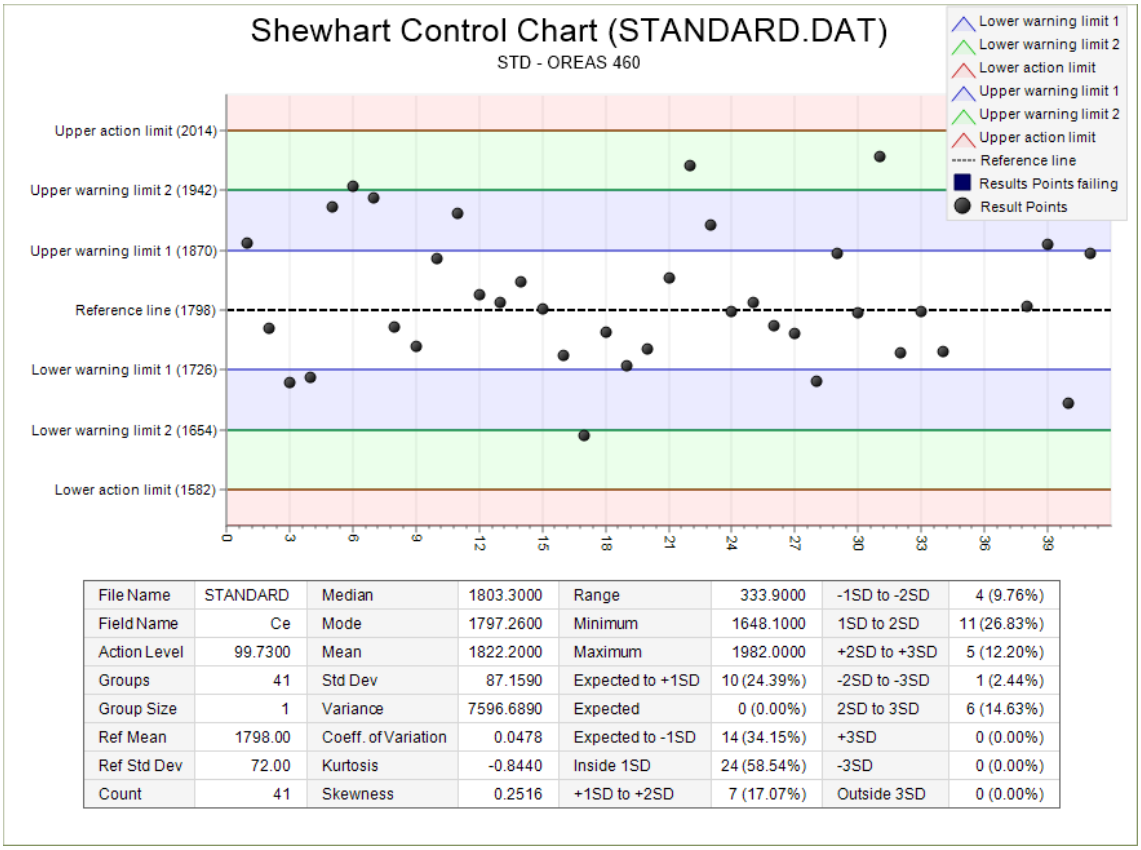

| File Name | STANDARD | Median | 186.2000 | Range | 23.5000 | -1SD to -2SD | 0 (0.00%) |
| --- | --- | --- | --- | --- | --- | --- | --- |
| Field Name | Ce | Mode | 177.0500 | Minimum | 176.9000 | 1SD to 2SD | 0 (0.00%) |
| Action Level | 99.7300 | Mean | 186.9273 | Maximum | 200.4000 | +2SD to +3SD | 0 (0.00%) |
| Groups | 11 | Std Dev | 7.3978 | Expected to +1SD | 3 (27.27%) | -2SD to -3SD | 0 (0.00%) |
| Group Size | 1 | Variance | 54.7282 | Expected | 0 (0.00%) | 2SD to 3SD | 0 (0.00%) |
| Ref Mean | 189.00 | Coeff. of Variation | 0.0396 | Expected to -1SD | 8 (72.73%) | +3SD | 0 (0.00%) |
| Ref Std Dev | 16.00 | Kurtosis | -0.5083 | Inside 1SD | 11 (100.00%) | -3SD | 0 (0.00%) |
| Count | 11 | Skewness | 0.4419 | +1SD to +2SD | 0 (0.00%) | Outside 3SD | 0 (0.00%) |

**Appendix III - Figure 8 – Standard OREAS 461, element Ce, Nau de Guerra Target.**



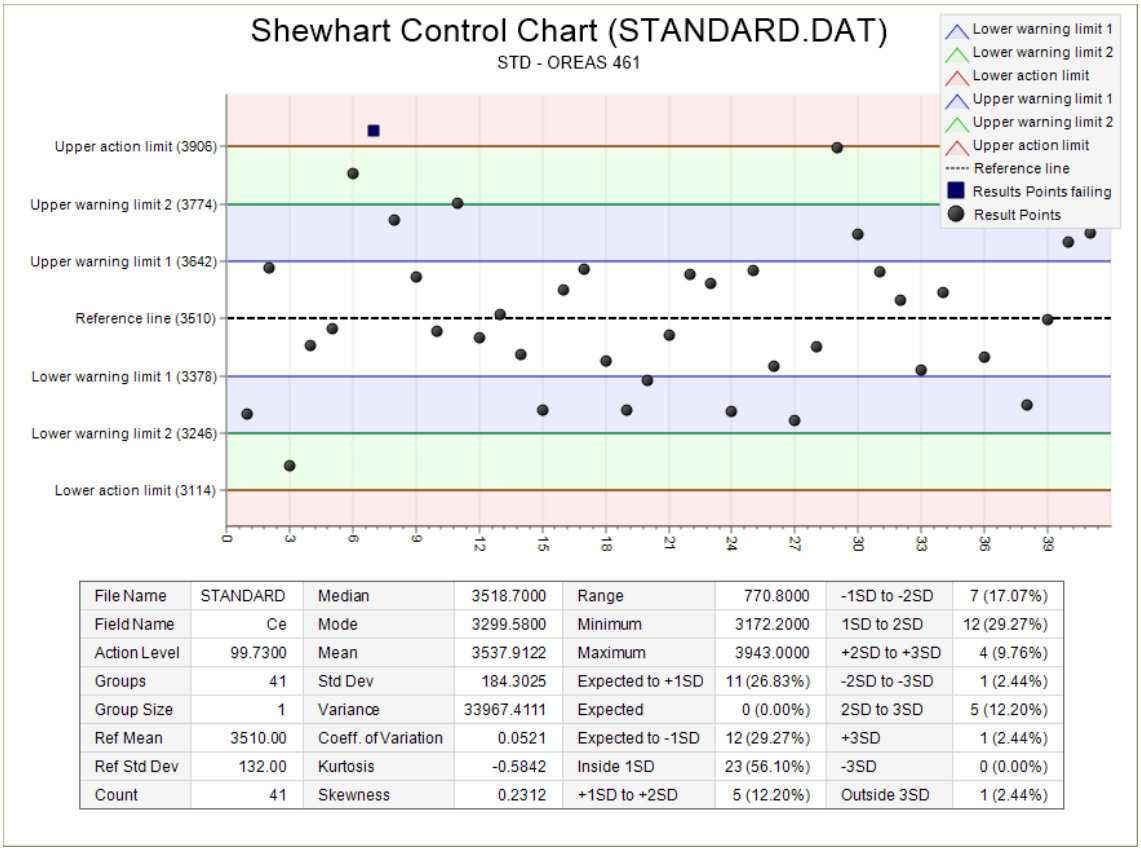

| File Name | STANDARD | Median | 186.2000 | Range | 23.5000 | -1SD to -2SD | 0 (0.00%) |
| --- | --- | --- | --- | --- | --- | --- | --- |
| Field Name | Ce | Mode | 177.0500 | Minimum | 176.9000 | 1SD to 2SD | 0 (0.00%) |
| Action Level | 99.7300 | Mean | 186.9273 | Maximum | 200.4000 | +2SD to +3SD | 0 (0.00%) |
| Groups | 11 | Std Dev | 7.3978 | Expected to +1SD | 3 (27.27%) | -2SD to -3SD | 0 (0.00%) |
| Group Size | 1 | Variance | 54.7282 | Expected | 0 (0.00%) | 2SD to 3SD | 0 (0.00%) |
| Ref Mean | 189.00 | Coeff. of Variation | 0.0396 | Expected to -1SD | 8 (72.73%) | +3SD | 0 (0.00%) |
| Ref Std Dev | 16.00 | Kurtosis | -0.5083 | Inside 1SD | 11 (100.00%) | -3SD | 0 (0.00%) |
| Count | 11 | Skewness | 0.4419 | +1SD to +2SD | 0 (0.00%) | Outside 3SD | 0 (0.00%) |

**Appendix III - Figure 9 – Standard SG-142, element Ce, Nau de Guerra Target.**



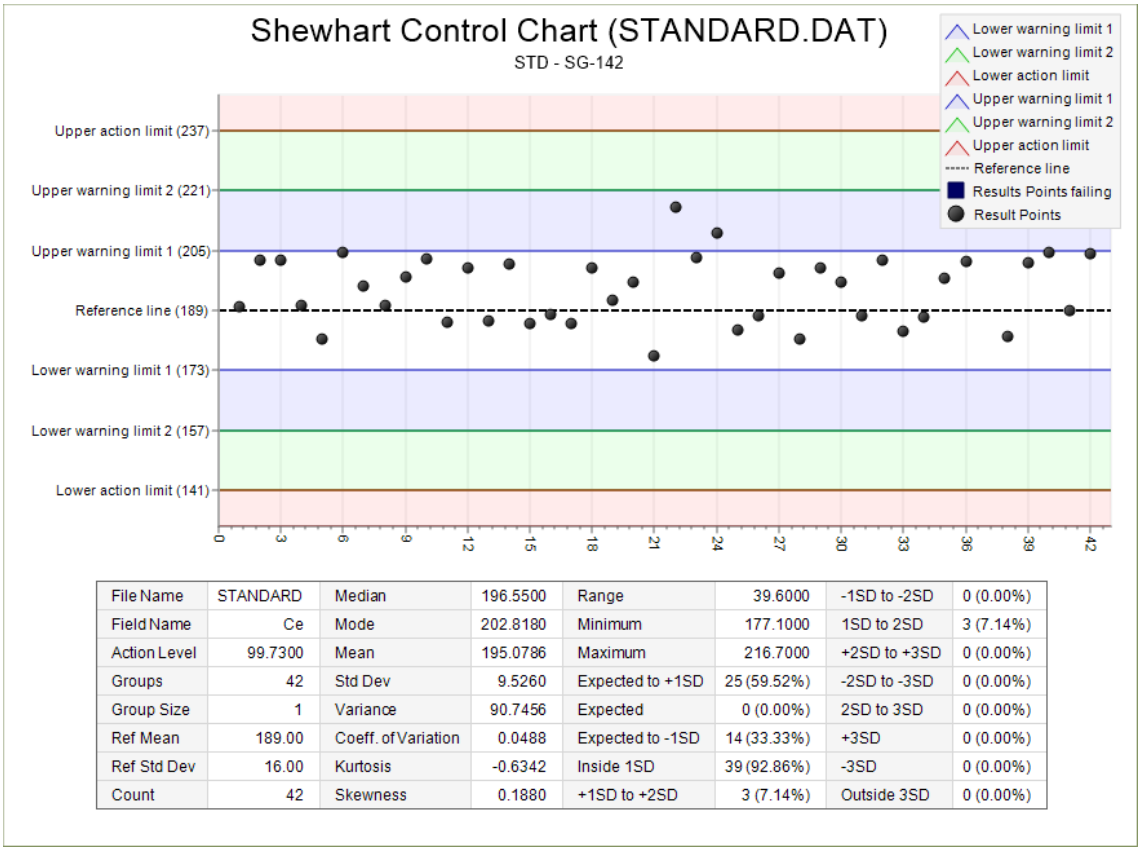

| File Name | STANDARD | Median | 1803.3000 | Range | 333.9000 | -1SD to -2SD | 4 (9.76%) |
| --- | --- | --- | --- | --- | --- | --- | --- |
| Field Name | Ce | Mode | 1797.2600 | Minimum | 1648.1000 | 1SD to 2SD | 11 (26.83%) |
| Action Level | 99.7300 | Mean | 1822.2000 | Maximum | 1982.0000 | +2SD to +3SD | 5 (12.20%) |
| Groups | 41 | Std Dev | 87.1590 | Expected to +1SD | 10 (24.39%) | -2SD to -3SD | 1 (2.44%) |
| Group Size | 1 | Variance | 7596.6890 | Expected | 0 (0.00%) | 2SD to 3SD | 6 (14.63%) |
| Ref Mean | 1798.00 | Coeff. of Variation | 0.0478 | Expected to -1SD | 14 (34.15%) | +3SD | 0 (0.00%) |
| Ref Std Dev | 72.00 | Kurtosis | -0.8440 | Inside 1SD | 24 (58.54%) | -3SD | 0 (0.00%) |
| Count | 41 | Skewness | 0.2516 | +1SD to +2SD | 7 (17.07%) | Outside 3SD | 0 (0.00%) |

**Appendix III - Figure 10 – Standard OREAS 460, element Ce, Balsamo e Alto da Serra Target.**



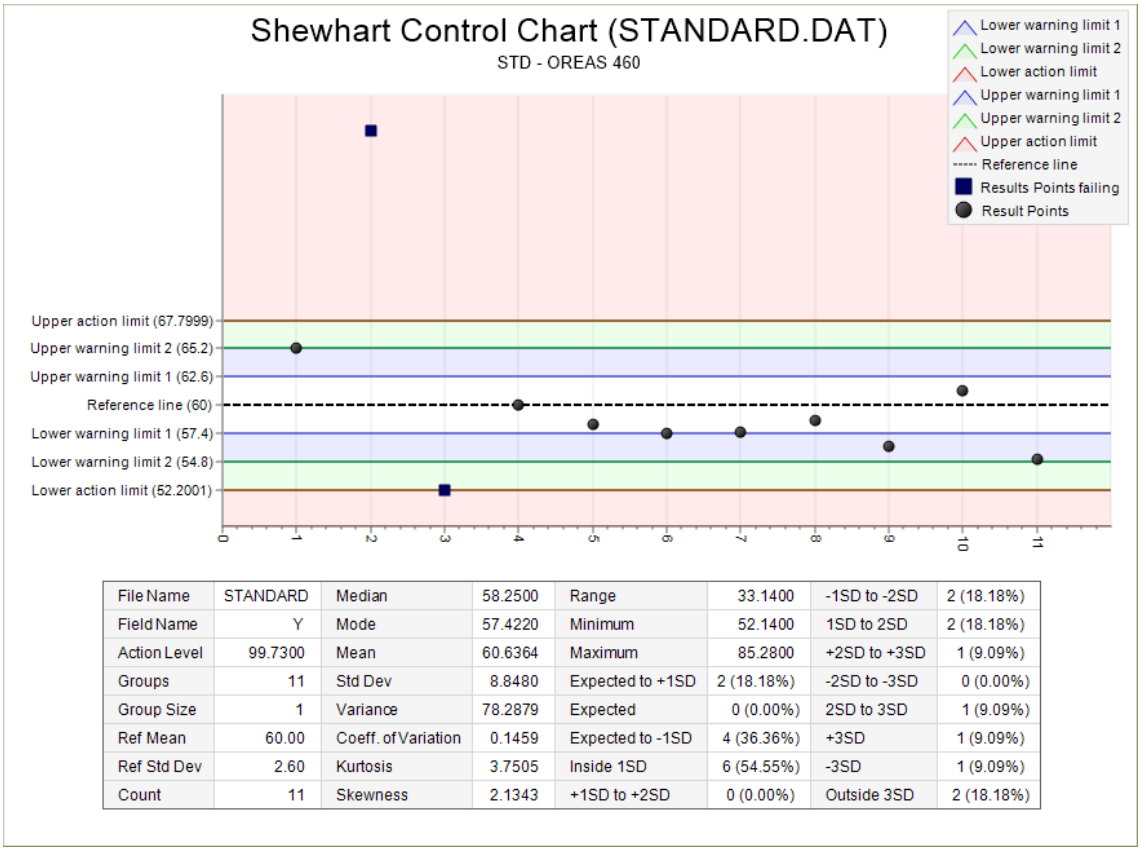

| File Name | STANDARD | Median | 3518.7000 | Range | 770.8000 | -1SD to -2SD | 7 (17.07%) |
|---|---|---|---|---|---|---|---|
| Field Name | Ce | Mode | 3299.5800 | Minimum | 3172.2000 | 1SD to 2SD | 12 (29.27%) |
| Action Level | 99.7300 | Mean | 3537.9122 | Maximum | 3943.0000 | +2SD to +3SD | 4 (9.76%) |
| Groups | 41 | Std Dev | 184.3025 | Expected to +1SD | 11 (26.83%) | -2SD to -3SD | 1 (2.44%) |
| Group Size | 1 | Variance | 33967.4111 | Expected | 0 (0.00%) | 2SD to 3SD | 5 (12.20%) |
| Ref Mean | 3510.00 | Coeff. of Variation | 0.0521 | Expected to -1SD | 12 (29.27%) | +3SD | 1 (2.44%) |
| Ref Std Dev | 132.00 | Kurtosis | -0.5842 | Inside 1SD | 23 (56.10%) | -3SD | 0 (0.00%) |
| Count | 41 | Skewness | 0.2312 | +1SD to +2SD | 5 (12.20%) | Outside 3SD | 1 (2.44%) |

**Appendix III - Figure 11 – Standard OREAS 461, element Ce, Balsamo e Alto da Serra Target.**



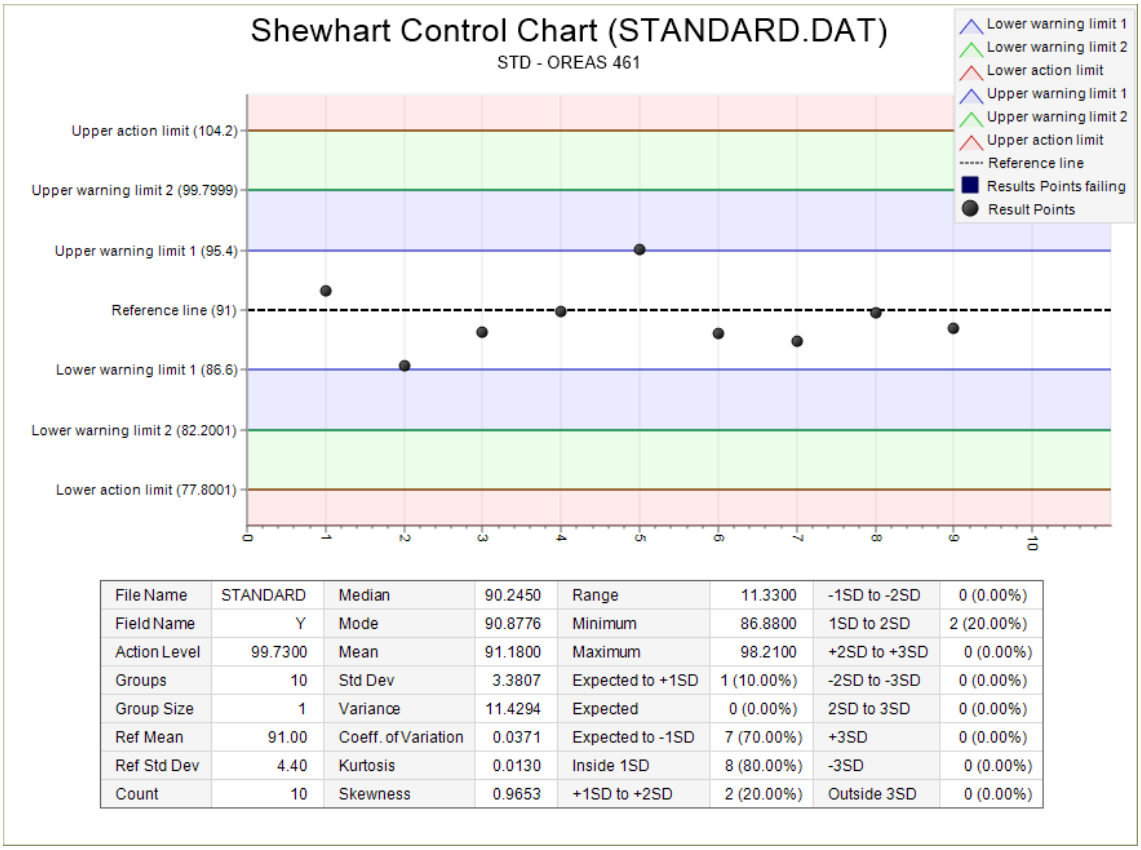

| File Name | STANDARD | Median | 196.5500 | Range | 39.6000 | -1SD to -2SD | 0 (0.00%) |
|---|---|---|---|---|---|---|---|
| Field Name | Ce | Mode | 202.8180 | Minimum | 177.1000 | 1SD to 2SD | 3 (7.14%) |
| Action Level | 99.7300 | Mean | 195.0786 | Maximum | 216.7000 | +2SD to +3SD | 0 (0.00%) |
| Groups | 42 | Std Dev | 9.5260 | Expected to +1SD | 25 (59.52%) | -2SD to -3SD | 0 (0.00%) |
| Group Size | 1 | Variance | 90.7456 | Expected | 0 (0.00%) | 2SD to 3SD | 0 (0.00%) |
| Ref Mean | 189.00 | Coeff. of Variation | 0.0488 | Expected to -1SD | 14 (33.33%) | +3SD | 0 (0.00%) |
| Ref Std Dev | 16.00 | Kurtosis | -0.6342 | Inside 1SD | 39 (92.86%) | -3SD | 0 (0.00%) |
| Count | 42 | Skewness | 0.1880 | +1SD to +2SD | 3 (7.14%) | Outside 3SD | 0 (0.00%) |

**Appendix III - Figure 12 – Standard SG-142, element Ce, Balsamo e Alto da Serra Target.**



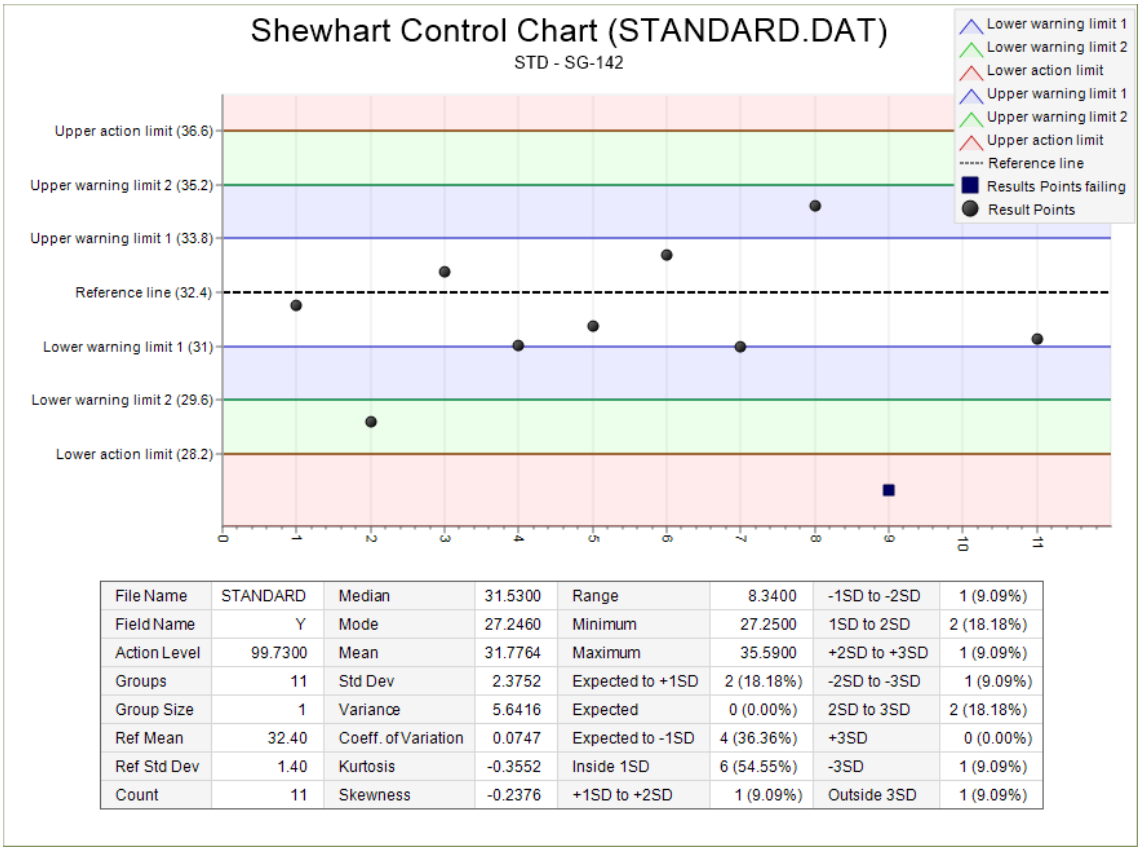

| File Name | STANDARD | Median | 58.2500 | Range | 33.1400 | -1SD to -2SD | 2 (18.18%) |
| --- | --- | --- | --- | --- | --- | --- | --- |
| Field Name | Y | Mode | 57.4220 | Minimum | 52.1400 | 1SD to 2SD | 2 (18.18%) |
| Action Level | 99.7300 | Mean | 60.6364 | Maximum | 85.2800 | +2SD to +3SD | 1 (9.09%) |
| Groups | 11 | Std Dev | 8.8480 | Expected to +1SD | 2 (18.18%) | -2SD to -3SD | 0 (0.00%) |
| Group Size | 1 | Variance | 78.2879 | Expected | 0 (0.00%) | 2SD to 3SD | 1 (9.09%) |
| Ref Mean | 60.00 | Coeff. of Variation | 0.1459 | Expected to -1SD | 4 (36.36%) | +3SD | 1 (9.09%) |
| Ref Std Dev | 2.60 | Kurtosis | 3.7505 | Inside 1SD | 6 (54.55%) | -3SD | 1 (9.09%) |
| Count | 11 | Skewness | 2.1343 | +1SD to +2SD | 0 (0.00%) | Outside 3SD | 2 (18.18%) |

**Appendix III - Figure 13 – Standard OREAS 460, element Y, Nau de Guerra Target.**



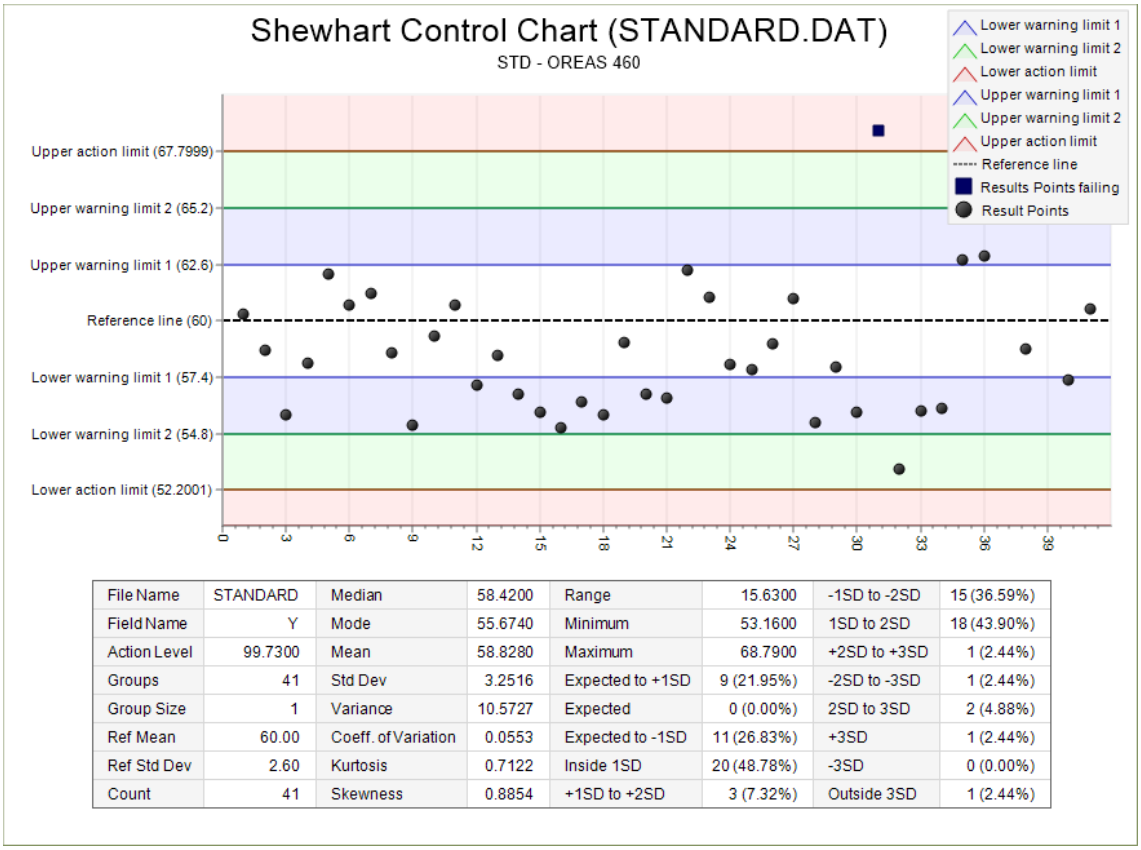

| File Name | STANDARD | Median | 90.2450 | Range | 11.3300 | -1SD to -2SD | 0 (0.00%) |
| --- | --- | --- | --- | --- | --- | --- | --- |
| Field Name | Y | Mode | 90.8776 | Minimum | 86.8800 | 1SD to 2SD | 2 (20.00%) |
| Action Level | 99.7300 | Mean | 91.1800 | Maximum | 98.2100 | +2SD to +3SD | 0 (0.00%) |
| Groups | 10 | Std Dev | 3.3807 | Expected to +1SD | 1 (10.00%) | -2SD to -3SD | 0 (0.00%) |
| Group Size | 1 | Variance | 11.4294 | Expected | 0 (0.00%) | 2SD to 3SD | 0 (0.00%) |
| Ref Mean | 91.00 | Coeff. of Variation | 0.0371 | Expected to -1SD | 7 (70.00%) | +3SD | 0 (0.00%) |
| Ref Std Dev | 4.40 | Kurtosis | 0.0130 | Inside 1SD | 8 (80.00%) | -3SD | 0 (0.00%) |
| Count | 10 | Skewness | 0.9653 | +1SD to +2SD | 2 (20.00%) | Outside 3SD | 0 (0.00%) |

**Appendix III - Figure 14 – Standard OREAS 461, element Y, Nau de Guerra Target.**



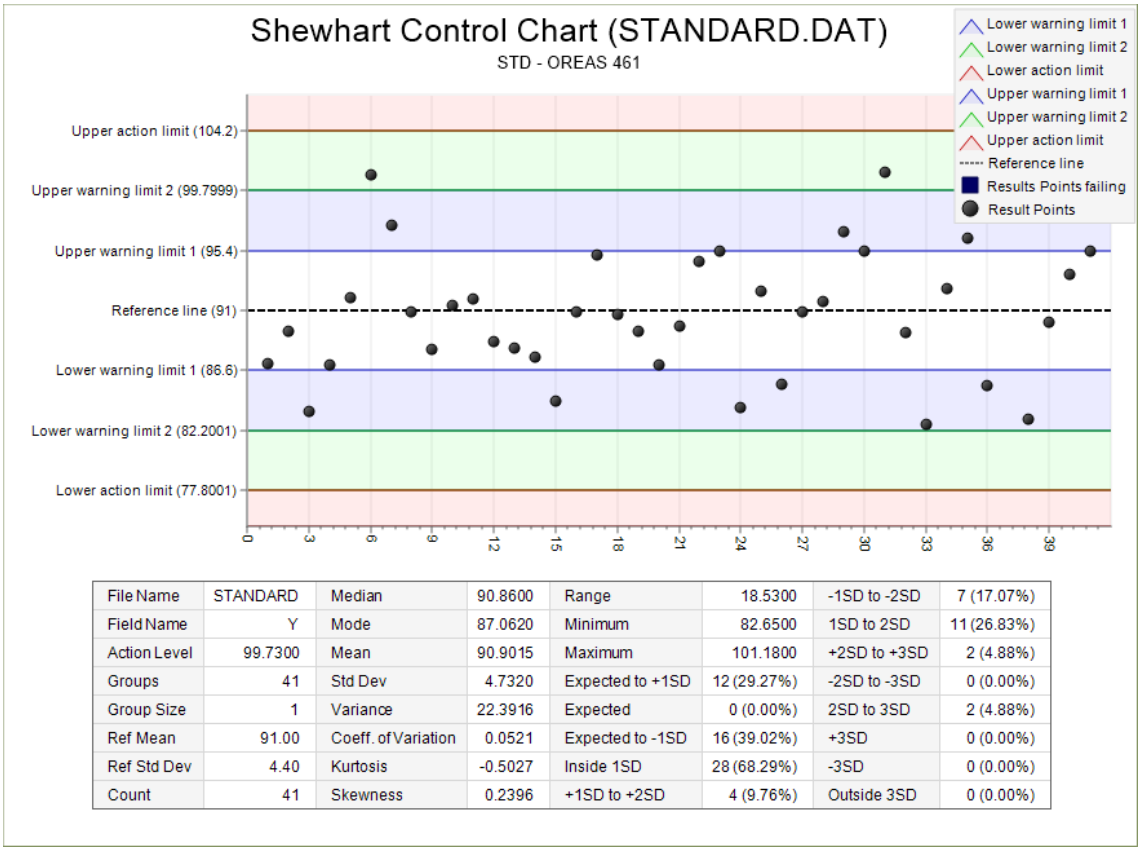

| File Name | STANDARD | Median | 31.5300 | Range | 8.3400 | -1SD to -2SD | 1 (9.09%) |
| --- | --- | --- | --- | --- | --- | --- | --- |
| Field Name | Y | Mode | 27.2460 | Minimum | 27.2500 | 1SD to 2SD | 2 (18.18%) |
| Action Level | 99.7300 | Mean | 31.7764 | Maximum | 35.5900 | +2SD to +3SD | 1 (9.09%) |
| Groups | 11 | Std Dev | 2.3752 | Expected to +1SD | 2 (18.18%) | -2SD to -3SD | 1 (9.09%) |
| Group Size | 1 | Variance | 5.6416 | Expected | 0 (0.00%) | 2SD to 3SD | 2 (18.18%) |
| Ref Mean | 32.40 | Coeff. of Variation | 0.0747 | Expected to -1SD | 4 (36.36%) | +3SD | 0 (0.00%) |
| Ref Std Dev | 1.40 | Kurtosis | -0.3552 | Inside 1SD | 6 (54.55%) | -3SD | 1 (9.09%) |
| Count | 11 | Skewness | -0.2376 | +1SD to +2SD | 1 (9.09%) | Outside 3SD | 1 (9.09%) |

**Appendix III - Figure 15 – Standard SG-142, element Yb, Nau de Guerra Target.**



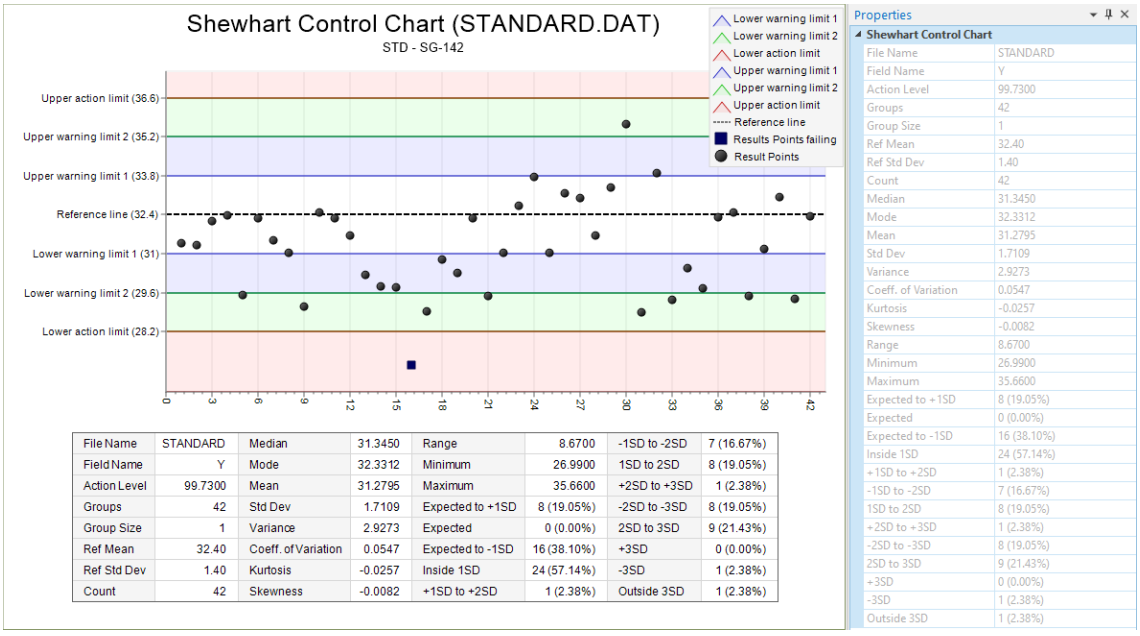

| File Name | STANDARD | Median | 58.4200 | Range | 15.6300 | -1SD to -2SD | 15 (36.59%) |
| --- | --- | --- | --- | --- | --- | --- | --- |
| Field Name | Y | Mode | 55.6740 | Minimum | 53.1600 | 1SD to 2SD | 18 (43.90%) |
| Action Level | 99.7300 | Mean | 58.8280 | Maximum | 68.7900 | +2SD to +3SD | 1 (2.44%) |
| Groups | 41 | Std Dev | 3.2516 | Expected to +1SD | 9 (21.95%) | -2SD to -3SD | 1 (2.44%) |
| Group Size | 1 | Variance | 10.5727 | Expected | 0 (0.00%) | 2SD to 3SD | 2 (4.88%) |
| Ref Mean | 60.00 | Coeff. of Variation | 0.0553 | Expected to -1SD | 11 (26.83%) | +3SD | 1 (2.44%) |
| Ref Std Dev | 2.60 | Kurtosis | 0.7122 | Inside 1SD | 20 (48.78%) | -3SD | 0 (0.00%) |
| Count | 41 | Skewness | 0.8854 | +1SD to +2SD | 3 (7.32%) | Outside 3SD | 1 (2.44%) |

**Appendix III - Figure 16 – Standard OREAS 460, element Y, Balsamo e Alto da Serra Target.**



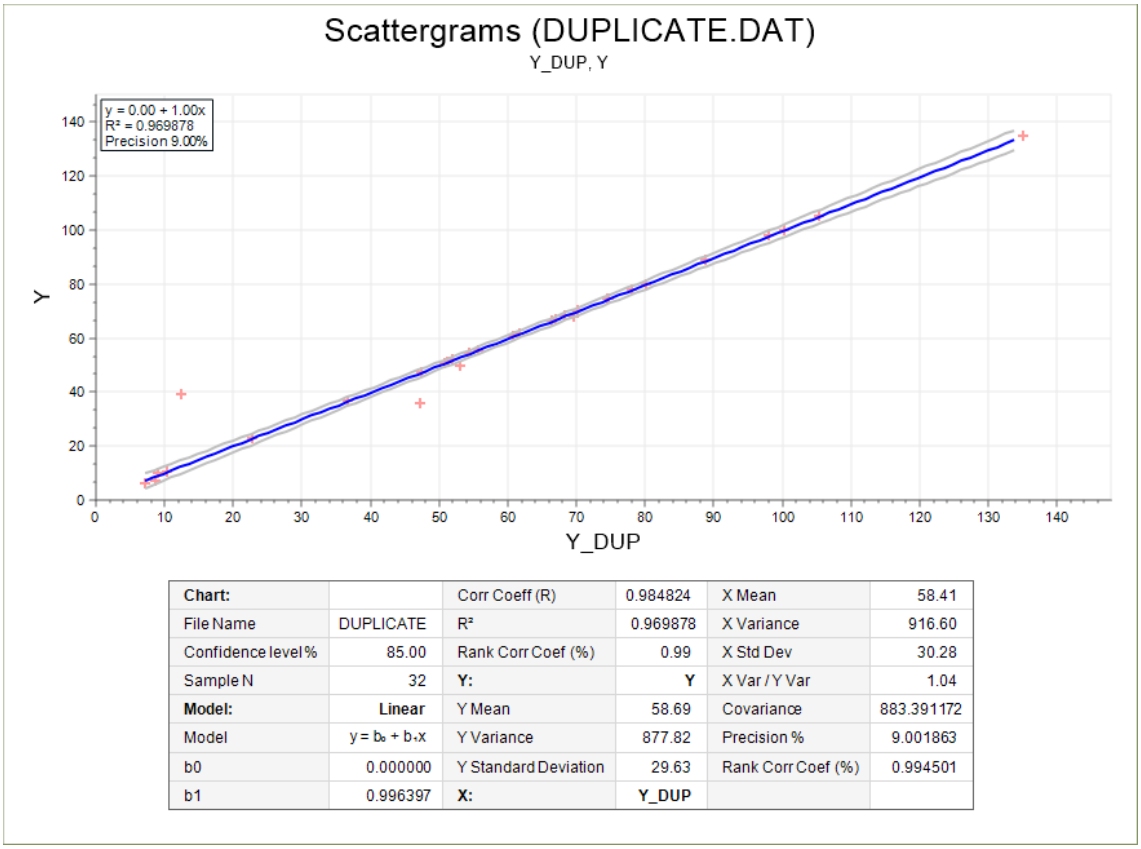

| File Name | STANDARD | Median | 90.8600 | Range | 18.5300 | -1SD to -2SD | 7 (17.07%) |
| --- | --- | --- | --- | --- | --- | --- | --- |
| Field Name | Y | Mode | 87.0620 | Minimum | 82.6500 | 1SD to 2SD | 11 (26.83%) |
| Action Level | 99.7300 | Mean | 90.9015 | Maximum | 101.1800 | +2SD to +3SD | 2 (4.88%) |
| Groups | 41 | Std Dev | 4.7320 | Expected to +1SD | 12 (29.27%) | -2SD to -3SD | 0 (0.00%) |
| Group Size | 1 | Variance | 22.3916 | Expected | 0 (0.00%) | 2SD to 3SD | 2 (4.88%) |
| Ref Mean | 91.00 | Coeff. of Variation | 0.0521 | Expected to -1SD | 16 (39.02%) | +3SD | 0 (0.00%) |
| Ref Std Dev | 4.40 | Kurtosis | -0.5027 | Inside 1SD | 28 (68.29%) | -3SD | 0 (0.00%) |
| Count | 41 | Skewness | 0.2396 | +1SD to +2SD | 4 (9.76%) | Outside 3SD | 0 (0.00%) |

**Appendix III - Figure 17 – Standard OREAS 461, element Y, Balsamo e Alto da Serra Target.**



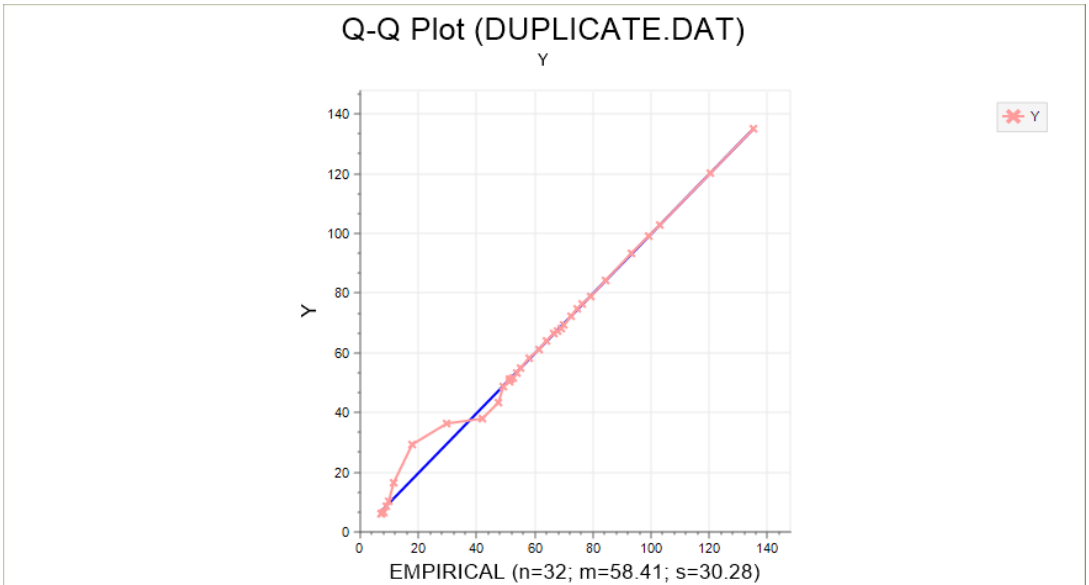

| File Name | STANDARD | Median | 31.3450 | Range | 8.6700 | -1SD to -2SD | 7 (16.67%) |
| --- | --- | --- | --- | --- | --- | --- | --- |
| Field Name | Y | Mode | 32.3312 | Minimum | 26.9900 | 1SD to 2SD | 8 (19.05%) |
| Action Level | 99.7300 | Mean | 31.2795 | Maximum | 35.6600 | +2SD to +3SD | 1 (2.38%) |
| Groups | 42 | Std Dev | 1.7109 | Expected to +1SD | 8 (19.05%) | -2SD to -3SD | 8 (19.05%) |
| Group Size | 1 | Variance | 2.9273 | Expected | 0 (0.00%) | 2SD to 3SD | 9 (21.43%) |
| Ref Mean | 32.40 | Coeff. of Variation | 0.0547 | Expected to -1SD | 16 (38.10%) | +3SD | 0 (0.00%) |
| Ref Std Dev | 1.40 | Kurtosis | -0.0257 | Inside 1SD | 24 (57.14%) | -3SD | 1 (2.38%) |
| Count | 42 | Skewness | -0.0082 | +1SD to +2SD | 1 (2.38%) | Outside 3SD | 1 (2.38%) |

**Appendix III - Figure 18 – Standard SG-142, element Yb, Balsamo e Alto da Serra Target.**



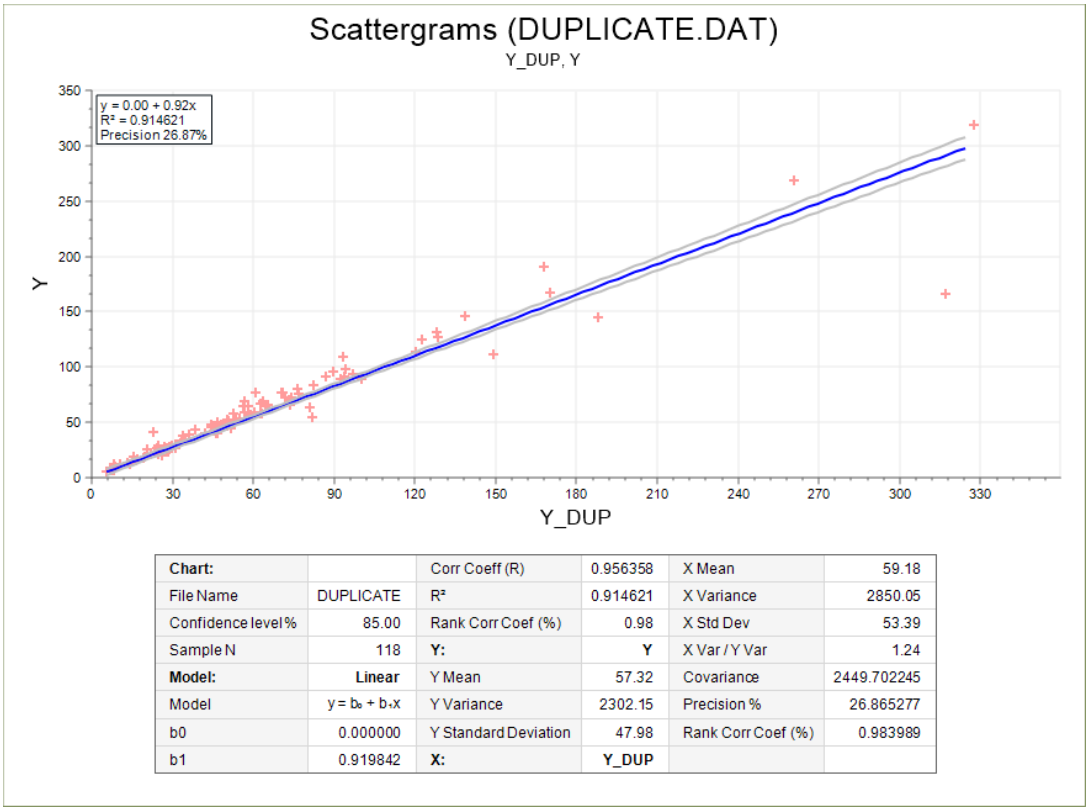

| Chart: | | Corr Coeff (R) | 0.984824 | X Mean | 58.41 |
| --- | --- | --- | --- | --- | --- |
| File Name | DUPLICATE | $R^2$ | 0.969878 | X Variance | 916.60 |
| Confidence level % | 85.00 | Rank Corr Coef (%) | 0.99 | X Std Dev | 30.28 |
| Sample N | 32 | **Y:** | **Y** | X Var / Y Var | 1.04 |
| **Model:** | **Linear** | Y Mean | 58.69 | Covariance | 883.391172 |
| Model | $y = b_0 + b_1x$ | Y Variance | 877.82 | Precision % | 9.001863 |
| b0 | 0.000000 | Y Standard Deviation | 29.63 | Rank Corr Coef (%) | 0.994501 |
| b1 | 0.996397 | **X:** | **Y_DUP** | | |

**Appendix III - Figure 19 – Linear Regression Diagram for Y ppm, field duplicate, class: Diamond Drilling, internal control results Nau de Guerra Target.**



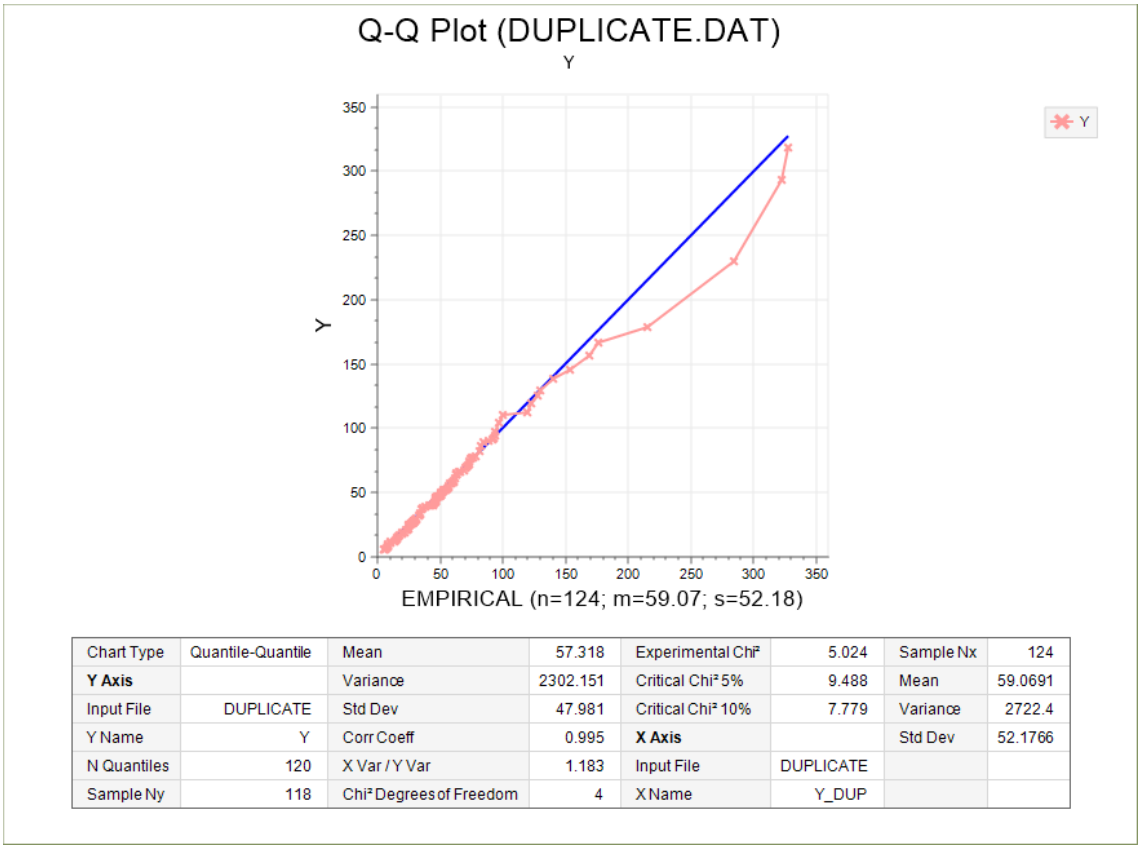

| Chart Type | Quantile-Quantile | Mean | 58.695 | Experimental Chi² | 0.200 | Sample Nx | 32 |
| --- | --- | --- | --- | --- | --- | --- | --- |
| **Y Axis** | | Variance | 877.824 | Critical Chi² 5% | nan | Mean | 58.4091 |
| Input File | DUPLICATE | Std Dev | 29.628 | Critical Chi² 10% | nan | Variance | 916.604 |
| Y Name | Y | Corr Coeff | 0.997 | **X Axis** | | Std Dev | 30.2755 |
| N Quantiles | 34 | X Var / Y Var | 1.044 | Input File | DUPLICATE | | |
| Sample Ny | 32 | Chi² Degrees of Freedom | 0 | X Name | Y_DUP | | |

**Appendix III - Figure 20 – Quantis plotting for Y ppm, field duplicate, class: Diamond Drilling, internal control results Nau de Guerra Target.**



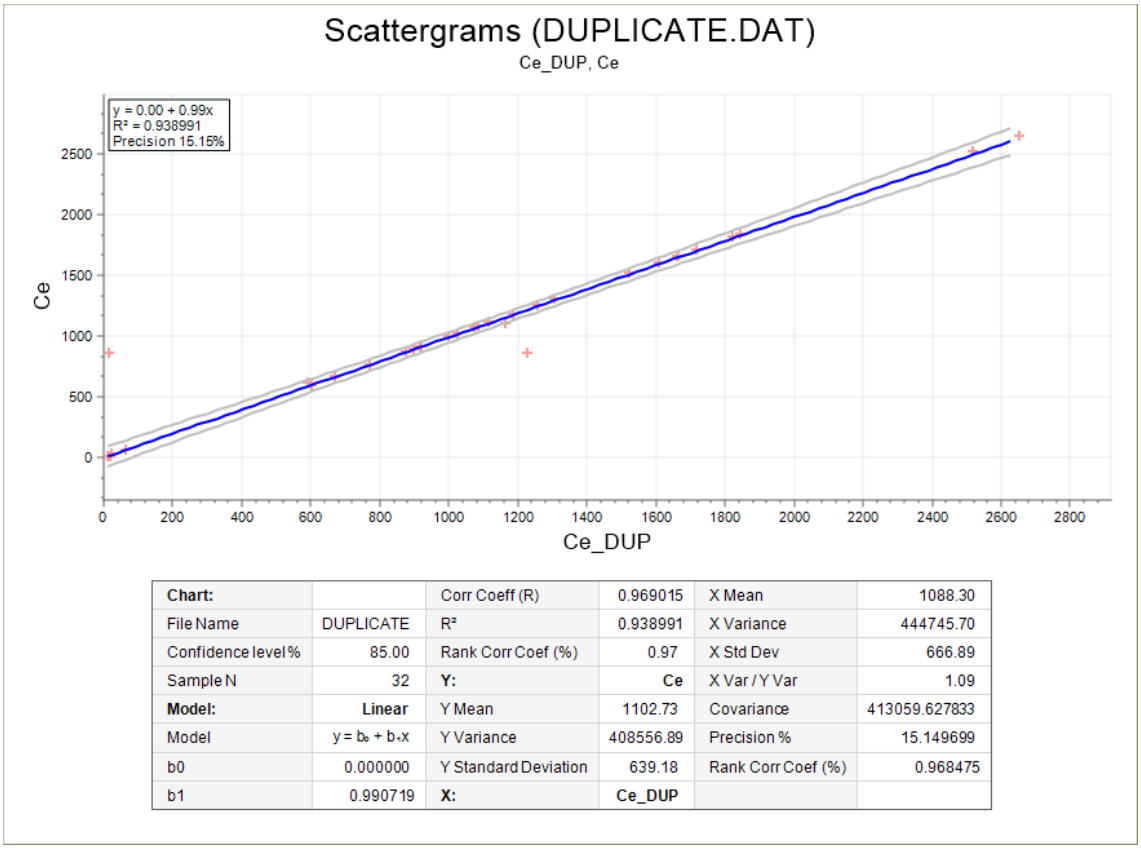

| **Chart:** | | Corr Coeff (R) | 0.956358 | X Mean | 59.18 |
| --- | --- | --- | --- | --- | --- |
| File Name | DUPLICATE | R² | 0.914621 | X Variance | 2850.05 |
| Confidence level % | 85.00 | Rank Corr Coef (%) | 0.98 | X Std Dev | 53.39 |
| Sample N | 118 | **Y:** | **Y** | X Var / Y Var | 1.24 |
| **Model:** | **Linear** | Y Mean | 57.32 | Covariance | 2449.702245 |
| Model | $y = b_0 + b_1 x$ | Y Variance | 2302.15 | Precision % | 26.865277 |
| b0 | 0.000000 | Y Standard Deviation | 47.98 | Rank Corr Coef (%) | 0.983989 |
| b1 | 0.919842 | **X:** | **Y_DUP** | | |

**Appendix III - Figure 21 – Linear Regression Diagram for Y ppm, field duplicate, class: Diamond Drilling, internal control results Balsamo and Alto da Serra Target.**



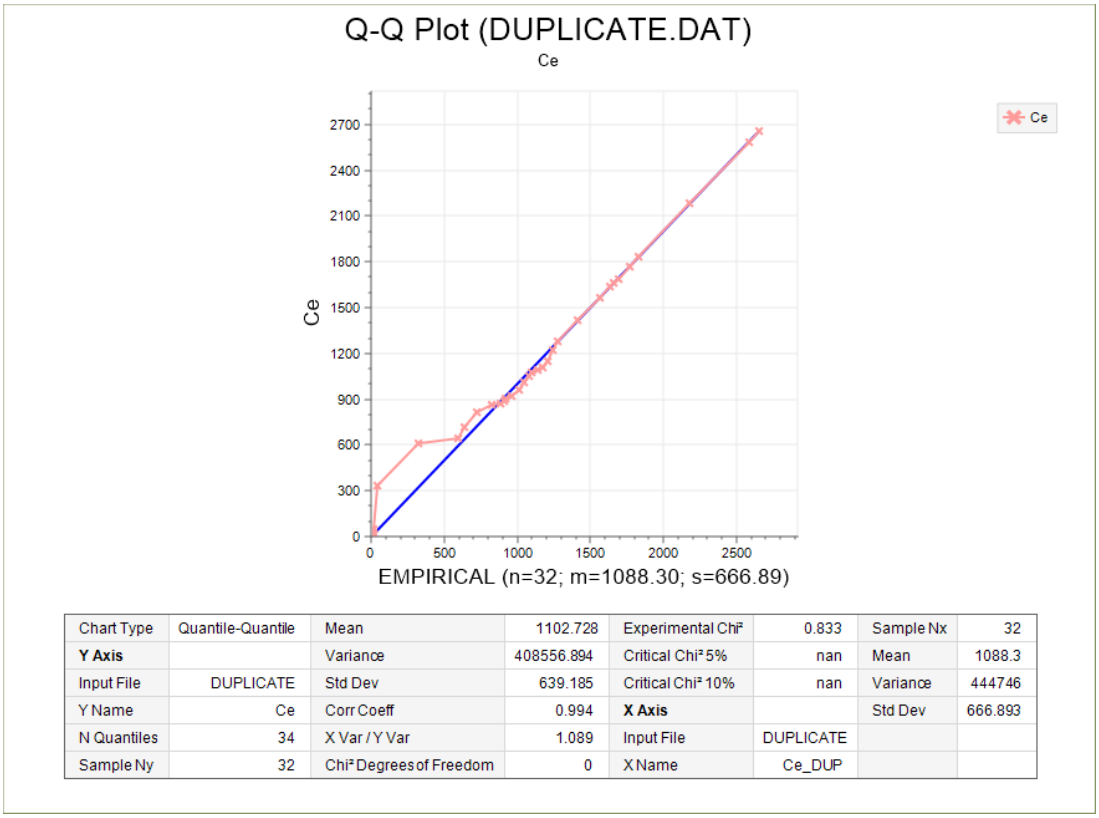

| | | | | | | | |
|---|---|---|---|---|---|---|---|
| Chart Type | Quantile-Quantile | Mean | 57.318 | Experimental Chi² | 5.024 | Sample Nx | 124 |
| **Y Axis** | | Variance | 2302.151 | Critical Chi² 5% | 9.488 | Mean | 59.0691 |
| Input File | DUPLICATE | Std Dev | 47.981 | Critical Chi² 10% | 7.779 | Variance | 2722.4 |
| Y Name | Y | Corr Coeff | 0.995 | **X Axis** | | Std Dev | 52.1766 |
| N Quantiles | 120 | X Var / Y Var | 1.183 | Input File | DUPLICATE | | |
| Sample Ny | 118 | Chi² Degrees of Freedom | 4 | X Name | Y_DUP | | |

**Appendix III - Figure 22 – Quantis plotting for Y ppm, field duplicate, class: Diamond Drilling, internal control results Balsamo and Alto da Serra Target.**



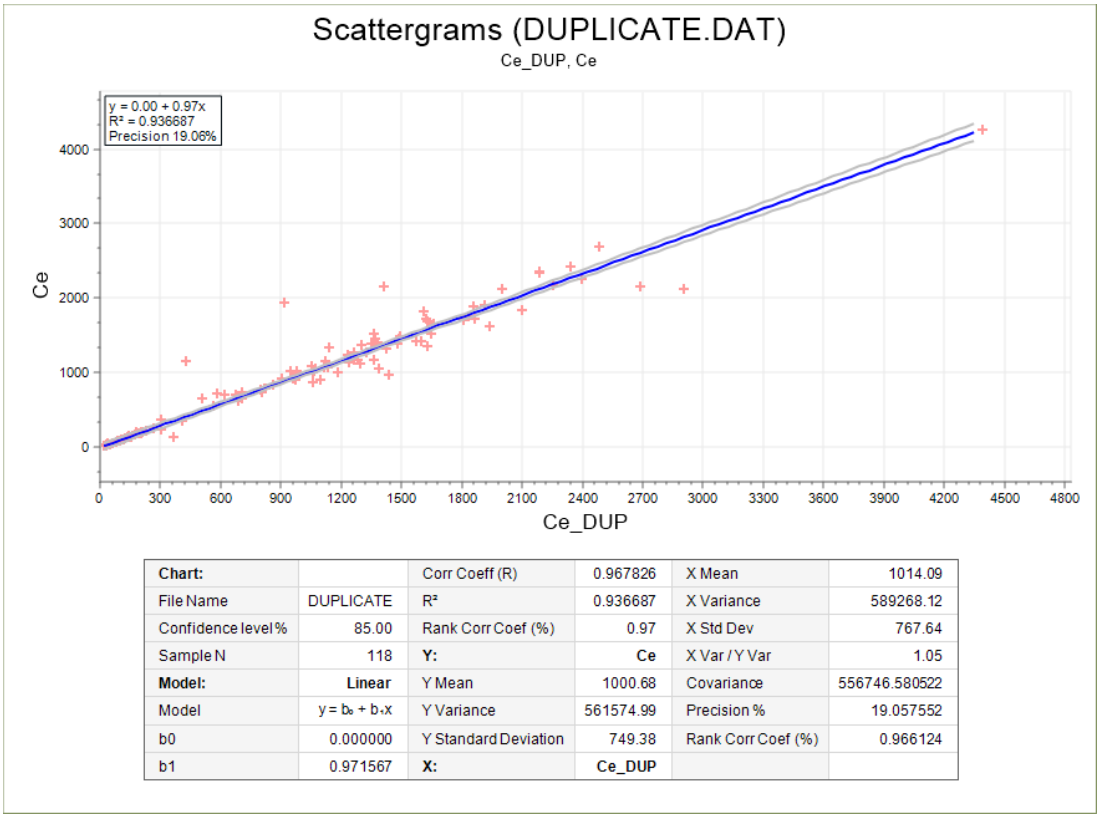

| Chart: | | Corr Coeff (R) | 0.969015 | X Mean | 1088.30 |
| --- | --- | --- | --- | --- | --- |
| File Name | DUPLICATE | $R^2$ | 0.938991 | X Variance | 444745.70 |
| Confidence level % | 85.00 | Rank Corr Coef (%) | 0.97 | X Std Dev | 666.89 |
| Sample N | 32 | **Y:** | **Ce** | X Var / Y Var | 1.09 |
| **Model:** | **Linear** | Y Mean | 1102.73 | Covariance | 413059.627833 |
| Model | $y = b_0 + b_1x$ | Y Variance | 408556.89 | Precision % | 15.149699 |
| b0 | 0.000000 | Y Standard Deviation | 639.18 | Rank Corr Coef (%) | 0.968475 |
| b1 | 0.990719 | **X:** | **Ce_DUP** | | |

**Appendix III - Figure 23 – Linear Regression Diagram for Ce ppm, field duplicate, class: Diamond Drilling, internal control results Nau de Guerra Target.**



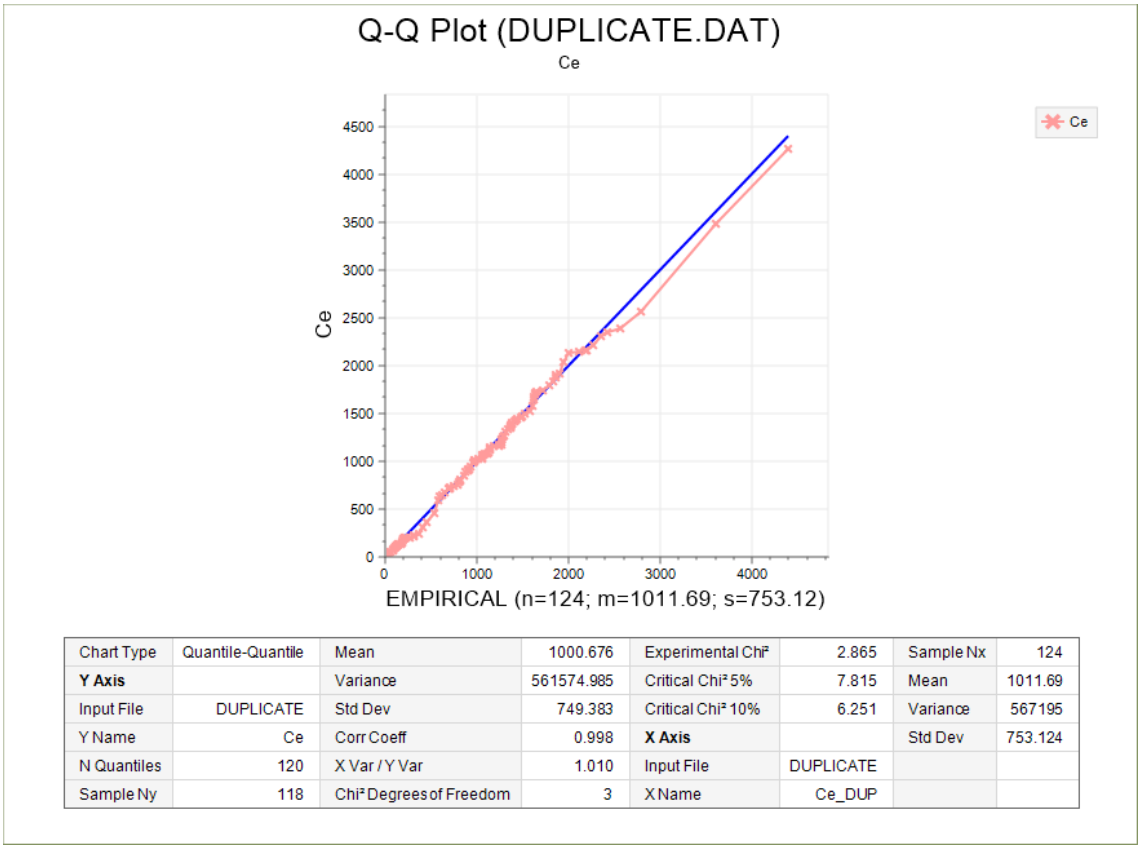

| | | | | | | | |
|---|---|---|---|---|---|---|---|
| Chart Type | Quantile-Quantile | Mean | 1102.728 | Experimental Chi² | 0.833 | Sample Nx | 32 |
| **Y Axis** | | Variance | 408556.894 | Critical Chi² 5% | nan | Mean | 1088.3 |
| Input File | DUPLICATE | Std Dev | 639.185 | Critical Chi² 10% | nan | Variance | 444746 |
| Y Name | Ce | Corr Coeff | 0.994 | **X Axis** | | Std Dev | 666.893 |
| N Quantiles | 34 | X Var / Y Var | 1.089 | Input File | DUPLICATE | | |
| Sample Ny | 32 | Chi² Degrees of Freedom | 0 | X Name | Ce_DUP | | |

**Appendix III - Figure 24 – Quantis plotting for Ce ppm, field duplicate, class: Diamond Drilling, internal control results Nau de Guerra Target.**



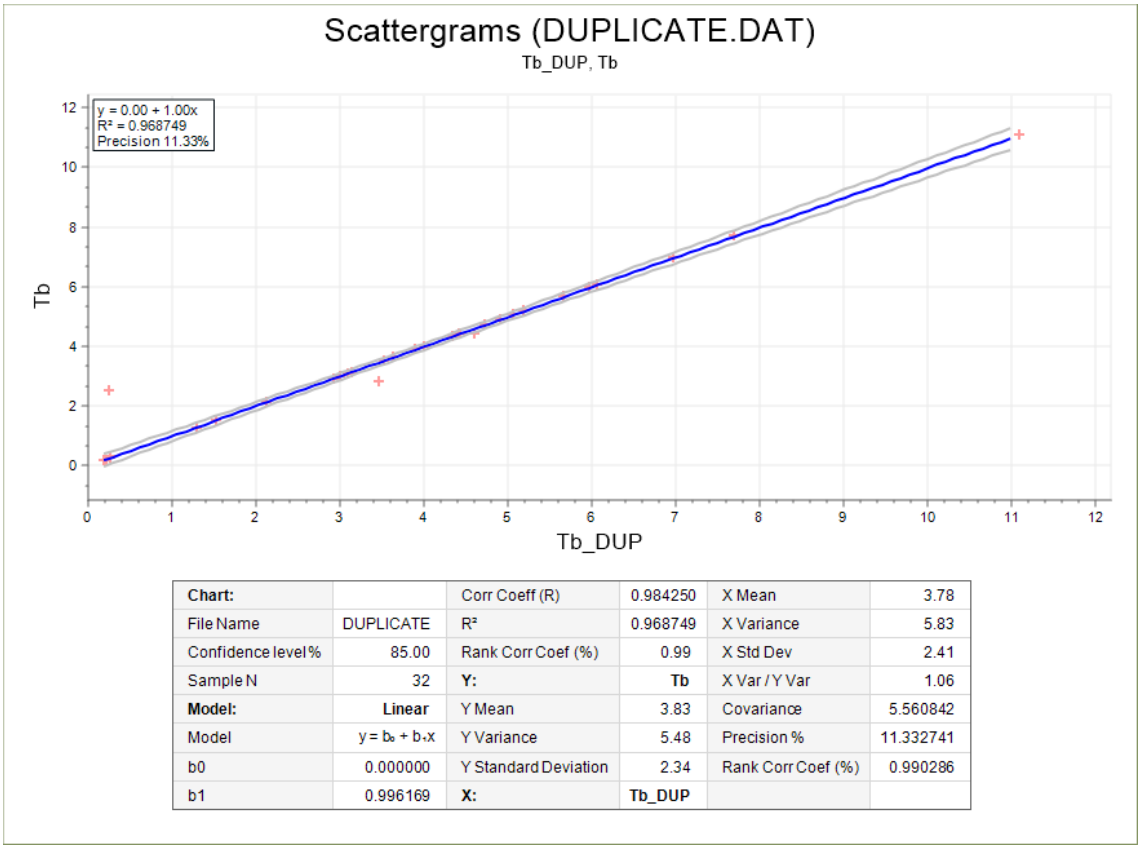

| | | | | | |
|---|---|---|---|---|---|
| **Chart:** | | Corr Coeff (R) | 0.967826 | X Mean | 1014.09 |
| File Name | DUPLICATE | R² | 0.936687 | X Variance | 589268.12 |
| Confidence level % | 85.00 | Rank Corr Coef (%) | 0.97 | X Std Dev | 767.64 |
| Sample N | 118 | **Y:** | **Ce** | X Var / Y Var | 1.05 |
| **Model:** | **Linear** | Y Mean | 1000.68 | Covariance | 556746.580522 |
| Model | $y = b_0 + b_1 x$ | Y Variance | 561574.99 | Precision % | 19.057552 |
| b0 | 0.000000 | Y Standard Deviation | 749.38 | Rank Corr Coef (%) | 0.966124 |
| b1 | 0.971567 | **X:** | **Ce_DUP** | | |

**Appendix III - Figure 25 – Linear Regression Diagram for Ce ppm, field duplicate, class: Diamond Drilling, internal control results Balsamo and Alto da Serra Target.**



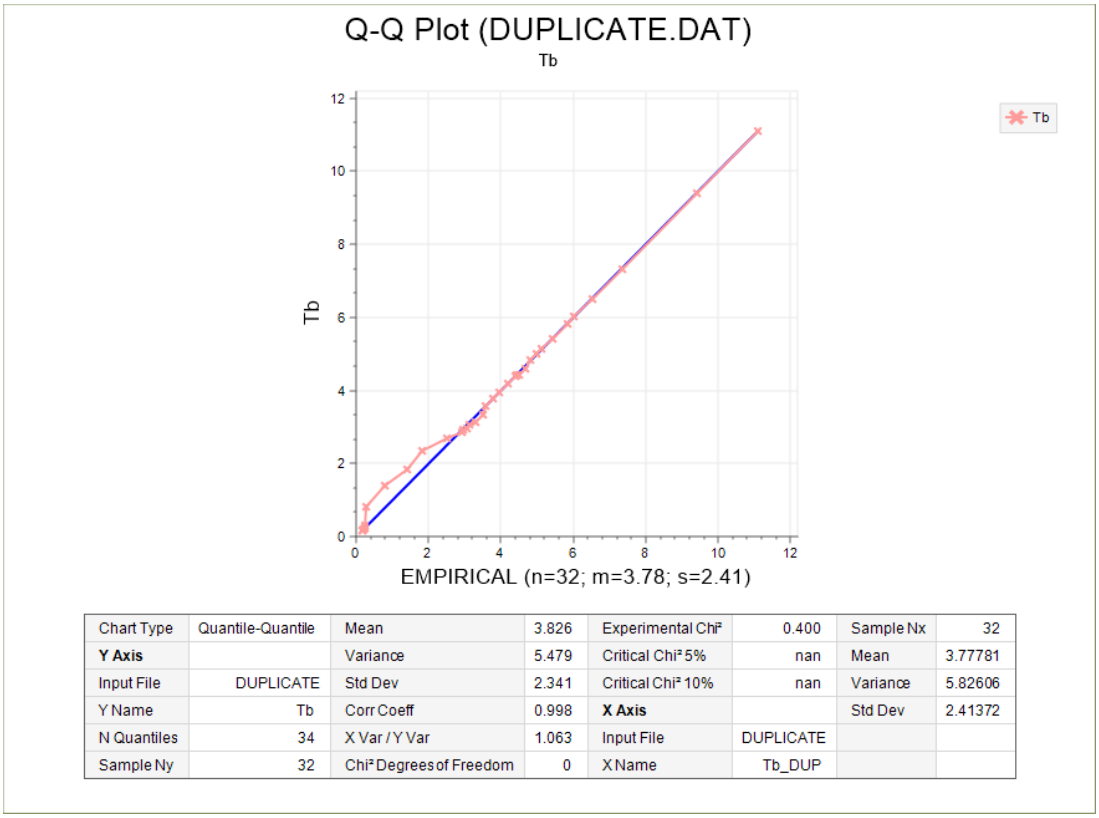

| Chart Type | Quantile-Quantile | Mean | 1000.676 | Experimental Chi² | 2.865 | Sample Nx | 124 |
| --- | --- | --- | --- | --- | --- | --- | --- |
| **Y Axis** | | Variance | 561574.985 | Critical Chi² 5% | 7.815 | Mean | 1011.69 |
| Input File | DUPLICATE | Std Dev | 749.383 | Critical Chi² 10% | 6.251 | Variance | 567195 |
| Y Name | Ce | Corr Coeff | 0.998 | **X Axis** | | Std Dev | 753.124 |
| N Quantiles | 120 | X Var / Y Var | 1.010 | Input File | DUPLICATE | | |
| Sample Ny | 118 | Chi² Degrees of Freedom | 3 | X Name | Ce_DUP | | |

**Appendix III - Figure 26 – Quantis plotting for Ce ppm, field duplicate, class: Diamond Drilling, internal control results Balsamo and Alto da Serra Target.**



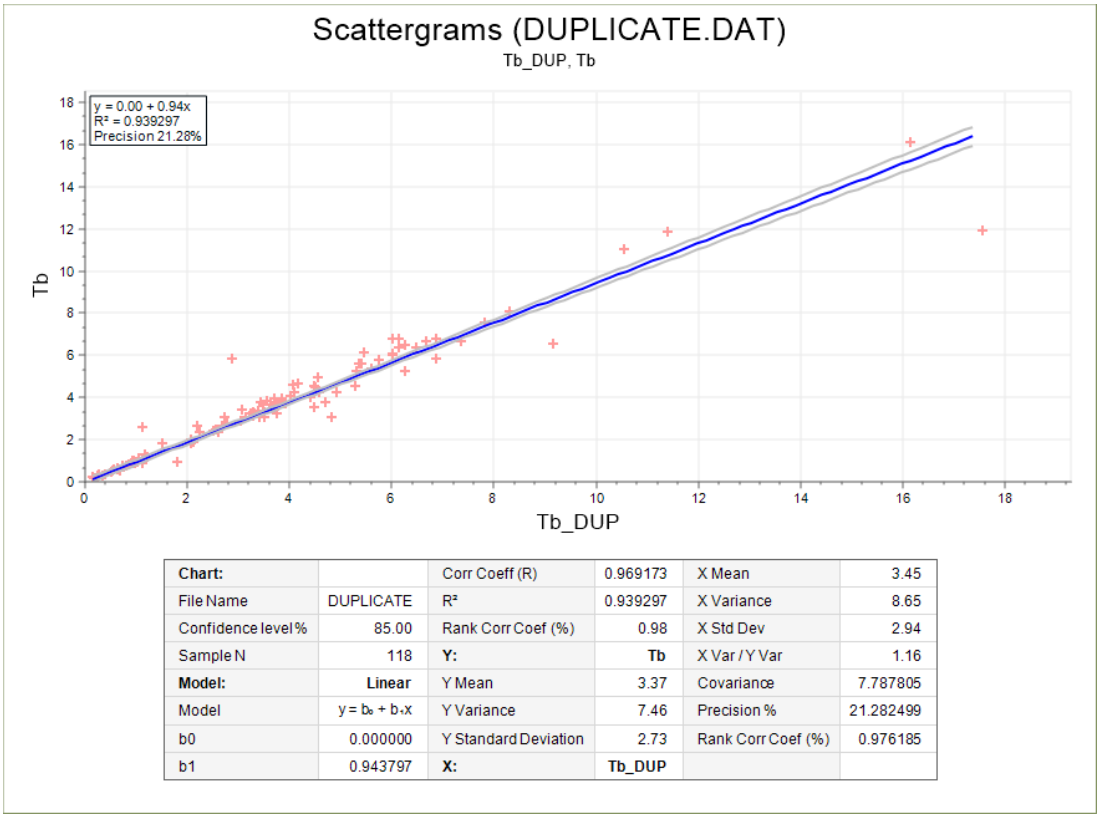

| Chart: | | Corr Coeff (R) | 0.984250 | X Mean | 3.78 |
| --- | --- | --- | --- | --- | --- |
| File Name | DUPLICATE | $R^2$ | 0.968749 | X Variance | 5.83 |
| Confidence level % | 85.00 | Rank Corr Coef (%) | 0.99 | X Std Dev | 2.41 |
| Sample N | 32 | **Y:** | **Tb** | X Var / Y Var | 1.06 |
| **Model:** | **Linear** | Y Mean | 3.83 | Covariance | 5.560842 |
| Model | $y = b_0 + b_1x$ | Y Variance | 5.48 | Precision % | 11.332741 |
| b0 | 0.000000 | Y Standard Deviation | 2.34 | Rank Corr Coef (%) | 0.990286 |
| b1 | 0.996169 | **X:** | **Tb_DUP** | | |

**Appendix III - Figure 27 – Linear Regression Diagram for Tb ppm, field duplicate, class: Diamond Drilling, internal control results Nau de Guerra Target.**



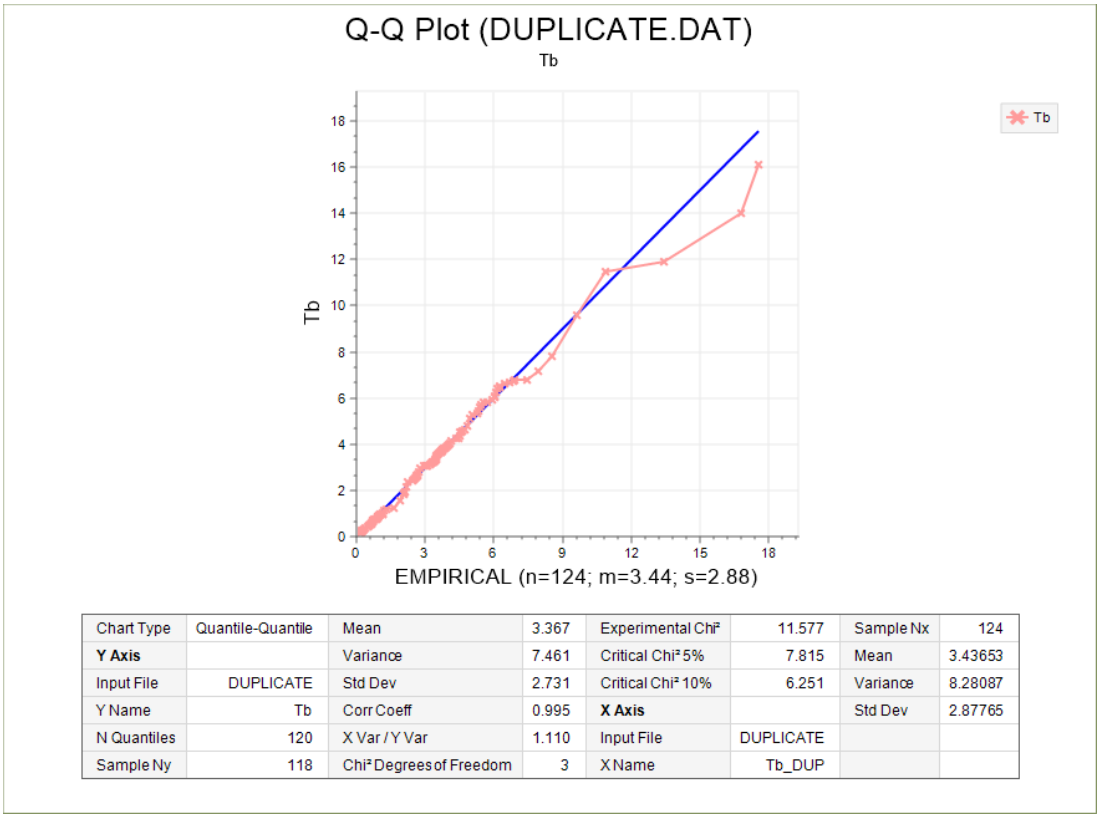

| | | | | | | | |
|---|---|---|---|---|---|---|---|
| Chart Type | Quantile-Quantile | Mean | 3.826 | Experimental Chi² | 0.400 | Sample Nx | 32 |
| **Y Axis** | | Variance | 5.479 | Critical Chi² 5% | nan | Mean | 3.77781 |
| Input File | DUPLICATE | Std Dev | 2.341 | Critical Chi² 10% | nan | Variance | 5.82606 |
| Y Name | Tb | Corr Coeff | 0.998 | **X Axis** | | Std Dev | 2.41372 |
| N Quantiles | 34 | X Var / Y Var | 1.063 | Input File | DUPLICATE | | |
| Sample Ny | 32 | Chi² Degrees of Freedom | 0 | X Name | Tb_DUP | | |

**Appendix III - Figure 28 – Quantis plotting for Tb ppm, field duplicate, class: Diamond Drilling, internal control results Nau de Guerra Target.**



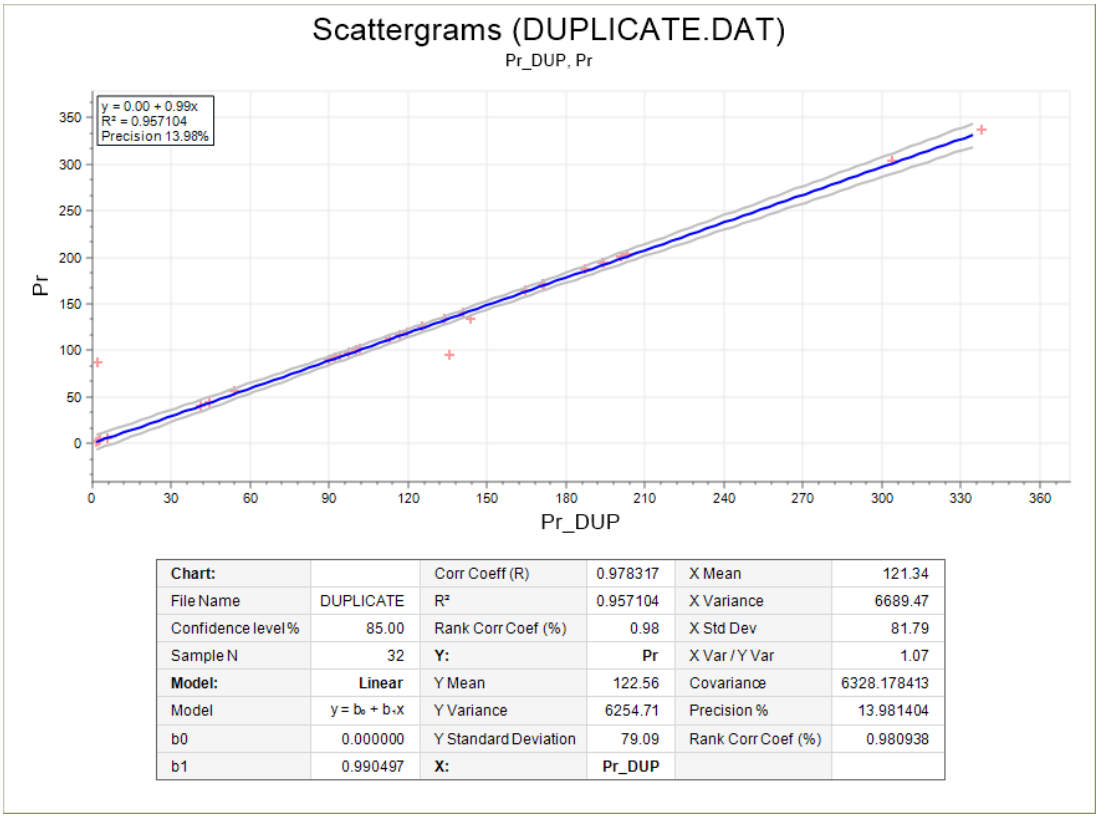

| | | | | | |
|---|---|---|---|---|---|
| **Chart:** | | Corr Coeff (R) | 0.969173 | X Mean | 3.45 |
| File Name | DUPLICATE | R² | 0.939297 | X Variance | 8.65 |
| Confidence level % | 85.00 | Rank Corr Coef (%) | 0.98 | X Std Dev | 2.94 |
| Sample N | 118 | **Y:** | **Tb** | X Var / Y Var | 1.16 |
| **Model:** | **Linear** | Y Mean | 3.37 | Covariance | 7.787805 |
| Model | $y = b_0 + b_1 x$ | Y Variance | 7.46 | Precision % | 21.282499 |
| b0 | 0.000000 | Y Standard Deviation | 2.73 | Rank Corr Coef (%) | 0.976185 |
| b1 | 0.943797 | **X:** | **Tb_DUP** | | |

**Appendix III - Figure 29 – Linear Regression Diagram for Tb ppm, field duplicate, class: Diamond Drilling, internal control results Balsamo and Alto da Serra Target.**



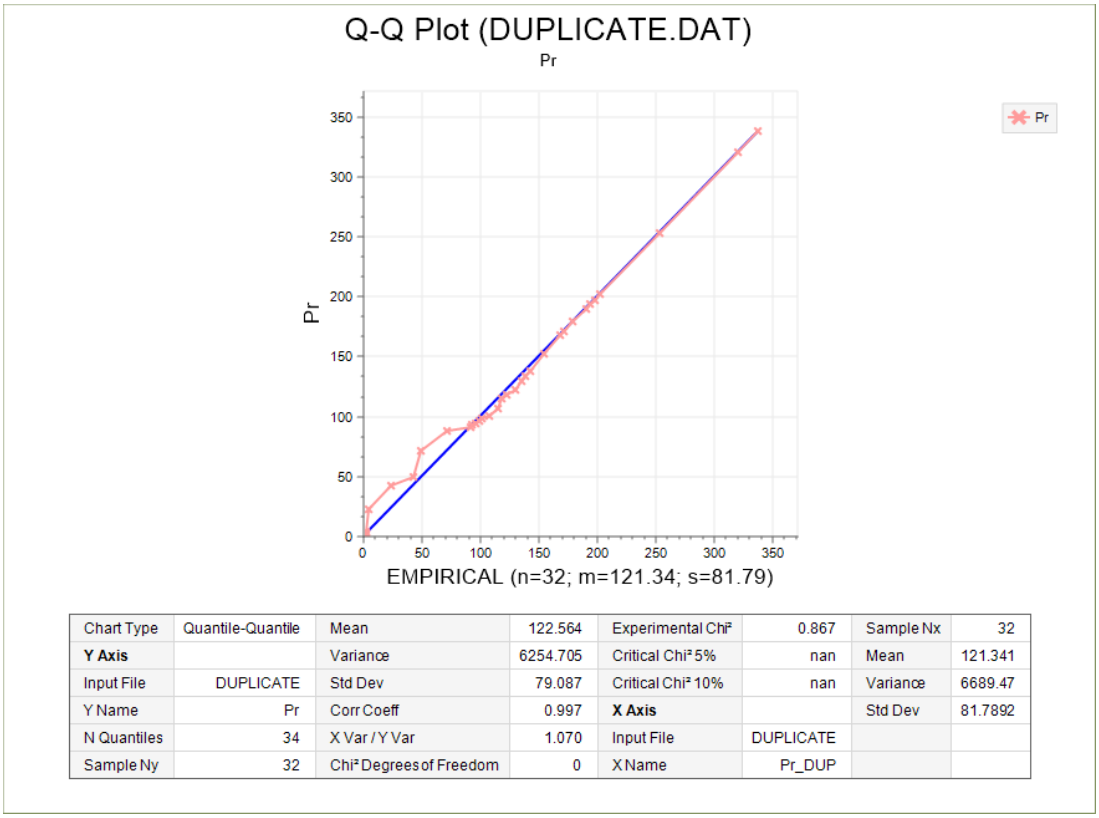

| | | | | | | | |
|---|---|---|---|---|---|---|---|
| Chart Type | Quantile-Quantile | Mean | 3.367 | Experimental Chi² | 11.577 | Sample Nx | 124 |
| **Y Axis** | | Variance | 7.461 | Critical Chi² 5% | 7.815 | Mean | 3.43653 |
| Input File | DUPLICATE | Std Dev | 2.731 | Critical Chi² 10% | 6.251 | Variance | 8.28087 |
| Y Name | Tb | Corr Coeff | 0.995 | **X Axis** | | Std Dev | 2.87765 |
| N Quantiles | 120 | X Var / Y Var | 1.110 | Input File | DUPLICATE | | |
| Sample Ny | 118 | Chi² Degrees of Freedom | 3 | X Name | Tb_DUP | | |

**Appendix III - Figure 30 – Quantis plotting for Tb ppm, field duplicate, class: Diamond Drilling, internal control results Balsamo and Alto da Serra Target.**



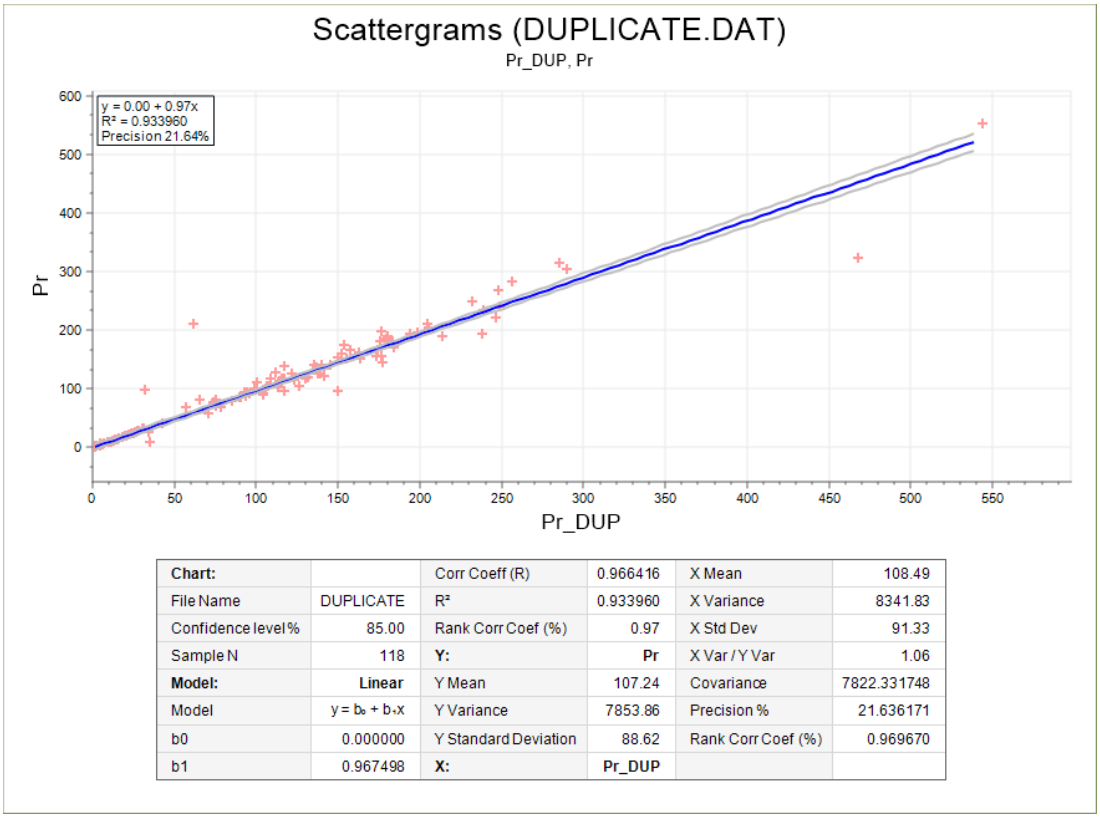

| | | | | | |
|---|---|---|---|---|---|
| **Chart:** | | Corr Coeff (R) | 0.978317 | X Mean | 121.34 |
| File Name | DUPLICATE | R² | 0.957104 | X Variance | 6689.47 |
| Confidence level % | 85.00 | Rank Corr Coef (%) | 0.98 | X Std Dev | 81.79 |
| Sample N | 32 | **Y:** | **Pr** | X Var / Y Var | 1.07 |
| **Model:** | **Linear** | Y Mean | 122.56 | Covariance | 6328.178413 |
| Model | $y = b_0 + b_1 x$ | Y Variance | 6254.71 | Precision % | 13.981404 |
| b0 | 0.000000 | Y Standard Deviation | 79.09 | Rank Corr Coef (%) | 0.980938 |
| b1 | 0.990497 | **X:** | **Pr_DUP** | | |

**Appendix III - Figure 31 – Linear Regression Diagram for Pr ppm, field duplicate, class: Diamond Drilling, internal control results Nau de Guerra Target.**



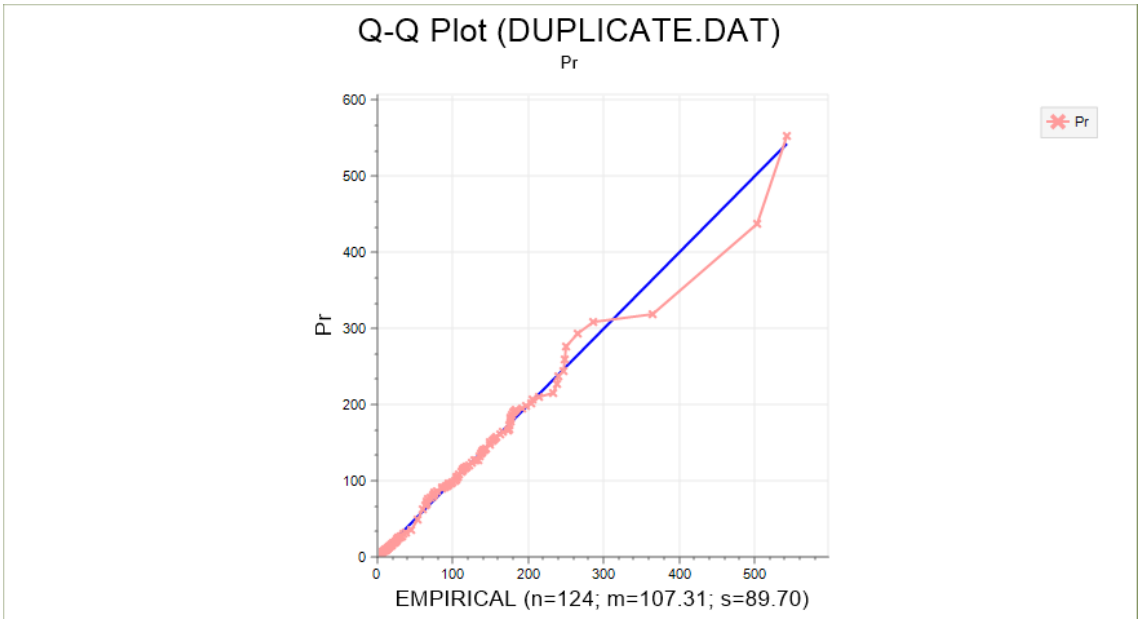

| Chart Type | Quantile-Quantile | Mean | 122.564 | Experimental Chi² | 0.867 | Sample Nx | 32 |
|---|---|---|---|---|---|---|---|
| **Y Axis** | | Variance | 6254.705 | Critical Chi² 5% | nan | Mean | 121.341 |
| Input File | DUPLICATE | Std Dev | 79.087 | Critical Chi² 10% | nan | Variance | 6689.47 |
| Y Name | Pr | Corr Coeff | 0.997 | **X Axis** | | Std Dev | 81.7892 |
| N Quantiles | 34 | X Var / Y Var | 1.070 | Input File | DUPLICATE | | |
| Sample Ny | 32 | Chi² Degrees of Freedom | 0 | X Name | Pr_DUP | | |

**Appendix III - Figure 32 – Quantis plotting for Pr ppm, field duplicate, class: Diamond Drilling, internal control results Nau de Guerra Target.**




| Chart: | | Corr Coeff (R) | 0.966416 | X Mean | 108.49 |
|---|---|---|---|---|---|
| File Name | DUPLICATE | R² | 0.933960 | X Variance | 8341.83 |
| Confidence level % | 85.00 | Rank Corr Coef (%) | 0.97 | X Std Dev | 91.33 |
| Sample N | 118 | **Y:** | **Pr** | X Var / Y Var | 1.06 |
| **Model:** | **Linear** | Y Mean | 107.24 | Covariance | 7822.331748 |
| Model | $y = b_0 + b_1 x$ | Y Variance | 7853.86 | Precision % | 21.636171 |
| b0 | 0.000000 | Y Standard Deviation | 88.62 | Rank Corr Coef (%) | 0.969670 |
| b1 | 0.967498 | **X:** | **Pr_DUP** | | |

**Appendix III - Figure 33 – Linear Regression Diagram for Pr ppm, field duplicate, class: Diamond Drilling, internal control results Balsamo and Alto da Serra Target.**




| Chart Type | Quantile-Quantile | Mean | 107.237 | Experimental Chi² | 8.211 | Sample Nx | 124 |
| --- | --- | --- | --- | --- | --- | --- | --- |
| **Y Axis** | | Variance | 7853.856 | Critical Chi² 5% | 7.815 | Mean | 107.309 |
| Input File | DUPLICATE | Std Dev | 88.622 | Critical Chi² 10% | 6.251 | Variance | 8046.42 |
| Y Name | Pr | Corr Coeff | 0.995 | **X Axis** | | Std Dev | 89.7018 |
| N Quantiles | 120 | X Var / Y Var | 1.025 | Input File | DUPLICATE | | |
| Sample Ny | 118 | Chi² Degrees of Freedom | 3 | X Name | Pr_DUP | | |

**Appendix III - Figure 34 – Quantis plotting for Pr ppm, field duplicate, class: Diamond Drilling, internal control results Balsamo and Alto da Serra Target.**

# APPENDIX IV - Geostatistics

# LIST OF FIGURES

Appendix IV - Figure 1- First axis to Y (ppm), Nau de GuerraTarget. ..... 218

Appendix IV - Figure 2- Second axis to Y (ppm), Nau de Guerra Target. ..... 218

Appendix IV - Figure 3 - Third axis to Y (ppm), Nau de GuerraTarget. ..... 219

Appendix IV - Figure 4 - Linear diagram of dependence between composite samples data and Y (ppm) grade estimates, Nau de Guerra Target. ..... 220

Appendix IV - Figure 5 - First axis to Y (ppm), Alto da SerraTarget. ..... 220

Appendix IV - Figure 6 - Second axis to Y (ppm), Alto da Serra Target. ..... 221

Appendix IV - Figure 7 - Third axis to Y (ppm), Alto da SerraTarget ..... 221

Appendix IV - Figure 8 - Linear diagram of dependence between composite samples data and Y (ppm) grade estimates, Alto da Serra Target ..... 222

Appendix IV - Figure 9 - First axis to Y (ppm), BalsamoTarget. ..... 223

Appendix IV - Figure 10 - Second axis to Y (ppm), Balsamo Target ..... 223

Appendix IV - Figure 11 - Third axis to Y (ppm), BalsamoTarget. ..... 224

Appendix IV - Figure 12 - Linear diagram of dependence between composite samples data and Y (ppm) grade estimates, Balsamo Target. ..... 225

Appendix IV - Figure 13 - First axis to Th (ppm), Nau de GuerraTarget. ..... 225

Appendix IV - Figure 14 - Second axis to Th (ppm), Nau de GuerraTarget. ..... 226

Appendix IV - Figure 15 - Third axis to Th (ppm), Nau de GuerraTarget. ..... 226

Appendix IV - Figure 16 - Linear diagram of dependence between composite samples data and Th (ppm) grade estimates, Nau de Guerra Target. ..... 227

Appendix IV - Figure 17 - First axis to Th (ppm), Alto da SerraTarget. ..... 228

Appendix IV - Figure 18 - Second axis to Th (ppm), Alto da SerraTarget. ..... 228

Appendix IV - Figure 19 - Third axis to Th (ppm), Alto da SerraTarget. ..... 229

Appendix IV - Figure 20 - Linear diagram of dependence between composite samples data and Th (ppm) grade estimates, Alto da Serra Target ..... 230

Appendix IV - Figure 21 - First axis to Th (ppm), BalsamoTarget. ..... 230

Appendix IV - Figure 22 - Second axis to Th (ppm), BalsamoTarget. ..... 231

Appendix IV - Figure 23 - Third axis to Th (ppm), BalsamoTarget. ..... 231

Appendix IV - Figure 24 - Linear diagram of dependence between composite samples data and Th (ppm) grade estimates, Balsamo Target. ..... 232

Appendix IV - Figure 25 - First axis to U (ppm), Nau de GuerraTarget..... 233

Appendix IV - Figure 26 - Second axis to U (ppm), Nau de GuerraTarget..... 233

Appendix IV - Figure 27 - Third axis to U (ppm), Nau de GuerraTarget..... 234

Appendix IV - Figure 28 - Linear diagram of dependence between composite samples data and U (ppm) grade estimates, Nau de Guerra Target..... 235

Appendix IV - Figure 29 - First axis to U (ppm), Alto da SerraTarget..... 235

Appendix IV - Figure 30 - Second axis to U (ppm), Alto da SerraTarget..... 236

Appendix IV - Figure 31 - Third axis to U (ppm), Alto da SerraTarget..... 236

Appendix IV - Figure 32 - Linear diagram of dependence between composite samples data and U (ppm) grade estimates, Alto da Serra Target..... 237

Appendix IV - Figure 33 - First axis to U (ppm), BalsamoTarget..... 238

Appendix IV - Figure 34 - Second axis to U (ppm), BalsamoTarget..... 238

Appendix IV - Figure 35 - Third axis to U (ppm), BalsamoTarget..... 239

Appendix IV - Figure 36 - Linear diagram of dependence between composite samples data and U (ppm) grade estimates, Balsamo Target..... 240

# LIST OF TABLES

Appendix IV - Table 1 - Cross-Validation verification results for Y (ppm), Nau de GuerraTarget. ..... 219

Appendix IV - Table 2 - Cross-Validation verification results for Y (ppm), Alto da SerraTarget..... 221

Appendix IV - Table 3 - Cross-Validation verification results for Y (ppm), BalsamoTarget. ..... 224

Appendix IV - Table 4 - Cross-Validation verification results for Th (ppm), Nau de GuerraTarget..... 226

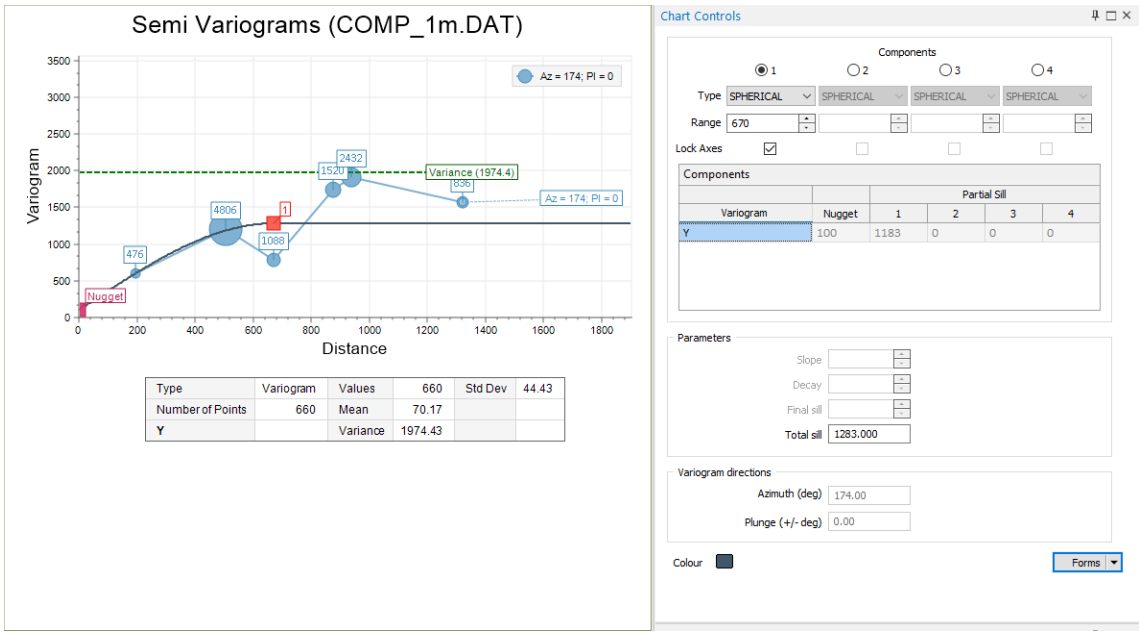
Appendix IV - Table 5 - Cross-Validation verification results for Th (ppm), Alto da SerraTarget..... 229

Appendix IV - Table 6 - Cross-Validation verification results for Th (ppm), BalsamoTarget. ..... 231

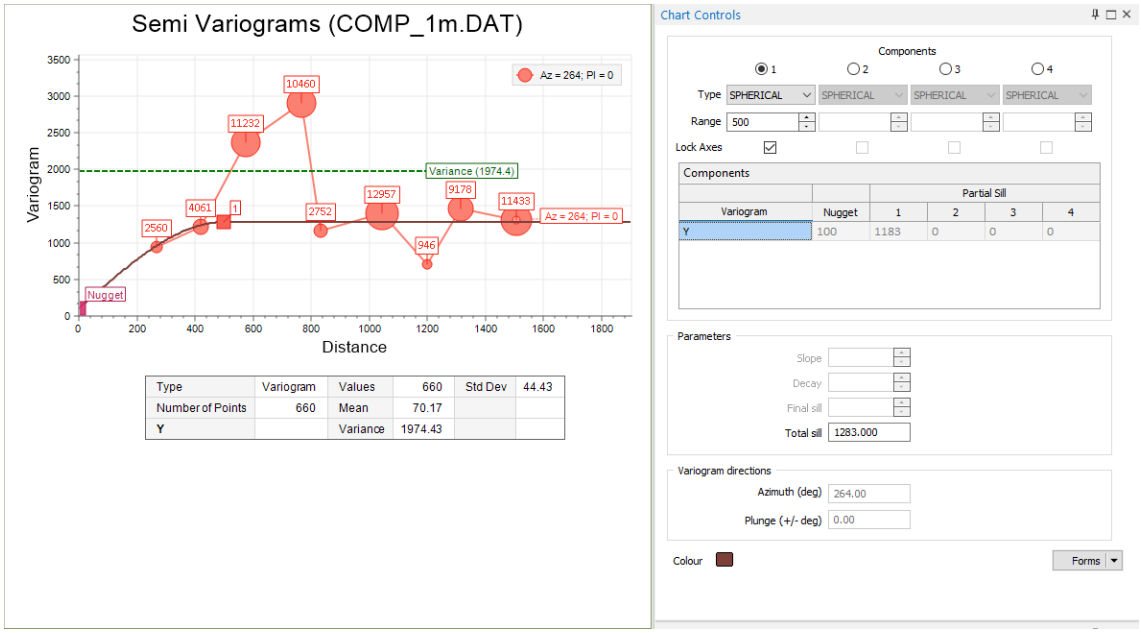
Appendix IV - Table 7 - Cross-Validation verification results for U (ppm), Nau de GuerraTarget. ..... 234

Appendix IV - Table 8 - Cross-Validation verification results for U (ppm), Alto da SerraTarget. ..... 236

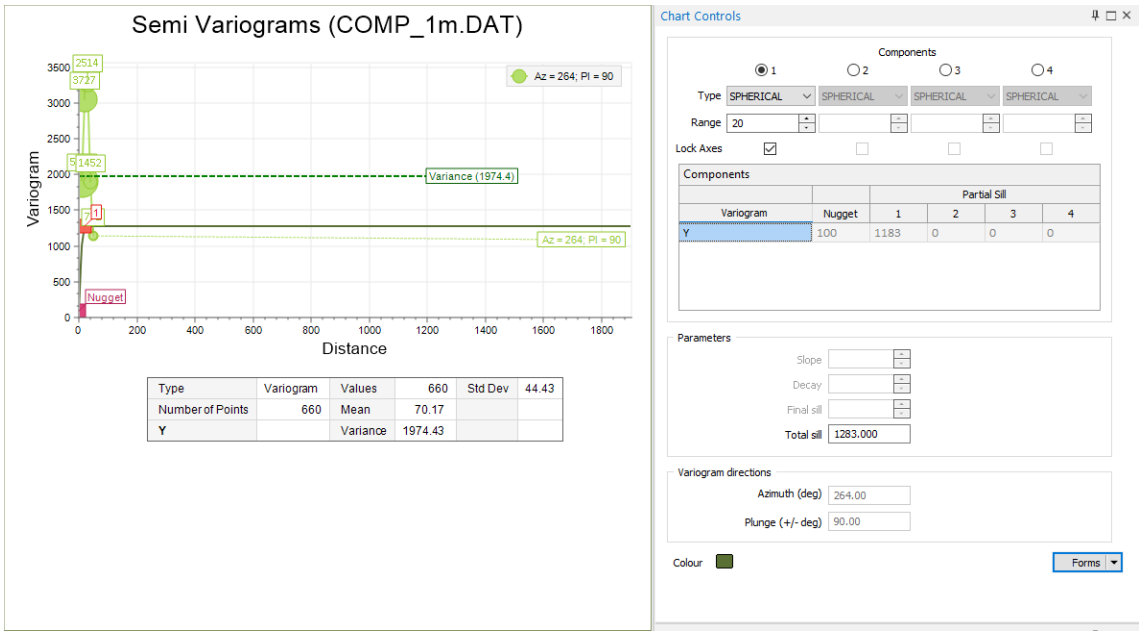
Appendix IV - Table 9 - Cross-Validation verification results for U (ppm), BalsamoTarget. ..... 239




**Appendix IV - Figure 1- First axis to Y (ppm), Nau de GuerraTarget.**



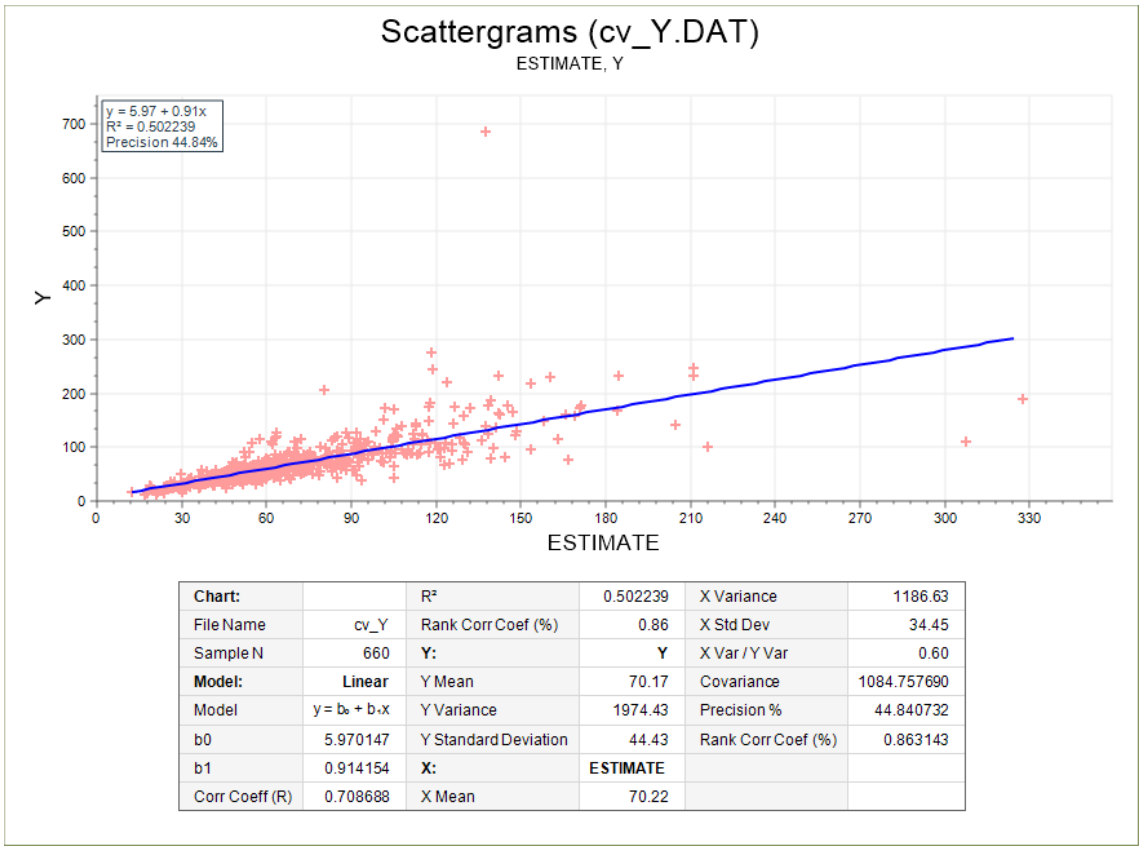

**Appendix IV - Figure 2- Second axis to Y (ppm), Nau de Guerra Target.**




**Appendix IV - Figure 3 - Third axis to Y (ppm), Nau de GuerraTarget.**

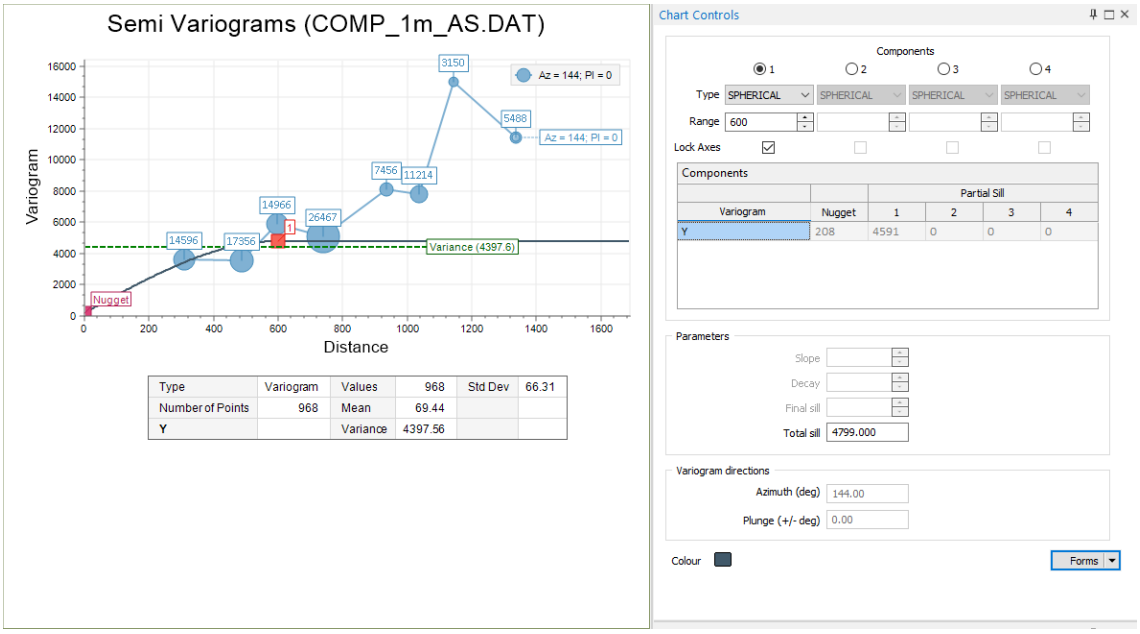
**Appendix IV - Table 1 - Cross-Validation verification results for Y (ppm), Nau de GuerraTarget.**

| Metadata Label | Metadata Value | Field Name | Mean | Std Dev |
| --- | --- | --- | --- | --- |
| Output File | cv_Y.DAT | | | |
| Input File | COMP_1m.DAT | | | |
| Analysis varb | Y | | | |
| Transformation | None | | | |
| Number of points | 660 | | | |
| Raw Data | | Y | 70.165151515 | 44.434541132 |
| Standard error | | STD_ERROR | 15.140158168 | 0.666333102 |
| Estimate | | ESTIMATE | 70.223426560 | 34.447424771 |
| Residual | | RESIDUAL | -0.058275045 | 31.488698601 |
| Error statistic | | ERROR_STAT | -0.002423321 | 2.096379670 |
| RMSE | | | 31.464888448 | |



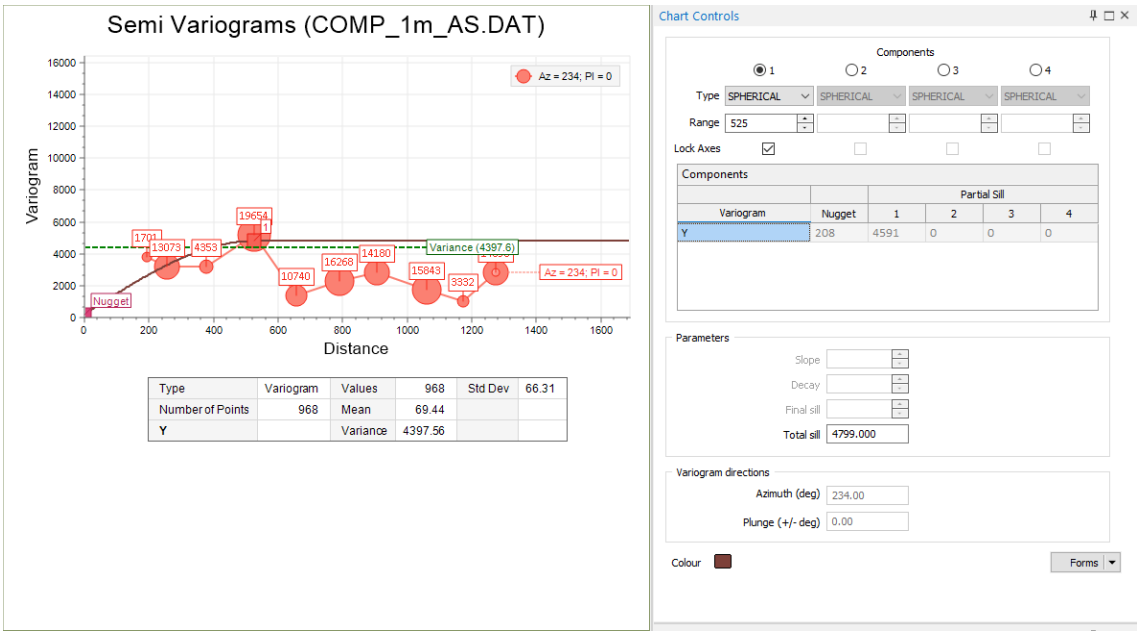

| Chart: | | R² | 0.502239 | X Variance | 1186.63 |
| --- | --- | --- | --- | --- | --- |
| File Name | cv_Y | Rank Corr Coef (%) | 0.86 | X Std Dev | 34.45 |
| Sample N | 660 | **Y:** | **Y** | X Var / Y Var | 0.60 |
| **Model:** | **Linear** | Y Mean | 70.17 | Covariance | 1084.757690 |
| Model | $y = b_0 + b_1 x$ | Y Variance | 1974.43 | Precision % | 44.840732 |
| b0 | 5.970147 | Y Standard Deviation | 44.43 | Rank Corr Coef (%) | 0.863143 |
| b1 | 0.914154 | **X:** | **ESTIMATE** | | |
| Corr Coeff (R) | 0.708688 | X Mean | 70.22 | | |

**Appendix IV - Figure 4 - Linear diagram of dependence between composite samples data and Y (ppm) grade estimates, Nau de Guerra Target.**



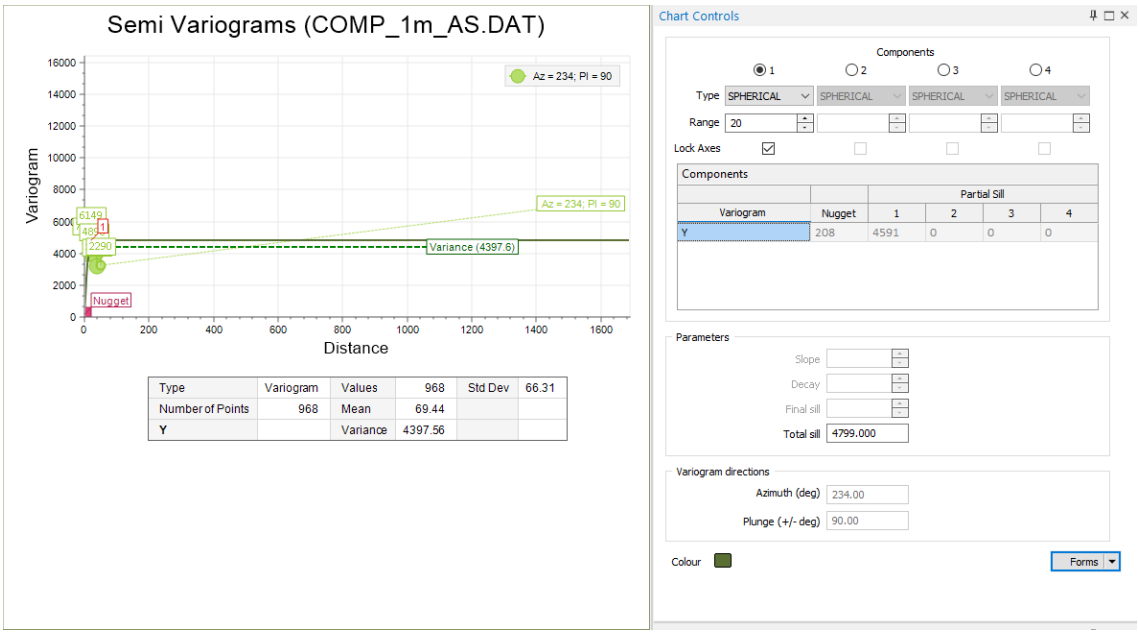

| Type | Variogram | Values | 968 | Std Dev | 66.31 |
| --- | --- | --- | --- | --- | --- |
| Number of Points | 968 | Mean | 69.44 | | |
| **Y** | | Variance | 4397.56 | | |

**Appendix IV - Figure 5 - First axis to Y (ppm), Alto da SerraTarget.**




| Type | Variogram | Values | 968 | Std Dev | 66.31 |
|---|---|---|---|---|---|
| Number of Points | 968 | Mean | 69.44 | | |
| Y | | Variance | 4397.56 | | |

**Appendix IV - Figure 6 - Second axis to Y (ppm), Alto da Serra Target.**



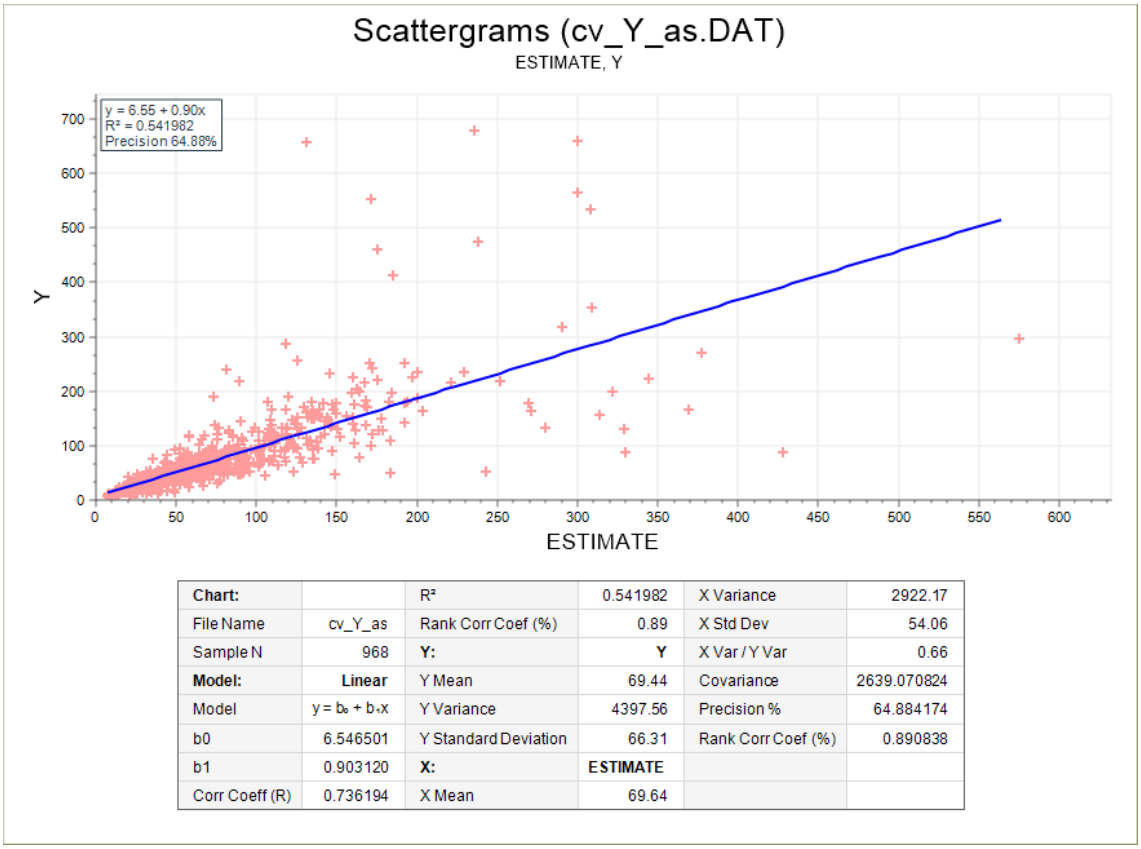

| Type | Variogram | Values | 968 | Std Dev | 66.31 |
|---|---|---|---|---|---|
| Number of Points | 968 | Mean | 69.44 | | |
| Y | | Variance | 4397.56 | | |

**Appendix IV - Figure 7 - Third axis to Y (ppm), Alto da SerraTarget.**

**Appendix IV - Table 2 - Cross-Validation verification results for Y (ppm), Alto da SerraTarget.**

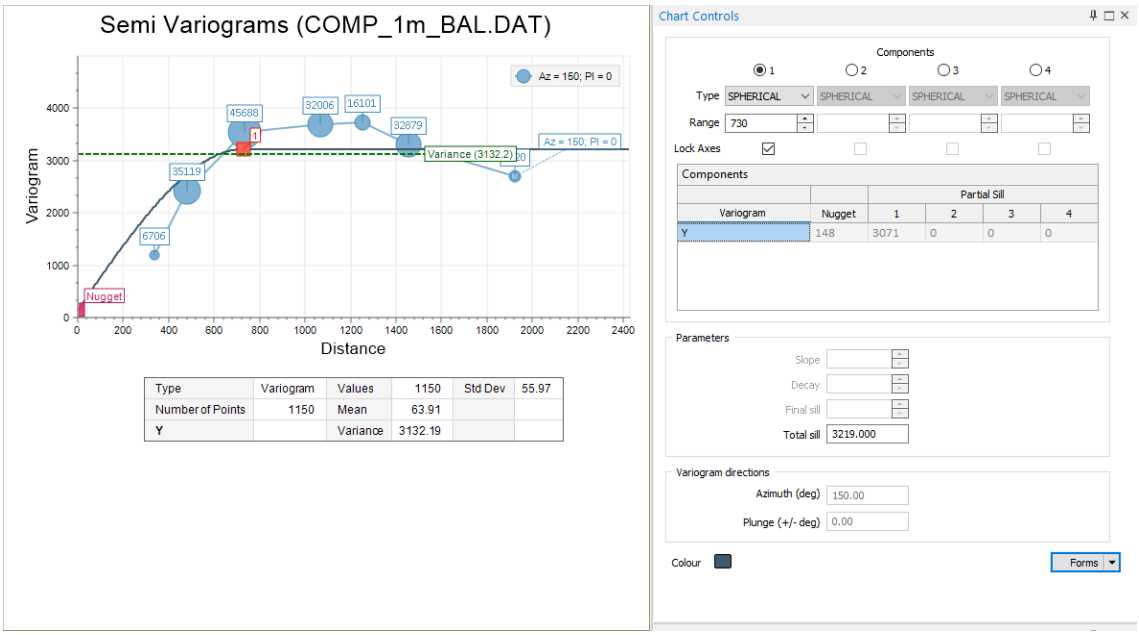
| Metadata Label | Metadata Value | Field Name | Mean | Std Dev |
|---|---|---|---|---|
| Output File | cv_Y_as.DAT | | | |
| Input File | COMP_1m_AS.DAT | | | |
| Analysis varb | Y | | | |
| Transformation | None | | | |
| Number of points | 968 | | | |
| Raw Data | | Y | 69.437871901 | 66.314115728 |

| Metadata Label | Metadata Value | Field Name | Mean | Std Dev |
|---|---|---|---|---|
| Standard error | | STD_ERROR | 25.556869640 | 1.389607483 |
| Estimate | | ESTIMATE | 69.637884021 | 54.057104016 |
| Residual | | RESIDUAL | -0.200012120 | 45.183966080 |
| Error statistic | | ERROR_STAT | -0.004678014 | 1.787148848 |
| RMSE | | | 45.161064139 | |

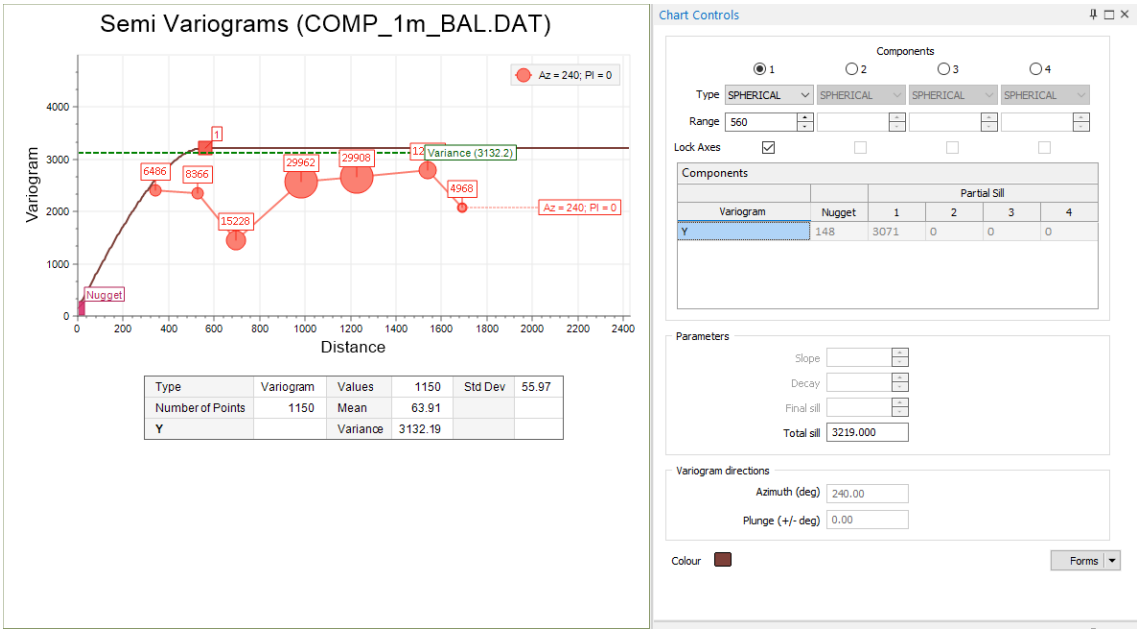



| Chart: | | R² | 0.541982 | X Variance | 2922.17 |
|---|---|---|---|---|---|
| File Name | cv_Y_as | Rank Corr Coef (%) | 0.89 | X Std Dev | 54.06 |
| Sample N | 968 | **Y:** | **Y** | X Var / Y Var | 0.66 |
| **Model:** | **Linear** | Y Mean | 69.44 | Covariance | 2639.070824 |
| Model | $y = b_0 + b_1 x$ | Y Variance | 4397.56 | Precision % | 64.884174 |
| b0 | 6.546501 | Y Standard Deviation | 66.31 | Rank Corr Coef (%) | 0.890838 |
| b1 | 0.903120 | **X:** | **ESTIMATE** | | |
| Corr Coeff (R) | 0.736194 | X Mean | 69.64 | | |

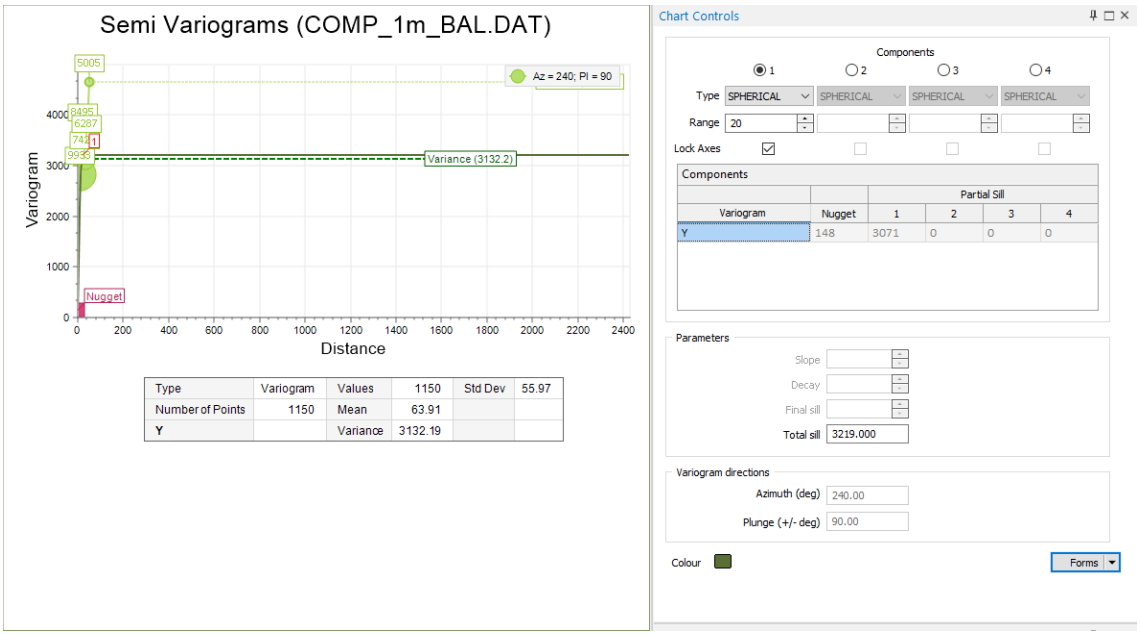
**Appendix IV - Figure 8 - Linear diagram of dependence between composite samples data and Y (ppm) grade estimates, Alto da Serra Target.**




**Appendix IV - Figure 9 - First axis to Y (ppm), BalsamoTarget.**



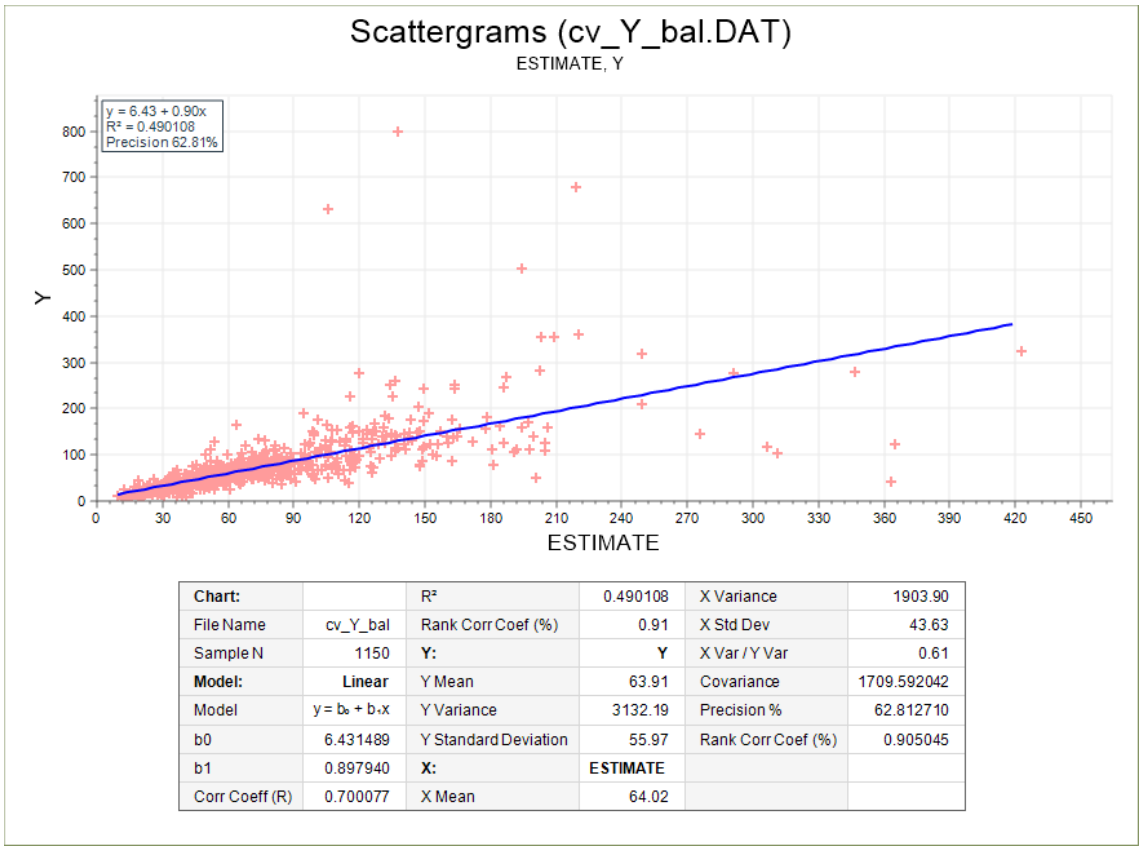

**Appendix IV - Figure 10 - Second axis to Y (ppm), Balsamo Target.**




**Appendix IV - Figure 11 - Third axis to Y (ppm), BalsamoTarget.**

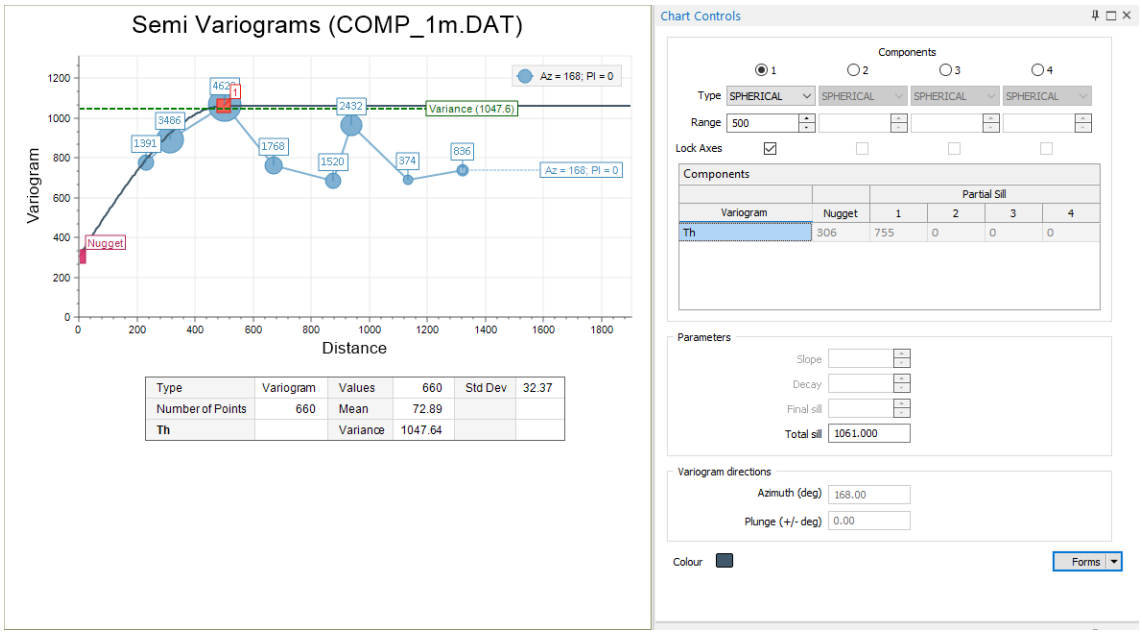
**Appendix IV - Table 3 - Cross-Validation verification results for Y (ppm), BalsamoTarget.**

| Metadata Label | Metadata Value | Field Name | Mean | Std Dev |
| --- | --- | --- | --- | --- |
| Output File | cv_Y_bal.DAT | | | |
| Input File | COMP_1m_BAL.DAT | | | |
| Analysis varb | Y | | | |
| Transformation | None | | | |
| Number of points | 1150 | | | |
| Raw Data | | Y | 63.914956522 | 55.965984624 |
| Standard error | | STD_ERROR | 21.106514053 | 0.977512948 |
| Estimate | | ESTIMATE | 64.017050267 | 43.633755738 |
| Residual | | RESIDUAL | -0.102093746 | 40.210844188 |
| Error statistic | | ERROR_STAT | -0.003285511 | 1.920881928 |
| RMSE | | | 40.193487072 | |




| Chart: | | R² | 0.490108 | X Variance | 1903.90 |
|---|---|---|---|---|---|
| File Name | cv_Y_bal | Rank Corr Coef (%) | 0.91 | X Std Dev | 43.63 |
| Sample N | 1150 | **Y:** | **Y** | X Var / Y Var | 0.61 |
| **Model:** | **Linear** | Y Mean | 63.91 | Covariance | 1709.592042 |
| Model | $y = b_0 + b_1 x$ | Y Variance | 3132.19 | Precision % | 62.812710 |
| b0 | 6.431489 | Y Standard Deviation | 55.97 | Rank Corr Coef (%) | 0.905045 |
| b1 | 0.897940 | **X:** | **ESTIMATE** | | |
| Corr Coeff (R) | 0.700077 | X Mean | 64.02 | | |

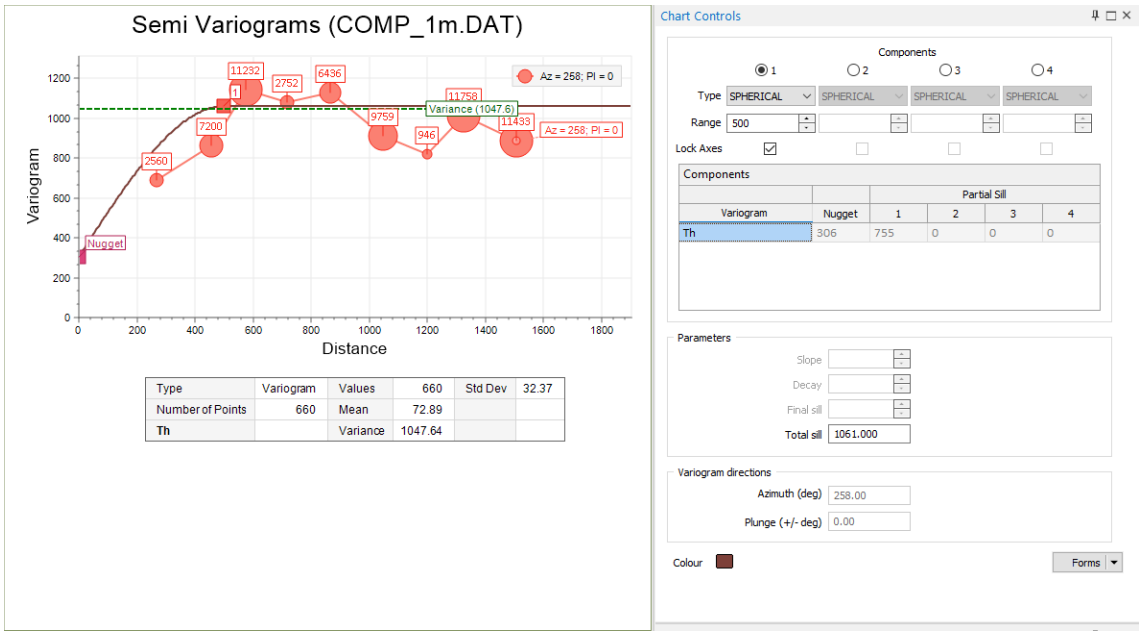
**Appendix IV - Figure 12 - Linear diagram of dependence between composite samples data and Y (ppm) grade estimates, Balsamo Target.**



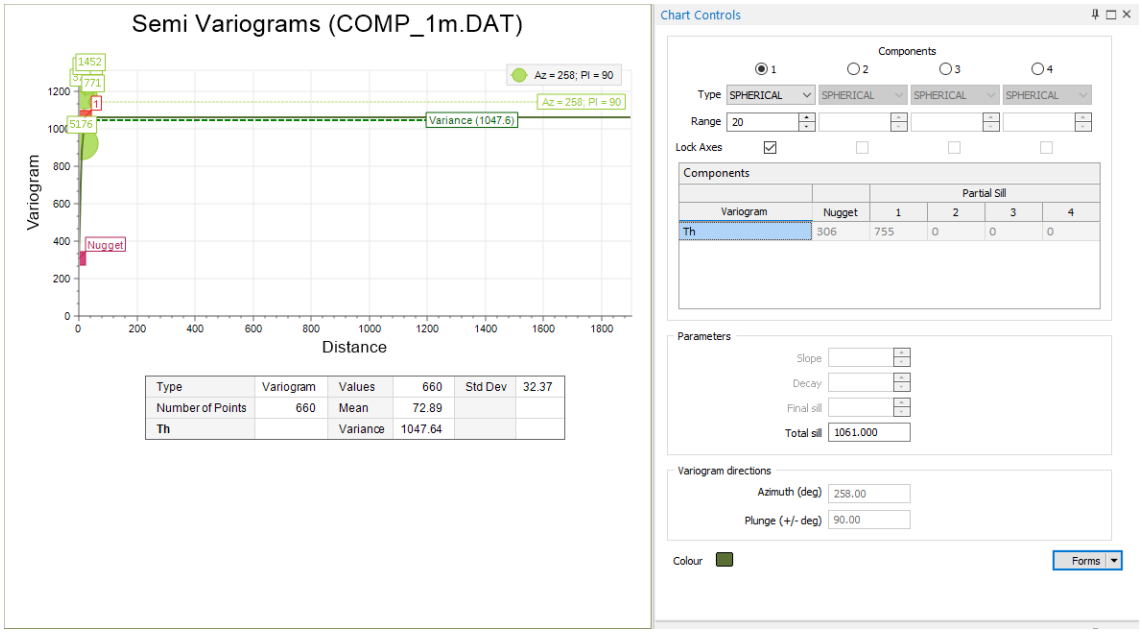

| Type | Variogram | Values | 660 | Std Dev | 32.37 |
|---|---|---|---|---|---|
| Number of Points | 660 | Mean | 72.89 | | |
| **Th** | | Variance | 1047.64 | | |

| Components | | | | | |
|---|---|---|---|---|---|
| | | Partial Sill | | | |
| Variogram | Nugget | 1 | 2 | 3 | 4 |
| Th | 306 | 755 | 0 | 0 | 0 |

**Appendix IV - Figure 13 - First axis to Th (ppm), Nau de GuerraTarget.**




**Appendix IV - Figure 14 - Second axis to Th (ppm), Nau de GuerraTarget.**

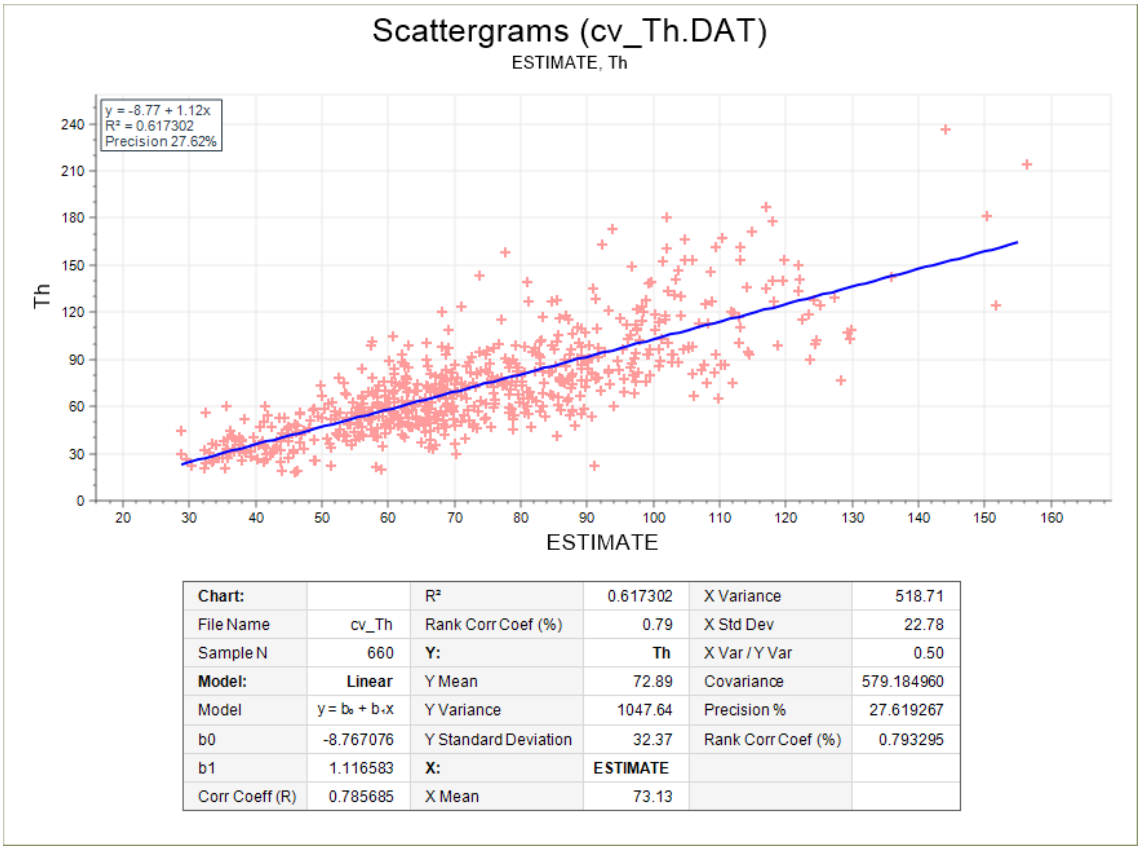



**Appendix IV - Figure 15 - Third axis to Th (ppm), Nau de GuerraTarget.**

**Appendix IV - Table 4 - Cross-Validation verification results for Th (ppm), Nau de GuerraTarget.**

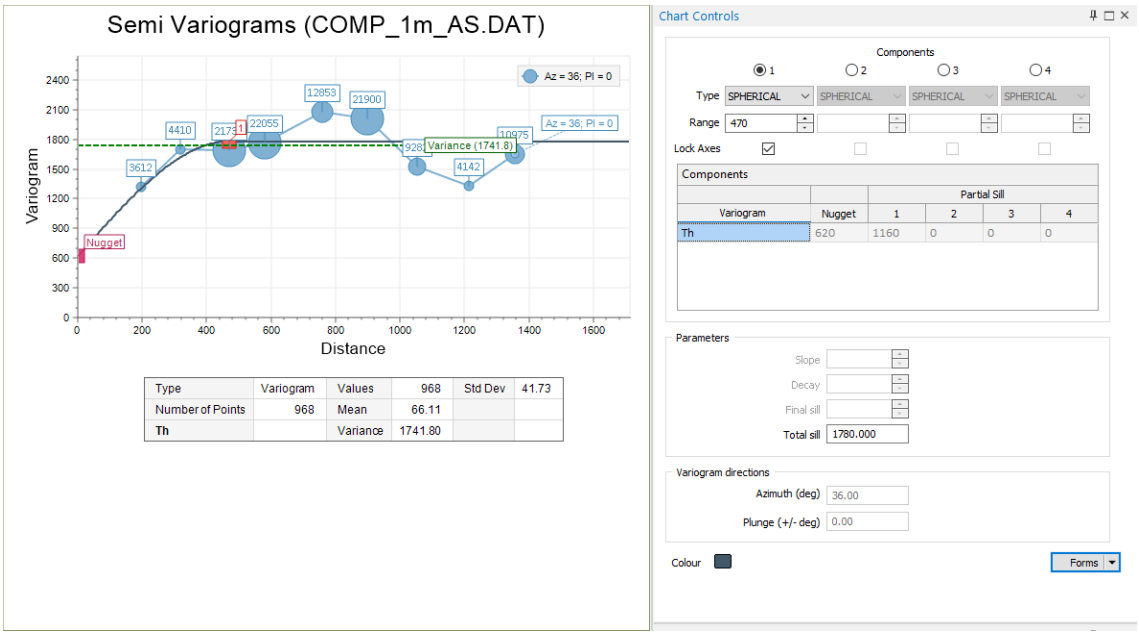
| Metadata Label | Metadata Value | Field Name | Mean | Std Dev |
|---|---|---|---|---|
| Output File | cv_Th.DAT | | | |
| Input File | COMP_1m.DAT | | | |
| Analysis varb | Th | | | |
| Transformation | None | | | |
| Number of points | 660 | | | |
| Raw Data | | Th | 72.890787879 | 32.367226310 |

| Metadata Label | Metadata Value | Field Name | Mean | Std Dev |
|---|---|---|---|---|
| Standard error | | STD_ERROR | 20.926984289 | 0.495696006 |
| Estimate | | ESTIMATE | 73.131906876 | 22.775246105 |
| Residual | | RESIDUAL | -0.241118997 | 20.198496328 |
| Error statistic | | ERROR_STAT | -0.008573512 | 0.962241812 |
| RMSE | | | 20.184628852 | |

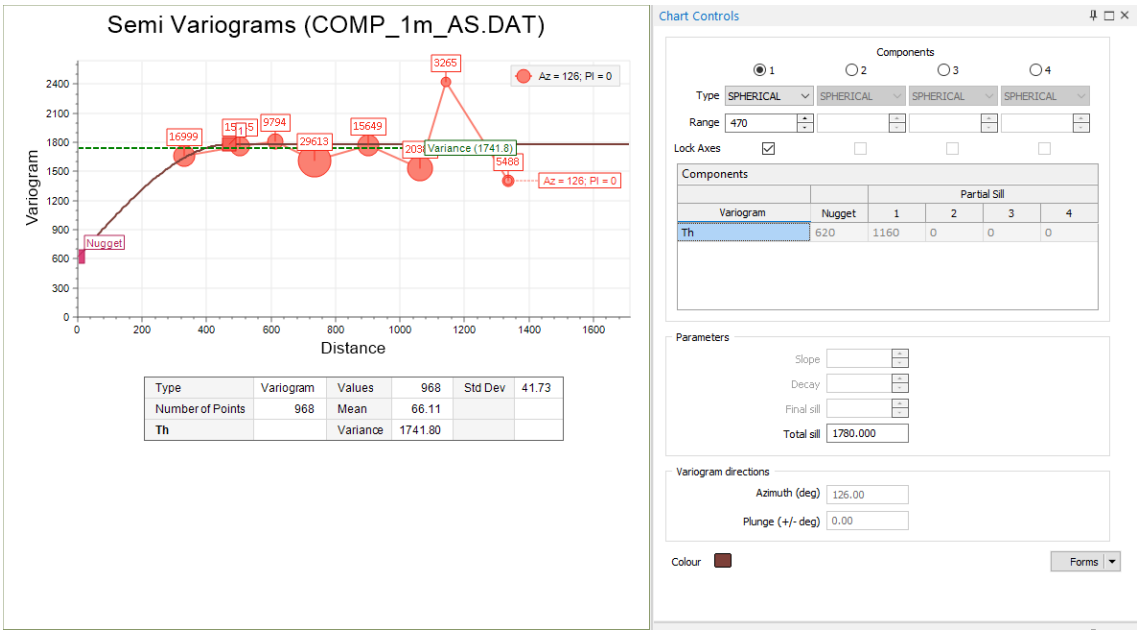



| Chart: | | R² | 0.617302 | X Variance | 518.71 |
|---|---|---|---|---|---|
| File Name | cv_Th | Rank Corr Coef (%) | 0.79 | X Std Dev | 22.78 |
| Sample N | 660 | **Y:** | **Th** | X Var / Y Var | 0.50 |
| **Model:** | **Linear** | Y Mean | 72.89 | Covariance | 579.184960 |
| Model | $y = b_0 + b_1x$ | Y Variance | 1047.64 | Precision % | 27.619267 |
| b0 | -8.767076 | Y Standard Deviation | 32.37 | Rank Corr Coef (%) | 0.793295 |
| b1 | 1.116583 | **X:** | **ESTIMATE** | | |
| Corr Coeff (R) | 0.785685 | X Mean | 73.13 | | |

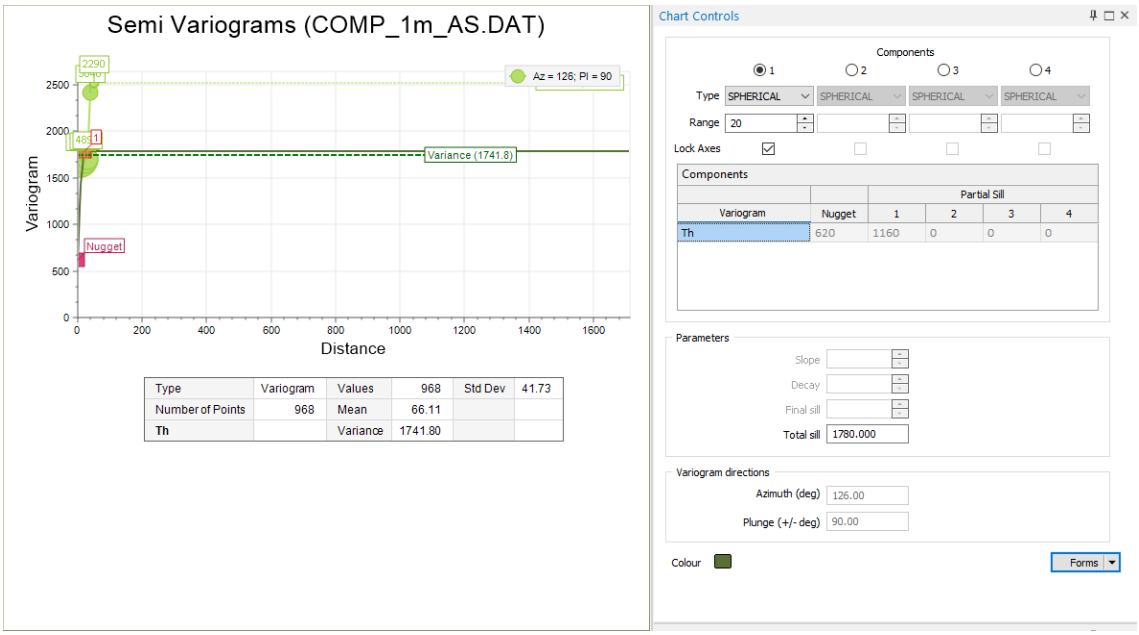
**Appendix IV - Figure 16 - Linear diagram of dependence between composite samples data and Th (ppm) grade estimates, Nau de Guerra Target.**




**Appendix IV - Figure 17 - First axis to Th (ppm), Alto da SerraTarget.**



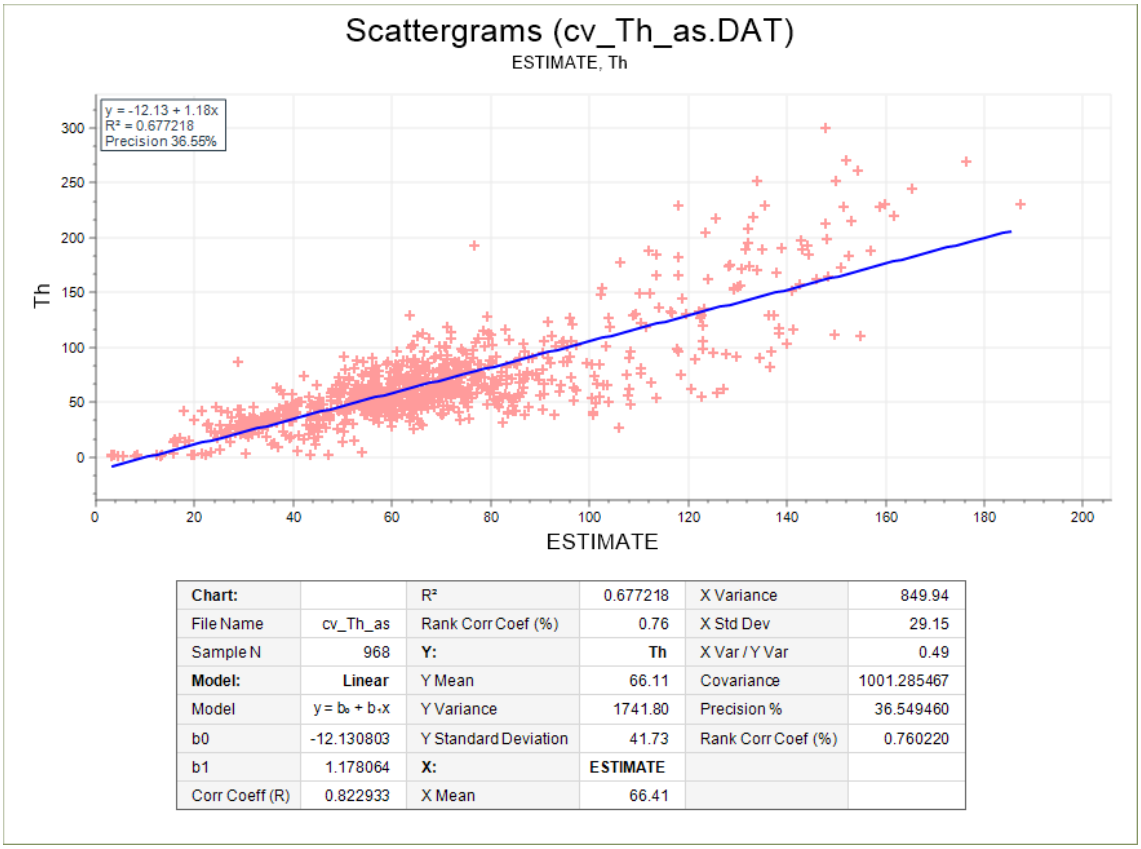

**Appendix IV - Figure 18 - Second axis to Th (ppm), Alto da SerraTarget.**




**Appendix IV - Figure 19 - Third axis to Th (ppm), Alto da SerraTarget.**

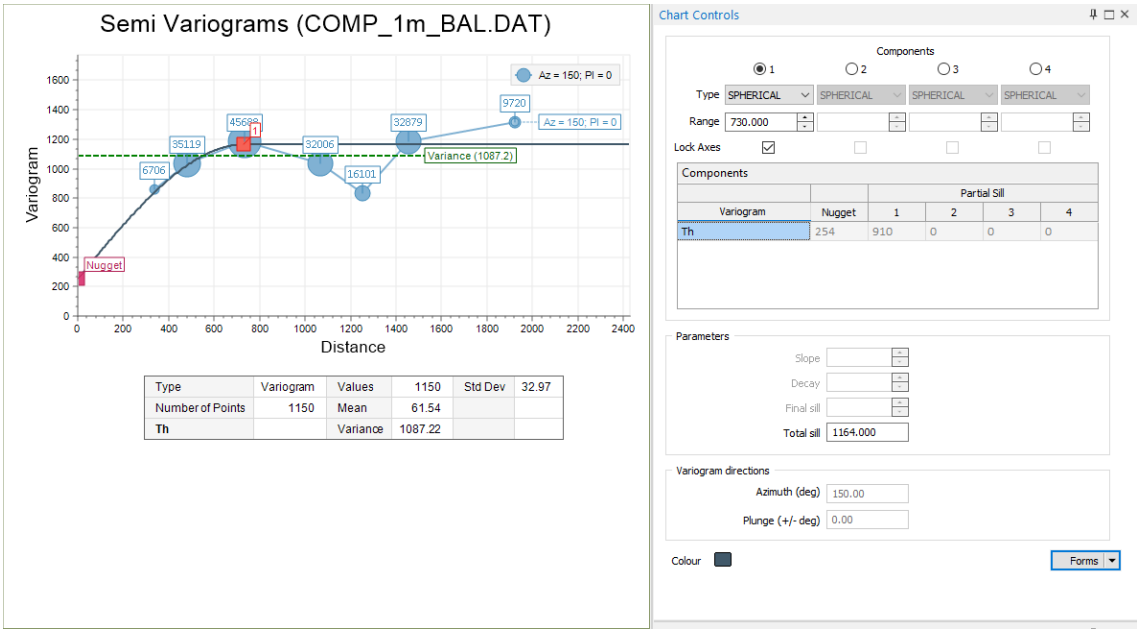
**Appendix IV - Table 5 - Cross-Validation verification results for Th (ppm), Alto da SerraTarget.**

| Metadata Label | Metadata Value | Field Name | Mean | Std Dev |
| --- | --- | --- | --- | --- |
| Output File | cv_Th_as.DAT | | | |
| Input File | COMP_1m_AS.DAT | | | |
| Analysis varb | Th | | | |
| Transformation | None | | | |
| Number of points | 968 | | | |
| Raw Data | | Th | 66.105475207 | 41.734869770 |
| Standard error | | STD_ERROR | 29.074353971 | 0.624321754 |
| Estimate | | ESTIMATE | 66.410895977 | 29.153757288 |
| Residual | | RESIDUAL | -0.305420770 | 24.272823988 |
| Error statistic | | ERROR_STAT | -0.008467356 | 0.837835448 |
| RMSE | | | 24.262205578 | |



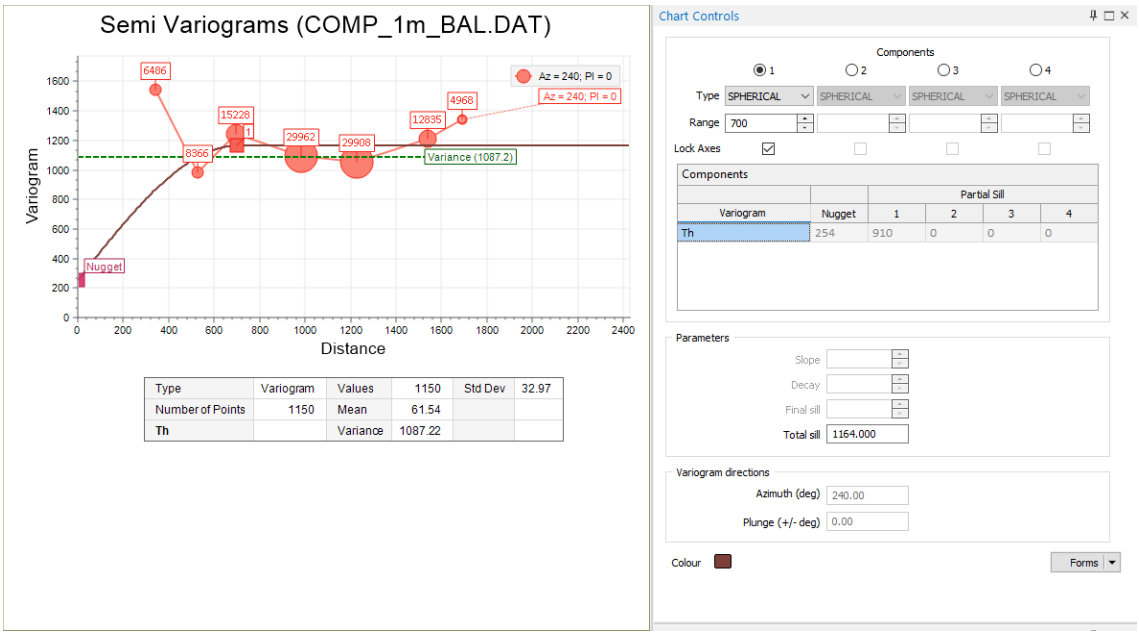

| Chart: | | R² | 0.677218 | X Variance | 849.94 |
|---|---|---|---|---|---|
| File Name | cv_Th_as | Rank Corr Coef (%) | 0.76 | X Std Dev | 29.15 |
| Sample N | 968 | **Y:** | **Th** | X Var / Y Var | 0.49 |
| **Model:** | **Linear** | Y Mean | 66.11 | Covariance | 1001.285467 |
| Model | $y = b_0 + b_1 x$ | Y Variance | 1741.80 | Precision % | 36.549460 |
| b0 | -12.130803 | Y Standard Deviation | 41.73 | Rank Corr Coef (%) | 0.760220 |
| b1 | 1.178064 | **X:** | **ESTIMATE** | | |
| Corr Coeff (R) | 0.822933 | X Mean | 66.41 | | |

**Appendix IV - Figure 20 - Linear diagram of dependence between composite samples data and Th (ppm) grade estimates, Alto da Serra Target.**

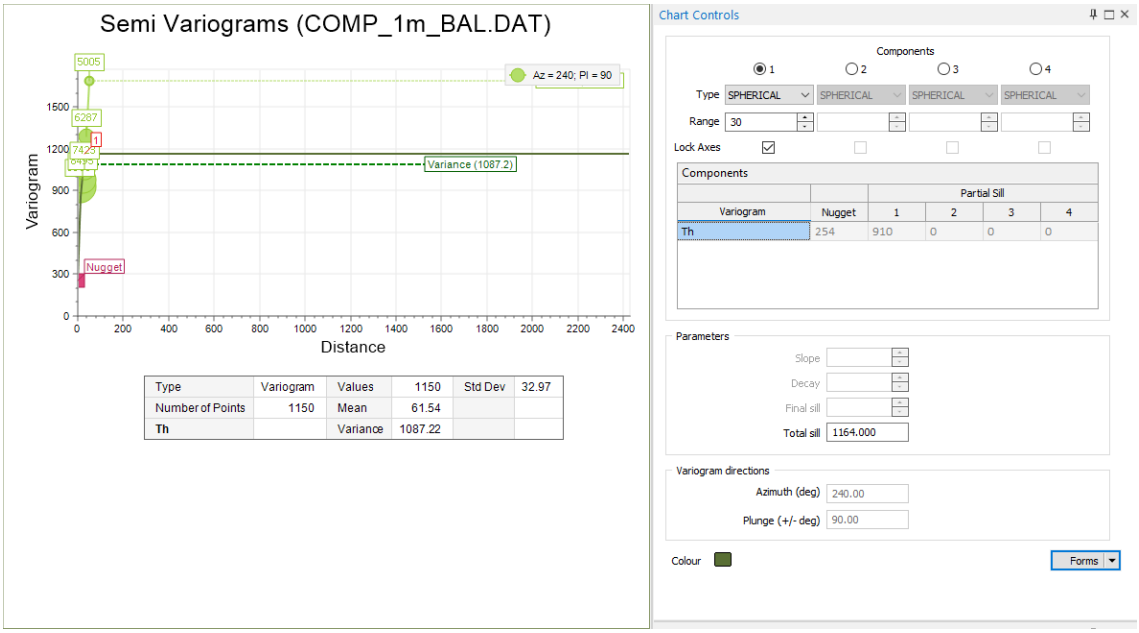



| Type | Variogram | Values | 1150 | Std Dev | 32.97 |
|---|---|---|---|---|---|
| Number of Points | 1150 | Mean | 61.54 | | |
| **Th** | | Variance | 1087.22 | | |

**Appendix IV - Figure 21 - First axis to Th (ppm), BalsamoTarget.**




**Appendix IV - Figure 22 - Second axis to Th (ppm), BalsamoTarget.**

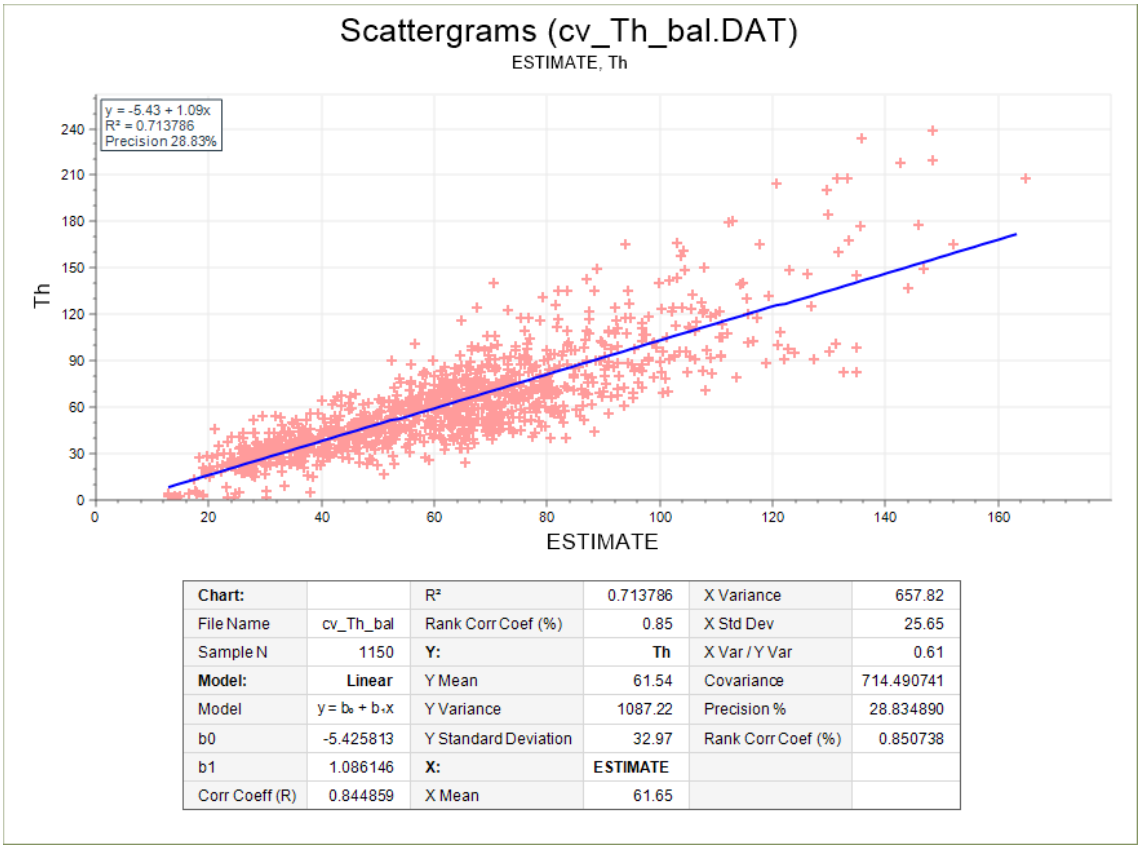



**Appendix IV - Figure 23 - Third axis to Th (ppm), BalsamoTarget.**

**Appendix IV - Table 6 - Cross-Validation verification results for Th (ppm), BalsamoTarget.**

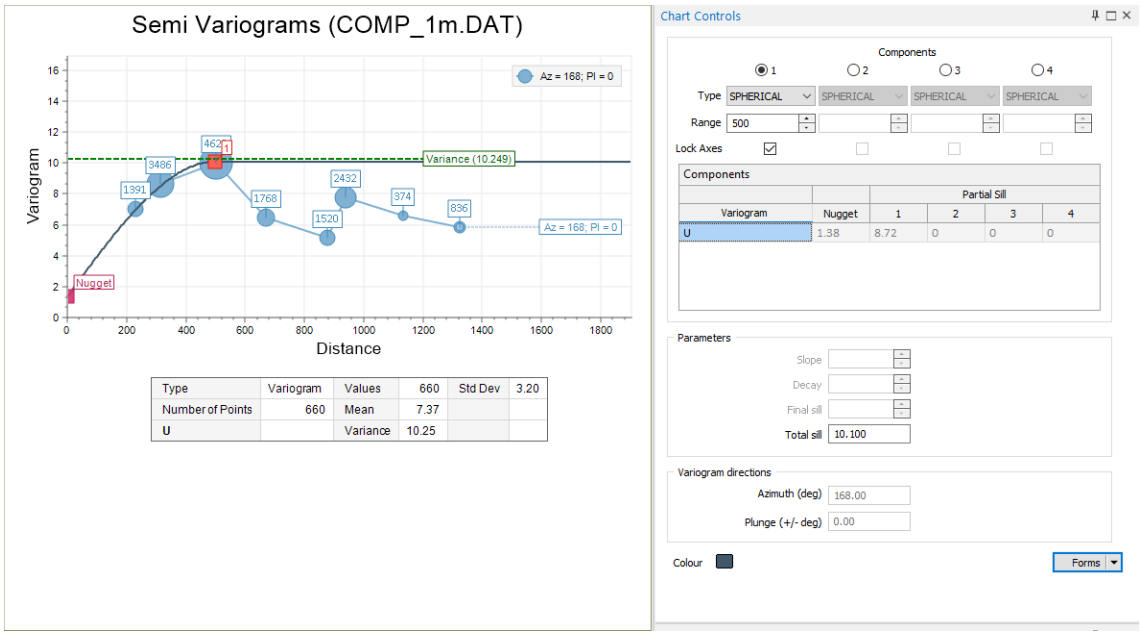
| Metadata Label | Metadata Value | Field Name | Mean | Std Dev |
| --- | --- | --- | --- | --- |
| Output File | cv_Th_bal.DAT | | | |
| Input File | COMP_1m_BAL.DAT | | | |
| Analysis varb | Th | | | |
| Transformation | None | | | |
| Number of points | 1150 | | | |
| Raw Data | | Th | 61.540086957 | 32.972990265 |
| Standard error | | STD_ERROR | 18.974277016 | 0.406110056 |

| Metadata Label | Metadata Value | Field Name | Mean | Std Dev |
|---|---|---|---|---|
| Estimate | | ESTIMATE | 61.654577944 | 25.648035914 |
| Residual | | RESIDUAL | -0.114490988 | 17.778029997 |
| Error statistic | | ERROR_STAT | -0.004604928 | 0.939151881 |
| RMSE | | | 17.770667557 | |



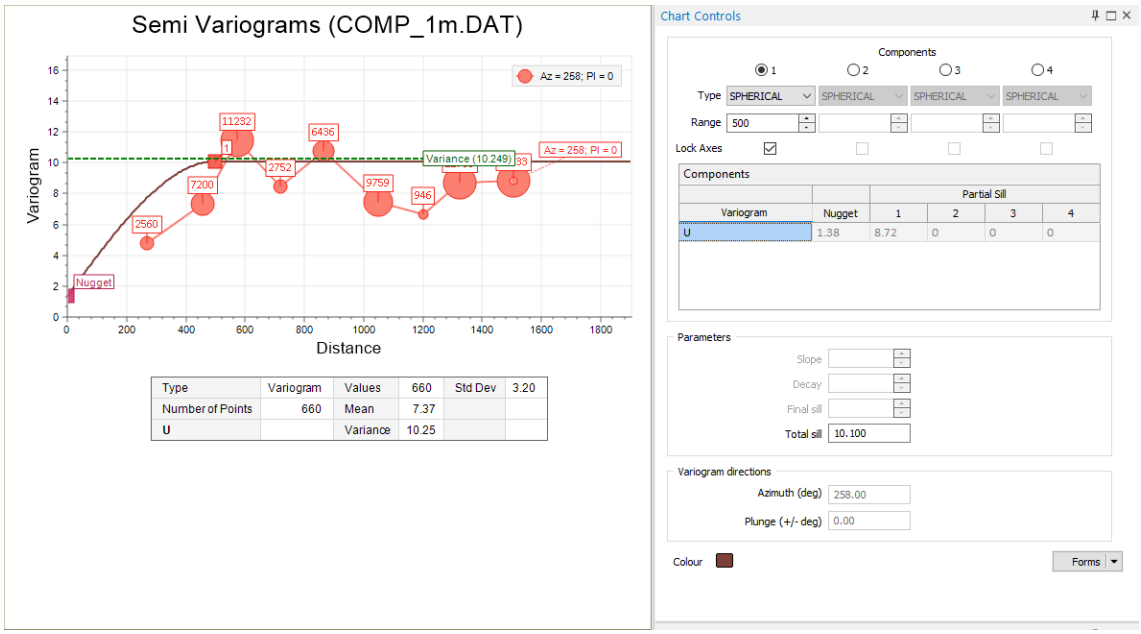

| Chart: | | R² | 0.713786 | X Variance | 657.82 |
|---|---|---|---|---|---|
| File Name | cv_Th_bal | Rank Corr Coef (%) | 0.85 | X Std Dev | 25.65 |
| Sample N | 1150 | **Y:** | **Th** | X Var / Y Var | 0.61 |
| **Model:** | **Linear** | Y Mean | 61.54 | Covariance | 714.490741 |
| Model | $y = b_0 + b_1x$ | Y Variance | 1087.22 | Precision % | 28.834890 |
| b0 | -5.425813 | Y Standard Deviation | 32.97 | Rank Corr Coef (%) | 0.850738 |
| b1 | 1.086146 | **X:** | **ESTIMATE** | | |
| Corr Coeff (R) | 0.844859 | X Mean | 61.65 | | |

**Appendix IV - Figure 24 - Linear diagram of dependence between composite samples data and Th (ppm) grade estimates, Balsamo Target.**



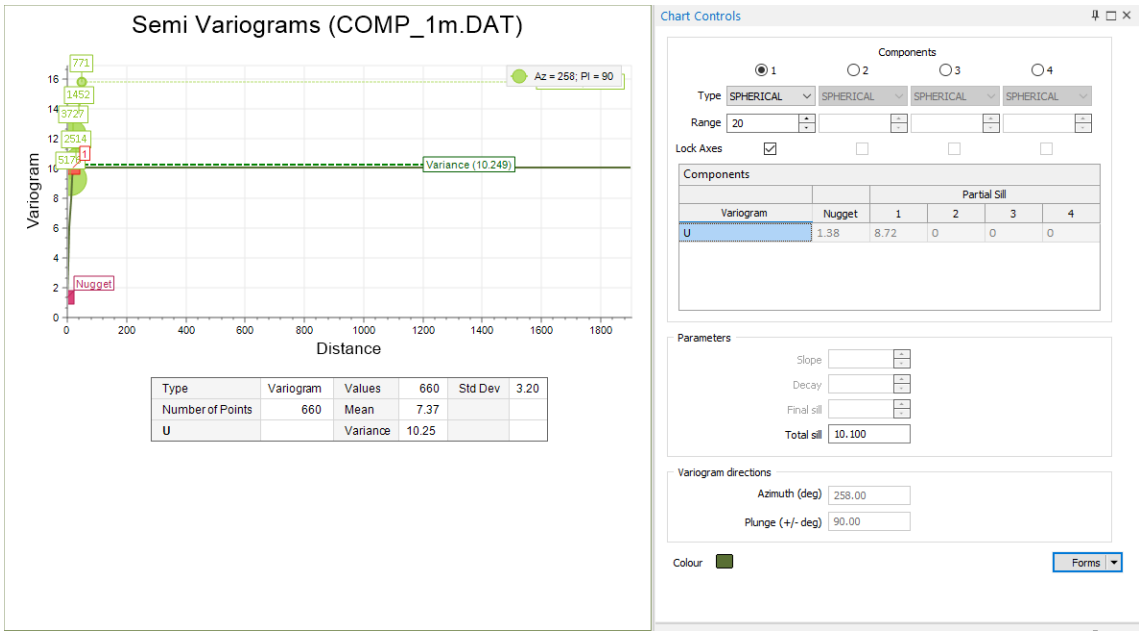

| Type | Variogram | Values | 660 | Std Dev | 3.20 |
| --- | --- | --- | --- | --- | --- |
| Number of Points | 660 | Mean | 7.37 | | |
| U | | Variance | 10.25 | | |

**Appendix IV - Figure 25 - First axis to U (ppm), Nau de GuerraTarget.**




| Type | Variogram | Values | 660 | Std Dev | 3.20 |
| --- | --- | --- | --- | --- | --- |
| Number of Points | 660 | Mean | 7.37 | | |
| U | | Variance | 10.25 | | |

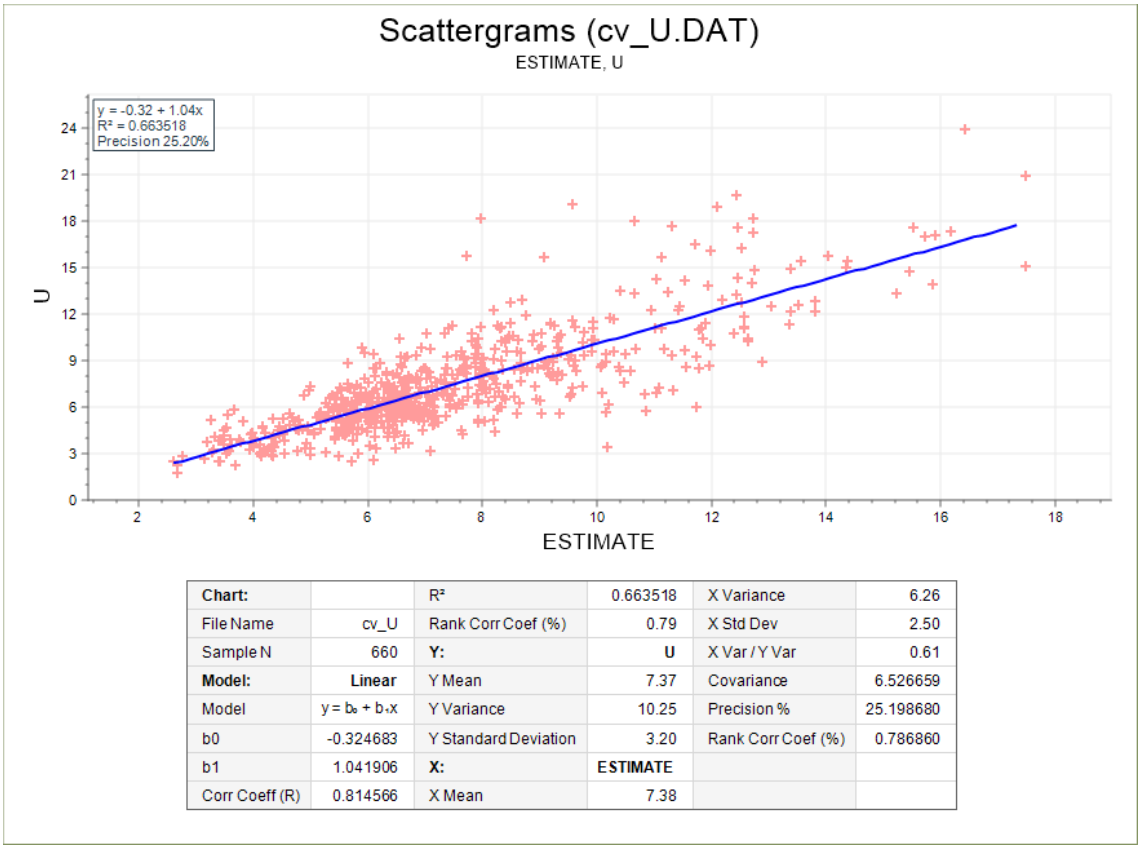
**Appendix IV - Figure 26 - Second axis to U (ppm), Nau de GuerraTarget.**




**Appendix IV - Figure 27 - Third axis to U (ppm), Nau de GuerraTarget.**

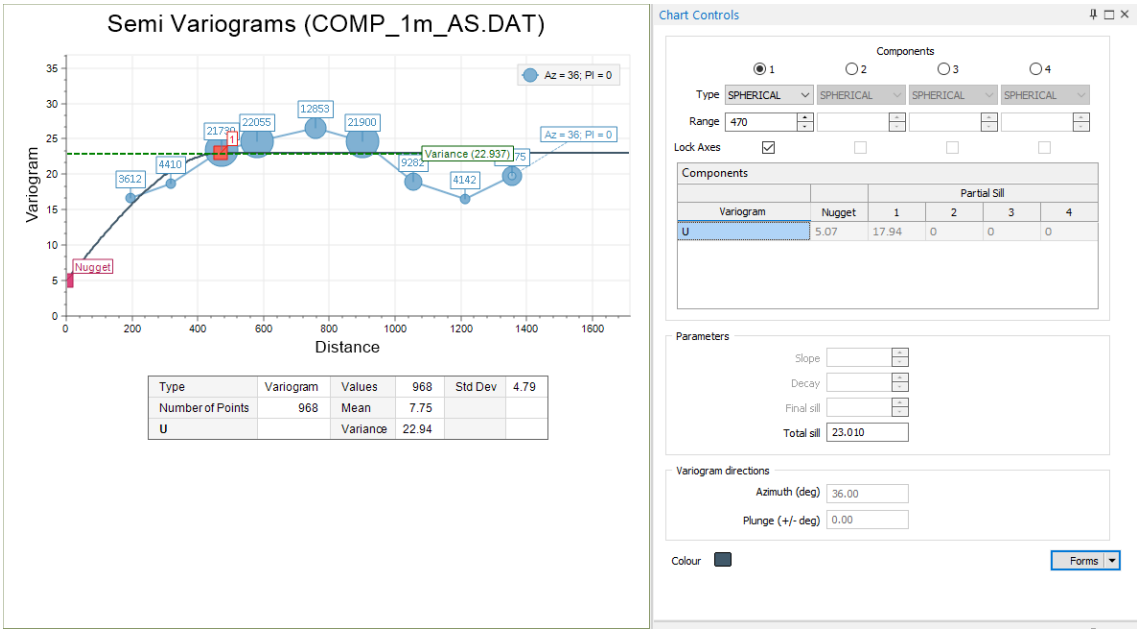
**Appendix IV - Table 7 - Cross-Validation verification results for U (ppm), Nau de GuerraTarget.**

| Metadata Label | Metadata Value | Field Name | Mean | Std Dev |
| --- | --- | --- | --- | --- |
| Output File | cv_U.DAT | | | |
| Input File | COMP_1m.DAT | | | |
| Analysis varb | U | | | |
| Transformation | None | | | |
| Number of points | 660 | | | |
| Raw Data | | U | 7.365860606 | 3.201352596 |
| Standard error | | STD_ERROR | 1.581436300 | 0.056469579 |
| Estimate | | ESTIMATE | 7.381226104 | 2.502829063 |
| Residual | | RESIDUAL | -0.015365498 | 1.859971542 |
| Error statistic | | ERROR_STAT | -0.006599539 | 1.169976576 |
| RMSE | | | 1.858625454 | |



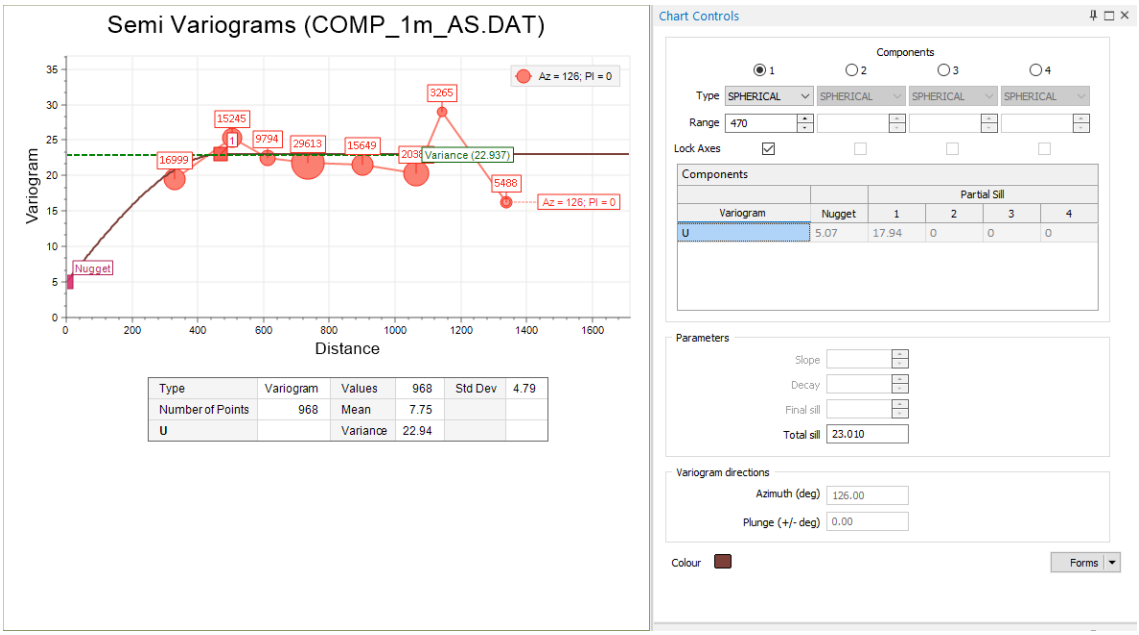

| Chart: | | R² | 0.663518 | X Variance | 6.26 |
| --- | --- | --- | --- | --- | --- |
| File Name | cv_U | Rank Corr Coef (%) | 0.79 | X Std Dev | 2.50 |
| Sample N | 660 | **Y:** | **U** | X Var / Y Var | 0.61 |
| **Model:** | **Linear** | Y Mean | 7.37 | Covariance | 6.526659 |
| Model | $y = b_0 + b_1 x$ | Y Variance | 10.25 | Precision % | 25.198680 |
| b0 | -0.324683 | Y Standard Deviation | 3.20 | Rank Corr Coef (%) | 0.786860 |
| b1 | 1.041906 | **X:** | **ESTIMATE** | | |
| Corr Coeff (R) | 0.814566 | X Mean | 7.38 | | |

**Appendix IV - Figure 28 - Linear diagram of dependence between composite samples data and U (ppm) grade estimates, Nau de Guerra Target.**

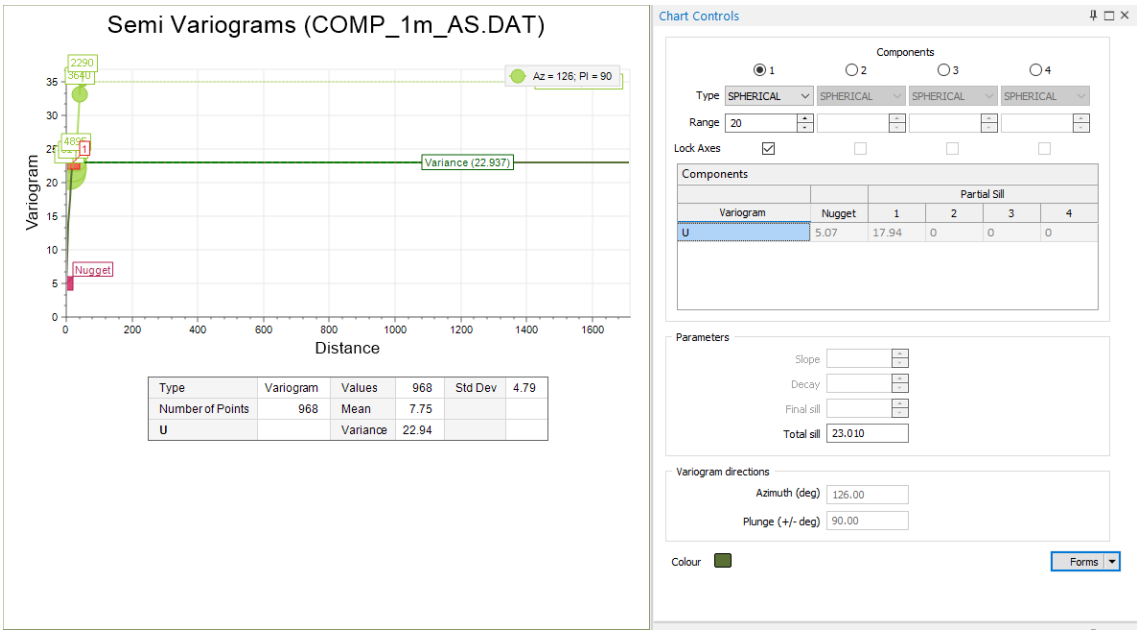



| Type | Variogram | Values | 968 | Std Dev | 4.79 |
| --- | --- | --- | --- | --- | --- |
| Number of Points | 968 | Mean | 7.75 | | |
| U | | Variance | 22.94 | | |

**Appendix IV - Figure 29 - First axis to U (ppm), Alto da SerraTarget.**




**Appendix IV - Figure 30 - Second axis to U (ppm), Alto da SerraTarget.**

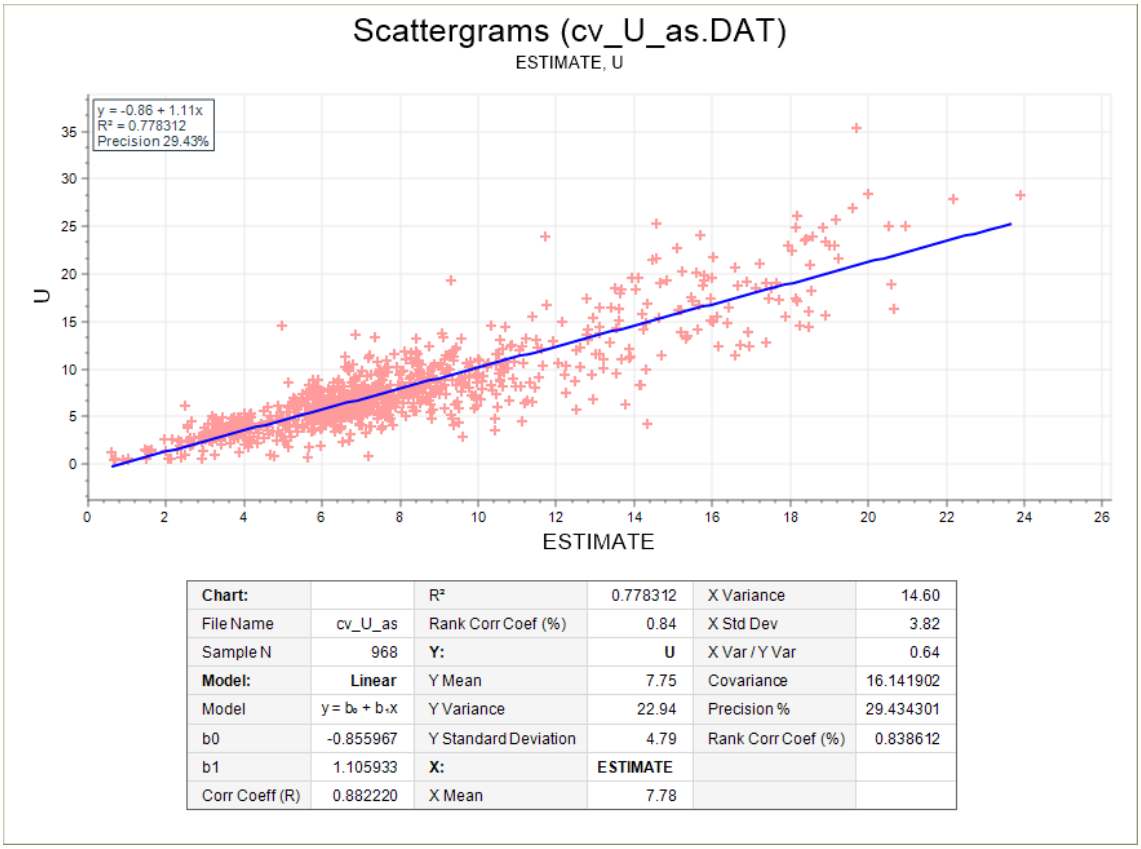



**Appendix IV - Figure 31 - Third axis to U (ppm), Alto da SerraTarget.**

**Appendix IV - Table 8 - Cross-Validation verification results for U (ppm), Alto da SerraTarget.**

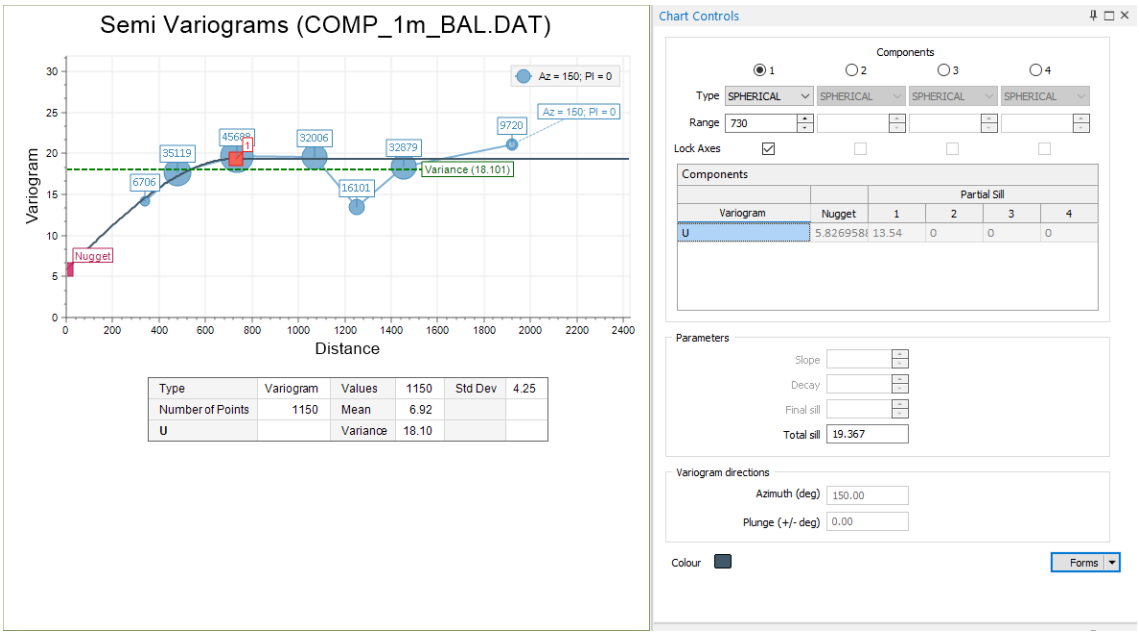
| Metadata Label | Metadata Value | Field Name | Mean | Std Dev |
|---|---|---|---|---|
| Output File | cv_U_as.DAT | | | |
| Input File | COMP_1m_AS.DAT | | | |
| Analysis varb | U | | | |
| Transformation | None | | | |
| Number of points | 968 | | | |
| Raw Data | | U | 7.751895661 | 4.789220634 |

| Metadata Label | Metadata Value | Field Name | Mean | Std Dev |
|---|---|---|---|---|
| Standard error | | STD_ERROR | 2.800141093 | 0.080145579 |
| Estimate | | ESTIMATE | 7.783351477 | 3.820436747 |
| Residual | | RESIDUAL | -0.031455816 | 2.290975080 |
| Error statistic | | ERROR_STAT | -0.008421844 | 0.820183364 |
| RMSE | | | 2.290007470 | |



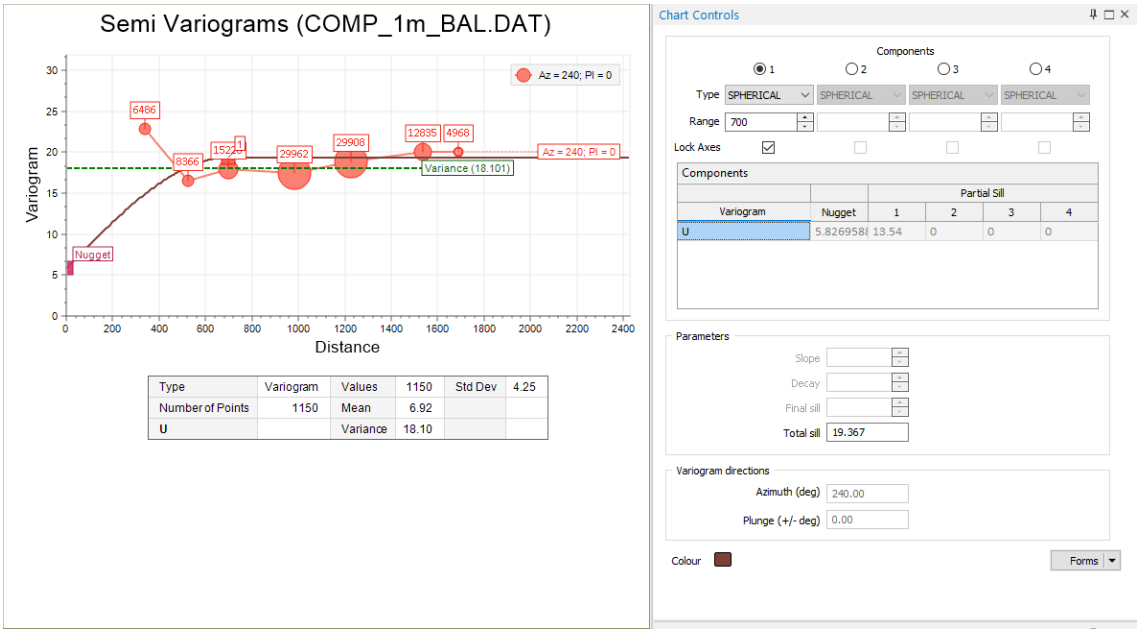

| Chart: | | R² | 0.778312 | X Variance | 14.60 |
|---|---|---|---|---|---|
| File Name | cv_U_as | Rank Corr Coef (%) | 0.84 | X Std Dev | 3.82 |
| Sample N | 968 | Y: | U | X Var / Y Var | 0.64 |
| Model: | Linear | Y Mean | 7.75 | Covariance | 16.141902 |
| Model | $y = b_0 + b_1 x$ | Y Variance | 22.94 | Precision % | 29.434301 |
| b0 | -0.855967 | Y Standard Deviation | 4.79 | Rank Corr Coef (%) | 0.838612 |
| b1 | 1.105933 | X: | ESTIMATE | | |
| Corr Coeff (R) | 0.882220 | X Mean | 7.78 | | |

**Appendix IV - Figure 32 - Linear diagram of dependence between composite samples data and U (ppm) grade estimates, Alto da Serra Target.**



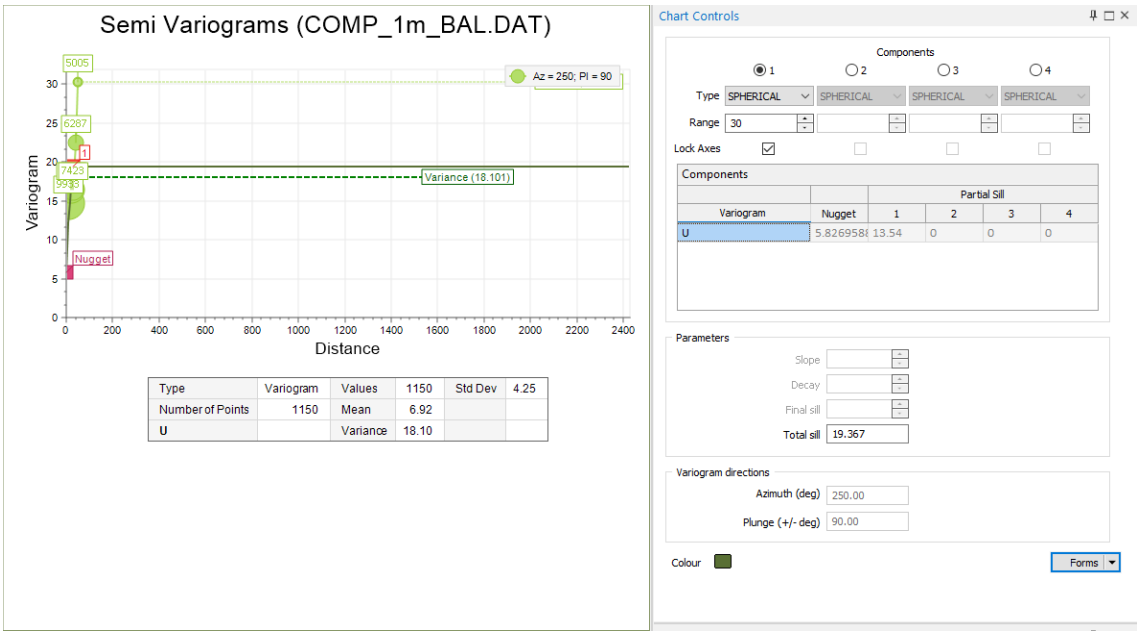

| Type | Variogram | Values | 1150 | Std Dev | 4.25 |
| --- | --- | --- | --- | --- | --- |
| Number of Points | 1150 | Mean | 6.92 | | |
| U | | Variance | 18.10 | | |

**Appendix IV - Figure 33 - First axis to U (ppm), BalsamoTarget.**




| Type | Variogram | Values | 1150 | Std Dev | 4.25 |
| --- | --- | --- | --- | --- | --- |
| Number of Points | 1150 | Mean | 6.92 | | |
| U | | Variance | 18.10 | | |

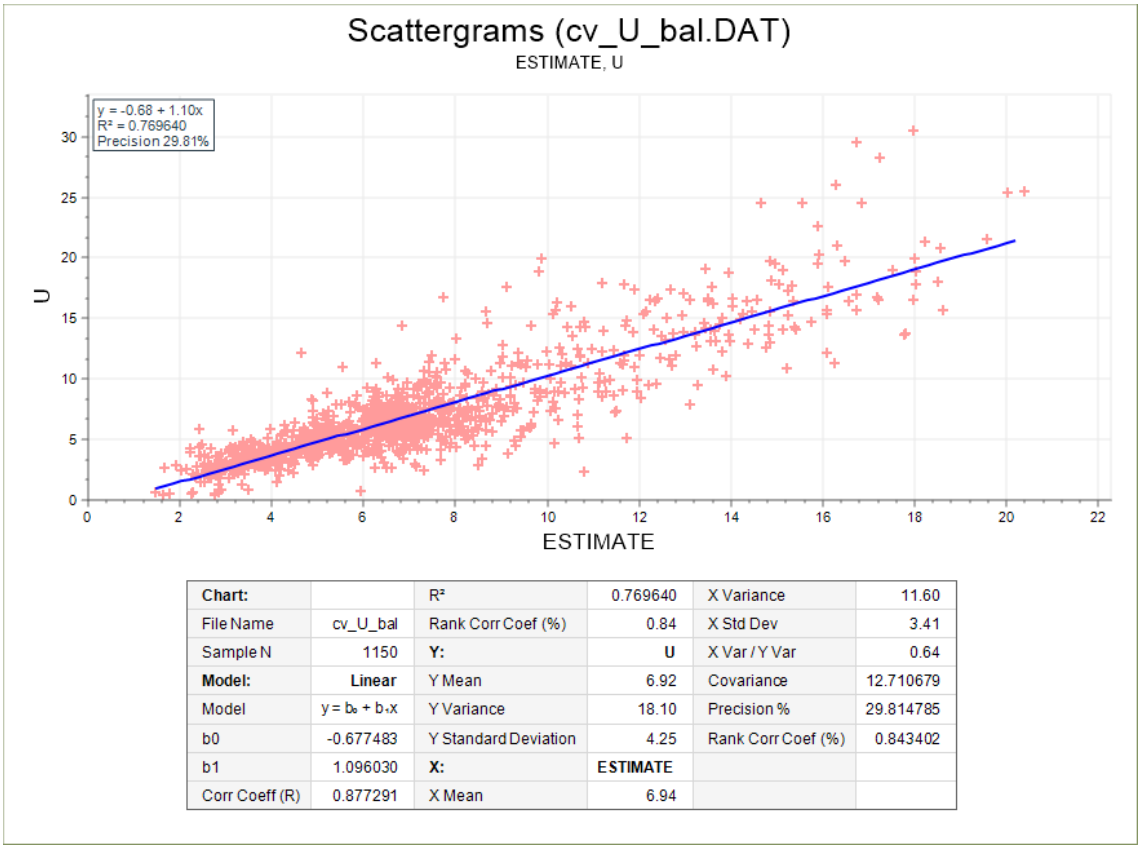
**Appendix IV - Figure 34 - Second axis to U (ppm), BalsamoTarget.**




**Appendix IV - Figure 35 - Third axis to U (ppm), BalsamoTarget.**

**Appendix IV - Table 9 - Cross-Validation verification results for U (ppm), BalsamoTarget.**

| Metadata Label | Metadata Value | Field Name | Mean | Std Dev |
|---|---|---|---|---|
| Output File | cv_U_bal.DAT | | | |
| Input File | COMP_1m_BAL.DAT | | | |
| Analysis varb | U | | | |
| Transformation | None | | | |
| Number of points | 1150 | | | |
| Raw Data | | U | 6.924817391 | 4.254531472 |
| Standard error | | STD_ERROR | 2.774796535 | 0.054154609 |
| Estimate | | ESTIMATE | 6.936217367 | 3.405439807 |
| Residual | | RESIDUAL | -0.011399975 | 2.068018305 |
| Error statistic | | ERROR_STAT | -0.003240773 | 0.745765764 |
| RMSE | | | 2.067150406 | |




| Chart: | | R² | 0.769640 | X Variance | 11.60 |
| --- | --- | --- | --- | --- | --- |
| File Name | cv_U_bal | Rank Corr Coef (%) | 0.84 | X Std Dev | 3.41 |
| Sample N | 1150 | **Y:** | **U** | X Var / Y Var | 0.64 |
| **Model:** | **Linear** | Y Mean | 6.92 | Covariance | 12.710679 |
| Model | $y = b_0 + b_1x$ | Y Variance | 18.10 | Precision % | 29.814785 |
| b0 | -0.677483 | Y Standard Deviation | 4.25 | Rank Corr Coef (%) | 0.843402 |
| b1 | 1.096030 | **X:** | **ESTIMATE** | | |
| Corr Coeff (R) | 0.877291 | X Mean | 6.94 | | |

**Appendix IV - Figure 36 - Linear diagram of dependence between composite samples data and U (ppm) grade estimates, Balsamo Target.**

# APPENDIX V – Resources Results

# LIST OF TABLES

Appendix V - Table 1 - Geological resources in situ – Nau de Guerra..... 243

Appendix V - Table 2 - Geological resources in situ – Alto da Serra ..... 244

Appendix V - Table 3 - Geological resources in situ – Balsamo..... 245

**Appendix V - Table 1 - Geological resources in situ – Nau de Guerra**

| CUT-OFF TREO+Y2O3 (ppm) | VOLUME m3 | TONNES t | DENSITY (t / m3) | TREO ppm | TREO less $Y_2O_3$ ppm | Y2O3 ppm | HREO ppm | LREO ppm | MREO ppm | Pr6O11 ppm | Nd2O3 ppm | Tb4O7 ppm | Dy2O3 ppm |
|---|---|---|---|---|---|---|---|---|---|---|---|---|---|
| 0 | 66,111,900.00 | 121,718,318.50 | 1.84 | 3,611.25 | 3,524.46 | 86.80 | 97.23 | 3,427.23 | 841.97 | 182.26 | 630.66 | 5.41 | 23.64 |
| 1000 | 65,889,200.00 | 121,330,679.50 | 1.84 | 3,619.92 | 3,532.94 | 86.98 | 97.45 | 3,435.49 | 844.08 | 182.71 | 632.25 | 5.42 | 23.69 |
| 1200 | 65,700,150.00 | 121,002,539.00 | 1.84 | 3,626.79 | 3,539.66 | 87.13 | 97.64 | 3,442.02 | 845.84 | 183.09 | 633.58 | 5.44 | 23.74 |
| 1300 | 65,637,850.00 | 120,892,760.00 | 1.84 | 3,628.94 | 3,541.77 | 87.17 | 97.70 | 3,444.07 | 846.38 | 183.20 | 633.99 | 5.44 | 23.75 |
| 1400 | 65,607,200.00 | 120,840,419.50 | 1.84 | 3,629.93 | 3,542.73 | 87.20 | 97.73 | 3,445.01 | 846.64 | 183.26 | 634.18 | 5.44 | 23.76 |
| 1500 | 65,582,500.00 | 120,795,880.50 | 1.84 | 3,630.73 | 3,543.52 | 87.22 | 97.75 | 3,445.77 | 846.83 | 183.30 | 634.32 | 5.44 | 23.77 |
| 2000 | 62,706,500.00 | 115,462,810.50 | 1.84 | 3,711.03 | 3,622.21 | 88.82 | 99.73 | 3,522.48 | 866.32 | 187.53 | 648.99 | 5.55 | 24.25 |
| 2500 | 57,097,650.00 | 105,052,936.00 | 1.84 | 3,854.12 | 3,762.36 | 91.76 | 103.52 | 3,658.83 | 901.55 | 195.09 | 675.51 | 5.77 | 25.17 |
| 3000 | 43,577,100.00 | 79,982,532.50 | 1.84 | 4,183.38 | 4,083.30 | 100.08 | 113.19 | 3,970.11 | 984.54 | 212.87 | 737.87 | 6.30 | 27.49 |
| 3500 | 31,594,050.00 | 57,845,591.50 | 1.83 | 4,549.70 | 4,439.10 | 110.60 | 124.72 | 4,314.38 | 1,077.29 | 232.67 | 807.42 | 6.94 | 30.27 |
| 4000 | 21,027,350.00 | 38,373,997.50 | 1.82 | 4,952.59 | 4,827.44 | 125.15 | 139.68 | 4,687.76 | 1,188.70 | 255.77 | 891.26 | 7.75 | 33.92 |
| 4500 | 11,289,150.00 | 20,495,958.50 | 1.82 | 5,567.22 | 5,423.75 | 143.47 | 157.88 | 5,265.86 | 1,343.89 | 290.25 | 1,006.62 | 8.76 | 38.26 |
| 5000 | 8,210,800.00 | 14,877,674.00 | 1.81 | 5,894.79 | 5,742.55 | 152.23 | 166.61 | 5,575.95 | 1,420.33 | 307.54 | 1,063.20 | 9.23 | 40.35 |

**Appendix V - Table 2 - Geological resources in situ – Alto da Serra**

| CUT-OFF TREO+Y2O3 (ppm) | VOLUME m3 | TONNES t | DENSITY (t / m3) | TREO ppm | TREO less $Y_2O_3$ ppm | Y2O3 ppm | HREO ppm | LREO ppm | MREO ppm | Pr6O11 ppm | Nd2O3 ppm | Tb4O7 ppm | Dy2O3 ppm |
|---|---|---|---|---|---|---|---|---|---|---|---|---|---|
| 0 | 137,644,100.00 | 244,395,414.50 | 1.78 | 3,510.09 | 3,416.98 | 93.11 | 99.51 | 3,317.47 | 832.77 | 178.63 | 624.21 | 5.49 | 24.44 |
| 1000 | 129,109,800.00 | 230,213,682.00 | 1.78 | 3,683.52 | 3,586.57 | 96.95 | 104.06 | 3,482.51 | 874.57 | 187.54 | 655.73 | 5.75 | 25.55 |
| 1200 | 128,772,000.00 | 229,624,547.50 | 1.78 | 3,690.19 | 3,593.07 | 97.12 | 104.24 | 3,488.83 | 876.19 | 187.89 | 656.95 | 5.76 | 25.59 |
| 1300 | 128,418,700.00 | 229,002,554.50 | 1.78 | 3,696.81 | 3,599.52 | 97.29 | 104.43 | 3,495.09 | 877.81 | 188.23 | 658.17 | 5.77 | 25.64 |
| 1400 | 127,749,450.00 | 227,828,634.50 | 1.78 | 3,708.91 | 3,611.34 | 97.57 | 104.75 | 3,506.59 | 880.75 | 188.86 | 660.39 | 5.79 | 25.72 |
| 1500 | 127,166,900.00 | 226,804,122.50 | 1.78 | 3,719.10 | 3,621.28 | 97.82 | 105.02 | 3,516.26 | 883.23 | 189.38 | 662.26 | 5.81 | 25.78 |
| 2000 | 122,778,600.00 | 219,073,035.50 | 1.78 | 3,788.23 | 3,688.60 | 99.63 | 106.97 | 3,581.63 | 900.23 | 192.99 | 675.07 | 5.91 | 26.26 |
| 2500 | 111,818,500.00 | 199,576,101.00 | 1.78 | 3,931.66 | 3,828.03 | 103.63 | 111.23 | 3,716.80 | 937.55 | 200.92 | 703.18 | 6.15 | 27.30 |
| 3000 | 79,072,900.00 | 141,063,119.00 | 1.78 | 4,409.29 | 4,290.42 | 118.87 | 126.64 | 4,163.79 | 1,063.75 | 227.60 | 798.07 | 6.98 | 31.10 |
| 3500 | 51,160,850.00 | 91,179,461.50 | 1.78 | 5,068.74 | 4,925.31 | 143.43 | 150.33 | 4,774.98 | 1,242.18 | 264.80 | 932.12 | 8.28 | 36.98 |
| 4000 | 33,628,000.00 | 59,874,108.00 | 1.78 | 5,759.81 | 5,592.76 | 167.06 | 175.44 | 5,417.31 | 1,435.50 | 304.42 | 1,078.24 | 9.67 | 43.17 |
| 4500 | 24,219,350.00 | 43,077,911.50 | 1.78 | 6,353.19 | 6,168.19 | 185.00 | 197.46 | 5,970.73 | 1,610.95 | 339.99 | 1,211.48 | 10.91 | 48.57 |
| 5000 | 17,579,550.00 | 31,256,634.50 | 1.78 | 6,970.41 | 6,781.16 | 189.25 | 214.16 | 6,567.00 | 1,800.70 | 379.26 | 1,357.06 | 11.93 | 52.46 |

**Appendix V - Table 3 - Geological resources in situ – Balsamo**

| CUT-OFF TREO+Y2O3 (ppm) | VOLUME m3 | TONNES t | DENSITY (t / m3) | TREO ppm | TREO less $Y_2O_3$ ppm | Y2O3 ppm | HREO ppm | LREO ppm | MREO ppm | Pr6O11 ppm | Nd2O3 ppm | Tb4O7 ppm | Dy2O3 ppm |
|---|---|---|---|---|---|---|---|---|---|---|---|---|---|
| 0 | 661,522,500.00 | 1,182,191,249.00 | 1.79 | 3,279.62 | 3,201.17 | 78.45 | 84.40 | 3,116.77 | 749.73 | 163.61 | 560.66 | 4.77 | 20.68 |
| 1000 | 640,828,400.00 | 1,145,624,208.50 | 1.79 | 3,357.88 | 3,278.31 | 79.57 | 85.99 | 3,192.32 | 768.70 | 167.82 | 574.98 | 4.87 | 21.04 |
| 1200 | 636,818,100.00 | 1,138,498,276.50 | 1.79 | 3,371.90 | 3,292.04 | 79.86 | 86.35 | 3,205.69 | 772.22 | 168.59 | 577.62 | 4.89 | 21.13 |
| 1300 | 623,763,850.00 | 1,115,547,171.50 | 1.79 | 3,415.73 | 3,334.82 | 80.91 | 87.58 | 3,247.24 | 783.76 | 171.10 | 586.28 | 4.96 | 21.43 |
| 1400 | 615,542,350.00 | 1,100,909,001.50 | 1.79 | 3,443.19 | 3,361.85 | 81.34 | 88.21 | 3,273.64 | 790.93 | 172.70 | 591.67 | 5.00 | 21.57 |
| 1500 | 608,686,250.00 | 1,088,676,465.00 | 1.79 | 3,465.59 | 3,383.81 | 81.78 | 88.75 | 3,295.06 | 796.47 | 173.91 | 595.83 | 5.03 | 21.70 |
| 2000 | 549,397,150.00 | 982,720,026.00 | 1.79 | 3,656.44 | 3,571.43 | 85.01 | 92.98 | 3,478.46 | 845.13 | 184.88 | 632.29 | 5.28 | 22.68 |
| 2500 | 467,357,550.00 | 836,206,187.00 | 1.79 | 3,896.56 | 3,808.50 | 88.05 | 97.69 | 3,710.81 | 906.08 | 198.77 | 678.00 | 5.56 | 23.75 |
| 3000 | 380,688,200.00 | 681,112,610.50 | 1.79 | 4,144.41 | 4,050.41 | 94.00 | 104.19 | 3,946.22 | 966.72 | 211.90 | 723.53 | 5.93 | 25.36 |
| 3500 | 244,874,300.00 | 438,065,369.50 | 1.79 | 4,645.52 | 4,536.89 | 108.62 | 118.82 | 4,418.07 | 1,091.54 | 239.27 | 816.42 | 6.76 | 29.10 |
| 4000 | 173,139,850.00 | 309,729,856.50 | 1.79 | 5,028.34 | 4,912.12 | 116.22 | 128.72 | 4,783.40 | 1,186.71 | 260.23 | 887.63 | 7.34 | 31.50 |
| 4500 | 115,183,800.00 | 206,015,922.00 | 1.79 | 5,448.49 | 5,321.74 | 126.75 | 141.21 | 5,180.53 | 1,294.86 | 283.96 | 968.16 | 8.08 | 34.66 |
| 5000 | 57,000,300.00 | 101,911,239.50 | 1.79 | 6,129.23 | 5,997.77 | 131.46 | 154.56 | 5,843.21 | 1,445.42 | 319.10 | 1,079.64 | 8.85 | 37.83 |

# APPENDIX VI – Preliminary Metallurgical Tests

# LIST OF CERTIFICATES

Verde Agritech – Declaração SGSGeosol.PDF